Klug Lisa Theresa Romana, M.Sc.

Lipids of *Pichia pastoris*

DISSERTATION

zur Erlangung des akademischen Grades eines

Doktors der Naturwissenschaften

eingereicht an der

Technischen Universität Graz

Betreuer: Ao. Univ.-Prof. Dipl.-Ing. Dr. techn. Günther Daum

Institut für Biochemie, Technische Universität Graz

Graz, 2014

EIDESSTATTLICHE ERKLÄRUNG

Ich erkläre an Eides statt, dass ich die vorliegende Arbeit selbstständig verfasst, andere als die angegebenen Quellen / Hilfsmittel nicht benutzt, und die den benutzten Quellen wörtlich und inhaltlich entnommene Stellen als solche kenntlich gemacht habe.

STATUTORY DECLARATION

I declare that I have authored this thesis independently, that I have not used other than the declared sources / resources, and that I have explicitly marked all material which has been quoted either literally or by content from the used sources.

Graz,……..... ….....

Danksagung

Meinem Betreuer, Günther Daum, möchte ich danken, dass er mir die Möglichkeit eine Dissertation unter seiner Obhut zu machen, gegeben hat und mich während dieser Zeit auf allen Ebenen unterstützt hat.

Meinen Co-AutorInnen und KollaboratorationspartnerInnen danke ich für die gute und erfolgreiche Zusammenarbeit.

Meinen Thesis Committee Mitgliedern, Kai-Uwe Fröhlich und Karl Lohner, danke ich für die konstruktiven Treffen in einer angenehmen Atmosphäre, für deren hilfreiche Ratschläge und deren Unterstützung.

Meinen lieben ArbeitskollegInnen danke ich für eine wunderbare Zeit, für unseren Zusammenhalt in den vielen Tagen zum Lachen und den wenigen Tagen zum Weinen, für unsere endlos langen Gespräche und Blödeleien aber natürlich auch für die vielen fachlichen Diskussionen und Ratschläge und hoffe, dass wir auch in Zukunft unseren freundschaftlichen Kontakt beibehalten werden. Namentlich nennen möchte ich insbesondere Heinzi, der mir immer tatkräftig beiseite gestanden hat und dadurch Vieles erleichtert hat, als auch Vasyl und Andi, die unser Pichia-Team erst komplett gemacht haben. Auch meinen liebenswerten (Nichtraucher-) Mädls Birgit, Barbara, Claudia, den drei Martinas, Ari, Francesca, Brigitte und Mirka bin ich dankbar, dass sie jeglichen Wetterkapriolen getrotzt und mich immer nach draußen begleitet haben. Ihr seid die Besten!

Meiner Familie, Mama, Papa und Flo als auch Gerald's Familie danke ich für ihr Verständnis und für die langjährige Unterstützung während meines ganzen Studiums.

Meinen Freunden, bei denen ich mich in den letzten Jahren oft rar gemacht habe, die aber trotzdem immer zu mir gehalten haben, möchte ich besonders danken.

Meinem zukünftigen Ehemann Gerald gebührt das größte Dankeschön. Mit seiner Liebe, seinem Verständnis, seiner Fürsorglichkeit und seinen Fähigkeiten mich aufzubauen und immer das Beste in mir zu sehen, hat er mich immer vorangetrieben und mich in meinem Tun bestärkt.

Abstract

During the last decades, lipids have gained much attention due to their involvement in several diseases. To study fundamental aspects of lipid metabolism, however, the yeast *Saccharomyces cerevisiae* has become a reliable model cell. In this Thesis, the first chapter is devoted to a compact overview of yeast lipid metabolism. Metabolic aspects, lipid storage and mobilization and regulatory problems have been addressed. The specific role of enzymes governing important steps of the different lipid metabolic pathways has been described. Beside *S. cerevisiae*, the yeast *Pichia pastoris* has become a valuable eukaryotic model organism which is frequently used as a tool for industrial protein production. Despite these important applications, cell biological aspects of *P. pastoris* including problems of biomembrane and lipid research have not been adequately addressed. Since eukaryotic cells are compartmentalized, techniques which allow isolation of these compartments (organelles) and subcellular membranes are required for studying various aspects of cell biology. Many reliable protocols for cell fractionation were designed for *S. cerevisiae*. We adopted and modified these methods for studying *P. pastoris* organelles in more detail. In this Thesis, optimized protocols for the isolation of the most important organelles from *P. pastoris* are provided, and standard methods for lipid analysis of *P. pastoris* organelles are described. The experimental focus of this Thesis was on *P. pastoris* microsomes which represent the endoplasmic reticulum. We developed a procedure to isolate microsomal membranes at high purity which were subjected to molecular analysis of lipids and proteins. Organelle lipidomics included a detailed analysis of glycerophospholipids, fatty acids, sterols and sphingolipids. The microsomal proteome analyzed by mass spectrometry identified typical proteins of the endoplasmic reticulum known from other cell types, especially *S. cerevisiae*, but also a number of unassigned gene products. As a contribution to *P. pastoris* lipid metabolism, we identified the cardiolipin synthase by expression in a *S. cerevisiae* mutant strain lacking this enzyme. Effects of the *P. pastoris* cardiolipin synthase on phospholipid formation and cell growth were shown. In summary, this Thesis contributes to our general knowledge of *P. pastoris* biomembrane biology and sets the stage to manipulate this microorganism for applied research.

Zusammenfassung

In den letzten Jahrzehnten hat das Interesse an Lipiden wegen ihrer Beteiligung an Krankheiten stark zugenommen. Um grundlegende Aspekte des Lipidstoffwechsels zu untersuchen wurde die Hefe *Saccharomyces cerevisiae* häufig als Modellorganismus verwendet. Das erste Kapitel dieser Dissertation gibt einen Überblick über den Lipidstoffwechsel der Hefe. Metabolismus, Lipidspeicherung und Mobilisierung sowie regulatorische Aspekte wurden behandelt. Die spezifische Rolle von Enzymen, die wichtige Schritte der verschiedenen Lipidstoffwechselwege katalysieren, wurde beschrieben. Neben *S. cerevisiae* hat sich die methylotrophe Hefe *Pichia pastoris,* die häufig für die industrielle Proteinproduktion verwendet wird, zu einem wertvollen eukaryotischen Modellorganismus entwickelt. Trotz der industriellen Anwendung wurden zellbiologische Aspekte von *P. pastoris* betreffend Biomembranen und Lipide noch nicht ausreichend untersucht. Da eukaryotische Zellen in Kompartimente (Organellen) unterteilt sind, wurden Techniken zur Isolierung dieser Organellen oder subzellulärer Membranen für zellbiologische Untersuchungen entwickelt. Viele Protokolle wurden in der Vergangenheit für die Zellfraktionierung von *S. cerevisiae* konzipiert. Wir haben diese Methoden modifiziert um *P. pastoris* Organellen im Detail zu untersuchen. Diese Dissertation beschreibt optimierte Protokolle für die Isolierung der wichtigsten Organellen von *P. pastoris* und Lipidanalysen von *P. pastoris* Organellen. Der experimentelle Schwerpunkt dieser Dissertation lag auf der Isolierung und Charakterisierung der Mikrosomen von *P. pastoris*, welche das endoplasmatischen Retikulum darstellen. Ein Protokoll zur Isolierung mikrosomaler Membranen mit hoher Reinheit wurde entwickelt um anschließend molekulare Analysen von Lipiden und Proteinen durchzuführen. Die Lipidanalysen der Mikrosomen umfassten die Glycerophospholipide, Fettsäuren, Sterole und Sphingolipide. Das mikrosomale Proteom wurde durch Massenspektrometrie analysiert. Es wurden nicht nur typische Proteine des endoplasmatischen Reticulum, die von anderen Zellarten und vor allem von *S. cerevisiae* bereits bekannt waren, identifiziert, sondern auch eine Reihe nicht zugewiesener Genprodukten. Als Beitrag zum Lipidmetabolismus von *P. pastoris* wurde die Cardiolipinsynthase dieses Mikroorganismus studiert. Expression des *P. pastoris* Gens in einer *S. cerevisiae* Deletionsmutante führte zur Komplementation von Defekten des Wachstums und der Lipidsynthese. Zusammenfassend stellt diese Arbeit einen Beitrag zum Verständnis der Membranbiologie von *P. pastoris* dar und bietet Information für die Manipulation dieses Mikroorganismus in der angewandten Forschung.

Table of content

Aims and Outline of this thesis

The methylotrophic yeast *Pichia pastoris* is a well characterized microorganism concerning its use in the industry as expression system for heterologous proteins. However, the knowledge about cell biological of this yeast is limited to a few issues such as peroxisome assembly and function, autophagy and secretion. Although some fundamental cell biological investigations have been performed recently, a broad understanding of *P. pastoris* organelles is still missing. Particularly, *P. pastoris* lipid metabolism, organelle lipidomic and proteomics require more detailed investigations.

The present Thesis was aimed to acquire information about the lipids and proteins from *P. pastoris* subcellular fractions. The first main topic of this Thesis is an introduction into yeast lipid metabolism. A detailed description of procedures for the isolation of *P. pastoris* organelles with the goal to analyze lipids and proteins is described in chapters III and IV. A major section of this thesis deals with *P. pastoris* microsomes representing the endoplasmic reticulum. Isolation and characterization of this organelle is described in detail in chapter V. The second major aim of this work was the identification of enzymes involved in *P. pastoris* lipid synthesize. The focus of this study was the identification of the mitochondrial phospholipid cardiolipin. These investigations are summarized in chapter VI.

In the following the content of the Thesis chapters is briefly described.

Chapter I is a short general introduction to *P. pastoris*. Advantages of this system for heterologous protein expression are presented. Some biochemical characteristics of *P. pastoris* membranes are mentioned pointing out the importance of *P. pastoris* as a model organism for fundamental research.

Chapter II reviews the lipid metabolism in *S. cerevisiae* at a glance. Synthesis, degradation and some regulatory aspects of fatty acid, membrane lipid and storage lipid metabolism and molecular biology are presented.

Chapter III summarizes techniques of subcellular fractionation which were specifically designated for the isolation of different *P. pastoris* organelles and biomembranes. This section is organized as stepwise protocols to obtain highly enriched and intact organelles and membrane compartments suitable for structural and functional analysis.

Chapter IV describes methods of detailed lipid analysis with the yeast *P. pastoris*. Optimized conventional lipid analysis and lipidomics techniques are rendered in the form of detailed protocols as guidance for lipidome analysis.

Chapter V is dedicated to the isolation and structural analysis of *P. pastoris* microsomes which represent the endoplasmic reticulum. Data presented here describe the lipidome and the proteome of this organelle.

Chapter VI reports identification of the cardiolipin synthase from *P. pastoris* by complementation studies with *S. cerevisiae* and describes an effect of enhanced enzyme synthesis on cell growth.

Chapter VII is a general discussion of this Thesis which summarizes the obtained results with some concluding remarks.

Chapter I

General introduction

The methylotrophic yeast Pichia pastoris

The methylotrophic yeast *Pichia pastoris* is one of four identified microbial genera beside *Hansenula*, *Candida* and *Torulopsis* which can use methanol as sole carbon source [1]. In the past years, methylotrophic yeasts attracted much attention in the industry because methanol is an inexpensive alternative growth supplement. Utilization of methanol as carbon source leads to the proliferation of peroxisomes [2,3]. Within these organelles enzymes for methanol metabolism are localized. The alcohol oxidase and the catalase are responsible for the degradation of methanol and the detoxification of hydrogen peroxide which is produced [4]. Peroxisome proliferation induced by methanol made *P. pastoris* a suitable organism to study peroxisomal genetics and biochemistry [5,6]. The existence of the inducible alcohol oxidase promoters *AOX1* and *AOX2* opened new perspectives for the industry. The *AOX1* promoter is strongly repressed by glucose or other carbon sources which is advantageous when large amounts of recombinant proteins produced may have a toxic effect to the cells. In contrast, induction of the promoter by methanol usually leads to immense overproduction of foreign proteins [7].

Another feature which favors *P. pastoris* for heterologous protein production is its preference for respiratory growth instead of fermentation where ethanol is synthesized as a toxic side product. Therefore, *P. pastoris* is able to grow to higher cell densities paralleled by higher yields of heterologous proteins [8]. *P. pastoris* can be easily manipulated by genetic means and possesses many post-translational protein processing properties similar to higher eukaryotes. Due to these features, proteins from higher eukaryotic cells which are expressed in *P. pastoris* have a good chance to be more correctly processed, folded and assembled into functional molecules than after expression in *S. cerevisiae* or *E. coli* [9–11]. *P. pastoris* is able to express foreign proteins either intracellularly or secrete them to the medium [12].

Therefore, *P. pastoris* has also become a model organism for studies of the protein secretory pathway [13].

Protein synthesis, processing and secretion in *P. pastoris* were intensively investigated to improve the expression of recombinant proteins for industrial purposes. However, many questions remain on cell biological and biochemical aspects of these processes. As an example, fundamental information about membrane functions and their lipid composition were missing although this knowledge may be very useful for industrial purposes. Our laboratory started to investigate *P. pastoris* organelles in some detail. These studies included the isolation of organelles at high purity and characterization of the lipidome and proteome. Moreover, the usage and influence of different carbon sources or incubation temperatures on growth and lipid composition were examined [14–17].

So far, procedures for the isolation of peroxisomes, mitochondria, microsomes and lipid droplets were successfully established. These highly purified subcellular fractions were used to determine membrane characteristics. Furthermore, intensive research was performed recently on the plasma membrane, the Golgi apparatus and the vacuoles (our own unpublished work). It was shown that the growth rate of *P. pastoris* was influences by the carbon source and the temperature. Methods for organelle isolation at high purity were adopted and, if required, improved from protocols which were previously designed for *Saccharomyces cerevisiae*. Lipid analysis of *P. pastoris* organelles revealed some characteristic differences to the corresponding cell compartments from *S. cerevisiae.*

An interesting feature of *P. pastoris* is the production of polyunsaturated fatty acids which influences membrane integrity and fluidity. The fatty acid composition was shown to depend on the carbon source used for cell cultivation. Another lipid class influencing membrane properties are sterols. Ergosterol is the predominant sterol found in *P. pastoris* organelles, while sterol precursor molecules are only present at low levels [14–17]. Interestingly, lipid droplets from *P. pastoris* store more triacylglycerols than steryl esters [16], while lipid droplets from *S. cerevisiae* contain equivalent amounts of these storage lipids [18,19]. Phosphatidylcholine and phosphatidylethanolamine are the two major membrane phospholipids found in *P. pastoris* subcellular fractions [14–17]. Growth of *P. pastoris* on methanol or oleic acid significantly increased the amount of cardiolipin in mitochondria, especially in the inner mitochondrial membrane, and changed the morphology and the number of mitochondria per cell as was also observed for peroxisomes [14,15].

Lipid studies on *P. pastoris* organelles open new perspectives for applied research, since membranes can be easily manipulated by the carbon source used for cultivation. The identification of enzymes involved in *P. pastoris* lipid metabolism also revealed new opportunities. Recently, two phosphatidylserine decarboxylases encoded by *PSD1* and *PSD2* [20] and the storage lipid synthases encoded by *LRO1*, *DGA1* and *ARE1* were identified in *P. pastoris* [21]. It was shown that deletion of the major phosphatidylethanolamine synthesizing enzyme Psd1p without external ethanolamine supply was lethal [20]. Several *P. pastoris* genes involved in fatty acid desaturation were also identified. Desaturation of fatty acids was shown to be essential for viability of *P. pastoris* [22,23]. Manipulating the sterol biosynthetic pathway and the enzymes involved may also be interesting for engineering industrial processes [24]. Thus, a fundamental knowledge of lipid metabolic pathways and membrane structural and functional features will be helpful to improve *P. pastoris* as an expression host and as a eukaryotic model organism.

References:

[1] K.N. Faber, W. Harder, G. Ab, M. Veenhuis, Review: methylotrophic yeasts as factories for the production of foreign proteins, Yeast, 11 (1995) 1331–1344.

[2] Y. Sakai, S. Subramani, Environmental response of yeast peroxisomes Aspects of organelle assembly and degradation, Cell Biochem. Biophys., 32 (2000) 51–61.

[3] C. Ma, G. Agrawal, S. Subramani, Peroxisome assembly: matrix and membrane protein biogenesis, J. Cell Biol., 193 (2011) 7–16.

[4] I.J. van der Klei, H. Yurimoto, Y. Sakai, M. Veenhuis, The significance of peroxisomes in methanol metabolism in methylotrophic yeast, Biochim. Biophys. Acta, 1763 (2006) 1453–1462.

[5] Role of the *PAS1* gene of *Pichia pastoris* in peroxisome biogenesis, J. Cell Biol., 127 (1994) 1259–1273.

[6] L.-A. Brown, A. Baker, Peroxisome biogenesis and the role of protein import, J. Cell. Mol. Med., 7 (2003) 388–400.

[7] S. Kim, S. Warburton, I. Boldogh, C. Svensson, L. Pon, M. d' Anjou, T.A. Stadheim, B.-K. Choi, Regulation of alcohol oxidase 1 (*AOX1*) promoter and peroxisome biogenesis in different fermentation processes in *Pichia pastoris*, J. Biotechnol., 166 (2013) 174–181.

[8] S. Christen, U. Sauer, Intracellular characterization of aerobic glucose metabolism in seven yeast species by 13C flux analysis and metabolomics, FEMS Yeast Res., 11 (2011) 263–272.

[9] A. Ramón, M. Marín, Advances in the production of membrane proteins in *Pichia pastoris*, Biotechnol. J., 6 (2011) 700–706.

[10] J. Bai, D.J. Swartz, I.I. Protasevich, C.G. Brouillette, P.M. Harrell, E. Hildebrandt, B. Gasser, D. Mattanovich, A. Ward, G. Chang, I.L. Urbatsch, A gene optimization strategy that enhances production of fully functional P-glycoprotein in *Pichia pastoris*, PLoS ONE, 6 (2011) e22577.

[11] J.L. Corchero, B. Gasser, D. Resina, W. Smith, E. Parrilli, F. Vázquez, I. Abasolo, M. Giuliani, J. Jäntti, P. Ferrer, M. Saloheimo, D. Mattanovich, S. Schwartz Jr., M.L. Tutino, A. Villaverde, Unconventional microbial systems for the cost-efficient production of high-quality protein therapeutics, Biotechnol. Advances, 31 (2013) 140–153.

[12] L.M. Damasceno, C.-J. Huang, C.A. Batt, Protein secretion in *Pichia pastoris* and advances in protein production, Appl. Microbiol. Biotechnol., 93 (2011) 31–39.

[13] M. Delic, M. Valli, A.B. Graf, M. Pfeffer, D. Mattanovich, B. Gasser, The secretory pathway: Exploring yeast diversity, FEMS Microbiol. Rev., 6 (2013) 872-914.

[14] T. Wriessnegger, G. Gübitz, E. Leitner, E. Ingolic, J. Cregg, B.J. de la Cruz, G. Daum, Lipid composition of peroxisomes from the yeast *Pichia pastoris* grown on different carbon sources, Biochim. Biophys. Acta, 1771 (2007) 455–461.

[15] T. Wriessnegger, E. Leitner, M.R. Belegratis, E. Ingolic, G. Daum, Lipid analysis of mitochondrial membranes from the yeast *Pichia pastoris*, Biochim. Biophys. Acta, 1791 (2009) 166–172.

[16] V.A. Ivashov, K. Grillitsch, H. Koefeler, E. Leitner, D. Baeumlisberger, M. Karas, G. Daum, Lipidome and proteome of lipid droplets from the methylotrophic yeast *Pichia pastoris*, Biochim. Biophys. Acta, (2012).

[17] L. Klug, P. Tarazona, C. Gruber, K. Grillitsch, B. Gasser, M. Trötzmüller, H. Köfeler, E. Leitner, I. Feussner, D. Mattanovich, F. Altmann, G. Daum, The lipidome and proteome of microsomes from the methylotrophic yeast *Pichia pastoris*, Biochim. Biophys. Acta, 1841 (2014) 215–226.

[18] R. Leber, E. Zinser, G. Zellnig, F. Paltauf, G. Daum, Characterization of lipid particles of the yeast *Saccharomyces cerevisiae*, Yeast, 10 (1994) 1421–1428.

[19] T. Czabany, A. Wagner, D. Zweytick, K. Lohner, E. Leitner, E. Ingolic, G. Daum, Structural and biochemical properties of lipid particles from the yeast *Saccharomyces cerevisiae*, J. Biol. Chem., 283 (2008) 17065–17074.

[20] T. Wriessnegger, A.J. Sunga, J.M. Cregg, G. Daum, Identification of phosphatidylserine decarboxylases 1 and 2 from *Pichia pastoris*, FEMS Yeast Res., 9 (2009) 911–922.

[21] V.A. Ivashov, G. Zellnig, K. Grillitsch, G. Daum, Identification of triacylglycerol and steryl ester synthases of the methylotrophic yeast *Pichia pastoris*, Biochim. Biophys. Acta, 1831 (2013) 1158–1166.

[22] X. Zhang, M. Li, D. Wei, L. Xing, Identification and characterization of a novel yeast omega3-fatty acid desaturase acting on long-chain n-6 fatty acid substrates from *Pichia pastoris*, Yeast, 25 (2008) 21–27.

[23] A.-Q. Yu, J.-C. Zhu, B. Zhang, L.-J. Xing, M.-C. Li, Knockout of fatty acid desaturase genes in *Pichia pastoris* GS115 and its effect on the fatty acid biosynthesis and physiological consequences, Arch. Microbiol., 194 (2012) 1023–1032.

[24] M. Hirz, G. Richter, E. Leitner, T. Wriessnegger, H. Pichler, A novel cholesterol-producing *Pichia pastoris* strain is an ideal host for functional expression of human Na,K-ATPase α3β1 isoform, Appl. Microbiol. Biotechnol., 97 (2013) 9465–9478.

Chapter II

Minireview

Yeast lipid metabolism at a glance

Lisa Klug and Günther Daum*

Institute of Biochemistry, Graz University of Technology, Graz, Austria

Running title: Yeast lipids

Key words:

Saccharomyces cerevisiae, Fatty acids, Phospholipids, Sphingolipids, Sterols, Triacylglycerols, Steryl esters, Lipid biosynthesis, Lipid degradation

*Corresponding author: Günther Daum, Institute of Biochemistry, Graz University of Technology, Petersgasse 12/II, A-8010 Graz, Austria.

Tel.: +43 316 873 6462; Fax: +43 316 873 6952; E-mail address: guenther.daum@tugraz.at

Abbreviations:

ATP, adenosine triphosphate; CDP, cytidinediphosphate; Cer, ceramide; Cho, choline; CL, cardiolipin; CoA, coenzyme A; CTP, cytidine triphosphate; DG, diacylglycerol; DHAP, dihydroxyacetone phosphate; DHCer, dihydroceramide; DHS, dihydrosphingosine; DPP, dimethylallyl pyrophosphate; ER, endoplasmic reticulum; ERAD, ER-associated protein degradation; Erg, ergosterol; Etn, ethanolamine; Etn-P, ethanolamine-phosphate; FA, fatty acids; FAS, fatty acid synthase; FFA, free fatty acids; FPP, farnesyl pyrophosphate; G3P, glycerol-3-phosphate; Glu-6-P, glucose-6-phosphate; GPP, geranyl pyrophosphate; GroPCho, glycerophosphocholine; GroPIns, glycerophosphoinositol; HMG-CoA, 3-hydroxy-3-methylglutaryl-Coenzyme A; HMGR, 3-hydroxy-3-methylglutaryl-Coenzyme A reductase; Ins, inositol; Ins-3-P, inositol-3-phosphate; IPC, inositol phosphorylceramide; IPP, isopentenyl pyrophosphate; LCB, long chain base; LCFA, long chain fatty acid; LD, lipid droplets; LPA, lyso-phosphatidic acid; MCFA, medium chain fatty acid; Mevalonate-5-P, mevalonate-5-phosphate; MG, monoacylglycerol; M(IP)2C, mannose-di-inositolphosphoryl ceramide; MIPC, mannose-inositolphosphoryl ceramide; Osh proteins, oxysterol-binding proteins; PA, phosphatidic acid; PC, phosphatidylcholine; PDRE, pleiotropic drug response element; PE, phosphatidylethanolamine; PI, phosphatidylinositol; PI-4-P, phosphatidylinositol-4-phosphate; PG, phosphatidylglycerol; PGP, phosphatidylglycerol-phosphate; PHCer, phytoceramide; PHS, phytosphingosine; PL, phospholipids; PRY proteins, pathogen-related yeast proteins; PS, phosphatidylserine; SE, steryl ester(s); SL, sphingolipids; SPT, serine palmitoyltransferase complex; SQ, squalene; SRE, sterol regulatory element; TG, triacylglycerol(s); TORC1/2, target of rapamycin complex 1/2; UASINO, inositol-responsive upstream activating sequence element; UPR, unfolded protein response; VLCFA, very long chain fatty acid.

Abstract

During the last decades, lipids have gained much attention due to their involvement in health and disease. Lipids are required for the formation of membranes and contribute to many different processes such as cell signaling, energy supply and cell death. Various organelles such as the endoplasmic reticulum, mitochondria, peroxisomes and lipid droplets are involved in lipid metabolism. The yeast Saccharomyces cerevisiae has become a reliable model organism to study biochemistry, molecular and cell biology of lipids. The availability of mutants bearing defects in lipid metabolic pathways and the ease of manipulation by culture conditions facilitated these investigations. Here, we summarize the current knowledge about lipid metabolism in yeast. We grouped this large topic into three sections dealing with (i) fatty acids; (ii) membrane lipids; and (iii) storage lipids. Fatty acids serve as building blocks for the synthesis of membrane lipids (phospholipids, sphingolipids) and storage lipids (triacylglycerols, steryl esters). Phospholipids, sterols and sphingolipids are essential components of cellular membranes. Recent investigations addressing lipid synthesis, degradation and storage as well as regulatory aspects are presented. The role of enzymes governing important steps of the different lipid metabolic pathways is described. Finally, the link between lipid metabolic and dynamic processes is discussed.

Introduction

Lipids are defined as organic substances which are soluble in nonpolar organic solvents, but not in water. They are rather small biomolecules which vary in their physical properties from highly hydrophobic to amphiphilic. Based on their structure and function, lipids are categorized into eight classes which are fatty acids, glycerolipids, glycerophospholipids, sterols and sterol derivatives, sphingolipids, prenol lipids, glycolipids and polyketides (Fahy et al., 2008; 2011). They are constituents of biological membranes or stored in distinct organelles and serve different functions, i.e., as energy source, structural elements, signaling molecules or as mediators of membrane fusion and apoptosis (Escribá et al., 2008; Rego et al., 2013). Lipids are important components of the cell envelope but also characteristic constituents of intracellular organelles (Van Meer et al., 2008). Major lipid synthesizing organelles are the endoplasmic reticulum (ER), the Golgi apparatus and mitochondria. Interestingly, some lipids are present in these organelles just at minor amounts (Fagone & Jackowski, 2009; Osman et al., 2010; Tamura et al., 2012). Therefore, a lipid transport system must exist to translocate lipids from their site of synthesis to their final destination (Achleitner et al., 1999; Schnabl et al., 2005; Peretti et al., 2008).

Due to the very well conserved mechanisms between all eukaryotes and due to other advantages, *Saccharomyces cerevisiae* has evolved as well-established lipid research model which has led to many new insights in this field. The construction of yeast mutant strains deficient in certain steps of lipid metabolism turned out to be a most useful instrument to study lipid biosynthesis, degradation and storage (Santos & Riezman, 2012). Yeast cell metabolism fulfills cellular lipid requirements by different pathways including *de novo* synthesis, uptake of external lipids and turnover of lipids. An excess of cellular lipids can be harmful for the cell and may lead to lipotoxicity (Garbarino et al., 2009; Eisenberg & Büttner, 2013). To overcome this unwanted effect lipids are stored in specialized organelles, the so called lipid droplets (LD). Upon requirement, stored lipids can be mobilized for energy production or synthesis of complex lipid (Czabany et al., 2007; Rajakumari et al., 2008).

In this minireview we describe synthesis, turnover and some regulatory aspects of lipids in *S. cerevisiae* at a glance. We have categorized the lipids into three groups depending on their function. First, we describe the role of fatty acids as basic building blocks for complex lipids; second, we discuss membrane lipids including phospholipids, sterols and sphingolipids; and finally we give a brief overview of storage lipids.

The basic modules: Fatty acids

Basic elements of complex lipids are fatty acids (FA). They can be incorporated into phospholipids and sphingolipids or serve as an energy reservoir in triacylglycerols (TG) and steryl esters (SE) stored in lipid droplets (LD). FA can also function as transcriptional regulators and signaling molecules, and can be involved in posttranslational modification of proteins. Free fatty acids (FFA) are carboxylic acids with hydrocarbon tails varying in chain length and degree of (un)saturation. These variations lead to the large variety of FA molecules and thus to the synthesis of many different lipid species. Yeast cells can get their FA either by (i) *de novo* synthesis; (ii) hydrolysis of complex lipids and delipidation of proteins; and (iii) from external sources by FA uptake (Tehlivets et al., 2007) (Figure 1).

The FA composition of *S. cerevisiae* is rather simple. Major FA are C16:1 (palmitoleic acid) and C18:1 (oleic acid) followed by C16:0 (palmitic acid) and C18:0 (stearic acid); and minor FA are C14:0 (myristic acid) and C26:0 (cerotic acid) (Viljoen et al. 1986; Tuller et al. 1999). The FA composition varies depending on growth conditions and in different subcellular membranes. Under standard growth conditions, about 80 mol % of total FA are monounsaturated (C18:1 ~ 50 %; and C16:1 ~30 %). Among the ~20 % of saturated fatty acid palmitic acid (C16:0) is the most prominent comprising 9 % of total fatty acids (Tuller et al., 1999; Martin et al., 2007). *De novo* synthesis of FA takes place in the cytosol and in mitochondria followed by elongation and desaturation in the ER. The initial step of FA synthesis is catalyzed by acetyl-CoA-carboxylase. For cytosolic FA synthesis, this enzyme is encoded by *ACC1* (Hasslacher et al., 1993), whereas *HFA1* codes for the mitochondrial acetyl-CoA-carboxylase (Hoja et al., 2004). In this reaction, acetyl-CoA derived from citrate degradation or from acetate is carboxylated to form malonyl-CoA which serves as a two carbon building block in the following FA synthesis reactions. Deletion of *ACC1* is lethal even with FA supplementation from the medium, but *Δhfa1* mutants are viable although unable to grow on non-fermentable carbon sources which is typical for strains with defective mitochondrial function (Tehlivets et al., 2007). The synthesis of FA is carried out in the cytosol by the hexameric fatty acid synthase (FAS) complex consisting of 6 Fas1p and 6 Fas2p subunits, each, which exhibit more than one enzymatic activity (Stoops & Wakil, 1978; Leibundgut et al., 2008). Fas1p harbors acetyl transferase, enoyl reductase, dehydratase and malonyl-palmitoyl transferase activities (Wieland et al., 1979; Leibundgut et al., 2008); and Fas2p contains acyl carrier protein, 3-ketoreductase, 3- ketosynthase and phosphopantheteine transferase activities (Mohamed et al., 1988; Fichtlscherer et al., 2000). Supplementation with

long chain FA (LCFA) is necessary to rescue *fas1* and *fas2* null mutants (Schüller et al., 1992).

In contrast, the mitochondrial FA synthase complex consists of six proteins, each harboring only one enzymatic activity. These proteins are: acyl-carrier protein Acp1p, β-ketoacyl-ACP synthase Cem1p, 3-oxoacyl-acyl-carrier-protein reductase Oar1p, 3-hydroxyacyl-thioester dehydratase Htd2p, enoyl-ACP reductase Etr1p and phosphopantetheine protein transferase Ppt2p. Both the cytosolic and the mitochondrial FAS machineries add two carbons from malonyl-CoA to a saturated acyl chain. While the mitochondrial FAS system primarily produces lipoic acid, a chain length up to C18 can be achieved by the cytosolic FA synthase (Hiltunen et al., 2010a). Whether the mitochondrial FAS complex also contributes to medium and long chain FA synthesis is still a matter of dispute, although its synthesis capacity was shown by enzymactic *in vitro* studies (Hiltunen et al., 2010b). Further elongation steps by addition of two carbons from malonyl-CoA, each, to very long chain fatty acids (VLCFA) up to C26 is carried out in the ER by different elongases encoded by *ELO1, ELO2* and *ELO3*. Elo1p functions as main elongase, whereas Elo2p and Elo3p are predominantly responsible for the assembly of VLCFA which are required for sphingolipid synthesis (Toke & Martin, 1996; Oh et al., 1997). Desaturation and hydroxylation of FA also take place in the ER. The introduction of double bonds into the acyl chains and thus their desaturation is performed by the acyl-CoA Δ9-desaturase Ole1p (Stukey et al., 1989; 1990). The expression of Ole1p can be regulated at the transcriptional level by varying growth conditions such as temperature, fatty acid supply, carbon source, or oxygen level (Martin et al., 2007). The transcriptional activation of Ole1p and its mRNA stability requires the proteasomal cleavage of the proteins Spt23p and Mga2p. An *mga2*Δ*spt23*Δ double deletion strain is not viable without supplementation of unsaturated FA (Zhang et al., 1999; Nakagawa et al., 2002; Kandasamy et al., 2004). Recently, it was shown that Sct1p (Gat2p), a glycerol-3-phosphate acyltransferase catalyzing the production of lyso-phosphatidic acid, competes with Ole1p for saturated FA. Deletion of *SCT1* increased desaturation of FA, and overexpression led to enhanced lyso-phosphatidic acid levels and decreased synthesis of unsaturated FA (De Smet et al., 2012). Hydroxylated FA are also found in yeast, predominantly as components of sphingolipids. The hydroxylation of C26 in ceramides is catalyzed by Scs7p, and in sphinganine by Sur2p (Haak et al., 1997).

Besides *de novo* synthesis, yeast cells can also take up FA from the environment either by diffusion or by transporters. Blocked *de novo* synthesis of FA can be completely rescued by the uptake of exogenous FA. The uptake of FFA in combination with their activation with

coenzyme A is performed by the acyl-CoA synthases Fat1p, Faa1p, Faa2p, Faa3p and Faa4p which are localized to the ER, LD, the plasma membrane and peroxisomes (Black & DiRusso, 2007). Internalized and activated FA are then rapidly used for the synthesis of complex lipids, stored in lipid droplets in form of TG and SE, or degraded by β-oxidation in peroxisomes. For the latter process, FA have to be imported into peroxisomes. Long chain fatty acids (LCFA) are translocated by the ABC transporter complex Pxa1p-Pxa2p (Van Roermund et al., 2012), whereas medium chain fatty acids (MCFA) are transported with the aid of Ant1p and Pex11p (Van Roermund et al., 2000; 2001). Activation of LCFA occurs in the cytosol, whereas MCFA are activated after import into peroxisomes by Faa2p. The initial step of FA degradation is the oxidation of acyl-CoA to trans-2-enoyl-CoA catalyzed by the acyl-CoA oxidase Fox1p (Pox1p). The toxic byproduct of this reaction, hydrogen peroxide, is degraded by the peroxisomal catalase Cta1p. Trans-2-enoyl-CoA is further converted to 3-ketoacyl-CoA by Fox2p (Mfe2p) with 3R-hydroxyacyl-CoA as intermediate. The thiolase Fox3p (Pot1p) catalyzes the final step of the β-oxidation where 3-ketoacyl-CoA is cleaved to acetyl-CoA and a C2-reduced acyl-CoA (Hiltunen et al., 2003; Poirier et al., 2006).

The membrane lipids: phospholipids, sterols and sphingolipids

Amphipathic molecules are best suited as components of biological membranes. Phospholipids (PL), also named glycerophospholipids, have such an amphipathic character due to their structure. They consist of a diacylglycerol (DG) as hydrophobic moiety and different polar head groups at the hydrophilic side. DG consists of a glycerol backbone which is esterified in the *sn*-1 and *sn*-2 positions with FA. The head group of the PL is linked to the *sn*-3 position. The diversity of PL molecules is due to combinations of possible FA in the DG moiety. In general, the FA at the *sn*-1 position is mostly saturated, and the FA in the *sn*-2 position unsaturated. Polar head groups determine the classification and the physical properties of the PL (Daum et al., 1998).

Major PL in total cell extracts from *S. cerevisiae* are phosphatidylcholine (PC), phosphatidylethanolamine (PE), phosphatidylinositol (PI) and phosphatidylserine (PS) (Table 1) However, the PL profile of different organelles varies (Zinser et al. 1991; Horvath et al. 2011). Moreover, the carbon source used for yeast cultivation affects the PL composition (Tuller et al., 1999). In an aqueous environment, PL form bilayers with the hydrophilic portions facing the environment and the hydrophobic FA forming the core of the membrane.

In cells, membrane forming PL contribute to the formation of organelles (Simons & Sampaio, 2011) whose lipid composition varies. As examples, the plasma membrane is enriched in PS, whereas cardiolipin (CL) and phosphatidylglycerol (PG) are predominantly found in mitochondria (Zinser et al., 1991). Besides PL, sphingolipids (SL) and sterols also contribute to the membrane architecture. SL are especially found in the plasma membrane, but also in other organelles at lower amounts (Van der Rest et al., 1995). Basic element of SL is a ceramide backbone which consists of a sphingoid long-chain base (LCB) linked via an amide bond to a FA. Inositol as a polar head group completes the structure of a SL molecule. Phytosphingosine (PHS) and dihydrosphingosine (DHS) are the two possible LCB in yeast. The chain length of DHS (16-20 carbons) and PHS (18-20 carbons) varies. In SL from *S. cerevisiae* the attached FA is predominantly a hydroxylated or non-hydroxylated cerotic acid (C26:0) (Dickson et al., 2006; Dickson, 2008). Another class of membrane lipids are the sterols. These components are non-polar lipids which are protected by SL head groups within the membrane. The major sterol in *S. cerevisiae* is ergosterol (Erg) which is, similar to SL, primarily embedded in the plasma membrane where it contributes to membrane integrity. Ergosterol is the final product of the complex sterol biosynthetic pathway. Precursor sterols are found only at low amounts in the yeast cell (Henneberry & Sturley, 2005).

Phospholipids

As shown in Figure 2, phosphatidic acid (PA) serves as a central metabolite in the *de novo* synthesis of PL. Its precursor, lyso-PA (LPA), is generated from glycerol-3-phosphate (G3P) catalyzed by G3P- acyltransferases encoded by *SCT1* (*GAT2*) and *GPT2* (*GAT1*) (Athenstaedt & Daum, 1997). LPA is further converted to PA by the LPA acyltransferases Slc1p, Slc4p (Jain et al., 2007; Benghezal et al., 2007) and Loa1p (Ayciriex et al., 2012). Sct1p and Gpt2p can also use dihydroxyacetone phosphate (DHAP) as a substrate forming acyl-DHAP as a product (Zheng & Zou, 2001) which is further converted to LPA by a reductase encoded by *AYR1* (Athenstaedt & Daum, 2000). Gene products of *SLC4* and *SCT1* are localized to the ER, whereas Gpt2p, Slc1p, Loa1p and Ayr1p are located to the ER and LD.

PA can contribute to two major lipid biosynthetic pathways. First, it can be cleaved by the phosphatidate phosphatases Pah1p, Dpp1p, Lpp1p and App1p to DG to enter the lipid storage pathway (Toke et al., 1998a; Toke et al. 1998b; Han et al., 2006; Chae et al., 2012).

Second, it contributes to PL synthesis via conversion to cytidine diphosphate-diacylglycerol (CDP-DG) catalyzed by the ER localized CDP-DG synthase Cds1p (Shen et al., 1996) or by the mitochondrial CDP-DG synthase Tam41p (Tamura et al., 2013) with cytidine triphosphate (CTP) as CDP donor. CDP-DG is the precursor molecule for all major phospholipids and can be combined with serine, inositol or G3P. Three different synthases use CDP-DG for the formation of PI, PS and PGP, respectively, namely (i) phosphatidylinositol synthase Pis1p, (ii) phosphatidylserine synthase Cho1p and (iii) phosphatidylglycerolphosphate (PGP) synthase Pgs1p (Zhao et al., 1998).

Inositol is either derived from glucose-6-phosphate catalyzed by the inositol-3-phosphate synthase Ino1p (Donahue & Henry, 1981; Dean-Johnson & Henry, 1989) and the inositol-3-phosphate phosphatase Inm1p (Lopez et al., 1999; Murray & Greenberg, 2000); or it is incorporated from the environment with the aid of the inositol permeases Itr1p and Itr2p (Nikawa et al., 1991). Pis1p catalyzes the synthesis of PI from CDP-DG and inositol (Nikawa & Yamashita, 1984).

Pgs1p uses CDP-DG in combination with G3P to synthesize PGP (Chang et al., 1998a). The phosphate group is removed from the molecule by the PGP phosphatase Gep4p resulting in PG (Osman et al., 2010) which can be further converted to CL by the cardiolipin synthase Crd1p (Tuller et al., 1998; Chang et al., 1998b). The structure of CL is unique among the PL because it contains two DG moieties. The acyltransferase Taz1p is responsible for the trimming of the final acyl chain composition of CL (Testet et al., 2005).

The PS synthase Cho1p uses CDP-DG and serine for the formation of PS (Letts et al., 1983). PS can be decarboxylated to PE by the PS-decarboxylases Psd1p localized to the inner mitochondrial membrane, or by the Golgi/vacuole associated Psd2p (Voelker, 1997). PC evolves as the last PL within the aminoglycerophospholipid biosynthetic pathway from PE by three methylation reactions catalyzed by Cho2p and Opi3p (Kodaki & Yamashita, 1987; Kodaki & Yamashita, 1989). Another route for the synthesis of PE and PC is the so-called Kennedy pathway, also known as CDP-ethanolamine/choline pathway which uses exogenous ethanolamine (Etn) and choline (Cho) as substrate for PE and PC synthesis (Bürgermeister et al., 2004). Both substrates are transported into the cell by an *HNM1*-encoded ethanolamine/choline transporter (Nikawa et al., 1990) and phosphorylated in the cytosol by respective kinases (Eki1p, ethanolamine kinase; and Cki1p, choline kinase) (Hosaka et al., 1989; Kim et al., 1998; Kim et al., 1999). Etn-phosphate can also be set free from sphingolipids by the dihydrosphingosine-1-P lyase Dpl1p (Kihara, 2013). Phosphorylated Etn and Cho are activated with CTP by cytidylyltransferases (Ect1p, ethanolamine phosphate

cytidylyltransferase; and Pct1p, choline phosphate cytidylyltransferase) to CDP-Etn and CDP-Cho, respectively (Min-Seok et al., 1996; Tsukagoshi et al., 1987; Carman & Han, 2011). Finally, a reaction with DG catalyzed by the phosphotransferases Ept1p (ethanolamine phosphotransferase) and Cpt1p (choline phosphotransferase) leads to PE and PC (Hjelmstad & Bell, 1987, 1988). DG used in the Kennedy pathway is derived from degradation of PA. This reaction is reversible, and PA can be re-synthesized from DG by the DG kinase Dgk1p (Han et al., 2008a). The Kennedy pathway of PL synthesis is highly active and essential when enzymes of the CDP-DG pathway are blocked. As an example, double deletions of *CHO2* and *OPI3* in yeast lead to cell death if choline is not provided from the growth medium (Tanaka et al., 2008).

Turnover of PL is provided by phospholipases and lipid phosphatases; and remodeling of acyl chains within the PL molecules is achieved by acyltransferases and transacylases. Some of these enzymes are specific for certain PL species, whereas others catalyze the degradation of PL in an unspecific way (Henry et al., 2012). Phospholipases are categorized in the four classes A, B, C and D. Representatives of these classes are the PC specific phospholipases Nte1p, Plb1p and Spo14p. The phospholipase Plb1p also cleaves PE (Lee et al., 1994). Cld1p acts a CL specific phospholipase A (Beranek et al., 2009), and Pgc1p as a PG specific phospholipase (Šimočková et al., 2008). Non-specific phospholipases are encoded by *PLB2* and *PLB3* (Merkel et al., 1999). Phospholipases B (Plb1p, Plb2p and Plb3) produce glycerophosphocholine (GroPCho) and glycerophosphoinositol (GroPIns) through degradation of PC and PI. These products are excreted into the growth medium, but can be re-absorbed by the cell via the GroPCho/GroPIns transporter Git1p (Patton-Vogt & Henry, 1998; Patton-Vogt, 2007). Phospholipases C (Plc1p and Pgc1p) form DG, inositol and G3P which can serve again as precursors for PL synthesis (Flick & Thorner, 1993; Šimočková et al., 2008). *SPO14* encodes a phospholipase D which catalyzes degradation of PC leading to PA and choline (Rudge & Engebrecht, 1999).

Besides phospholipases, phosphatases contribute to PL degradation by dephosphorylation of different substrates. These enzymes, e.g. Ymr1p, Fig4p, Inp51p, Inp54p and Sac1p, are either specific for a certain polyphosphoinositide, or they use any polyphosphoinositide as a substrate such as phosphatases encoded by *INP52* and *INP53* (Henry et al., 2012). The lipid phosphate phosphatases Dpp1p and Lpp1p are also rather unspecific but do not use polyphosphoinositides as substrates. They catalyze dephosphorylation of DG pyrophosphate, LPA and PA, but also of sphingoid base and isoprenoid phosphates (Wu et al., 1996; Toke et al., 1998a; Toke et al., 1998b). PA is also

substrate of the specific PA phosphatase Pah1p which is involved in the *de novo* synthesis of PL and TG (Han et al., 2007). Recently, a novel PA phosphatase encoded by *APP1* has been identified (Chae et al., 2012). In contrast, Phm8p cleaves LPA to monoacylglycerol and phosphate (Reddy et al., 2008). However, PL are also modified by remodeling of their acyl chains. Acyltransferases like Psi1p and Taz1p, and the acyl-CoA binding protein Acb1p catalyze changes of the acyl chain composition of PL (Le Guédard et al., 2009; Rijken et al., 2009). Additionally, triacylglycerol lipases encoded by *TGL3*, *TGL4* and *TGL5* were also identified as acyltransferases involved in PL acyl chain remodeling (Rajakumari & Daum, 2010a, 2010b).

PL synthesis can be modulated by regulation of enzyme expression or by regulation of enzyme catalytic activities. Gene expression is influenced by various growth conditions such as temperature, growth medium, pH, and nutrients. Many *cis*- and *trans*-acting elements are responsible for the regulation of gene expression. The inositol-responsive *cis*-acting element (UAS_{INO}) and the trans-acting factors Ino2p, Ino4p and Opi1p are prominent examples to regulate different enzymes of the CDP-DG and the Kennedy pathway as well as the transporters Itr1p and Hnm1p (Henry et al., 2012). The repressor Opi1p competes with the UAS_{INO} for the binding of Ino2p. When Opi1p binds Ino2p, the expression of Ino1p is repressed and the synthesis of inositol is blocked (Bailis et al., 1992; Lai & McGraw, 1994). The activity of Opi1p as a repressor is regulated by its cellular location. Under inositol rich growth conditions, Opi1p is found in the nucleus where it represses *INO1* and other UAS_{INO} genes. Under inositol starvation Opi1p is localized to the ER/nuclear membrane which allows derepression of the UAS_{INO} genes (Loewen et al., 2004; Wilson et al., 2011). The integral membrane protein Scs2p and PA are necessary for the association of Opi1p to the nuclear/ER membrane due to the lack of a trans-membrane domain in the protein. Furthermore, the interaction of the Opi1p-Scs2p aggregate with the Yet1p-Yet3p complex is necessary to maintain Opi1p at the ER. Absence of Scs2p or Yet3p leads to nuclear localization and to an increased repressor activity of Opi1p (Loewen et al., 2004; Wilson et al., 2011).

PA levels can be regulated by several enzymes, but the PA phosphatase Pah1p and the DG kinase Dgk1p are the most important enzymes with that respect. Overexpression of Pah1p leads to PA depletion and thus to increased repression of Ino1p by Opi1p in the nucleus. In contrast, deletion of *PAH1* stimulates PL synthesis (Han et al., 2006). The level of PA can be enhanced by overexpression of Dgk1p which leads to nuclear/ER membrane localization of the repressor Opi1p and to de-repression of UAS_{INO} controlled gene expression thus

increasing PL synthesis (Han et al., 2008b; Fakas et al., 2011). Dgk1p expression itself is regulated by the essential transcription factor Reb1p which also activates the expression of other lipid metabolic genes (Qiu et al., 2013). Besides this enzymatic regulation, the presence of inositol or zinc in the growth medium as well as the growth phase affects the gene expression under the control of UAS_{INO}. Zinc activates the expression of these genes, whereas inositol has the opposite effect. In the exponential growth phase, the expression of UAS_{INO} controlled genes is induced when inositol is absent, but the expression is also repressed even when inositol is absent as cells enter the stationary growth phase (Griac & Henry, 1999; Henry et al., 2012).

Regulation of PL synthesis can also occur via phosphorylation of enzymes at a serine or threonine residue by protein kinases such as protein kinase A and C, casein kinase II and cyclin-dependent kinase (Choi et al., 2011). The repressor Opi1p, the PS synthase Cho1p, the PA phosphatase Pah1p, the choline kinase Cki1p, and the CTP synthases encoded by *URA7* and *URA8* are regulated by phosphorylation (Carman & Han, 2011). As an example, the Pah1p activity is reduced after phosphorylation of the enzyme by the Pho85p-Pho80p protein kinase- cyclin complex, by the cyclin-dependent kinase 1 (Cdk1p = Cdc28p) or by the protein kinase A (Choi et al., 2012; Su et al., 2012).

Sterols

While various cell compartments are involved in PL synthesis and degradation, the synthesis of another class of membrane lipids, the sterols, mainly takes place in the ER. Newly synthesized sterols formed in this organelle have to be transported to their final destination. In fungi, the major sterol is ergosterol (Erg) which is the end product of the yeast sterol biosynthetic pathway and the equivalent of mammalian cholesterol (Henneberry & Sturley, 2005; Nielsen 2009). The sterol concentration in the ER is low but increased in organelles of the secretory route with the highest concentration in the plasma membrane (Zinser et al., 1993).

Sterols are necessary for maintaining membrane integrity and essential for the viability of eukaryotic cells. Ergosterol consists of a four-ring structure, an acyl side chain and a hydrophilic hydroxyl group which facilitates insertion into membranes. The structure of ergosterol differs from cholesterol by two additional double bonds between C7 and C8 in the

ring and between C22 and C23 in the side chain, respectively, and an additional methyl group at C24 of the side chain (Sturley, 2000). Ergosterol is synthesized through a most complicated pathway involving almost 30 enzymes known as Erg proteins (Figure 3). Yeast sterol biosynthesis starts with condensation of two acetyl-CoA molecules to gain acetoacetyl-CoA catalyzed by Erg10p (Hiser et al., 1994). Condensation of a third acetyl-CoA to acetoacetyl-CoA catalyzed by Erg13p yields 3-hydroxy-3-methylglutaryl-CoA (HMG-CoA) (Miziorko, 2011) which is further reduced to mevalonate by the HMG-CoA reductases Hmg1p and Hmg2p (Basson et al., 1986). This step is a major metabolic check point due to feedback inhibition of the reductases by sterol intermediates (Bard & Downing, 1981). In the next reaction, mevalonate is phosphorylated by the mevalonate kinase Erg12p (Oulmouden & Karst, 1990). A further phosphorylation catalyzed by the Erg8p phosphomevalonate kinase leads to mevalonate-5-pyrophosphate (Tsay & Robinson, 1991). Isopentenyl pyrophosphate (IPP) is built in the next step through decarboxylation by the mevalonate pyrophosphate decarboxylase Erg19p (Berges et al., 1997). The IPP isomerase encoded by *IDI1* converts IPP into dimethylallyl pyrophosphate (DPP) (Anderson et al., 1989a) which condensates in the next step with another IPP molecule to geranyl pyrophosphate (GPP). If an additional IPP molecule is added, farnesyl pyrophosphate (FPP) is formed. Both reactions are catalyzed by Erg20p, the geranyl/farnesyl pyrophosphate synthase (Anderson et al., 1989b). Then, squalene synthase encoded by *ERG9* forms squalene (SQ) from two molecules FPP (Jennings et al., 1991). In an oxygen dependent reaction, epoxidation of SQ catalyzed by the SQ epoxidase Erg1p leads to squalene epoxide (Jandrositz et al., 1991) which is then metabolized to lanosterol by the lanosterol synthase Erg7p (Corey et al., 1994). Conversion of lanosterol to zymosterol is achieved by various demethylation, reduction and desaturation reactions catalyzed by gene products of *ERG11* and *ERG24-ERG28.* The sterol C-24 methyltransferase Erg6p forms fecosterol from zymosterol, the isomerase Erg2p converts fecosterol to episterol which is then further desaturated and reduced to the final product ergosterol. These last steps are accomplished by the enzymes Erg3p, Erg5p and Erg4p, respectively (Kristan & Rižner, 2012).

Balance and regulation of sterol synthesis are very important to avoid accumulation of free sterols which may become toxic for the cell. Regulation of sterol levels is mainly achieved by feedback mechanisms at transcriptional, translational and post-translational stages (Espenshade & Hughes, 2007). As examples, an excess of sterol induces proteasomal degradation of the HMG-CoA reductase (HMGR) which leads to reduced sterol synthesis. Targeting of HMGR to the proteasome is accomplished by the ER-associated protein

degradation (ERAD) pathway. Recognition of HMGR by the ERAD component Hrd1p requires the chaperones Nsg1p and Nsg2p (homologs of mammalian INSIG proteins) and specific sterol signals. Hrd1p, an ubiquitin ligase complex localized in the ER membrane, is responsible for the release of HMGR from the ER to the cytoplasm where it is degraded by the proteasome (Burg & Espenshade, 2011). Recently, another ERAD factor was identified as an important regulator of sterol homeostasis. This ubiquitin ligase encoded by *DOA10* is controlled by intracellular lanosterol levels and necessary for degradation of the squalene epoxidase Erg1p (Foresti et al., 2013). Since sterol biosynthesis requires oxygen, a transcriptional regulation of genes involved in this pathway is induced under oxygen reduced conditions when sterol levels are low. The transcription factors Ecm22p and Upc2p are such regulators which activate the transcription of sterol synthesizing enzymes by binding to the sterol regulatory element (SRE) within the promoter region (Davies & Rine, 2006). Under oxygen starvation, Upc2p also induces the expression of *AUS1* and *PDR11* which code for ATP binding cassette transporters responsible for sterol uptake from the environment (Zavrel et al., 2013).

Although multiple regulatory mechanisms for sterol homeostasis exist, yeast cells may produce sterols in excess under aerobic conditions. To avoid toxic effects, yeast cells are either able to store sterols in the form of steryl esters in lipid droplets (see below) or secrete them as sterol acetates into the medium. Besides detoxification, sterol acetylation also contributes to the elimination of damaged lipids. Sterol acetylation is catalyzed by the alcohol acetyltransferase Atf2p; and deacetylation of sterol acetates is accomplished by the sterol deacetylase Say1p (Tiwari et al., 2007). Both enzymes are localized to ER membranes. For secretion into the environment, acetylated sterols have to be transported to the plasma membrane. Pathogen-related yeast (PRY) proteins which were recently identified bind sterol acetates, retain them soluble and facilitate their secretion (Choudhary & Schneiter, 2012).

Sterol transport between organelles as well as the release into the medium is mostly ATP-dependent either in a vesicular or non-vesicular manner (Jacquier & Schneiter, 2012). Non-selective transport of newly synthesized lipids from the ER to the PM appears to occur by vesicle flux through the secretory pathway. It has been shown that ergosterol transport from the ER to the PM is still maintained in a *sec18* mutant where vesicular transport is inactive. This result suggested that other, non-vesicular transport routes are available (Sullivan et al., 2006). Due to the insolubility of sterols in aqueous solution, lipid transport was assumed to occur through organelle membrane contact or lipid binding/transfer proteins.

Such soluble proteins transiently "solubilize" bound lipids during the transport process. In yeast seven proteins harboring such a function have been identified. They are homologs of the mammalian oxysterol-binding proteins and were named Osh proteins (Osh1-Osh7) (Schulz & Prinz, 2007). Lack of all seven Osh proteins leads to cell death accompanied by increased intracellular ergosterol levels. Most Osh proteins are localized to membrane contact sites (Beh et al., 2001). Recently, participation of Osh proteins in sphingolipid (SL) homeostasis was also suggested through studies with Osh4p (Kes1p) (LeBlanc et al., 2013). This protein activates the phosphatidylinositol-4-phosphate (PI-4-P) phosphatase Sac1p, which produces a pool of PI as a precursor for the synthesis of SL by dephosphorylation of PI-4-P (Brice et al., 2009). Deletion of *OSH4* altered SL levels dramatically which prevented a correct incorporation of the membrane raft associated plasma membrane ATPase Pma1p into the plasma membrane. Pma1p is normally transported from the Golgi to the PM induced by SL signaling (LeBlanc et al., 2013).

Another protein which is involved in sterol transport and exogenous sterol uptake is encoded by *ARV1*. Deletion of this gene leads to increased sterol levels in the ER and in vacuolar membranes and to decreased sterol incorporation into the plasma membrane (Tinkelenberg et al., 2000). Furthermore, involvement of Arv1p in SL homeostasis has been reported (Swain et al., 2002); and most recently, Ruggles et al. (2013) identified Arv1p as protective factor against lipotoxicity due to modulation of fatty acid metabolism (Ruggles et al., 2013).

Defects of the human sterol transporters hNpc1p and hNpc2p cause cholesterol accumulation in lysosomes and are involved in the neurodegenerative Niemann-Pick type c disease (Liscum, 2000; Munkacsi et al., 2007). In *S. cerevisiae,* Ncr1p and Npc2p were identified as homologs of the human proteins. Both enzymes functionally complement the loss of the respective human orthologs. However, deletion of *NCR1* or *NPC2* neither showed severe growth defects nor effects on the sterol distribution of the cells (Malathi et al., 2004; Zhang et al., 2004; Berger et al., 2005).

Sphingolipids

Sterol and SL homeostasis comprises a complex interfering network (Swain et al., 2002). Concerted regulation may arise from the same site of sterol and SL synthesis. As for

sterols, the ER is also the major site of SL synthesis. Consequently, SL have to be transported to other organelles, especially to the plasma membrane where the highest SL concentration is found.

The basic unit of yeast SL contains a long chain base (LCB) (sphingoid backbone); a saturated fatty acid which is amide-linked to the LCB to form a ceramide (Cer); and an inositol phosphate which is attached to the Cer at C1 (Schneiter, 1999). *De novo* synthesis of SL (Figure 4) starts with condensation of a serine and a fatty acyl-CoA, mostly palmitoyl-CoA or stearyl-CoA, catalyzed by the serine palmitoyltransferase (SPT) complex. SPT exists of three enzymes encoded by *LCB1*, *LCB2* and *TSC3* (Nagiec et al., 1994; Gable et al., 2000). The product of this reaction, 3-ketodihydrosphingosine (ketosphinganine), is further converted to dihydrosphingosine (DHS) by the 3-ketosphinganine reductase Tsc10p (Beeler et al., 1998). DHS is the first LCB which can be hydroxylated by Sur2p to another LCB, namely phytosphingosine (PHS). Both LCBs can enter two possible routes. The first option includes phosphorylation catalyzed by Lcb4p and Lcb5p and further degradation by the DHS phosphate lyase Dpl1p to hexadecanal and ethanolamine-1-phosphate which is recycled for PL synthesis. This phosphorylation step is reversible, and the reverse reaction is catalyzed by Lcb3p (Ysr2p) and Ysr3p (Dickson & Lester, 2002). The second route leads to complex SL. The ceramide synthase complex, comprising Lag1p, Lac1p and Lip1p, catalyzes acyl-CoA dependent acetylation of the LCB with VLCFA to yield dihydroceramide (DHCer) and phytoceramide (PHCer) (Schorling et al., 2001; Vallee & Riezman, 2005). Palmitoyl-CoA serves as precursor for the synthesis of VLCFA in the ER. The elongation of the FA is accomplished by enzymes encoded by the three genes *ELO2*, *ELO3* and *TSC13* (Oh et al., 1997; Kohlwein et al., 2001); and the protein Acb1p serves as an acyl-CoA transporter to the elongation machinery (Gaigg et al., 2001). After incorporation into DHCer or PHCer, the VLCFA can be modified by α-hydroxylation catalyzed by Scs7p (Haak et al., 1997). Recently, it was demonstrated that the two acyltransferases Dga1p and Lro1p, which were originally identified as TG synthases, are also responsible for O-acetylation of Cer. This process may serve as a storage or detoxification pathway of Cer (Voynova et al., 2012). Minor ceramide synthase activity was also assigned to the alkaline dihydroceramidases Ydc1p and Ypc1p, especially in the absence of the ceramide synthase complex. Under normal conditions, however, Ydc1p and Ypc1p catalyze hydrolysis of DHCer/PHCer to FFA and DHS/PHS (Mao et al., 2000a; 2000b).

Ceramides are simple SL molecules without head groups. The first more complex yeast SL in the biosynthetic pathway is formed by addition of an inositol phosphate group to ceramide. This reaction is accomplished by the inositolphosphoryl ceramide (IPC) synthase Aur1p yielding IPC (Nagiec et al., 1997). The activity of Aur1p is regulated by Kei1p, an essential protein which forms a complex with Aur1p. Absence of Kei1p results in reduced IPC synthesis and mis-localization of Aur1p from the Golgi apparatus to vacuoles (Sato et al., 2009). It was shown that deletion of the *SAC1* gene, which produces PI by dephosphorylation of PI-4-P, limits the availability of PI for the synthesis of IPC by Aur1p accompanied by decreased formation of complex SL and increased amounts of LCB. SL synthesis was not completely blocked indicating that another source of PI is used for this synthesis pathway (Brice et al., 2009). Furthermore, reduction of IPC synthesis to 50 % occurs during inositol starvation (Jesch et at., 2010), while inositol supplementation increases the level of complex SL and reduces ceramide levels (Alvarez-Vasquez et al., 2005). The next component in the pathway, mannose-inositolphosphoryl ceramide (MIPC), is formed from IPC by mannosylation with the aid of the Csg1p, Csg2p and Csh1p complex (Uemura et al., 2003). If a second inositol phosphate group is attached to MIPC by Ipt1p, mannose-diinositolphosphoryl ceramide ($M(IP)_2C$) is synthesized (Dickson et al., 1997).

Catabolism of inositol containing SL is achieved by inositolphosphosphingolipid phospholipase C encoded by *ISC1*. This enzyme is activated by anionic PL (PS, CL and PG) and hydrolyzes the head groups of the complex SL to yield the ceramides DHCer and PHCer (Sawai et al., 2000). These ceramides are further cleaved to FFA and LCB (DHS and PHS) by Ydc1p and Ypc1p. Phosphorylation of LCB catalyzed by Lcb4p and Lcb5p yields phosphorylated intermediates (DHS-P and PHS-P) which are further degraded by the DHS phosphate lyase Dpl1p to hexadecanal and ethanolamine-1-phosphate as already mentioned above. The resulting ethanolamine-1-phosphate enters the Kennedy pathway as a precursor for the synthesis of PE (Schuiki et al., 2010). Thus, metabolic routes of the major lipid classes are linked to each other, although details of this complex, wide spreading network still need to be elucidated.

The biosynthesis of yeast SL has been investigated intensively in the past, but little is known about the regulation of SL metabolism and homeostasis. One mechanism of regulation, which connects the protein quality control and SL biosynthesis has been reported recently (Han et al., 2010). The ER proteins Orm1p and Orm2p bind to the SPT and inhibit its activity. Double deletion of *ORM1* and *ORM2* leads to increased LCB levels. Furthermore,

the unfolded protein response (UPR) in the ER is constitutively activated, the stress resistance is decreased and the ER-to-Golgi transport is compromised. Orm proteins can be inactivated by phosphorylation. This reaction is catalyzed by the protein kinase Ypk1p which is induced when SL synthesis is impaired and should be restored, or under heat stress conditions (Roelants et al., 2011). As a response to low SL levels, the plasma membrane proteins Slm1p and Slm2p stimulate the target of rapamycin complex 2 (TORC2) which further activates the protein kinase Ypk1p (Niles & Powers, 2012). TORC1 controls the phosphorylation of Orm proteins as response to nutrients. Nitrogen starvation inhibits TORC1 which leads to increased Orm protein phosphorylation by the protein kinase Npr1p, while excess of nutrients results in the opposite effect (Shimobayashi et al., 2013).

Another event regulating SL synthesis is phosphorylation of Lcb4p. The interaction of the cyclin dependent kinase Pho85p with its two cyclin partners encoded by *PCL1* and *PCL2* leads to phosphorylation of Lcb4p decreasing the concentration of sphingoid base phosphates (Iwaki et al., 2005). Some SL synthesizing enzymes like Ipt1p, Lcb2p, Sur2p and Lac1p contain a pleiotropic drug response element (PDRE) within their promoter region. Upon stimulation, the transcriptional activators Pdr1p and Pdr3p bind to these elements, induce gene expression and thus SL synthesis (Kolaczkowski et al., 2004).

These findings suggest a coordinated regulation of the plasma membrane lipid composition by transcriptional activation of SL biosynthesis and activity of membrane transporter proteins. As described above, a connection between SL and PL synthesis, sterols and plasma membrane lipid composition has also been shown for Osh4p. It functions as activator of the PI synthesizing enzyme Sac1p. Noteworthy, the produced PI is further used for the synthesis of SL (Alfaro et al., 2011).

Synthesis and storage of non-polar lipids

Yeast cells are able to overcome a possible toxic effect of sterols and free fatty acids (FFA) by converting them into largely inert molecules and storing them in special organelles. Sterols are esterified to steryl esters (SE), and FFA are linked to a glycerol backbone to form triacylglycerols (TG). These non-polar lipids are not suitable as membrane constituents, but serve as energy source and precursors for membrane lipid synthesis. The storage organelles of these lipids are the so-called lipid droplets (LD) (Zweytick et al., 2000a). Biogenesis of LD is still a matter of dispute. Two models, the “lensing model” and the “bicelle formation model”,

suggest that LD bud off from the ER when TG accumulate between the two leaflets of the ER membrane and a critical size has been reached (Walther & Farese, 2009). The "lensing model" describes the formation of the envelope only from the outer leaflet of the ER membrane (Guo et al., 2009), whereas the "bicelle formation model" suggests development of the PL monolayer from both ER membrane leaflets (Ploegh, 2007). Another possibility of LD formation is defined by the "secretory vesicle model" which is based on the evolvement of LD from secretory vesicles which are filled with TG. However, recent evidence is more in favor with the budding models (Guo et al., 2009; Kohlwein et al., 2013).

Mature LD have a diameter of about 300 - 400 nm and are covered by a PL monolayer which contains a small amount of proteins (Tauchi-Sato et al., 2002). This surface monolayer of LD consists mostly of PC, PI and PE. Proteome analysis identified many LD proteins as enzymes of lipid metabolism (Athenstaedt et al., 1999; Grillitsch et al., 2011; Natter et al., 2005). Most LD proteins do not contain transmembrane domains, and many of them appear to be dually localized to LD and to the ER. When TG and SE synthesis is blocked, LD are no longer formed and LD proteins remain in the ER (Sandager et al., 2002; Sorger et al., 2004; Schmidt et al., 2013). The ratio of TG to SE in LD from *S. cerevisiae* is approximately 1:1 (Leber et al., 1994). The core of LD made of TG is surrounded by several shells of SE (Czabany et al., 2008).

As already mentioned above, a central precursor for TG and PL synthesis is PA synthesized from glycerol-3-phosphate (G3P) or dihydroxyacetone phosphate (DHAP) (see Figure 2). If PA is cleaved by the phosphatidate phosphatase Pah1p to diacylglycerol (DG) it becomes the direct precursor for TG synthesis. Dpp1p, Lpp1p and App1p also exhibit minor phosphatidate phosphatase activity (Han et al., 2006; Chae et al., 2012). Other pathways of DG formation are degradation of PL by phospholipases or deacetylation of TG. For the formation of TG, the intermediate DG has to be acetylated at the *sn*-3 position. This step can be accomplished in an acyl-CoA independent or dependent reaction (Oelkers et al., 2000; Sorger & Daum, 2002). The acyl-CoA independent reaction utilizes PL as acyl donor. The gene product of *LRO1* transfers an acyl group mainly from PC and PE to the *sn*-3 position of DG (Oelkers et al., 2000). Dga1p, the other acyltransferase, requires oleoyl-CoA or palmitoyl-CoA as co-substrates (Sorger & Daum, 2002). The two SE synthases Are1p and Are2p are also able to catalyze acyl-CoA dependent TG formation, although only with minor efficiency (Oelkers et al., 2002). Lro1p and the two SE synthases are located to the ER, whereas dual localization of Dga1p to LD and the ER has been reported (Sorger & Daum, 2003). Presence

of all four enzymes in the ER makes this organelle the major site of storage lipid synthesis (Jacquier et al., 2011). Recently, Dga1p and Lro1p were also described to O-acetylate ceramides (Voynova et al., 2012).

SE are formed by reaction of an activated FA, mainly palmitoyl-CoA and oleyl-CoA, with the hydroxyl group at the C3-position of a sterol molecule (see Figure 3). The two enzymes catalyzing this reaction, Are1p and Are2p, share about 50 % sequence homology but differ in their substrate specificities. Both enzymes use ergosterol as a substrate, but Are1p preferentially esterifies sterol intermediates like lanosterol (Yang et al., 1996; Zweytick et al., 2000b). Under standard growth conditions Are2p functions as the major SE synthase, but under anaerobic growth conditions when ergosterol biosynthesis is blocked esterification of ergosterol precursors by Are1p is enhanced (Valachovic et al., 2001). In an *are1*Δ*are2*Δ double mutant SE synthesis is completely inhibited suggesting that the two Are proteins are the only SE synthases in yeast. Interestingly, the double mutation does no influence the growth phenotype, although the total sterol pattern is changed. In such strains, the overall sterol biosynthesis is decreased, but the level of free sterol is increased (Zweytick et al., 2000b). These findings suggest that sterol biosynthesis and SE formation are connected through a regulatory mechanism. Indeed, in the double mutant strain the expression of Erg3p, a sterol synthesizing enzyme, is down-regulated; and the squalene epoxidase Erg1p is destabilized leading to a block in sterol synthesis (Arthington-Skaggs et al., 1996; Sorger et al., 2004). Furthermore, Arv1p has been identified as essential component in the absence of sterol esterification (Tinkelenberg et al., 2000). Deletion of *ARV1* in the *are1*Δ*are2*Δ double mutant strain leads to synthetic lethality, changes in the cellular sterol level and composition, decreased sterol uptake and *de novo* synthesis, and restricted synthesis of complex SL. For biochemical investigations a gene knockdown strain has been recently applied, where the *ARV1* expression was decreased through perturbation of the mRNA (Ruggles et al., 2013).

A quadruple mutant lacking Dga1p, Lro1p, Are1p and Are2p and thus the complete storage lipid formation machinery cannot form non-polar lipids and LD. Nevertheless, this strain is viable and shows only minor alterations in the growth behavior under standard conditions (Sandager et al., 2002). Growth of the quadruple mutant on oleate, however, leads to a lipotoxic effect resulting in growth retardation and changes in the membrane lipid composition (Petschnigg et al., 2009; Connerth et al., 2010). Electron and fluorescence microscopic studies revealed morphological alterations due to lipotoxic stress. In the quadruple mutant, an excess of unsaturated FA is directed to phospholipid synthesis resulting

in enhanced proliferation and enlargement of ER membranes. These data demonstrate that FA uptake is not limited by the cellular requirements; FA are channeled to membrane phospholipid synthesis in the absence of TG synthesis; UPR is not involved in enhanced membrane proliferation in mutants defective in TG synthesis; and FA-induced cell death is not an immediate response to oleic acid exposure, but rather the consequence of induced defects in membrane trafficking.

If required, yeast cells can mobilize TG and SE to provide sterols, FA and DG for the synthesis of membrane lipids or for the production of energy. Degradation of TG is mainly achieved by the TG lipases Tgl3p, Tgl4p and Tgl5p which are located to LD (Athenstaedt & Daum, 2003; 2005) (see Figure 2). In the absence of LD, Tgl3p is retained in the ER without exhibiting lipase activity (Schmidt et al., 2013). Recently, Ayr1p which was originally identified as a 1-acyl DHAP acyltransferase (Athenstaedt & Daum, 2000) was shown to act also as a TG lipase (Ploier et al., 2013). So far, no specific yeast DG lipase has been identified, but Tgl3p was shown to use also DG as substrates, although at low activity (Kurat et al., 2006). Degradation of monoacylglycerols (MG) is accomplished by the MG lipase Yju3p (Heier et al., 2010). An additional TG lipase encoded by *TGL2* and localized to mitochondria has also been identified, but its physiological role remained obscure (Ham et al., 2010).

The gene products of *TGL1*, *YEH1* and *YEH2* were identified as SE hydrolases which cleave SE to sterols and FFA (Müllner et al., 2005; Köffel et al., 2005). Tgl1p and Yeh1p are components of LD, but Yeh2p, the major SE hydrolase under standard conditions, is located to the cell periphery, most likely to the plasma membrane. A *tgl1*Δ*yeh1*Δ*yeh2*Δ triple deletion leads to complete loss of SE degradation suggesting that these genes encode the only SE hydrolases in yeast (Köffel et al., 2005). Under anaerobic conditions, mobilization of SE is accomplished only by Yeh1p while the two other hydrolases are completely inactive (Köffel & Schneiter, 2006).

Non-polar lipids of the yeast have been regarded only as storage molecules for a long time, but recent studies revealed other functions, especially of TG. An involvement of TG in iron, PL and SL metabolism, lipotoxicity and cell cycle progression has been described (Kohlwein, 2010). It has been demonstrated that TG degradation by Tgl4p is activated by cyclin-dependent protein kinase 1 (CDK1) at the checkpoint between the Gap1 phase and the DNA synthesis phase in the cell cycle (Kurat et al., 2009). Deficient lipolysis requires FA supply from *de novo* synthesis and delays the cell cycle. CDK1 is also involved in the down-

regulation of TG synthesis by phosphorylation of Pah1p. Inhibition of Pah1p occurs between the Gap2 phase and the mitosis in the cell cycle (Choi et al., 2011). These findings suggest concerted regulation of TG lipolysis, TG synthesis, PL metabolism and cell growth.

Recently, the LPA acyltransferase Loa1p localized to the ER was also shown to play a regulatory role in LD biogenesis and TG formation (Ayciriex et al., 2012). Deletion of *LOA1* yielded enhanced amounts of LD but at smaller sizes, whereas overexpression showed exactly the opposite effect. Loss of Loa1p reduced the level of oleic acid containing PA, PC, DG and TG species and simultaneously increased the amount of molecular species containing C16 acyl chains in these lipids. Deletion of *LDH1* was also demonstrated to affect the size of LD and lead to accumulation of storage lipids and PL, suggesting a role of of this protein in mobilization of storage lipids from LD (Debelyy et al., 2011). Ldh1p which was identified as LD protein harbors minor TG lipase activity and is involved in TG and PL metabolism. The morphology of LD was also shown to be subject of regulation (Fei et al., 2008). Deletion of the yeast seipin homologue *FLD1* enhances the amounts of non-polar lipids, leads to an increased size of LD, and provokes aggregation of LD.

Conclusion and perspectives

Sequencing of the *S. cerevisiae* genome has set the stage for identifying and characterizing genes and gene products involved in lipid metabolism. The homology of yeast genes to those of higher eukaryotes has led to substantial progress in the field of lipid research and to a better general understanding of the role of lipids in various cellular processes. Nevertheless, a number of questions still remained open. While lipid metabolic pathways and most of the enzymes involved have been studied in some detail, regulatory aspects on the transcriptional level, by lipids themselves or by the influence of different growth conditions still need clarification. Also the field of lipid sensing and signaling requires further elucidation. Finally, studies of lipid transport between organelles and the assembly of lipids into cellular membranes will be a task for the future. Such investigations will lead to a better understanding of the links within the lipid metabolic and dynamic networks.

References

Achleitner G, Gaigg B, Krasser A, Kainersdorfer E, Kohlwein SD, Perktold A, Zellnig G & Daum G (1999) Association between the endoplasmic reticulum and mitochondria of yeast facilitates interorganelle transport of phospholipids through membrane contact. *Eur. J. Biochem.* **264**: 545–553.

Alfaro G, Johansen J, Dighe SA, Duamel G, Kozminski KG & Beh CT (2011) The sterol-binding protein Kes1/Osh4p is a regulator of polarized exocytosis. *Traffic* **12**: 1521–1536.

Alvarez-Vasquez F, Sims KJ, Cowart LA, Okamoto Y, Voit EO & Hannun YA (2005) Simulation and validation of modelled sphingolipid metabolism in *Saccharomyces cerevisiae*. *Nature* **433**: 425–430.

Anderson MS, Muehlbacher M, Street IP, Proffitt J & Poulter CD (1989a) Isopentenyl diphosphate:dimethylallyl diphosphate isomerase. An improved purification of the enzyme and isolation of the gene from *Saccharomyces cerevisiae*. *J. Biol. Chem.* **264**: 19169–19175.

Anderson MS, Yarger JG, Burck CL & Poulter CD (1989b) Farnesyl diphosphate synthetase. Molecular cloning, sequence, and expression of an essential gene from *Saccharomyces cerevisiae*. *J. Biol. Chem.* **264**: 19176–19184.

Arthington-Skaggs BA, Crowell DN, Yang H, Sturley SL & Bard M (1996) Positive and negative regulation of a sterol biosynthetic gene (*ERG3*) in the post-squalene portion of the yeast ergosterol pathway. *FEBS Letters* **392**: 161–165.

Athenstaedt K & Daum G (1997) Biosynthesis of phosphatidic acid in lipid particles and endoplasmic reticulum of *Saccharomyces cerevisiae*. *J. Bacteriol.* **179**: 7611–7616.

Athenstaedt K & Daum G (2000) 1-Acyldihydroxyacetone-phosphate reductase (Ayr1p) of the yeast *Saccharomyces cerevisiae* encoded by the open reading frame YIL124w is a major component of lipid particles. *J. Biol. Chem.* **275**: 235–240.

Athenstaedt K & Daum G (2005) Tgl4p and Tgl5p, two triacylglycerol lipases of the yeast *Saccharomyces cerevisiae* are localized to lipid particles. *J. Biol. Chem.* **280**: 37301–37309.

Athenstaedt K & Daum G (2003) *YMR313c/TGL3* encodes a novel triacylglycerol lipase located in lipid particles of *Saccharomyces cerevisiae*. *J. Biol. Chem.* **278**: 23317–23323.

Athenstaedt K, Zweytick D, Jandrositz A, Kohlwein SD & Daum G (1999) Identification and characterization of major lipid particle proteins of the yeast *Saccharomyces cerevisiae*. *J. Bacteriol.* **181**: 6441–6448.

Ayciriex S et al. (2012) *YPR139c/LOA1* encodes a novel lysophosphatidic acid acyltransferase associated with lipid droplets and involved in TAG homeostasis. *Mol. Biol. Cell.* **23**: 233–246.

Bailis AM, Lopes JM, Kohlwein SD & Henry SA (1992) Cis and trans regulatory elements required for regulation of the *CHO1* gene of *Saccharomyces cerevisiae*. *Nucleic Acids Res.* **20**: 1411–1418.

Bard M & Downing JF (1981) Genetic and biochemical aspects of yeast sterol regulation involving 3-hydroxy-3-methylglutaryl coenzyme A reductase. *J. Gen. Microbiol.* **125**: 415–420.

Basson ME, Thorsness M & Rine J (1986) *Saccharomyces cerevisiae* contains two functional genes encoding 3-hydroxy-3-methylglutaryl-coenzyme A reductase. *Proc. Natl. Acad. Sci. U. S. A.* **83**: 5563–5567.

Beeler T, Bacikova D, Gable K, Hopkins L, Johnson C, Slife H & Dunn T (1998) The *Saccharomyces cerevisiae TSC10/YBR265w* gene encoding 3-ketosphinganine reductase is identified in a screen for temperature-sensitive suppressors of the Ca^{2+}-sensitive csg2Δ mutant. *J. Biol. Chem.* **273**: 30688–30694.

Beh CT, Cool L, Phillips J & Rine J (2001) Overlapping functions of the yeast oxysterol-binding protein homologues. *Genetics* **157**: 1117–1140.

Benghezal M, Roubaty C, Veepuri V, Knudsen J & Conzelmann A (2007) *SLC1* and *SLC4* encode partially redundant acyl-coenzyme A 1-acylglycerol-3-phosphate O-acyltransferases of budding yeast. *J. Biol. Chem.* **282**: 30845–30855.

Beranek A, Rechberger G, Knauer H, Wolinski H, Kohlwein SD & Leber R (2009) Identification of a cardiolipin-specific phospholipase encoded by the gene *CLD1* (*YGR110W*) in yeast. *J. Biol. Chem.* **284**: 11572–11578.

Berger AC, Vanderford TH, Gernert KM, Nichols JW, Faundez V & Corbett AH (2005) *Saccharomyces cerevisiae* Npc2p is a functionally conserved homologue of the human Niemann-Pick disease type C 2 protein, hNPC2. *Eukaryot. Cell* **4**: 1851–1862.

Berges T, Guyonnet D & Karst F (1997) The *Saccharomyces cerevisiae* mevalonate diphosphate decarboxylase is essential for viability, and a single Leu-to-Pro mutation in a conserved sequence leads to thermosensitivity. *J. Bacteriol.* **179**: 4664–4670.

Black PN & DiRusso CC (2007) Yeast acyl-CoA synthetases at the crossroads of fatty acid metabolism and regulation. *Biochim. Biophys. Acta* **1771**: 286–298.

Brice SE, Alford CW & Cowart LA (2009) Modulation of sphingolipid metabolism by the phosphatidylinositol-4-phosphate phosphatase Sac1p through regulation of phosphatidylinositol in *Saccharomyces cerevisiae*. *J. Biol. Chem.* **284**: 7588–7596.

Burg JS & Espenshade PJ (2011) Regulation of HMG-CoA reductase in mammals and yeast. *Prog. Lipid Res.* **50**: 403–410.

Bürgermeister M, Birner-Grünberger R, Nebauer R & Daum G (2004) Contribution of different pathways to the supply of phosphatidylethanolamine and phosphatidylcholine to mitochondrial membranes of the yeast *Saccharomyces cerevisiae*. *Biochim. Biophys. Acta* **1686**: 161–168.

Carman GM & Han G-S (2011) Regulation of phospholipid synthesis in the yeast *Saccharomyces cerevisiae*. *Annu. Rev. Biochem.* **80**: 859–883.

Chae M, Han G-S & Carman GM (2012) The *Saccharomyces cerevisiae* actin patch protein App1p is a phosphatidate phosphatase enzyme. *J. Biol. Chem.* **287**: 40186–40196.

Chang S-C, Heacock PN, Clancey CJ & Dowhan W (1998a) The *PEL1* Gene (renamed *PGS1*) encodes the phosphatidylglycerophosphate synthase of *Saccharomyces cerevisiae*. *J. Biol. Chem.* **273**: 9829–9836.

Chang S-C, Heacock PN, Mileykovskaya E, Voelker DR & Dowhan W (1998b) Isolation and characterization of the gene (*CLS1*) encoding cardiolipin synthase in *Saccharomyces cerevisiae*. *J. Biol. Chem.* **273**: 14933–14941.

Choi H-S, Su W-M, Morgan JM, Han G-S, Xu Z, Karanasios E, Siniossoglou S & Carman GM (2011) Phosphorylation of phosphatidate phosphatase rRegulates its membrane association and physiological functions in *Saccharomyces cerevisiae*. *J. Biol. Chem.* **286**: 1486–1498.

Choudhary V & Schneiter R (2012) Pathogen-related yeast (PRY) proteins and members of the CAP superfamily are secreted sterol-binding proteins. *Proc. Natl. Acad. Sci. U. S. A.* **109**: 16882–16887.

Connerth M, Czabany T, Wagner A, Zellnig G, Leitner E, Steyrer E & Daum G (2010) Oleate inhibits steryl ester synthesis and causes liposensitivity in yeast. *J. Biol. Chem.* **285**: 26832–26841.

Corey EJ, Matsuda SP & Bartel B (1994) Molecular cloning, characterization, and overexpression of *ERG7*, the *Saccharomyces cerevisiae* gene encoding lanosterol synthase. *Proc. Natl. Acad. Sci. U. S. A.* **91**: 2211–2215.

Czabany T, Athenstaedt K & Daum G (2007) Synthesis, storage and degradation of neutral lipids in yeast. *Biochim. Biophys. Acta* **1771**: 299–309.

Czabany T, Wagner A, Zweytick D, Lohner K, Leitner E, Ingolic E & Daum G (2008) Structural and biochemical properties of lipid particles from the yeast *Saccharomyces cerevisiae*. *J. Biol. Chem.* **283**: 17065–17074.

Daum G, Lees ND, Bard M & Dickson RC (1998) Biochemistry, cell biology and molecular biology of lipids of *Saccharomyces cerevisiae*. *Yeast* **14**: 1471–1510.

Davies BSJ & Rine J (2006) A role for sterol levels in oxygen sensing in *Saccharomyces cerevisiae*. *Genetics* **174**: 191–201.

Dean-Johnson M & Henry SA (1989) Biosynthesis of inositol in yeast. Primary structure of myo-inositol-1-phosphate synthase (EC 5.5.1.4) and functional analysis of its structural gene, the *INO1* locus. *J. Biol. Chem.* **264**: 1274–1283.

Debelyy MO, Thoms S, Connerth M, Daum G & Erdmann R (2011) Involvement of the *Saccharomyces cerevisiae* hydrolase Ldh1p in lipid homeostasis. *Eukaryot. Cell* **10**: 776–781.

Dickson RC (2008) Thematic review series: Sphingolipids. New insights into sphingolipid metabolism and function in budding yeast. *J. Lipid Res.* **49**: 909–921.

Dickson RC & Lester RL (2002) Sphingolipid functions in *Saccharomyces cerevisiae*. *Biochim. Biophys. Acta* **1583**: 13–25.

Dickson RC, Nagiec EE, Wells GB, Nagiec MM & Lester RL (1997) Synthesis of mannose-(inositol-P)2-ceramide, the major sphingolipid in *Saccharomyces cerevisiae*, requires the *IPT1* (*YDR072c*) Gene. *J. Biol. Chem.* **272**: 29620–29625.

Dickson RC, Sumanasekera C & Lester RL (2006) Functions and metabolism of sphingolipids in *Saccharomyces cerevisiae*. *Progr. Lipid Res.* **45**: 447–465.

Donahue TF & Henry SA (1981) myo-Inositol-1-phosphate synthase. Characteristics of the enzyme and identification of its structural gene in yeast. *J. Biol. Chem.* **256**: 7077–7085.

Eisenberg T & Büttner S (2013) Lipids and cell death in yeast. *FEMS Yeast Res.* doi: 10.1111/1567-1364.12105.

Escribá PV et al. (2008) Membranes: a meeting point for lipids, proteins and therapies. *J. Cell. Mol. Med.* **12**: 829–875.

Espenshade PJ & Hughes AL (2007) Regulation of sterol synthesis in eukaryotes. *Annual. Rev. Genet.* **41**: 401–427.

Fagone P & Jackowski S (2009) Membrane phospholipid synthesis and endoplasmic reticulum function. *J. Lipid Res.* **50**: S311–S316.

Fahy E et al. (2008) Update of the LIPID MAPS comprehensive classification system for lipids. *J. Lipid Res.* **50**: S9–S14.

Fahy E, Cotter D, Sud M & Subramaniam S (2011) Lipid classification, structures and tools. *Biochim. Biophys. Acta* **1811**: 637–647.

Fakas S, Konstantinou C & Carman GM (2011) *DGK1*-encoded diacylglycerol kinase activity is required for phospholipid synthesis during growth resumption from stationary phase in *Saccharomyces cerevisiae*. *J. Biol. Chem.* **286**: 1464–1474.

Fei W et al. (2008) Fld1p, a functional homologue of human seipin, regulates the size of lipid droplets in yeast. *J. Cell Biol.* **180**: 473–482.

Fichtlscherer F, Wellein C, Mittag M & Schweizer E (2000) A novel function of yeast fatty acid synthase. *Eur. J. Biochem.* **267**: 2666–2671.

Flick JS & Thorner J (1993) Genetic and biochemical characterization of a phosphatidylinositol-specific phospholipase C in *Saccharomyces cerevisiae*. *Mol. Cell Biol.* **13**: 5861–5876.

Foresti O, Ruggiano A, Hannibal-Bach HK, Ejsing CS & Carvalho P (2013) Sterol homeostasis requires regulated degradation of squalene monooxygenase by the ubiquitin ligase Doa10/Teb4. *eLife* **2**:e00953. DOI: 10.7554/eLife.00953

Gable K, Slife H, Bacikova D, Monaghan E & Dunn TM (2000) Tsc3p is an 80-amino acid protein associated with serine palmitoyltransferase and required for optimal enzyme activity. *J. Biol. Chem.* **275**: 7597–7603.

Gaigg B et al. (2001) Depletion of acyl-coenzyme A-binding protein affects sphingolipid synthesis and causes vesicle accumulation and membrane defects in *Saccharomyces cerevisiae*. *Mol. Biol. Cell* **12**: 1147–1160.

Garbarino J et al. (2009) Sterol and diacylglycerol acyltransferase deficiency triggers fatty acid-mediated cell death. *J. Biol. Chem.* **284**: 30994–31005.

Griac P & Henry SA (1999) The yeast inositol-sensitive upstream activating sequence, UASINO, responds to nitrogen availability. *Nucleic Acids Res.* **27**: 2043–2050.

Grillitsch K, Connerth M, Köfeler H, Arrey TN, Rietschel B, Wagner B, Karas M & Daum G (2011) Lipid particles/droplets of the yeast *Saccharomyces cerevisiae* revisited: Lipidome meets Proteome. *Biochim. Biophys. Acta* **1811**: 1165–1176.

Le Guédard M et al. (2009) *PSI1* is responsible for the stearic acid enrichment that is characteristic of phosphatidylinositol in yeast. *FEBS Journal* **276**: 6412–6424.

Guo Y, Cordes KR, Farese RV & Walther TC (2009) Lipid droplets at a glance. *J. Cell Sci.* **122**: 749–752.

Haak D, Gable K, Beeler T & Dunn T (1997) Hydroxylation of *Saccharomyces cerevisiae* ceramides requires Sur2p and Scs7p. *J. Biol. Chem.* **272**: 29704–29710.

Ham HJ, Rho HJ, Shin SK & Yoon H-J (2010) The *TGL2* gene of *Saccharomyces cerevisiae* encodes an active acylglycerol lipase located in the mitochondria. *J. Biol. Chem.* **285**: 3005–3013.

Han G-S, Siniossoglou S & Carman GM (2007) The cellular functions of the yeast lipin homolog Pah1p are dependent on its phosphatidate phosphatase activity. *J. Biol. Chem.* **282**: 37026–37035.

Han G-S, O'Hara L, Carman GM & Siniossoglou S (2008b) An unconventional diacylglycerol kinase that regulates phospholipid synthesis and nuclear membrane growth. *J. Biol. Chem.* **283**: 20433–20442.

Han G-S, O'Hara L, Siniossoglou S & Carman GM (2008a) Characterization of the Yeast *DGK1*-encoded CTP-dependent diacylglycerol kinase. *J. Biol. Chem.* **283**: 20443–20453.

Han G-S, Wu W-I & Carman GM (2006) The *Saccharomyces cerevisiae* lipin homolog is a Mg^{2+}-dependent phosphatidate phosphatase enzyme. *J. Biol. Chem.* **281**: 9210–9218.

Han S, Lone MA, Schneiter R & Chang A (2010) Orm1 and Orm2 are conserved endoplasmic reticulum membrane proteins regulating lipid homeostasis and protein quality control. *Proc. Natl. Acad. Sci. U. S. A.* **107**: 5851–5856.

Hasslacher M, Ivessa AS, Paltauf F. & Kohlwein SD (1993) Acetyl-CoA carboxylase from yeast is an essential enzyme and is regulated by factors that control phospholipid metabolism. *J. Biol. Chem.* **268**: 10946–10952.

Heier C, Taschler U, Rengachari S, Oberer M, Wolinski H, Natter K, Kohlwein SD, Leber R & Zimmermann R (2010) Identification of Yju3p as functional orthologue of

mammalian monoglyceride lipase in the yeast *Saccharomyces cerevisiae*. *Biochim. Biophys. Acta* **1801**: 1063–1071.

Henneberry AL & Sturley SL (2005) Sterol homeostasis in the budding yeast, *Saccharomyces cerevisiae*. *Semin. Cell Dev. Biol.* **16**: 155–161.

Henry SA, Kohlwein SD & Carman GM (2012) Metabolism and regulation of glycerolipids in the yeast *Saccharomyces cerevisiae*. *Genetics* **190**: 317–349.

Hiltunen JK, Chen Z, Haapalainen AM, Wierenga RK & Kastaniotis AJ (2010a) Mitochondrial fatty acid synthesis – An adopted set of enzymes making a pathway of major importance for the cellular metabolism. *Progr. Lipid Res.* **49**: 27–45.

Hiltunen JK, Autio KJ, Schonauer MS, Kursu VAS, Dieckmann CL & Kastaniotis AJ (2010b) Mitochondrial fatty acid synthesis and respiration. *Biochim. Biophys. Acta* **1797**: 1195–1202.

Hiltunen JK, Mursula AM, Rottensteiner H, Wierenga RK, Kastaniotis AJ & Gurvitz A (2003) The biochemistry of peroxisomal β-oxidation in the yeast *Saccharomyces cerevisiae*. *FEMS Microbiol. Rev.* **27**: 35–64.

Hiser L, Basson ME & Rine J (1994) *ERG10* from *Saccharomyces cerevisiae* encodes acetoacetyl-CoA thiolase. *J. Biol. Chem.* **269**: 31383–31389.

Hjelmstad RH & Bell RM (1987) Mutants of *Saccharomyces cerevisiae* defective in sn-1,2-diacylglycerol cholinephosphotransferase. Isolation, characterization, and cloning of the *CPT1* gene. *J. Biol. Chem.* **262**: 3909–3917.

Hjelmstad RH & Bell RM (1988) The sn-1,2-diacylglycerol ethanolaminephosphotransferase activity of *Saccharomyces cerevisiae*. Isolation of mutants and cloning of the *EPT1* gene. *J. Biol. Chem.* **263**: 19748–19757.

Hoja U, Marthol S, Hofmann J, Stegner S, Schulz R, Meier S, Greiner E & Schweizer E (2004) *HFA1* encoding an organelle-specific acetyl-CoA carboxylase controls mitochondrial fatty acid synthesis in *Saccharomyces cerevisiae*. *J. Biol. Chem.* **279**: 21779–21786.

Horvath SE, Wagner A, Steyrer E & Daum G (2011) Metabolic link between phosphatidylethanolamine and triacylglycerol metabolism in the yeast *Saccharomyces cerevisiae*. *Biochim Biophys Acta* **1811**: 1030–1037.

Hosaka K, Kodaki T & Yamashita S (1989) Cloning and characterization of the yeast *CKI* gene encoding choline kinase and its expression in *Escherichia coli*. *J. Biol. Chem.* **264**: 2053–2059.

Iwaki S, Kihara A, Sano T & Igarashi Y (2005) Phosphorylation by Pho85 cyclin-dependent kinase acts as a signal for the down-regulation of the yeast sphingoid long-chain base kinase Lcb4 during the stationary phase. *J. Biol. Chem.* **280**: 6520–6527.

Jacquier N, Choudhary V, Mari M, Toulmay A, Reggiori F & Schneiter R (2011) Lipid droplets are functionally connected to the endoplasmic reticulum in *Saccharomyces cerevisiae*. *J. Cell Sci.* **124**: 2424–2437.

Jacquier N & Schneiter R (2012) Mechanisms of sterol uptake and transport in yeast. *J. Steroid Biochem. Mol. Biol.* **129**: 70–78.

Jain S, Stanford N, Bhagwat N, Seiler B, Costanzo M, Boone C & Oelkers P (2007) Identification of a novel lysophospholipid acyltransferase in *Saccharomyces cerevisiae*. *J. Biol. Chem.* **282**: 30562–30569.

Jandrositz A, Turnowsky F & Högenauer G (1991) The gene encoding squalene epoxidase from *Saccharomyces cerevisiae*: cloning and characterization. *Gene* **107**: 155–160.

Jennings SM, Tsay YH, Fisch TM & Robinson GW (1991) Molecular cloning and characterization of the yeast gene for squalene synthetase. *Proc. Natl. Acad. Sci. U. S. A.* **88**: 6038–6042.

Jesch SA., Gaspar ML., Stefan CJ, Aregullin MA & Henry SA (2010) Interruption of inositol sphingolipid synthesis triggers Stt4p-dependent protein kinase C signaling. *J. Biol. Chem.* **285**: 41947–41960.

Kandasamy P, Vemula M, Oh C-S, Chellappa R & Martin CE (2004) Regulation of unsaturated fatty acid biosynthesis in *Saccharomyces*; The endoplasmic reticulum membrane protein, Mga2p, a transcription activator of the *OLE1* gene, regulates the stability of the *OLE1* mRNA through exosome-mediated mechanisms. *J. Biol. Chem.* **279**: 36586–36592.

Kihara A (2013) Sphingosine 1-phosphate is a key metabolite linking sphingolipids to glycerophospholipids. *Biochim. Biophys. Acta*. DOI:10.1016/j.bbalip.2013.08.014

Kim K, Kim K-H, Storey MK, Voelker DR & Carman GM (1999) Isolation and characterization of the *Saccharomyces cerevisiae EKI1* gene encoding ethanolamine kinase. *J. Biol. Chem.* **274**: 14857–14866.

Kim K-H, Voelker DR, Flocco MT & Carman GM (1998) Expression, purification, and characterization of choline kinase, product of the *CKI* gene from *Saccharomyces cerevisiae*. *J. Biol. Chem.* **273**: 6844–6852.

Kodaki T & Yamashita S (1987) Yeast phosphatidylethanolamine methylation pathway. Cloning and characterization of two distinct methyltransferase genes. *J. Biol. Chem.* **262**: 15428–15435.

Kodaki T & Yamashita S (1989) Characterization of the methyltransferases in the yeast phosphatidylethanolamine methylation pathway by selective gene disruption. *Eur. J. Biochem.* **185**: 243–251.

Köffel R, Tiwari R, Falquet L & Schneiter R (2005) The *Saccharomyces cerevisiae YLL012/YEH1, YLR020/YEH2,* and *TGL1* genes encode a novel family of membrane-anchored lipases that are required for steryl ester hydrolysis. *Mol. Cell. Biol.* **25**: 1655–1668.

Köffel R & Schneiter R (2006) Yeh1 constitutes the major steryl ester hydrolase under heme-deficient conditions in *Saccharomyces cerevisiae*. *Eukaryot. Cell* **5**: 1018–1025.

Kohlwein SD (2010) Triacylglycerol Homeostasis: Insights from Yeast. *J. Biol. Chem.* **285**: 15663–15667.

Kohlwein SD, Eder S, Oh C-S, Martin CE, Gable K, Bacikova D & Dunn T (2001) Tsc13p is required for fatty acid elongation and localizes to a novel structure at the nuclear-vacuolar interface in *Saccharomyces cerevisiae*. *Mol. Cell Biol.* **21**: 109–125.

Kohlwein SD, Veenhuis M & Van der Klei IJ (2013) Lipid droplets and peroxisomes: Key players in cellular lipid homeostasis or a matter of fat--Store 'em up or Burn'em down. *Genetics* **193**: 1–50.

Kolaczkowski M, Kolaczkowska A, Gaigg B, Schneiter R & Moye-Rowley WS (2004) Differential regulation of ceramide synthase components LAC1 and LAG1 in *Saccharomyces cerevisiae*. *Eukaryot. Cell* **3**: 880–892.

Kristan K & Rižner TL (2012) Steroid-transforming enzymes in fungi. *J. Steroid Biochem. Mol. Biol.* **129**: 79–91.

Kurat CF et al. (2006) Obese yeast: Triglyceride lipolysis is functionally conserved from mammals to yeast. *J. Biol. Chem.* **281**: 491–500.

Kurat CF, Wolinski H, Petschnigg J, Kaluarachchi S, Andrews B, Natter K & Kohlwein SD (2009) Cdk1/Cdc28-dependent activation of the major triacylglycerol lipase Tgl4 in yeast links lipolysis to cell-cycle progression. *Mol. Cell* **33**: 53–63.

Lai K & McGraw P (1994) Dual control of inositol transport in *Saccharomyces cerevisiae* by irreversible inactivation of permease and regulation of permease synthesis by *INO2*, *INO4*, and *OPI1*. *J. Biol. Chem.* **269**: 2245–2251.

Leber R, Zinser E, Zellnig G, Paltauf F & Daum G (1994) Characterization of lipid particles of the yeast, *Saccharomyces cerevisiae*. *Yeast* **10**: 1421–1428.

LeBlanc MA, Fairn GD, Russo SB, Czyz O, Zaremberg V, Cowart LA & McMaster CR (2013) The yeast oxysterol binding protein Kes1 maintains sphingolipid levels. PLoS ONE 8(4): e60485. doi:10.1371/journal.pone.0060485.

Lee KS, Patton JL, Fido M, Hines LK, Kohlwein SD, Paltauf F, Henry SA & Levin DE (1994) The *Saccharomyces cerevisiae PLB1* gene encodes a protein required for lysophospholipase and phospholipase B activity. *J. Biol. Chem.* **269**: 19725–19730.

Leibundgut M, Maier T, Jenni S & Ban N (2008) The multienzyme architecture of eukaryotic fatty acid synthases. *Curr. Opin. Struc. Biol.* **18**: 714–725.

Letts VA, Klig LS, Bae-Lee M, Carman GM & Henry SA (1983) Isolation of the yeast structural gene for the membrane-associated enzyme phosphatidylserine synthase. *Proc. Natl. Acad. Sci. U. S. A.* **80**: 7279–7283.

Liscum L (2000) Niemann–Pick type C mutations cause lipid traffic jam. *Traffic* **1**: 218–225.

Loewen CJR, Gaspar ML, Jesch SA, Delon C, Ktistakis NT, Henry SA & Levine TP (2004) Phospholipid metabolism regulated by a transcription factor sensing phosphatidic acid. *Science* **304**: 1644–1647.

Lopez F, Leube M, Gil-Mascarell R, Navarro-Aviñó JP & Serrano R (1999) The yeast inositol monophosphatase is a lithium- and sodium-sensitive enzyme encoded by a non-essential gene pair. *Mol. Microbiol.* **31**: 1255–1264.

Malathi K et al. (2004) Mutagenesis of the putative sterol-sensing domain of yeast Niemann Pick C-related protein reveals a primordial role in subcellular sphingolipid distribution. *J. Cell Biol.* **164**: 547–556.

Mao C, Xu R, Bielawska A & Obeid LM (2000a) Cloning of an alkaline ceramidase from *Saccharomyces cerevisiae*; an enzyme with reverse (CoA-independent) ceramide synthase activity. *J. Biol. Chem.* **275**: 6876–6884.

Mao C, Xu R, Bielawska A, Szulc ZM & Obeid LM (2000b) Cloning and characterization of a *Saccharomyces cerevisiae* alkaline ceramidase with specificity for dihydroceramide. *J. Biol. Chem.* **275**: 31369–31378.

Martin CE, Oh C-S & Jiang Y (2007) Regulation of long chain unsaturated fatty acid synthesis in yeast. *Biochim. Biophys. Acta* **1771**: 271–285.

Van Meer G, Voelker DR & Feigenson GW (2008) Membrane lipids: where they are and how they behave. *Nat. Rev. Mol. Cell Biol.* **9**: 112–124.

Merkel O, Fido M, Mayr JA, Prüger H, Raab F, Zandonella G, Kohlwein SD & Paltauf F (1999) Characterization and function in vivo of two novel phospholipases B/lysophospholipases from *Saccharomyces cerevisiae*. *J. Biol. Chem.* **274**: 28121–28127.

Min-Seok R, Kawamata Y, Nakamura H, Ohta A & Takagi M (1996) Isolation and characterization of *ECT1* gene encoding CTP: phosphoethanolamine cytidylyltransferase of *Saccharomyces cerevisiae*. *J. Biochem.* **120**: 1040–1047.

Miziorko HM (2011) Enzymes of the mevalonate pathway of isoprenoid biosynthesis. *Arch. Biochem. Biophys.* **505**: 131–143.

Mohamed AH, Chirala SS, Mody NH, Huang WY & Wakil SJ (1988) Primary structure of the multifunctional alpha subunit protein of yeast fatty acid synthase derived from *FAS2* gene sequence. *J. Biol. Chem.* **263**: 12315–12325.

Müllner H, Deutsch G, Leitner E, Ingolic E & Daum G (2005) *YEH2/YLR020c* encodes a novel steryl ester hydrolase of the yeast *Saccharomyces cerevisiae*. *J. Biol. Chem.* **280**: 13321–13328.

Munkacsi AB, Porto AF & Sturley SL (2007) Niemann-Pick type C disease proteins: orphan transporters or membrane rheostats? *Future Lipidol.* **2**: 357–367.

Murray M & Greenberg ML (2000) Expression of yeast *INM1* encoding inositol monophosphatase is regulated by inositol, carbon source and growth stage and is decreased by lithium and valproate. *Mol. Microbiol.* **36**: 651–661.

Nagiec MM, Baltisberger JA, Wells GB, Lester RL & Dickson RC (1994) The *LCB2* gene of *Saccharomyces* and the related *LCB1* gene encode subunits of serine palmitoyltransferase, the initial enzyme in sphingolipid synthesis. *Proc. Natl. Acad. Sci. U. S. A.* **91**: 7899–7902.

Nagiec MM, Nagiec EE, Baltisberger JA, Wells GB, Lester RL & Dickson RC (1997) Sphingolipid Synthesis as a Target for Antifungal Drugs; complementation of the

inositol phosphorylceramide synthase defect in a mutant strain of *Saccharomyces cerevisiae* by the *AUR1* gene. *J. Biol. Chem.* **272**: 9809–9817.

Nakagawa Y, Sakumoto N, Kaneko Y & Harashima S (2002) Mga2p is a putative sensor for low temperature and oxygen to induce *OLE1* transcription in *Saccharomyces cerevisiae*. *Biochem. Biophys. Res.Comm.* **291**: 707–713.

Natter K, Leitner P, Faschinger A, Wolinski H, McCraith S, Fields S & Kohlwein SD (2005) The spatial organization of lipid synthesis in the yeast *Saccharomyces cerevisiae* derived from large scale green fluorescent protein tagging and high resolution microscopy. *Mol. Cell Proteomics* **4**: 662–672.

Nielsen J (2009) Systems biology of lipid metabolism: From yeast to human. *FEBS Lett.* **583**: 3905–3913.

Nikawa J, Hosaka K, Tsukagoshi Y & Yamashita S (1990) Primary structure of the yeast choline transport gene and regulation of its expression. *J. Biol. Chem.* **265**: 15996–16003.

Nikawa J, Tsukagoshi Y & Yamashita S (1991) Isolation and characterization of two distinct myo-inositol transporter genes of *Saccharomyces cerevisiae*. *J. Biol. Chem.* **266**: 11184–11191.

Nikawa J & Yamashita S (1984) Molecular cloning of the gene encoding CDP diacylglycerol–inositol 3-phosphatidyl transferase in *Saccharomyces cerevisiae. Eur. J. Biochem.* **143**: 251–256.

Niles BJ & Powers T (2012) Plasma membrane proteins Slm1 and Slm2 mediate activation of the AGC kinase Ypk1 by TORC2 and sphingolipids in *S. cerevisiae*. *Cell Cycle* **11**: 3745–3749.

Oelkers P, Cromley D, Padamsee M, Billheimer JT & Sturley SL (2002) The *DGA1* gene determines a second triglyceride synthetic pathway in yeast. *J. Biol. Chem.* **277**: 8877–8881.

Oelkers P, Tinkelenberg A, Erdeniz N, Cromley D, Billheimer JT & Sturley SL (2000) A lecithin cholesterol acyltransferase-like gene mediates diacylglycerol esterification in yeast. *J. Biol. Chem.* **275**: 15609–15612.

Oh C-S, Toke DA, Mandala S & Martin Charles E. (1997) *ELO2* and *ELO3*, homologues of the *Saccharomyces cerevisiae ELO1* gene, function in fatty acid elongation and are required for sphingolipid formation. *J. Biol. Chem.* **272**: 17376–17384.

Osman C, Haag M, Wieland FT, Brugger B & Langer T (2010) A mitochondrial phosphatase required for cardiolipin biosynthesis: the PGP phosphatase Gep4. *EMBO J.* **29**: 1976–1987.

Oulmouden A & Karst F (1990) Isolation of the *ERG12* gene of *Saccharomyces cerevisiae* encoding mevalonate kinase. *Gene* **88**: 253–257.

Patton-Vogt J (2007) Transport and metabolism of glycerophosphodiesters produced through phospholipid deacylation. *Biochim. Biophys. Acta* **1771**: 337–342.

Patton-Vogt JL & Henry SA (1998) *GIT1*, a gene encoding a novel transporter for glycerophosphoinositol in *Saccharomyces cerevisiae*. *Genetics* **149**: 1707–1715.

Peretti D, Dahan N, Shimoni E, Hirschberg K & Lev S (2008) Coordinated lipid transfer between the endoplasmic reticulum and the Golgi complex requires the VAP proteins and is essential for Golgi-mediated transport. *Mol. Biol. Cell* **19**: 3871–3884.

Petschnigg J, Wolinski H, Kolb D, Zellnig G, Kurat CF, Natter K & Kohlwein SD (2009) Good fat, essential cellular requirements for triacylglycerol synthesis to maintain membrane homeostasis in yeast *J. Biol. Chem.* **284**: 30981–30993.

Ploegh HL (2007) A lipid-based model for the creation of an escape hatch from the endoplasmic reticulum. *Nature* **448**: 435–438.

Ploier B, Scharwey M, Koch B, Schmidt C, Schatte J, Rechberger G, Kollroser M, Hermetter A & Daum G (2013) Screening for hydrolytic enzymes revealed Ayr1p as a novel triacylglycerol lipase in *Saccharomyces cerevisiae. J. Biol. Chem.* doi: 10.1074/jbc.M113.509927.

Poirier Y, Antonenkov VD, Glumoff T & Hiltunen JK (2006) Peroxisomal β-oxidation—A metabolic pathway with multiple functions. *Biochim. Biophys. Acta* **1763**: 1413–1426.

Qiu Y, Fakas S, Han G-S, Barbosa AD, Siniossoglou S & Carman GM (2013) Transcription factor Reb1p regulates *DGK1*-encoded diacylglycerol kinase and lipid metabolism in *Saccharomyces cerevisiae*. *J. Biol. Chem.* doi: 10.1074/jbc.M113.507392.

Rajakumari S & Daum G (2010a) Janus-faced enzymes yeast Tgl3p and Tgl5p catalyze lipase and acyltransferase reactions. *Mol. Biol. Cell* **21**: 501–510.

Rajakumari S & Daum G (2010b) Multiple functions as lipase, steryl ester hydrolase, phospholipase, and acyltransferase of Tgl4p from the yeast *Saccharomyces cerevisiae*. *J. Biol. Chem.* **285**: 15769–15776.

Rajakumari S, Grillitsch K & Daum G (2008) Synthesis and turnover of non-polar lipids in yeast. *Prog. Lipid Res.* **47**: 157–171.

Reddy VS, Singh AK & Rajasekharan R (2008) The *Saccharomyces cerevisiae PHM8* gene encodes a soluble magnesium-dependent lysophosphatidic acid phosphatase. *J. Biol. Chem.* **283**: 8846–8854.

Rego A, Trindade D, Chaves SR, Manon S, Costa V, Sousa MJ & Côrte-Real M (2013) The yeast model system as a tool towards the understanding of apoptosis regulation by sphingolipids. *FEMS Yeast Res.* doi: 10.1111/1567-1364.12096

Van der Rest ME, Kamminga AH, Nakano A, Anraku Y, Poolman B & Konings WN (1995) The plasma membrane of *Saccharomyces cerevisiae*: structure, function, and biogenesis. *Microbiol. Rev.* **59**: 304–322.

Rijken PJ, Houtkooper RH, Akbari H, Brouwers JF, Koorengevel MC, De Kruijff B, Frentzen M, Vaz FM & De Kroon AIPM (2009) Cardiolipin molecular species with shorter acyl chains accumulate in *Saccharomyces cerevisiae* mutants lacking the acyl coenzyme A-binding Pprotein Acb1p. *J. Biol. Chem.* **284**: 27609–27619.

Roelants FM, Breslow DK, Muir A, Weissman JS & Thorner J (2011) Protein kinase Ypk1 phosphorylates regulatory proteins Orm1 and Orm2 to control sphingolipid homeostasis in *Saccharomyces cerevisiae*. *Proc. Natl. Acad. Sci. U. S. A.* **108**: 19222–19227.

Van Roermund CWT, Drissen R, Van den Berg M, Ijlst L, Hettema EH, Tabak HF, Waterham HR & Wanders RJA (2001) Identification of a peroxisomal ATP carrier required for medium-chain fatty acid -oxidation and normal peroxisome proliferation in *Saccharomyces cerevisiae*. *Mol. Cell. Biol.* **21**: 4321–4329.

Van Roermund CWT, IJlst L, Majczak W, Waterham HR, Folkerts H, Wanders RJA & Hellingwerf KJ (2012) Peroxisomal fatty acid uptake mechanism in *Saccharomyces cerevisiae. J. Biol. Chem.* **287**: 20144–20153.

Van Roermund CWT, Tabak HF, Van den Berg M, Wanders RJA & Hettema EH (2000) Pex11p plays a primary role in medium-chain fatty acid oxidation, a process that affects peroxisome number and size in *Saccharomyces cerevisiae*. *J. Cell Biol.* **150**: 489–498.

Rudge SA & Engebrecht J (1999) Regulation and function of PLDs in yeast. *Biochim. Biophys. Acta* **1439**: 167–174.

Ruggles KV et al. (2013) A functional, genome-wide evaluation of liposensitive yeast identifies the *"ARE2* required for viability" (*ARV1*) gene product as a major component of eukaryotic fatty acid resistance. *J. Biol. Chem.* 10.1074/jbc.M113.515197.

Sandager L, Gustavsson MH, Ståhl U, Dahlqvist A, Wiberg E, Banas A, Lenman M, Ronne H & Stymne S (2002) Storage lipid synthesis is non-essential in Yeast. *J. Biol. Chem.* **277**: 6478–6482.

Santos AXS & Riezman H (2012) Yeast as a model system for studying lipid homeostasis and function. *FEBS Lett.* **586**: 2858–2867.

Sato K, Noda Y & Yoda K (2009) Kei1: A novel subunit of inositolphosphorylceramide synthase, essential for its enzyme activity and golgi localization. *Mol. Biol. Cell* **20**: 4444–4457.

Sawai H, Okamoto Y, Luberto C, Mao C, Bielawska A, Domae N & Hannun YA (2000) Identification of *ISC1* (*YER019w*) as inositol phosphosphingolipid phospholipase C in *Saccharomyces cerevisiae*. *J. Biol. Chem.* **275**: 39793–39798.

Schmidt C, Athenstaedt K, Koch B, Ploier B & Daum G (2013) Regulation of the yeast triacylglycerol lipase Tgl3p by formation of nonpolar lipids. *J. Biol. Chem.* **288**: 19939–19948.

Schnabl M, Daum G & Pichler H (2005) Multiple lipid transport pathways to the plasma membrane in yeast. *Biochim. Biophys. Acta* **1687**: 130–140.

Schneiter R (1999) Brave little yeast, please guide us to Thebes: sphingolipid function in *S. cerevisiae. BioEssays* **21**: 1004–1010.

Schorling S, Vallée B, Barz WP, Riezman H & Oesterhelt D (2001) Lag1p and Lac1p are essential for the acyl-CoA–dependent ceramide synthase reaction in *Saccharomyces cerevisiae*. *Mol. Biol. Cell* **12**: 3417–3427.

Schuiki I, Schnabl M, Czabany T, Hrastnik C & Daum G (2010) Phosphatidylethanolamine synthesized by four different pathways is supplied to the plasma membrane of the yeast *Saccharomyces cerevisiae*. *Biochim. Biophys. Acta* **1801**: 480–486.

Schüller H-J, Förtsch B, Rautenstrauss B, Wolf DH & Schweizer E (1992) Differential proteolytic sensitivity of yeast fatty acid synthetase subunits α and β contributing to a balanced ratio of both fatty acid synthetase components. *Eur. J. Biochem.* **203**: 607–614.

Schulz TA & Prinz WA (2007) Sterol transport in yeast and the oxysterol binding protein homologue (OSH) family. *Biochim. Biophys. Acta* **1771**: 769–780.

Shen H, Heacock PN, Clancey CJ & Dowhan W (1996) The *CDS1* gene encoding CDP-diacylglycerol synthase in *Saccharomyces cerevisiae* is essential for cell growth. *J. Biol. Chem.* **271**: 789–795.

Shimobayashi M, Oppliger W, Moes S, Jeno P & Hall MN (2013) TORC1-regulated protein kinase Npr1 phosphorylates Orm to stimulate complex sphingolipid synthesis. *Mol. Biol. Cell* **24**: 870–881.

Šimočková M, Holič R, Tahotná D, Patton-Vogt J & Griač P (2008) Yeast Pgc1p (*YPL206c*) controls the amount of phosphatidylglycerol via a phospholipase C-type degradation mechanism. *J. Biol. Chem.* **283**: 17107–17115.

Simons K & Sampaio JL (2011) Membrane organization and lipid rafts. Cold Spring Harb. Perspect. Biol. **3**:a004697

De Smet CH, Vittone E, Scherer M, Houweling M, Liebisch G, Brouwers JF & De Kroon AIPM (2012) The yeast acyltransferase Sct1p regulates fatty acid desaturation by competing with the desaturase Ole1p. *Mol. Biol. Cell* **23**: 1146–1156.

Sorger D & Daum G (2003) Triacylglycerol biosynthesis in yeast. *Appl. Microbiol. Biotechnol.* **61**: 289–299.

Sorger D, Athenstaedt K, Hrastnik C & Daum G (2004) A yeast strain lacking lipid particles Bbears a defect in ergosterol formation. *J. Biol. Chem.* **279**: 31190–31196.

Sorger D & Daum G (2002) Synthesis of triacylglycerols by the acyl-coenzyme A:diacyl-glycerol acyltransferase Dga1p in lipid particles of the yeast *Saccharomyces cerevisiae*. *J. Bacteriol.* **184**: 519–524.

Stoops JK & Wakil SJ (1978) The isolation of the two subunits of yeast fatty acid synthetase. *Biochem. Biophys. Res. Comm.* **84**: 225–231.

Stukey JE, McDonough VM & Martin CE (1989) Isolation and characterization of *OLE1*, a gene affecting fatty acid desaturation from *Saccharomyces cerevisiae*. *J. Biol. Chem.* **264**: 16537–16544.

Stukey JE, McDonough VM & Martin CE (1990) The *OLE1* gene of *Saccharomyces cerevisiae* encodes the delta 9 fatty acid desaturase and can be functionally replaced by the rat stearoyl-CoA desaturase gene. *J. Biol. Chem.* **265**: 20144–20149.

Sturley SL (2000) Conservation of eukaryotic sterol homeostasis: new insights from studies in budding yeast. *Biochim. Biophys. Acta* **1529**: 155–163.

Sullivan DP, Ohvo-Rekilä H, Baumann NA, Beh CT & Menon AK (2006) Sterol trafficking between the endoplasmic reticulum and plasma membrane in yeast. *Biochem. Soc. Trans.* **34**: 356–358.

Swain E, Stukey J, McDonough V, Germann M, Liu Y, Sturley SL & Nickels JT (2002) Yeast cells lacking the *ARV1* gene harbor defects in sphingolipid metabolism; complementation by human *ARV1*. *J. Biol. Chem.* **277**: 36152–36160.

Tamura Y et al. (2013) Tam41 is a CDP-diacylglycerol synthase required for cardiolipin biosynthesis in mitochondria. *Cell Metab.* **17**: 709–718.

Tamura Y, Onguka O, Itoh K, Endo T, Iijima M, Claypool SM & Sesaki H (2012) Phosphatidylethanolamine biosynthesis in mitochondria; phosphatidylserine (PS) trafficking is independent of a PS decarboxylase and intermembrane space proteins Ups1p and Ups2p. *J. Biol. Chem.* **287**: 43961–43971.

Tanaka K et al. (2008) Incorporation and remodeling of extracellular phosphatidylcholine with short acyl residues in *Saccharomyces cerevisiae*. *Biochim. Biophys. Acta* **1781**: 391–399.

Tauchi-Sato K, Ozeki S, Houjou T, Taguchi R & Fujimoto T (2002) The surface of lipid droplets is a phospholipid monolayer with a unique fatty acid composition. *J. Biol. Chem.* **277**: 44507–44512.

Tehlivets O, Scheuringer K & Kohlwein SD (2007) Fatty acid synthesis and elongation in yeast. *Biochim. Biophys. Acta* **1771**: 255–270.

Testet E, Laroche-Traineau J, Noubhani A, Coulon D, Bunoust O, Camougrand N, Manon S, Lessire R & Bessoule JJ (2005) Ypr140wp, "the yeast tafazzin", displays a mitochondrial lysophosphatidylcholine (lyso-PC) acyltransferase activity related to triacylglycerol and mitochondrial lipid synthesis. *Biochem. J.* **387**: 617-626.

Tinkelenberg AH, Liu Y, Alcantara F, Khan S, Guo Z, Bard M & Sturley SL (2000) Mutations in yeast *ARV1* alter intracellular sterol distribution and are complemented by human *ARV1*. *J. Biol. Chem.* **275**: 40667–40670.

Tiwari R, Köffel R & Schneiter R (2007) An acetylation/deacetylation cycle controls the export of sterols and steroids from S. cerevisiae. *EMBO J.* **26**: 5109–5119.

Toke DA, Bennett WL, Dillon DA, et al. (1998a) Isolation and characterization of the *Saccharomyces cerevisiae DPP1* gene encoding diacylglycerol pyrophosphate phosphatase. *J. Biol. Chem.* **273**: 3278–3284.

Toke DA, Bennett WL, Oshiro J, Wu W-I, Voelker DR & Carman GM (1998b) Isolation and characterization of the *Saccharomyces cerevisiae LPP1* gene encoding a Mg^{2+}-independent phosphatidate phosphatase. *J. Biol. Chem.* **273**: 14331–14338.

Toke DA & Martin CE (1996) Isolation and characterization of a gene affecting fatty acid elongation in *Saccharomyces cerevisiae*. *J. Biol. Chem.* **271**: 18413–18422.

Tsay YH & Robinson GW (1991) Cloning and characterization of *ERG8*, an essential gene of *Saccharomyces cerevisiae* that encodes phosphomevalonate kinase. *Mol. Cell Biol.* **11**: 620–631.

Tsukagoshi Y, Nikawa J & Yamashita S (1987) Molecular cloning and characterization of the gene encoding cholinephosphate cytidylyltransferase in *Saccharomyces cerevisiae*. *Eur. J. Biochem.* **169**: 477–486.

Tuller G, Hrastnik C, Achleitner G, Schiefthaler U, Klein F & Daum G (1998) *YDL142c* encodes cardiolipin synthase (Cls1p) and is non-essential for aerobic growth of *Saccharomyces cerevisiae*. *FEBS Lett.* **421**: 15–18.

Tuller G, Nemec T, Hrastnik C & Daum G (1999) Lipid composition of subcellular membranes of an FY1679-derived haploid yeast wild-type strain grown on different carbon sources. *Yeast* **15**: 1555–1564.

Uemura S, Kihara A, Inokuchi J & Igarashi Y (2003) Csg1p and newly identified Csh1p function in mannosylinositol phosphorylceramide synthesis by interacting with Csg2p. *J. Biol. Chem.* **278**: 45049–45055.

Valachovic M, Hronská L & Hapala I (2001) Anaerobiosis induces complex changes in sterol esterification pattern in the yeast *Saccharomyces cerevisiae*. *FEMS Microbiol. Lett.* **197**: 41–45.

Vallee B & Riezman H (2005) Lip1p: a novel subunit of acyl-CoA ceramide synthase. *EMBO J.* **24**: 730–741.

Viljoen BC, Kock JL & Lategan PM (1986) Long-chain fatty acid composition of selected genera of yeasts belonging to the Endomycetales. *Anton. V. Leeuwen.* **52**: 45–51.

Voelker DR (1997) Phosphatidylserine decarboxylase. *Biochim. Biophys. Acta* **1348**: 236–244.

Voynova NS, Vionnet C, Ejsing CS & Conzelmann A (2012) A novel pathway of ceramide metabolism in *Saccharomyces cerevisiae*. *Biochem. J.* **447**: 103–114.

Walther TC & Farese Jr. RV (2009) The life of lipid droplets. *Biochim. Biophys. Acta* **1791**: 459–466.

Wieland F, Renner L, Verfürth C & Lynen F (1979) Studies on the multi-enzyme complex of yeast fatty-acid synthetase. *Eur. J. Biochem.* **94**: 189–197.

Wilson JD, Thompson SL & Barlowe C (2011) Yet1p-Yet3p interacts with Scs2p-Opi1p to regulate ER localization of the Opi1p repressor. *Mol. Biol. Cell* **22**: 1430–1439.

Wu W-I, Liu Y, Riedel B, Wissing JB, Fischl AS & Carman GM (1996) Purification and characterization of diacylglycerol pyrophosphate phosphatase from *Saccharomyces cerevisiae*. *J. Biol. Chem.* **271**: 1868–1876.

Yang H, Bard M, Bruner DA, Gleeson A, Deckelbaum RJ, Aljinovic G, Pohl TM, Rothstein R & Sturley SL (1996) Sterol esterification in yeast: A two-gene process. *Science* **272**: 1353–1356.

Zavrel M, Hoot SJ & White TC (2013) Comparison of sterol import under aerobic and anaerobic conditions in three fungal species, *Candida albicans*, *Candida glabrata*, and *Saccharomyces cerevisiae*. *Eukaryot. Cell* **12**: 725–738.

Zhang S, Skalsky Y & Garfinkel DJ (1999) *MGA2* or *SPT23* is required for transcription of the delta9 fatty acid desaturase gene, *OLE1*, and nuclear membrane integrity in *Saccharomyces cerevisiae. Genetics* **151**: 473–483.

Zhang S, Ren J, Li H, Zhang Q, Armstrong JS, Munn AL & Yang H (2004) Ncr1p, the yeast ortholog of mammalian Niemann Pick C1 protein, is dispensable for endocytic transport. *Traffic* **5**: 1017–1030.

Zhao M, Rua D, Hajra AK & Greenberg ML (1998) Enzymatic synthesis of [^{3}H]cytidine 5′-diphospho-1,2-diacyl-sn-glycerol. *Anal. Biochem.* **258**: 48–52.

Zheng Z & Zou J (2001) The Initial Step of the glycerolipid pathway; identification of glycerol 3-phosphate/dihydroxyacetone phosphate dual substrate acyltransferases in *Saccharomyces cerevisiae*. *J. Biol. Chem.* **276**: 41710–41716.

Zinser E, Paltauf F & Daum G (1993) Sterol composition of yeast organelle membranes and subcellular distribution of enzymes involved in sterol metabolism. *J. Bacteriol.* **175**: 2853–2858.

Zinser E, Sperka-Gottlieb CD, Fasch EV, Kohlwein SD, Paltauf F & Daum G (1991) Phospholipid synthesis and lipid composition of subcellular membranes in the unicellular eukaryote *Saccharomyces cerevisiae*. *J. Bacteriol.* **173**: 2026–2034.

Zweytick D, Leitner E, Kohlwein SD, Yu C, Rothblatt J & Daum G (2000a) Contribution of Are1p and Are2p to steryl ester synthesis in the yeast *Saccharomyces cerevisiae*. *Eur. J. Biochem.* **267**: 1075–1082.

Zweytick D, Athenstaedt K & Daum G (2000b) Intracellular lipid particles of eukaryotic cells. *Biochim. Biophys. Acta* **1469**: 101–120.

Table 1: Phospholipid composition of organelles from *S. cerevisiae.*

Phospholipid compositions of yeast cells and organelles are shown as summarized previously by Zinser et al., 1991; and Horvath et al., 2011. PC, phosphatidylcholine; PE, phosphatidylethanolamine; PI, phosphatidylinositol; PS, phosphatidylserine; CL, cardiolipin; PA, phosphatidic acid; others, other phospholipids such as lyso-phospholipids, phosphatidylglycerol, dimethylphosphatidylethanolamine; nd, not detectable.

	Mol % of total phospholipids						
Cell Fraction	**PC**	**PE**	**PI**	**PS**	**CL**	**PA**	**others**
Homogenate	51.0	25.0	11.4	5.1	3.7	1.1	2.7
Plasma membrane	11.3	24.6	27.2	32.2	nd	3.3	1.4
Endoplasmic reticulum	38.9	18.6	22.4	6.4	0.3	3.4	10.0
Mitochondria	33.4	22.7	20.6	3.3	7.2	1.7	10.1
Peroxisomes	39.8	17.4	22.0	2.5	2.7	6.1	10.5

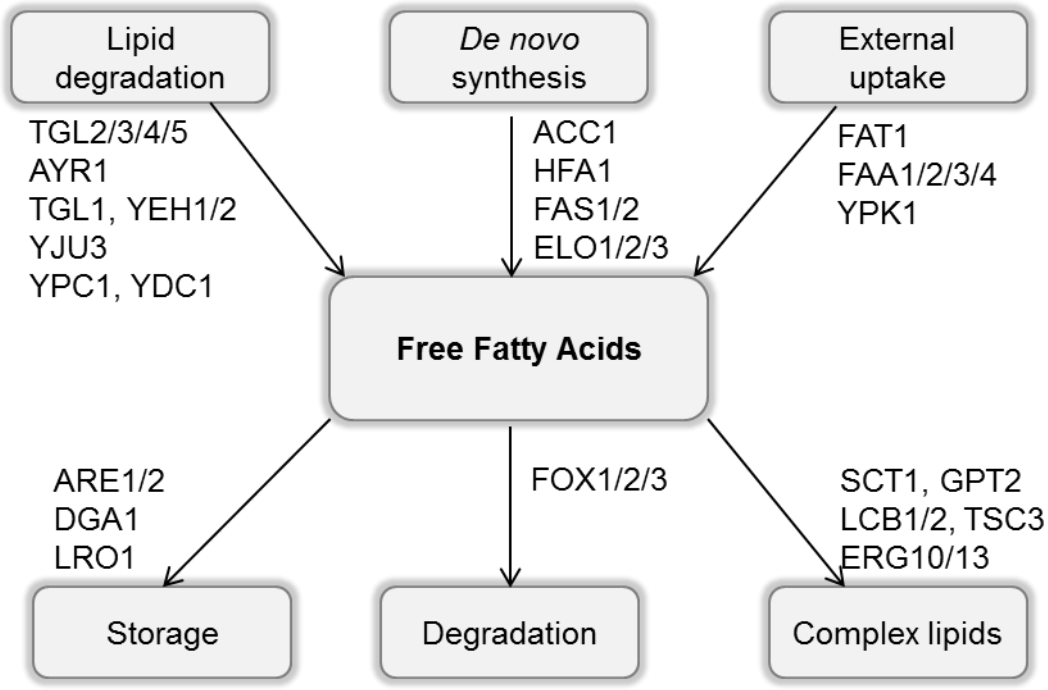

Figure 1: Fatty acid metabolism in the yeast *S. cerevisiae*

Fatty acids are derived from (i) degradation of storage and complex lipids; (ii) *de novo* synthesis; and (iii) uptake from the environment. They can be incorporated into storage lipids or complex membrane lipids, or degraded by β-oxidation. Enzymes catalyzing these processes are described in the text.

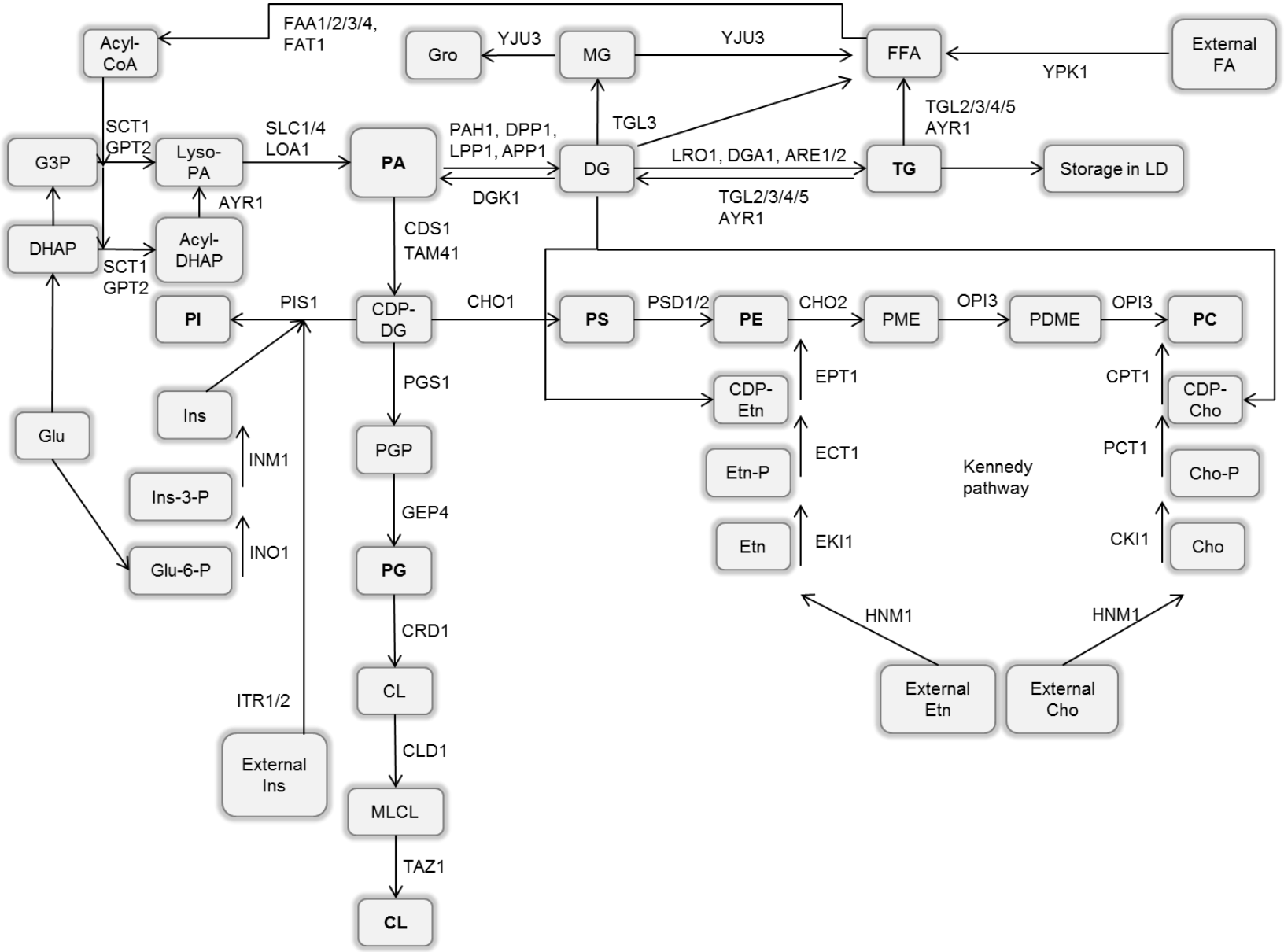
Acyl-CoA
FAA1/2/3/4, FAT1
Gro
YJU3
MG
YJU3
FFA
External FA
YPK1
G3P
SCT1 GPT2
Lyso-PA
SLC1/4 LOA1
PA
PAH1, DPP1, LPP1, APP1
DG
TGL3
LRO1, DGA1, ARE1/2
TG
TGL2/3/4/5 AYR1
Storage in LD
DGK1
TGL2/3/4/5 AYR1
AYR1
DHAP
Acyl-DHAP
SCT1 GPT2
CDS1 TAM41
PI
PIS1
CDP-DG
CHO1
PS
PSD1/2
PE
CHO2
PME
OPI3
PDME
OPI3
PC
CDP-Etn
EPT1
CPT1
CDP-Cho
Glu
Ins
INM1
PGP
PCT1
Ins-3-P
ECT1
Etn-P
Kennedy pathway
Cho-P
GEP4
Glu-6-P
INO1
PG
Etn
EKI1
CKI1
Cho
HNM1
HNM1
CRD1
External Etn
External Cho
ITR1/2
CL
External Ins
CLD1
MLCL
TAZ1
CL

Figure 2: Phospholipid and triacylglycerol biosynthesis in the yeast *S. cerevisiae*

Phosphatidic acid serves as a central intermediate in the biosynthesis of phospholipids and triacylglycerols. The different branches of the glycerolipid biosynthetic network, the lipid products and the enzymes involved are described in the text. Glu-6-P, glucose-6-phosphate; Ins-3-P, inositol-3-phosphate; Ins, inositol; acyl-DHAP, acyldihydroxyacetone phosphate; G3P, glycerol-3-phosphate; lyso-PA, lysophosphatidic acid; CDP-DG, cytidinediphosphatediacylglycerol; TG, triacylglycerol; MG, monoacylglycerol; Gro, glycerol; (F)FA, (free) fatty acids; CoA, Coenzyme A; PGP, phosphatidylglycerolphosphate; PG, phosphatidylglycerol; PME, phosphatidylmethylethanolamine; PDME, phosphatidyldimethyl-ethanolamine; CDP-Etn, cytidinediphosphate ethanolamine; Etn, ethanolamine; Etn-P, ethanolamine phosphate; Cho, choline; Cho-P, choline phosphate; CDP-Cho, cytidinediphosphate choline; MLCL, monolysocardiolipin; PI, phosphatidylinositol; PS, phosphatidylserine; PE, phosphatidylethanolamine; PC, phosphatidylcholine; CL, cardiolipin.

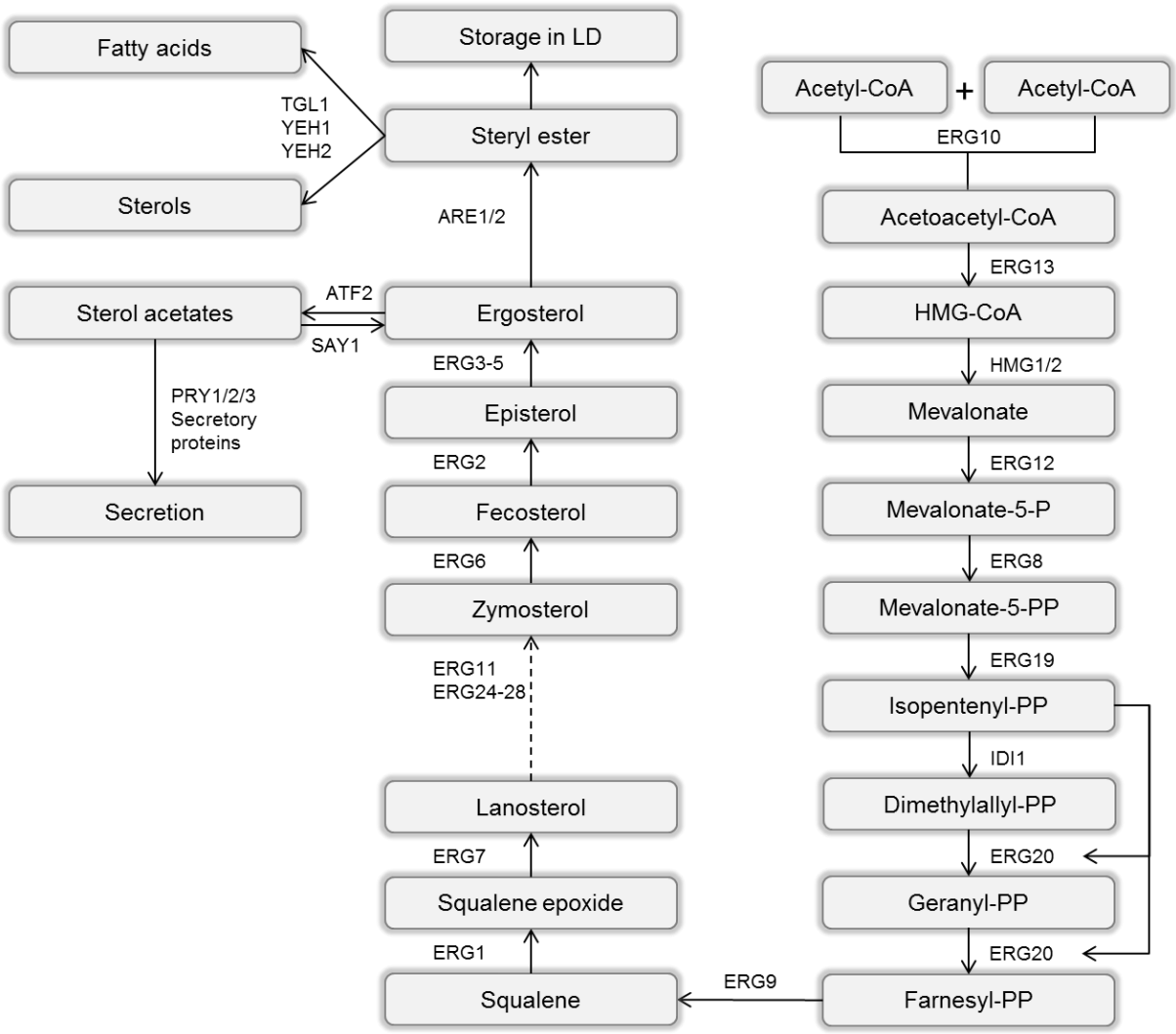

Figure 3: Sterol and sterol ester metabolism in the yeast *S. cerevisiae*

The graph shows an overview of synthesis intermediates, end products and enzymes which are involved in the individual steps of sterol metabolism. CoA, Coenzyme A; HMG-CoA, 3-hydroxy-3-methylglutaryl-CoA; P, phosphate; LD, lipid droplet.

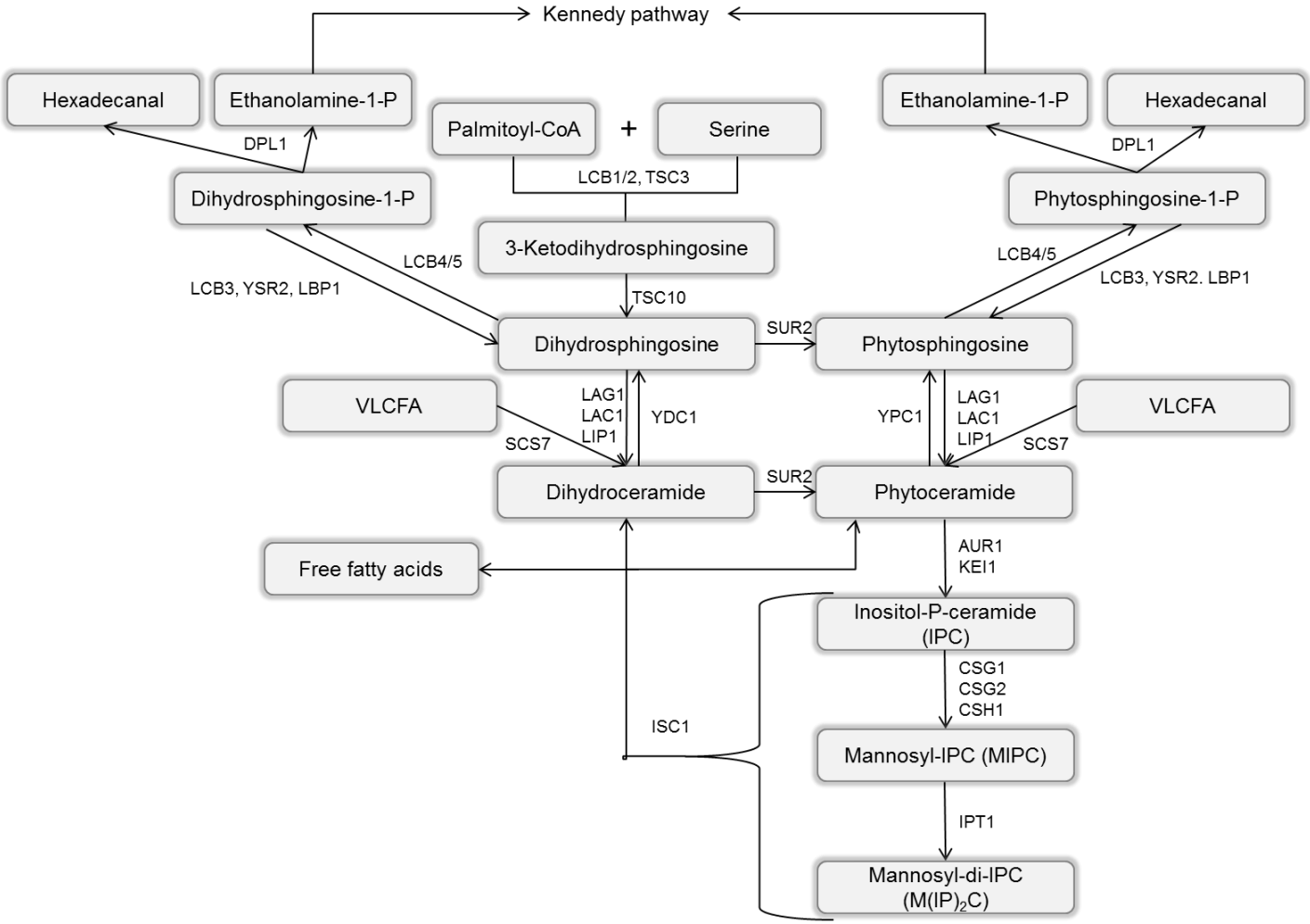

Figure 4: Sphingolipid metabolism in the yeast *S. cerevisiae*.

The biosynthetic network of sphingolipid synthesis in the yeast with the most important intermediates, end products and enzymes is shown. For a detailed description see text. P, phosphate; PP, pyrophosphate; CoA, Coenzyme A; VLCFA, very long chain fatty acid;

Chapter III

Isolation of organelles from *Pichia pastoris*

Vasyl Ivashov[1*], Lisa Klug[1*], Karlheinz Grillitsch[2] and Günther Daum[1]

[1]Institute of Biochemistry, Graz University of Technology, Austria; [2]Austrian Centre of Industrial Biotechnology, Graz, Austria

*Contributed equally to this paper and should be considered as co-first-authors

Running title: Organelles from *Pichia pastoris*

Corresponding author: Günther Daum, Institute of Biochemistry, Graz University of Technology; Petersgasse 12/2, A-8010 Graz, Austria; Tel.: +43 316 873 6462; Fax: +43 316 873 6952; E-mail: guenther.daum@tugraz.at

Summary

Pichia pastoris is widely used for heterologous protein expression but fundamental knowledge about its cell biology is largely missing. Since eukaryotic cells are compartmentalized and have an internal endomembrane system, techniques which allow isolation of these compartments (organelles) or subcellular membranes are required for studying various aspects of cell biology such as organelle biogenesis, membrane traffic, segregation of metabolic pathways and metabolite transport inside the cell. Many reliable protocols for cell fractionation were designed for the model yeast *Saccharomyces cerevisiae.* We adopted and modified these methods to study organelles from *Pichia pastoris* which is frequently used for applied biotechnology and industrial purposes. In this chapter we will describe optimized protocols for the isolation of the most important organelles from *Pichia pastoris* and briefly address applications of these techniques for cell biological investigations.

Key words

Organelles, endoplasmic reticulum, plasma membrane, vacuole, Golgi, lipid droplets, peroxisomes, mitochondria

1 Introduction

Eukaryotic cells are structurally and functionally organized in compartments called organelles. These structures are surrounded by lipid membranes with specific membrane proteins embedded. Membranes segregate the interior of organelles from the environment and therefore allow spatial separation of metabolic pathways inside the cell. Each organelle has its distinct subset of membrane and luminal proteins which fulfill structural, metabolic or regulatory functions. Such proteins can be localized exclusively to one organelle but may also be present in several compartments with related functions. To address the various questions of cell biology, molecular biology and biochemistry, isolation of organelles and cellular membranes is required. These methods are also employed to study cell biology of the yeast *Pichia pastoris* in fundamental and applied research. As examples, isolated organelles can be used to investigate their biogenesis, structural or functional properties, their components by -omics studies, and the role of individual enzyme, metabolic pathways or transport processes ***(1–3)***. Recombinant proteins which are expressed heterologously in *Pichia pastoris* move in many cases gradually from their site of synthesis to the cell periphery. The process of protein secretion which includes protein folding and protein modifications is linked to vesicle flux from the endoplasmic reticulum via Golgi to the plasma membrane. Production and secretion of proteins may lead to their accumulation in a certain organelle or in the cytoplasm ***(4, 5)***. Also in this case, organelle isolation techniques are useful tools to follow the traffic routes of such recombinant proteins.

Here we describe optimized protocols designed for isolation and quality control of organelles from *Pichia pastoris*. Techniques for yeast organelle isolation with a focus on *Saccharomyces cerevisiae* were established and described previously ***(6)***. Most of these methods are based on cell disruption and a combination of differential and density gradient centrifugation steps followed by quality control of the obtained fractions ***(7)***. Although some general principles and strategies can be applied for cell fractionation of different yeast species, each isolation procedure should be optimized for each cell type and for different culture conditions. In this chapter, we provide guidelines for the isolation of subcellular fractions from *Pichia pastoris*. Moreover, we describe the quality control of organelles which is essential for the evaluation of cell fractionation and for subsequent cell biological investigations.

2 Materials

2.1 Equipment

The basic equipment required is similar for most organelle preparation procedures.

1. 2 L shaking flasks with baffles.
2. High speed centrifuge, fixed angle rotors (e.g., SLC-3000, F21S) and centrifugation tubes (500 and 50 ml).
3. Ultracentrifuge, swing-out rotors (e.g., AH629, TH641), fixed angle rotor (e.g., T865) and centrifuge tubes.
4. Dounce homogenizer with large clearance pestle (L-pestle).
5. Cell disruptor with cooling device.
6. Glass beads, diameter 0.3 mm.

2.2 Reagents

2.2.1 Spheroplast preparation

1. Buffer SP-A: 0.1 M Tris/SO_4, pH 9.4.
2. Buffer SP-B: 1.2 M sorbitol in 20 mM KH_2PO_4/KOH, pH 7.4.
3. Dithiothreitol (DTT).
4. Zymolyase (see Note 1).

2.2.2 Isolation of peroxisomes

1. Growth media containing methanol or oleic acid (see Note 2).
2. Buffers and chemicals for spheroplast preparation (see section 2.2.1.).
3. Breaking buffer: 5 mM MES, pH 6.0, 1 M sorbitol, 1 mM KCl, 1 mM Na_2EDTA, 0.1 % ethanol, 2 mM phenylmethylsulfonyl fluoride (PMSF).
4. Gradients: 50 %, 35 %, 30 % and 24 % Accudenz (w/v) in 5 mM MES, pH 6.0, 1 mM KCl, 0.24 M sucrose.
5. 10 mM Tris/HCl, pH 7.4.

2.2.3 Isolation of mitochondria and microsomes

1. Growth media have to be chosen according to experimental requirements (see Note 3).
2. Buffers and chemicals for spheroplast preparation (see section 2.2.1.).
3. Buffer C: 0.6 M mannitol, 10 mM Tris/HCl, pH 7.4.
4. Buffer D: 10 mM Tris/HCl, pH 7.4.
5. 1 M PMSF stock in dimethylsulfoxid (DMSO).

2.2.4 Isolation of Golgi

1. Growth media should be chosen according to experimental requirements.
2. Buffers and chemicals for spheroplast preparation (see section 2.2.1.).
3. Lysis buffer: 0.6 M sorbitol, 10 mM triethanolamine hydrochloride/NaOH, pH 7.2, 1 mM EDTA.
4. MES buffer: 10 mM Mes/Tris, pH 7.2.
5. Tris buffer: 10 mM Tris/HCl, pH 7.4.
6. 40 % sucrose/MES: 40 % sucrose, 60 % MES buffer.
7. 35 % sucrose/MES: 35 % sucrose, 65 % MES buffer.
8. 30 % sucrose/MES: 30 % sucrose, 70 % MES buffer.
9. 25 % sucrose/MES: 25 % sucrose, 75 % MES buffer.
10. 5 M sorbitol.
11. 1 M PMSF stock in DMSO.

2.2.5 Isolation of vacuoles

1. Any rich growth media.
2. Buffers and chemicals for spheroplast preparation (see section 2.2.1.).
3. Stock solution: 10 mM MES/Tris, pH 6.9, 0.2 mM EDTA, 2 mM PMSF.
4. Breaking buffer: 12 % Ficoll (w/w) in stock solution.
5. 6 % Ficoll (w/w) in stock solution.
6. 3.5 % Ficoll (w/w) in stock solution.
7. 1.5 % Ficoll (w/w) in stock solution.

2.2.6 Isolation of lipid droplets

1. Any rich growth media.
2. Buffers and chemicals for spheroplast preparation (see section 2.2.1.).

3. Stock solution: 10 mM MES/Tris, pH 6.9, 0.2 mM EDTA, 2 mM PMSF.
4. Buffer LD-A: 12 % Ficoll (w/w) in stock solution.
5. Buffer LD-B: 4 % Ficoll (w/w) in stock solution.
6. Buffer LD-D: 0.25 M Sorbitol in stock solution.

2.2.7 Isolation of plasma membrane

1. Any rich growth media.
2. Solution 1: 0.5 M Tris/HCl, pH 8.5.
3. Solution 2: 0.5 M EDTA/NaOH, pH 8.0.
4. TE buffer: 10 mM Tris/HCl, 0.2 mM EDTA, pH 7.5.
5. TED: 10 mM Tris/HCl, 0.2 mM EDTA, pH 7.5, 0.2 mM DTT (see Note 4).
6. TEDG buffer: 80 % TE buffer, 20 % glycerol, 0.2 mM DTT, pH 7.5. (see Note 4).
7. 53 % sucrose/TED: 53 % sucrose, 47 % TE buffer, 0.2 mM DTT (see Note 4).
8. 43 % sucrose/TED: 43 % sucrose, 57 % TE buffer, 0.2 mM DTT (see Note 4).
9. MES buffer: 5 mM MES, 0.2 mM EDTA, pH 6.0.
10. 53 % sucrose/MES: 53 % sucrose, 47 % MES buffer.
11. 43 % sucrose/MES: 43 % sucrose, 57 % MES buffer.
12. 38 % sucrose/MES: 38 % sucrose, 62 % MES buffer.
13. 1 M PMSF stock in DMSO.
14. Dithiothreitol (DTT).

3 Methods

3.1 Spheroplast preparation

Yeast spheroplast preparation based on the treatment with Zymolyase® 20T has been described previously ***(8)***. This procedure is prerequisite for most isolation protocols described here and allows digestion/removal of the cell wall making cells susceptible for gentle mechanical and osmotic disintegration.

1. When the culture has reached the desired growth phase, cells are harvested by centrifugation at 2,500 x g for 4 min.

2. Cell pellets are washed once with deionized water and the cell wet weight (CWW) is estimated.
3. Suspend cells in pre-warmed (30°C) buffer SP-A: Use 0.5 g CWW/ml buffer and add 0.66 mg/ml DTT per ml SP-A. Incubate with shaking at 30°C for 10 min.
4. Centrifuge cells at 2,500 x g for 4 min. Remove supernatant, wash cell pellet with 1-2 volumes buffer SP-B and centrifuge at 2,500 x g for 4 min.
5. Resuspend cell pellet in pre-warmed (30°C) buffer SP-B. Use 0.15 g CWW/ml, add Zymolyase 20T (2 mg/g CWW) and incubate with shaking at 30°C.
6. Conversion of whole cells to spheroplasts takes approximately 30-60 minutes (see Note 5).
7. Harvest spheroplasts by centrifugation at 2,500 x g for 4 min. Remove supernatant carefully without suspending the pellet.
8. Wash spheroplasts with ice-cold SP-B and centrifuge as described above (see Note 6). After this step, spheroplasts are ready for disintegration.

3.2 Isolation of peroxisomes

The protocol for the isolation of peroxisomes from *Pichia pastoris* was adapted from procedures described previously ***(1, 9)***.

1. Inoculate YPM or YPO media with an aliquot of a YPD grown preculture to an OD_{600} of 0.1. Grow cells to the late logarithmic phase in shaking flasks at the desired temperature. The time of cultivation depends on the growth conditions. Typically, 3-5 L main culture will yield peroxisome samples with a total amount of 1.5–2 mg protein.
2. Harvest cells and prepare spheroplasts (see section 3.1.).
3. Preparation of homogenate: Add an equal volume of breaking buffer and disintegrate spheroplasts with 10 strokes in a Dounce Homogenizer using a loose (L) fitting pestle. Save an aliquot of the homogenate if needed and store at -80°C.
4. Centrifuge the homogenate for 5 min at 3,000 x g to remove cell debris and high density components. Collect supernatant in a fresh tube. Resuspend the pellet in an equal volume of breaking buffer and repeat homogenization and centrifugation. Discard pellet and combine cell-free supernatants.
5. Centrifuge supernatant at 30,000 x g for 30 min.
6. Discard supernatant, add 2-3 volumes of breaking buffer to the pellet and resuspend in a Dounce homogenizer by 3-5 strokes.

7. Load suspension on top of a step gradient composed of 5 ml 50 %, 10 ml 35 %, 10 ml 30 %, 7 ml 24 % of Accudenz (w/v) in 5 mM MES, pH 6.0, l mM KCl, 0.24 M sucrose (see Note 7).
8. Centrifuge gradient at 122,000 x g for 2 h. After centrifugation, peroxisomes form a band at the interface of 35 % and 30 % Accudenz. Collect the peroxisomal fraction carefully with a syringe by inserting the needle from the side of the tube. As a byproduct of this centrifugation step, a fraction enriched in mitochondria can be collected from the 30 % - 24 % Accudenz interphase.
9. Wash peroxisomes with 4 volumes of breaking buffer and centrifugation at 30,000 x g for 30 min. Remove supernatant. The pellet containing purified peroxisomes can be suspended in a small volume of any buffer for further analysis.

3.3 Isolation of mitochondria

The isolation of mitochondria from *Pichia pastoris* has been reported previously ***(2)***.

1. Pre-cultures grown to the stationary phase are used for inoculating main cultures in Erlenmeyer flasks with baffles. Cells are grown at the desired cultivation conditions (temperature, growth media and carbon source, aeration). Typically, cells are harvested when they have reached the late exponential growth phase (see Note 8).
2. Harvest cells by centrifugation at room temperature (RT) at 2,500 x g for 5 min.
3. Wash cells with deionized water and prepare spheroplasts (see section 3.1.).
4. Suspend spheroplast pellet in buffer C (1 ml/g CWW) and add 1 M PMSF (2 µl/g CWW).
5. Transfer cells into a Dounce homogenizer and disintegrate them with 15 strokes on ice using an L-pestle.
6. Centrifuge for 5 min at 5,100 x g at 4°C. Rinse the homogenizer with 10 ml buffer C to collect residual material.
7. Collect supernatant (homogenate) and store on ice.
8. Repeat steps 7 to 9 twice. Add PMSF each time. Combine all three supernatants, withdraw 1-3 ml homogenate samples and store them at -80°C for further analysis. The pellet can be discarded after the third round of cell disintegration.
9. Sediment the homogenate (combined supernatants) for 10 min at 12,000 x g at 4°C.

10. Remove the supernatant and clean the inside of the centrifugation tube carefully with a paper towel to avoid contamination with other organelles without suspending the pellet. The supernatant contains the cytosol and microsomes (see section 3.4.).
11. The pellet is suspended in 30 ml buffer C and transferred to a new centrifugation tube.
12. Centrifuge for 5 min at 5,100 x g at 4°C to remove all cell debris.
13. Transfer supernatant into a new centrifugation tube and centrifuge for 10 min at 12,000 x g at 4°C.
14. Remove the supernatant and clean the inside of the tube carefully with a paper towel to reduce the risk of contamination with other subcellular fractions. Mitochondria (pellet) are suspended in 1-2 ml buffer D depending on the size of the pellet. Samples can be stored at -80°C for further analysis.

3.4 Isolation of microsomes

The isolation of microsomes from *Pichia pastoris* as described recently ***(10)*** can be performed as a continuation of the isolation protocol of mitochondria (see section 3.3.). Typically 30-40 g of cells will yield a microsomal fraction containing 1-2 mg protein.

1.-10. These steps are identical to section 3.3.

11. After centrifugation at 12,000 x g for 10 min at 4°C, transfer supernatant to a new centrifuge tube. The supernatant contains the cytosol and microsomes, the pellet contain the mitochondria.
12. Centrifuge supernatant for 30 min at 20,000 x g at 4°C using a fixed angle rotor.
13. Discard pellet which contains an intermediate/mixed fraction. Transfer supernatant to a new centrifuge tube and centrifuge for 30 min at 30,000 x g at 4°C.
14. The pellet contains the 30,000 x g microsomal fraction. Transfer supernatant to a new centrifuge tube and centrifuge supernatant for 30 min at 40,000 x g at 4°C. Suspend the 30,000 x g pellet in 1-2 ml buffer D depending on the size of the pellet. The resuspended pellet can be stored at -80°C till further analysis.
15. After centrifugation at 40,000 x g, the resulting pellet contains the 40,000 x g microsomal fraction. Transfer the supernatant to ultracentrifugation tubes and centrifuge for 45 min at 100,000 x g at 4°C using a fixed angle rotor. Suspend the 40,000 x g pellet in 1-2 ml buffer D depending on the size of the pellet and store the sample at -80°C until further analysis.

16. After ultracentrifugation at 100,000 x g, the supernatant (cytosol) is removed; the 100,000 x g microsomal pellet is suspended in 1-2 ml buffer D and stored at -80°C for further analysis. Cytosol samples can also be collected and stored at -80°C.

3.5 Isolation of the Golgi

The isolation of the Golgi follows a procedure developed recently in our lab (Grillitsch *et al.*, manuscript in preparation).

1. Pre-cultures grown to the stationary phase are used for inoculating main cultures in baffled Erlenmeyer flasks.
2. Cells are incubated until they have reached the mid exponential to late exponential growth phase (see Note 9).
3. Harvest cells by centrifugation at room temperature at 2,500 x g for 5 min using a fixed angle rotor.
4. Wash cells with deionized water and prepare spheroplasts as described in section 3.1.
5. Suspend sedimented spheroplasts in lysis buffer (1 ml/1.5 g CWW) and add PMSF (2 µl/g CWW). Disintegration of spheroplasts for the isolation of Golgi is critical and requires gentle handling and moderate mechanical force.
6. Homogenize spheroplasts in suspension using a Dounce homogenizer by disintegrating with 3 strokes on ice using an L-pestle.
7. Transfer homogenized suspension into a beaker and fill up with approximately 2-3 volumes of lysis buffer.
8. Incubate spheroplasts under slight agitation on a magnetic stirrer for 20 min at 4°C.
9. Add sorbitol from a 5 M stock to a final concentration of 1 M. Take into account that the suspension already contains 0.6 M sorbitol from the lysis buffer.
10. Sediment intact spheroplasts and cell debris for 5 min at 3,600 x g at 4°C using a fixed angle rotor.
11. Discard pellet, withdraw 1-2 ml from the supernatant (homogenate) and store at -80°C for further analysis.
12. To obtain loading material for density gradient ultracentrifugation the cleared homogenate is subjected to several steps of differential centrifugation (Figure 1). First, high speed centrifugation is performed at 12,000 x g at 4°C for 10 min (pellet 1, P1).
13. To remove residual mitochondria the supernatant of the previous centrifugation step is centrifuged for 20 min at 20,000 x g at 4°C (pellet 2, P2).

14. The supernatant resulting from step 14 is centrifuged at 30,000 x g for 30 min at 4°C. In the obtained pellet fraction (pellet 3, P3) cis-Golgi marker proteins are enriched. This sample is loaded onto the final sucrose density gradient to obtain enriched and purified cis-Golgi fractions (see step 19). The sample should be stored on ice.
15. The resulting supernatant of step 15 is centrifuged at 40,000 x g for 30 min at 4°C (pellet 4, P4).
16. Transfer supernatant to an ultracentrifuge tube and separate soluble cytosol from membranes (mostly vesicle populations) by centrifugation at 200,000 x g at 4°C using a fixed angle rotor. The pellet (pellet 5, P5) is enriched in trans-Golgi marker proteins and loaded onto the final sucrose density gradient to obtain enriched and purified trans-Golgi (see step 19). The sample should be stored on ice.
17. Preparation of sucrose density gradients: The gradient consists of 2.5 ml, each, of sucrose/MES with concentrations of 40 %, 35 %, 30 % and 25 % sucrose. High quality of gradients is critical for successful separation of subcellular fractions.
18. Pellet fractions obtained after 30,000 x g (P3) and 200,000 x g (P5) centrifugation are resuspended in MES buffer (10 mM, pH 7.2). Samples are well homogenized in a Dounce homogenizer before loading onto a sucrose density gradient for separate isolation of cis- and trans-Golgi fractions. Ultracentrifugation using a swing out rotor is performed for at least 5 h at 200,000 x g at 4°C (see Note 10).
19. After ultracentrifugation, samples are taken from the four phase separation zones (cis F1-F4, trans F1-F4) with the aid of a syringe (approximately 1.5 ml per sample). Samples can be either frozen directly in sucrose solution or sedimented in a final centrifugation step. For sedimentation samples should be diluted 5-fold with 10 mM Tris/HCl, pH 7.4, and centrifuged at 200,000 x g for 45 min at 4°C using a fixed angle rotor.
20. Samples should be critically evaluated for the enrichment of Golgi markers, e.g. Emp47p, and the absence of other subcellular fractions. Depending on the strain, cultivation conditions, and experimental handling the best enrichment of highly purified fractions of cis- or trans-Golgi, respectively, may vary in cis F1-F4 and trans F1-F4.
21. Pellet fractions generated throughout this isolation procedure can be suspended in appropriate volumes of 10 mM Tris/HCl, pH 7.4, and used as loading controls when testing the quality of the final Golgi samples. Samples should be kept at -80°C.

3.6 Isolation of vacuoles

A number of protocols have been published for the isolation of vacuoles from yeast. Most of these methods are based on gradient centrifugation and floatation ***(11, 12)***. Here we present a modified protocol for the isolation of *Pichia pastoris* vacuoles which yields highly enriched samples (Ivashov *et al*., manuscript in preparation).

1. Inoculate YPD media or any other rich media with a preculture grown on YPD to a final OD_{600} of 0.1. Grow cells to the mid stationary phase (16-17 h) in shaking flasks at 30°C. The cultivation time depends on growth conditions. Typically, 50 g cells will yield a vacuolar fraction containing 2-3 mg protein.
2. Harvest cells by centrifugation at 2,500 x g for 4 min.
3. Remove supernatant, wash cells with deionized water and sediment them at 2,500 x g for 4 min.
4. Spheroplasts preparation has been described in section 3.1. As the whole procedure is time consuming, steps after spheroplasts preparation may be continued on the next day. Spheroplasts can be frozen in liquid nitrogen and then thawed quickly on a 30°C water bath. Noteworthy, storage of spheroplasts overnight reduces the yield of vacuoles to ~50%.
5. For the preparation of the homogenate, suspend spheroplasts in 1.5 to 2 volumes of ice-cold breaking buffer. Disintegrate spheroplasts with 30 strokes in a Dounce Homogenizer using a loose fitting pestle. Utilization of complex protease inhibitors is strongly recommended (see Note11). Save homogenate sample if needed for further analysis and store at -80°C.
6. Load 25 ml of homogenate, each, to the bottom of ultracentrifuge tubes and overlay with 6% Ficoll solution to the top of the tube. Centrifuge at 140,000 x g for 90 min using a swing-out rotor, e.g. AH629. Collect the floating layers from each tube.
7. Add an equal volume of 6 % Ficoll solution to the combined floating layers and mix with 6 strokes in a Dounce homogenizer. Load suspension to the bottom of ultracentrifuge tube and overlay carefully with stock solution to the top of the tube. Centrifuge at 140,000 x g for 2 h.
8. Withdraw the band from the interphase of 6 % Ficoll layer and stock solution with the aid of a syringe. This fraction contains crude vacuoles.
9. Add 2 volumes of 6 % Ficoll to crude vacuoles and load to the bottom of an ultracentrifuge tube. Overlay the suspension with 3.5 % Ficoll solution to the top of

the tube. Centrifuge at 140,000 x g for 3 h. Collect the floating layer and, if present, any dispersed white fraction beneath.

10. Dilute the collected fraction with 5-6 volumes of 1.5 % Ficoll. Centrifuge suspension at 100,000 x g for 30 min. Discard the supernatant, but avoid dispersing the pellet which contains purified vacuoles. Suspend vacuoles in 2-3 ml of stock solution or any buffer required for further experiments and store at -80°C.

3.7 Isolation of lipid droplets

A protocol for the isolation of highly purified lipid droplets from *Pichia pastoris* has been described previously ***(3)***.

1. Inoculate YPD media or any other rich media with a preculture grown on YPD to a final OD_{600} of 0.1. Grow cells to the early stationary phase in shaking flasks at 30°C. The cultivation time depends on growth conditions. Lipid droplets are formed during growth on any media, but the highest yield can be obtained from cells grown on YPO. Typically, 100 g of cells grown on YPD will yield lipid droplets containing 250-350 µg protein. Please note that the amount of proteins in lipid droplets compared to lipid components is very low.
2. Harvest cells by centrifugation at 2,500 x g for 4 min.
3. Remove supernatant, wash cells with deionized water and sediment them at 2,500 x g for 4 min.
4. Prepare spheroplasts as described in section 3.1.
5. To prepare the homogenate suspend spheroplasts in an equal volume of ice-cold buffer LD-A. Disintegrate spheroplasts with 30 strokes in a Dounce Homogenizer using a loose fitting pestle.
6. Centrifuge the homogenate at 6,000 x g for 5 min and save supernatant. Add an equal volume of buffer LD-A to the remaining pellet, repeat disintegration in a Dounce Homogenizer by 15 strokes and centrifuge again at 6,000 x g for 5 min. Discard pellet and combine supernatants.
7. Centrifuge combined supernatants at 12,000 x g for 15 min. Save supernatant and discard pellet.
8. Load 25 ml of the supernatant, each, to the bottom of ultracentrifuge tubes and overlay with buffer LD-B to the top of the tube. Centrifuge at 140,000 x g for 1 h. Collect floating layers from the top of tubes and combine.

9. Suspend floating layer in 10 volumes of buffer LD-B and mix by 5-7 strokes in a Dounce homogenizer. Fill samples into ultracentrifuge tube and centrifuge at 140,000 x g for 1 h. Collect the floating layer.
10. Suspend the floating layer in an equal volume of buffer LD-B and load to the bottom of ultracentrifuge tube. Overlay suspension with buffer LD-D. Centrifuge at 140,000 x g for 90 min. The resulting floatate contains highly purified lipid droplets. Collect lipid droplets from the top of the tube using a sampler and store at -80°C.

3.8 Isolation of Plasma Membrane

A procedure for the isolation of plasma membrane from *Pichia pastoris* was recently developed in our lab (Grillitsch *et al*., manuscript submitted). Typically, 30 g of cells yield plasma membrane samples containing 2-3 mg protein.

1. Stationary grown pre-cultures are used to inoculate main cultures in baffled Erlenmeyer flasks.
2. Incubation conditions can vary depending on experimental requirements. However, cells should be incubated until they have reached the late exponential growth phase.
3. Harvest cells by centrifugation at room temperature at 2,500 x g for 5 min using a fixed angle rotor.
4. Wash cells once with deionized water and estimate cell wet weight (CWW).
5. Yeast cells are suspended in breaking buffer (20 g CWW in 84 deionized water; 5 ml of 0.5 M TrisCl, pH 8.5; 1 ml of 0.5 M EDTA, pH 8.0; 0.25 ml of 0.2 M PMSF).
6. Disintegrate cells mechanically by using glass beads under constant cooling and vigorous shaking for 3 min in any tissue/cell disintegrator. Let the glass beads sediment and collect supernatant on ice. After disintegration of the entire cell pellet, glass beads are washed once with TEDG buffer.
7. Cell extracts are cleared of unbroken cells and residual glass beads by centrifugation at 1,000 x g for 10 min using a fixed angle rotor. Discard pellet.
8. The resulting supernatant (homogenate) is centrifuged at 35,000 x g for 30 min to sediment bulk membranes using a fixed angle rotor. Suspend the pellet in TEDG-buffer and store on ice until loading the sucrose density gradient. Samples should be homogenized with 10 strokes in a Dounce homogenizer using a loose-fitting pestle.

9. Preparation of sucrose density gradients: 1 volume of 53 % sucrose in TED-buffer and 2 volumes of 43 % sucrose in TED-buffer. Do not load samples from more than 20 g CWW per gradient (total volume ~40ml).
10. Centrifuge for at least 3.5 h at 100,000 x g at 4°C using a swing out rotor.
11. After ultracentrifugation harvest the crude plasma membrane fraction at the 43/53 % sucrose interface with the aid of a syringe.
12. Dilute the sample 3- to 4-fold with deionized water and centrifuge for 20 min at 45,000 x g at 4°C using a fixed angle rotor to sediment membranes. Suspend the pellet in MES-buffer and store on ice until loading the sucrose density gradient. Samples should be homogenized with 10 strokes in a Dounce homogenizer using a loose-fitting pestle.
13. Preparation of the second sucrose density gradient: 1 volume of 53 %, 43 % and 38 % sucrose, each, in MES-buffer. Do not load samples from more than 20 g CWW per gradient.
14. Centrifuge for at least 2.5 h at 100,000 x g at 4°C using a swing out rotor (see Note 12).
15. After ultracentrifugation harvest the plasma membrane fraction at the interface between 53 % and 43 % sucrose.
16. Dilute the plasma membrane fraction 5-fold with Tris/HCl buffer (10 mM, pH 7.4) and centrifuge for 20 min at 45,000 x g at 4°C using a fixed angle rotor.
17. Discard supernatant without dispersing the pellet (PM2) which is not very stable.
18. Suspend pellet in Tris/HCl buffer (10 mM, pH 7.4) and store the plasma membrane fraction at -80°C for further analysis.

3.9 Quality Control of Isolated Organelles

Quality control of organelle fractions obtained by procedures described above is essential to ensure enrichment and purity. These tests are routinely carried out by Western blot analysis. For this purpose, 5-15 µg of precipitated protein from organelle fractions of interest and homogenate sample as a control are subjected to SDS polyacrylamide electrophoresis (SDS-PAGE), transferred to nitrocellulose or PVDF membrane and probed with primary antibodies recognizing typical marker proteins of particular organelles. By comparing intensities of bands from organelle samples and homogenate the enrichment factor can be estimated, provided that the amount of protein loaded onto each lane is exactly the same. Typical

examples of yeast organelle marker proteins are: mitochondrial porin Por1p; plasma membrane ATPase Pma1p; sterol 24-C-methyltransferase Erg6p from lipid droplets, vacuolar carboxypeptidase Y (CPY; Prc1p), Pex3p from peroxisomes; beta-subunit of the endoplasmic reticulum resident oligosaccharyl transferase glycoprotein complex Wbp1p; and glyceraldehyde-3-phosphate dehydrogenase (GAPDH) from the cytosol. Specific antibodies raised against *Pichia pastoris* proteins are rare. In many cases, antibodies raised against the *Saccharomyces cerevisiae* orthologs can be used, although sometimes immunoreactions are weak. Another possibility to test for organelle markers is the use of hybrid proteins containing GFP, HIS, HA or any other tag. When these hybrids are expressed in *Pichia pastoris* under the native promoter, they can be detected with commercially available primary antibodies specific for the respective tag. Alternatively to Western Blot analysis marker enzyme assays can be performed to assess the quality of organelle preparations ***(6, 13)***.

High enrichment of organelles over the homogenate is desirable for cell fractionation experiments (Fig. 2A). In most cases, however, organelle preparations still contain impurities of other subcellular compartments. These contaminations can be due to naturally occurring tight association of organelles (e.g. ER and Golgi, ER and lipid droplets, mitochondria and peroxisomes) ***(14–17)*** or to artifacts created during the cell fractionation procedure. Therefore, it is important to check organelle purity, e.g. by Western Blot analysis as shown in Fig. 2B. If signals of "foreign" markers are present in homogenate but largely absent from the organelle fraction of interest, the purity can be regarded as high. The presence of markers from other organelles in the sample at the amounts comparable to homogenate would, however, indicate low quality of the respective cell fraction.

4 Notes

1. Instead of zymolyase, lyticase can be used for spheroplasts preparation following the manufacturer's instructions.
2. For the isolation of most organelles rich growth media like YPD (1 % yeast extract, 2 % peptone, 2 % glucose) are suitable. For isolation of peroxisomes, media containing methanol (0.5 -2 %; YPM) or oleic acid (0.2 %; YPO) as carbon sources are required to induce the proliferation of peroxisomes. In principle, however, different growth media (minimal or complex media) can be used depending on the scientific problem.
3. Repression of mitochondria proliferation by high glucose concentrations has to be taken into account. Utilization of non-fermentable carbon sources such as glycerol or lactate may be advantageous for increasing the yield of mitochondria.
4. DTT must be added directly before use of the buffer. Buffers containing DTT are not considered for long term storage.
5. Withdraw samples of 10 µl, each, prior to the addition of zymolyase and at different time points of incubation with zymolyase during the spheroplasting procedure. Samples are diluted 1000-fold in deionized water. To monitor the efficiency of zymolyase treatment compare untreated to treated samples. When the solution of zymolyase treated samples turns clear, spheroplasting is complete. In case of inefficient conversion of intact cells to spheroplasts, the incubation time can be extended, or amounts of the enzyme may be increased.
6. After spheroplasts were obtained, all further steps should be performed on ice using ice-cold buffers. All centrifugation steps should be performed at 4°C.
7. Step gradients should be loaded carefully to avoid mixing of layers. Correct handling results in sharp border lines of interphases which are clearly visible. If no border lines are visible, gradients should be discarded.
8. Cells grown on glucose (30-40 g CWW) will yield mitochondria fractions containing 5-6 mg protein. Please note that the amount of mitochondria obtained highly depends on the carbon source utilized. Growth of cells on fermentable carbon sources will increase the yield markedly.
9. For the isolation of Golgi fractions cells should be harvested at latest when they have reached the late exponential phase. Depletion of nutrients or starvation of cell should be strictly avoided, because all conditions provoking autophagy might negatively affect the yield of Golgi.

10. In case no clear phase separation has been achieved after 5 h of ultracentrifugation, the centrifugation period can be extended. Another reason for unsuccessful separation may be overloading of gradients. The maximum load of gradients has to be defined empirically. As a rule of thumb, single gradients for the isolation of trans-Golgi can be loaded with the double amount of material compared to single gradients used for the isolation of cis-Golgi.
11. If inhibition of proteolysis is crucial for further experiments, commercially available protease inhibitor cocktails can be added to the breaking buffer and all other buffers at amounts recommended by the manufacturer. Since vacuoles harbor many highly active proteases, the use of complex protease inhibitor cocktails and not only PMSF is strongly recommended.
12. Ultracentrifugation of the second density gradient can be continued overnight.

Acknowledgements

This work was supported by the Austrian Science Fund FWF (project TRP009 and DK Molecular Enzymology to GD), the Federal Ministry of Economy, Family and Youth (BMWFJ), the Federal Ministry of Traffic, Innovation and Technology (bmvit), the Styrian Business Promotion Agency SFG, the Standortagentur Tirol and ZIT – Technology Agency of the City of Vienna through the COMET-Funding Program managed by the Austria Research Promotion Agency FFG, and by the Austrian Centre of Industrial Biotechnology (ACIB GmbH). We are grateful to Dr. Tamara Wriessnegger for providing unpublished results of Western blot analyses of mitochondria fractions.

References

1. T. Wriessnegger, G. Gübitz, E. Leitner, et al. (2007) Lipid composition of peroxisomes from the yeast *Pichia pastoris* grown on different carbon sources, Biochim. Biophys. Acta, 1771, 455–461.

2. T. Wriessnegger, E. Leitner, M.R. Belegratis, et al. (2009) Lipid analysis of mitochondrial membranes from the yeast *Pichia pastoris*, Biochim. Biophys. Acta, 1791, 166–172.

3. V.A. Ivashov, K. Grillitsch, H. Koefeler, et al. (2013) Lipidome and proteome of lipid droplets from the methylotrophic yeast *Pichia pastoris*, Biochim. Biophys. Acta, 1831, 282–290.

4. A. Lenassi Zupan, S. Trobec, V. Gaberc-Porekar, et al. (2004) High expression of green fluorescent protein in *Pichia pastoris* leads to formation of fluorescent particles, J. Biotechnol., 109, 115–122.

5. G. Yang, T. Liu, W. Peng, et al. (2006) Expression and localization of recombinant human EDG-1 receptors in *Pichia pastoris*, Biotechnol. Letters, 28, 1581–1586.

6. E. Zinser and G. Daum (1995) Isolation and biochemical characterization of organelles from the yeast *Saccharomyces cerevisiae*, Yeast, 11, 493–536.

7. S.E. Rieder and S.D. Emr (2001) Overview of subcellular fractionation procedures for the yeast *Saccharomyces cerevisiae*, Curr. Protoc. Cell Biol., Chapter 3, Unit 3.7.

8. G. Daum, P.C. Böhni, and G. Schatz (1982) Import of proteins into mitochondria. Cytochrome b_2 and cytochrome c peroxidase are located in the intermembrane space of yeast mitochondria, J. Biol. Chem., 257, 13028–13033.

9. K.N. Faber, J.A. Heyman, and S. Subramani (1998) Two AAA family peroxins, PpPex1p and PpPex6p, interact with each other in an ATP-dependent manner and are associated with different subcellular membranous structures distinct from peroxisomes, Mol. Cell. Biol., 18, 936–943.

10. L. Klug, P. Tarazona, C. Gruber, et al. (2014) The lipidome and proteome of microsomes from the methylotrophic yeast *Pichia pastoris*, Biochim. Biophys. Acta, 1841, 215-226.

11. J. Sinha, B.A. Plantz, M. Inan, et al. (2005) Causes of proteolytic degradation of secreted recombinant proteins produced in methylotrophic yeast *Pichia pastoris*: case study with recombinant ovine interferon-tau, Biotechnol. Bioeng., 89, 102–112.

12. E. Wiederhold, T. Gandhi, H.P. Permentier, et al. (2009) The yeast vacuolar membrane proteome, Mol. Cell. Prot., 8, 380–392.

13. B. Gaigg, R. Simbeni, C. Hrastnik, et al. (1995) Characterization of a microsomal subfraction associated with mitochondria of the yeast, *Saccharomyces cerevisiae*. Involvement in synthesis and import of phospholipids into mitochondria, Biochim. Biophys. Acta, 1234, 214–220.

14. A. Toulmay and W.A. Prinz (2011) Lipid transfer and signaling at organelle contact sites: the tip of the iceberg, Curr. Op. Cell Biol., 23, 458–463.

15. A.A. Rowland and G.K. Voeltz (2012) Endoplasmic reticulum-mitochondria contacts: function of the junction, Nat. Rev. Mol. Cell Biol., 13, 607–625.

16. T. Levine and C. Loewen (2006) Inter-organelle membrane contact sites: through a glass, darkly, Curr. Opin. Cell Biol., 18, 371–378.

17. D. Binns, T. Januszewski, Y. Chen, et al. (2006) An intimate collaboration between peroxisomes and lipid bodies, J. Cell Biol., 173, 719–731.

Figures and legends

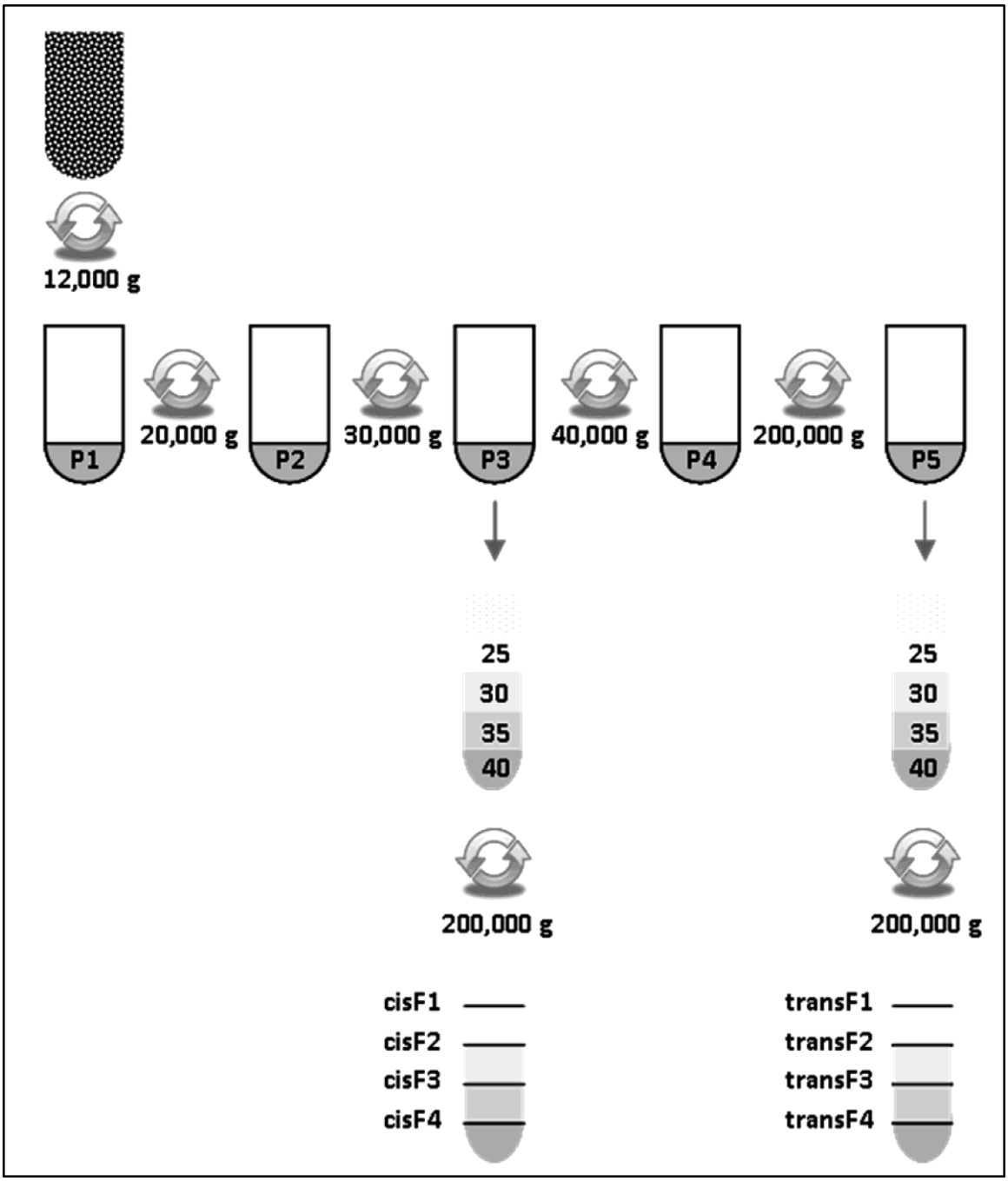

Figure 1: Chart flow of differential and density gradient ultracentrifugation steps for the isolation of Golgi fractions.

P1-5 pellet fractions are sedimented after centrifugation as indicated. Pellet fractions P3 and P5 are used for loading sucrose density gradients (40/35/30/25 % sucrose). Fractions cisF1-F4 and transF1-F4 are harvested from gradients and tested for the enrichment of Golgi marker proteins.

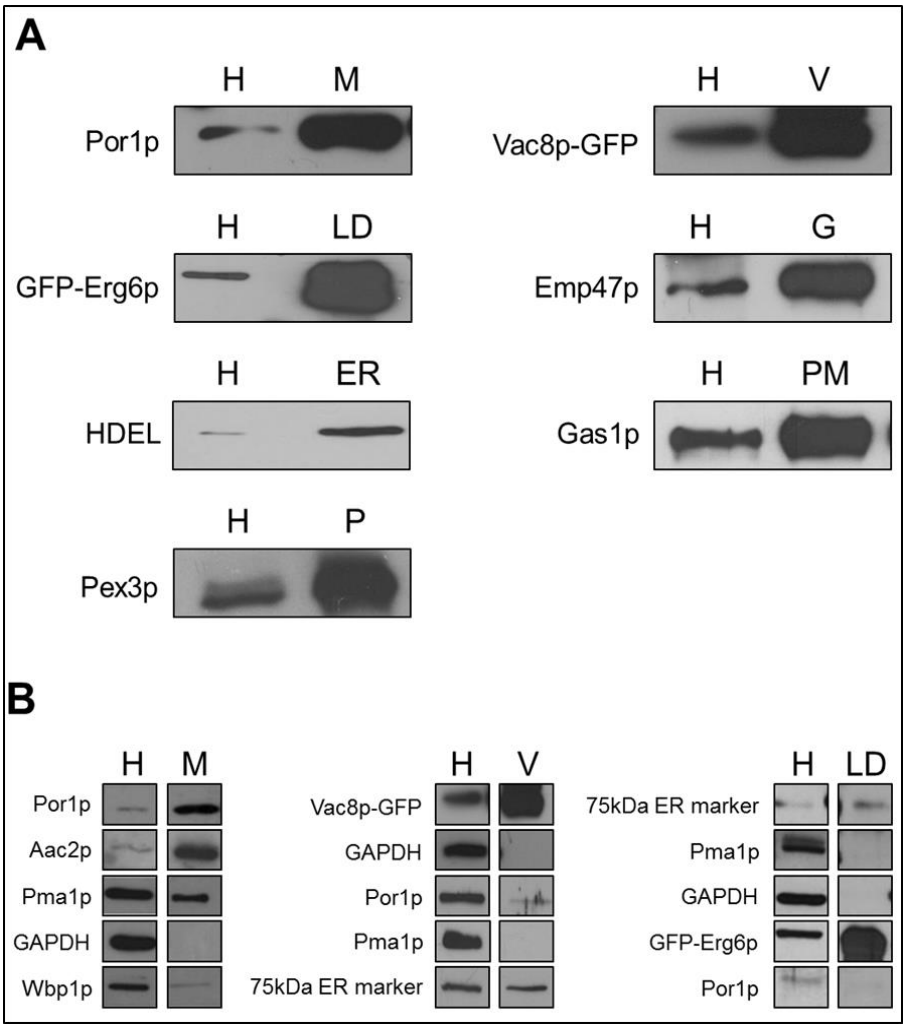

Figure 2: Enrichment and quality control of isolated organelles

A - Western Blot analysis showing the enrichment of organelle fractions over cell homogenate. Antibodies raised against organelle marker proteins were Por1p, Aac2p, Pex3p, Emp47p, and Gas1p. Commercially available GFP-reactive antibodies were applied for detecting fusion constructs of Erg6p and Vac8p, respectively. Commercially available HDEL-antibody recognizes the retention signal motif HDEL of the endoplasmic reticulum resident protein BiP. Ten µg of organelle protein and homogenate were applied. H- homogenate, M- mitochondria, LD- lipid droplets, ER- endoplasmic reticulum 40,000 x g microsomes, P- peroxisomes, V- vacuoles, G- trans-Golgi fraction, PM- plasma membrane.

B – Evaluation of cross-contamination by Western Blot analysis. Ten µg of organelle proteins and homogenate were applied. H- homogenate, M- mitochondria, V- vacuoles, LD- lipid droplets. Organelle marker proteins were mitochondrial Por1p and Aac2p; plasma membrane ATPase Pma1p; cytosolic GAPDH; endoplasmic reticulum 75 kDa marker protein and Wbp1p; vacuolar Vac8p-GFP fusion protein; and lipid droplet GFP-Erg6p fusion protein.

Chapter IV

Pichia Lipidomics

Lisa Klug[1*], Vasyl Ivashov[1*], Karlheinz Grillitsch[2] and Günther Daum[1]

[1]Institute of Biochemistry, Graz University of Technology, Austria; [2]Austrian Centre of Industrial Biotechnology, Graz, Austria

*Contributed equally to this paper and should be considered as co-first-authors

Running title: Pichia Lipidomics

Corresponding author: Günther Daum, Institute of Biochemistry, Graz University of Technology; Petersgasse 12/2, A-8010 Graz, Austria; Tel.: +43 316 873 6462; Fax: +43 316 873 6952; E-mail: guenther.daum@tugraz.at

Summary

The yeast *Pichia pastoris* has become a valuable eukaryotic model organism which is frequently used as a tool for industrial protein production. Despite these important applications, cell biological aspects of *Pichia pastoris* including problems of biomembrane and lipid research have not been adequately addressed. As lipids play an important role in various cell biological processes such as compartmentation, transport processes and signaling, our laboratory has started a systematic approach to study this class of biomolecules in some detail. In this chapter we describe materials and protocols for lipid analysis with *P. pastoris*. Standard methods for fatty acid, phospholipid and sterol analyses are presented.

Key words

Lipids, fatty acids, phospholipids, sterols, triacylglycerols

1 Introduction

Lipids are a major group of biomolecules characterized by their hydrophobic properties. They are essential components of all biological membranes but also serve as storage molecules to provide a source of energy and building blocks for membrane biogenesis. Moreover, lipids are signaling molecules and involved in many cellular processes like membrane fusion or induction of apoptosis *(1–3)*. Lipids can be classified in eight distinct groups based on their structure and function. These classes are fatty acids, glycerolipids, glycerophospholipids, sphingolipids, sterols and sterol derivatives, prenol lipids, glycolipids and polyketides *(4, 5)*. Biosynthesis of lipids occurs mainly in the endoplasmic reticulum, the Golgi apparatus and mitochondria. Consequently, newly synthesized lipids have to be transported to the other organelles which are devoid of lipid synthesizing enzymes *(6, 7)*.

Yeast organelles are characterized by their specific lipid composition *(8, 9)*. Such studies have been extensively performed with *Saccharomyces cerevisiae*, whereas lipids of the biotechnologically important yeast *P. pastoris* have not been studied in much detail. In the present chapter, different techniques for the analysis of lipids from *P. pastoris* are described. Most of these methods are adopted from protocols used for *S. cerevisiae*. The first step in lipid analysis is the extraction from cellular material. Different chromatographic methods such as thin layer chromatography (TLC) and gas lipid chromatography (GLC) are employed to separate and quantify individual lipid classes and species *(1)*. More detailed lipidome studies are performed by mass spectrometry techniques *(10, 11)*. Here, we provide basic lab protocols for lipid analysis of *P. pastoris* with a focus on the most common lipid classes.

2 Materials

Use deionized water for preparation of all solutions and organic solvents of analytical grade purity. Use preferably glassware when working with organic solvents. Prepare and store all reagents at room temperature unless mentioned otherwise. Waste disposal regulations should be considered.

2.1 Lipid extraction

2.1.1 Equipment

1. 12 ml glass tubes with Teflon liner caps.
2. Vibrax orbital shaker with glass tube attachment.
3. Table top centrifuge.
4. Water-jet or vacuum pump.
5. Glass Pasteur pipettes.
6. Glass pipettes.
7. Compressed nitrogen supply.

2.1.2 Reagents

1. $CHCl_3$/Methanol (2:1; v/v).
2. 0.034% $MgCl_2$ in water.
3. 2M KCl in water/methanol (4:1; v/v).
4. Methanol/H_2O/$CHCl_3$ (48:47:3; per vol.).

2.2 Fatty acid analysis by gas liquid chromatography

2.2.1 Equipment

1. 12 ml glass tubes with Teflon liner caps.
2. Oven (100°C).
3. Vibrax orbital shaker with glass tube attachment.
4. Table top centrifuge.

5. Glass Pasteur pipettes.
6. Glass pipettes.
7. GLC-sample vials with caps.
8. Microsyringe.
9. Gas liquid chromatograph with autosampler.

2.2.2 Reagents

1. 2.5 % H_2SO_4 (v/v) in methanol.
2. Light petroleum.
3. Deionized water.
4. Fatty acid methyl ester standards.

2.3 Phospholipid analysis

2.3.1 Equipment

1. TLC glass chambers.
2. Silica gel 60 TLC plates.
3. Glass pipettes.
4. Microsyringe.
5. Hairdryer.
6. Glass tubes with tight-fitting glass lids.
7. Oven (100°C).
8. Heating block (180°C) with inlets for glass tubes fixed at 45° angle.
9. Iodine vapor chamber.
10. Glassware cleaned with phosphate free detergent: pipettes, graduated cylinders, bottles etc.

2.3.2 Reagents

1. $CHCl_3$/Methanol (2:1; v/v).
2. Double distilled water.
3. TLC solvent for the first direction: $CHCl_3$/methanol/25 % NH_3 (65:35:5; per vol.).

4. TLC solvent for the second direction: $CHCl_3$/acetone/methanol/acetic acid/water (50:20:10:10:5; per vol.).
5. Acid mixture: 90 % H_2SO_4 (conc.), 10 % $HClO_4$ (72 %).
6. 0.26 % Ammonium heptamolybdate in water.
7. ANSA solution: 40 g $K_2S_2O_5$, 1.25 g Na_2SO_3, 0.63 g 1-anilinonaphthalene-8-sulfonic acid (ANS-acid) dissolved in 250 ml double distilled water.
8. Phosphate standard: 1 mg P/ml (73 mg $K_2HPO_4 \times 3H_2O$ in 10 ml double distilled water).

2.4 Sphingolipid analysis by UPLC-nano ESI-MS

2.4.1 Equipment

1. 12 ml Pyrex glass tubes with Teflon liner caps.
2. Glass vials with caps.
3. Water bath.
4. Vortex.
5. Sonicator.
6. Table top centrifuge.
7. Ultra Performance Liquid Chromatograph followed by nano-electrospray ionization mass spectrometer (UPLC-nano ESI-MS/MS).

2.4.2 Reagents

1. Internal standard mix: 0.15 nmol *N*-(dodecanoyl)-sphing-4-enine, 0.15 nmol *N*-(dodecanoyl)-1-β-glucosyl-sphing-4-enine, 4.5 nmol C17 sphinganine (Avanti Polar Lipids, Inc., Alabaster, AL, USA).
2. Propan-2-ol/hexane/water (60:26:14; per vol.).
3. Tetrahydrofuran/methanol/water (4:4:1; per vol.).

2.5 Non-polar lipid analysis

2.5.1 Equipment

1. TLC glass chambers.

2. Silica gel 60 TLC plates.
3. Microsyringe.
4. Oven (100°C).
5. Hairdryer.
6. TLC scanner.

2.5.2 Reagents

1. TLC solvent 1: light petroleum/diethyl ether/acetic acid (70:30:2; per vol.).
2. TLC solvent 2: light petroleum/diethyl ether (49:1; v/v).
3. Charring solution: 0.63 g $MnCl_2 \times 4\ H_2O$, 60 ml water, 60 ml methanol and 4 ml H_2SO_4 (conc.).
4. Lipid standards (1 mg/ml): ergosterol, cholesterol oleate, squalene, fatty acids, triolein, 1,2-diolein, monoolein.
5. Chloroform/acetone/acetic acid (90:8:1; per vol.) for the analysis of diacylglycerols.

2.6 Sterol analysis

2.6.1 Equipment

1. 12 ml glass tubes with Teflon liner caps.
2. Water bath.
3. Vibrax orbital shaker with glass tube attachment.
4. Table top centrifuge.
5. Compressed nitrogen supply.
6. Gas Liquid Chromatograph coupled with mass selective detector.

2.6.2 Reagents

1. Methanol.
2. 0.5% (w/v) pyrogallol in methanol.
3. 60% (w/v) aqueous KOH.
4. Internal cholesterol standard (2 mg/ml) in ethanol.
5. *n*-Heptane.
6. Pyridine.

7. N'O'-bis(trimethylsilyl)-trifluoracetamide.
8. Ethyl acetate.

2.7 Mass spectrometry of non-polar lipids and phospholipids

2.7.1 Equipment

1. Glass HPLC acquisition vials.
2. HPLC coupled with FT-ICR-MS hybrid mass spectrometer.

2.7.2 Reagents

1. $CHCl_3$/methanol (1:1; v/v).
2. Solvent A: 1 % ammonium acetate, 0.1 % formic acid in water.
3. Solvent B: 1 % ammonium acetate, 0.1 % formic acid in acetonitrile/2-propanol (5:2; v/v).
4. Internal standards: triacylglycerol (TG) species 51:0; and phosphatidylcholine species (PC) 24:0.

3 Methods

3.1 Lipid extraction

Lipids with the exception of sphingolipids are extracted as described by Folch et al. *(12)*. The amount of biological material to be used for extraction depends on the type of analysis and the sample. In principle, the amounts of lipids can be referred to the protein content, cell dry weight or OD_{600}. Here, we provide guidelines referring lipid to protein amounts. For analyzing lipids from total cell extracts we recommend the following amounts of protein from the cell homogenate. For phospholipid analysis, lipids are extracted from samples containing 1-2 mg protein; for diacylglycerol analysis samples containing 0.4 mg protein are used; triacylglycerols are analyzed from samples containing 0.2 mg protein; and analysis of sterols and fatty acids as well as species analysis of phospholipids, diacylglycerols, triacylglycerols and sphingolipids are performed with samples containing 0.3 mg protein. Extracted lipids are dried under a stream of nitrogen and stored at -20°C.

3.1.1 Extraction of fatty acids, phospholipids, sterols and non-polar lipids

1. Transfer appropriate amount of sample to a glass tube (see Note 1) and add 3 ml $CHCl_3$/methanol (2:1; v/v). Lipids are extracted by vigorous shaking on a Vibrax for 30 min.
2. After addition of 1 ml 0.034 % $MgCl_2$, extraction is continued for another 30 min with vigorous shaking.
3. Phase separation is accomplished by centrifugation in a table top centrifuge at 250 x g for 3 min.
4. Remove upper aqueous phase and as much as possible of the white intermediate layer of precipitated proteins without disturbing the lower organic phase (see Note 2).
5. Add 2 ml 2 N KCl/methanol (4:1; v/v), shake on a Vibrax for 10 min and centrifuge as described above.
6. Remove the aqueous phase and proteins without disturbing the lower organic phase.

7. Add 2 ml of methanol/H_2O/ $CHCl_3$ (48:47:3; per vol.). Shake for 10 min on a Vibrax and centrifuge as described above.
8. Remove the aqueous phase with the remaining proteins.
9. Dry the organic phase completely under the stream of nitrogen (see Note 3).
10. Dissolve dry lipids in an appropriate volume of $CHCl_3$/methanol (2:1 or 1:1; v/v) prior to analysis.

3.1.2 Extraction of sphingolipids for mass spectrometry

1. Cell fractions containing 0.3 mg protein are spiked with an internal standard mixture of 0.15 nmol *N*-(dodecanoyl)-sphing-4-enine; 0.15 nmol *N*-(dodecanoyl)-1-β-glucosyl-sphing-4-enine; and 4.5 nmol C17 sphinganine as an extraction control.
2. Samples are suspended in 6 ml propan-2-ol/hexane/water (60:26:14; per vol.) and incubated at 60°C for 30 min slightly modifying a protocol described previously *(13)*.
3. During incubation, samples are shortly vortexed and sonicated after 0, 10, 20 and 30 min.
4. Extracts are cleared from cell debris by centrifugation, transferred to new tubes and dried under a stream of nitrogen.
5. Extracted sphingolipids are re-dissolved in 800 µl tetrahydrofuran/methanol/water (4:4:1; per vol.) *(14)* and stored under argon at -20°C.

3.2 Fatty acid analysis by gas-liquid chromatography

1. Dissolve dried lipid extracts in 1 ml of a 2.5 % (v/v) H_2SO_4 in methanol and close tubes tightly.
2. Heat samples in the oven at 85°C for 90 min (see Note 1).
3. Let the samples cool down and add 1 ml H_2O and 3 ml light petroleum.
4. Extract the formed fatty acid methyl esters by shaking the tubes on a Vibrax for 30 min.
5. Centrifuge the samples for phase separation for 5 min at 250 x g.
6. Transfer the upper organic phase to a new tube.

7. Repeat the extraction step by adding 3 ml of light petroleum to the remaining aqueous phase for 30 min.
8. Centrifuge as described above. Combine the organic phases of the two extraction steps.
9. Remove solvent under a stream of nitrogen.
10. Dissolve the samples in 100 µl light petroleum for GLC-analysis and transfer to glass acquisition vials.
11. Fatty acid methyl esters are separated by GLC using a capillary column (e.g., 15 m x 0.25 mm i.d. x 0.50 µm film thickness) with helium as carrier gas.
12. Fatty acids are identified by comparison of retention times with a mix of commercially available fatty acid methyl ester standards which is analyzed separately.

3.3 Phospholipid analysis

3.3.1 Analysis of individual phospholipids

1. Phospholipids are extracted (see. Section 3.1.1) from cell homogenates or specific subcellular fractions containing 1-3 mg protein and dried under a stream of nitrogen.
2. Dried lipids are dissolved in 50 µl $CHCl_3$/methanol (2:1; v/v) and applied as a spot on a Silica gel 60 TLC plate (see Note 4).
3. After evaporation of the solvent, the plate is developed in the first dimension using a TLC chamber saturated with first developing solvent for ~50 min (see Note 5).
4. Withdraw TLC plate from the chamber and dry with a hairdryer until the smell of ammonia has disappeared (see Note 6).
5. Develop the plate in the second direction using chloroform/acetone/methanol/acetic acid/water (50:20:10:10:5; per vol.) for 50 min (Fig. 1) (see Note 5).
6. Withdraw TLC plate from the chamber and dry with a hairdryer (see Note 6).
7. Phospholipids are visualized by staining with iodine vapor, and spots are marked with a pencil (Fig. 1B) (see Note 7).
8. Phospholipids are quantified by the procedure of Broekhuyse *et al. (15)*. Silica gel with the identified lipid spots are scrapped off and transferred to phosphate-free glass tubes with the aid of a phosphate-free razor blade, scalpel or spatula (see Note 8). In

addition, unstained areas of the TLC plate are analyzed as blanks for correction of the background.

9. Remove residual moisture by drying samples in an oven for 10 min at 100°C.
10. After cooling down the samples, add 0.2 ml conc. H_2SO_4/72 % $HClO_4$ (9:1, v/v) to each tube and mix briefly.
11. Incubate the tubes in a heating block at 180°C for 30 min to hydrolyze samples (see Note 9).
12. Cool samples down to room temperature and add 4.8 ml of a freshly prepared solution containing 500 vol. of 0.26 % ammonium molybdate and 22 vol. of ANSA.
13. Close the tubes tightly with a lid and incubate them in an oven at 100°C for 30 min. Phosphate containing samples turn blue.
14. Cool the sample down and sediment silica gel by centrifugation at 250 x g for 3 min in a table top centrifuge.
15. Quantification of phospholipids is achieved by measuring the absorption at a wavelength of 830 nm. Values have to be corrected for the blank. For calculation of the absolute amounts of individual phospholipids a series of phosphorus standards is required.

3.3.2 Quantification of total phospholipids

1. Lipids are extracted as described in section 3.1.1, dissolved in chloroform/methanol (2:1; v/v) and transferred to phosphate free glass tubes. Samples are brought to complete dryness either by evaporation in an oven or under a stream of nitrogen.
2. Samples and phosphorus standards are directly subjected to hydrolysis. The following steps are performed as described in section 3.3.1 starting at step 10. Centrifugation at step 15 is omitted.
3. Amounts of total phospholipids are calculated from a standard curve using inorganic phosphate at known amounts (0.5, 1, 2, 4, and 8 µg phosphorus per tube are recommended). Obtained values correspond to µg phosphorus per mg protein. Values are multiplied by the factor of 25, the approximate ratio of molar masses of phosphorus and an average phospholipid, to yield µg phospholipid/mg protein.

3.4 Sphingolipid analysis

Analysis is performed by Ultra Performance Liquid Chromatography followed by nano-electrospray ionization mass spectrometry (UPLC-nano ESI-MS/MS) *(16, 17)*.

1. For analysis, sphingolipids extracted as described in section 3.1.2 are solubilized by gentle heating and sonication.
2. Sphingolipid analysis is initiated by Ultra Performance Liquid Chromatography (UPLC) (see Note 10).

   Aliquots of 2 µl are injected in the partial loop with needle overfill mode. The flow rate is set at 0.12 ml/min, and the separation temperature at 35°C. Inositol containing sphingolipids are separated by elution with a linear gradient of solvents A and B as follows: 65 % solvent B held for 2 min, linear increase to 100 % solvent B for 8 min, 100 % solvent B held for 2 min, and equilibration to 65 % solvent B in 2 min. Ceramides (Cer) and hexosylceramides (HexCer) are separated as follows: 80 % solvent B held for 2 min, linear increase to 100 % solvent B for 8 min, 100 % solvent B held for 2 min and equilibration to 80 % solvent B in 2 min. Solvent B is tetrahydrofuran/methanol/20 mM ammonium acetate containing 0.1 % (v/v) acetic acid; and solvent A is methanol/20 mM ammonium acetate containing 0.1 % (v/v) acetic acid.
3. Chip-based nano-electrospray ionization is achieved in the positive ion mode with 5 µm internal diameter nozzles, a flow rate of 209 nl/ min, and a voltage of 1.5 kV.
4. Detection of sphingolipid molecular species is carried out with a tandem mass spectrometer by monitoring (i) the transition from $[M+H]^+$ molecular ions to dehydrated long chain base (LCB) fragments for Cer, HexCer and LCB; and (ii) the loss of phosphoinositol containing head groups for inositol containing sphingolipids. Dwell time is 30 ms (see Note 11).

3.5 Non-polar lipid analysis by thin layer chromatography

The profile of the major *P. pastoris* non polar lipids has been reported previously *(18)*. Here we provide a protocol suitable for quantitative analysis of non-polar lipids from *P. pastoris* total cell extracts or subcellular fractions. The sample size used for lipid extraction varies. For

total cell extracts we recommend to use samples containing 0.3 mg protein. If isolated lipid droplets are used for analysis, samples containing 0.5-1 µg protein are sufficient. Dissolve dried lipids in 15-30 µl (or any appropriate volume) of $CHCl_3$/methanol (2:1; v/v) prior to loading on TLC plates.

3.5.1 Separation of non-polar lipids by a two-step procedure

This procedure allows proper separation of sterols, free fatty acids, steryl esters and triacylglycerols.

1. Prepare two glass TLC chambers by filling one chamber with 50-100 ml of the first running solvent solution and the second chamber with 50-100 ml of the second running solvent solution (see Note 5).
2. Load TLC plates with samples either manually (see Note 12) or with a sample loading device. Leave 1.5 cm space from the bottom and side margins of TLC plates. Load each sample as a narrow 0.8-1 cm wide band leaving 1-1.5 cm space in between. Load each TLC plate with at least three lanes containing standards with increasing amounts of the respective component (see Note 13).
3. First step separation: Develop the TLC in an ascending manner until the solvent front reaches half of the plate (~5 min, see Note 14). Remove plate and dry with the hairdryer (see Note 6).
4. Second step separation: Develop the TLC using the second solvent system in the same direction as in the first step until the solvent front reaches the top of the plate (~20 min) (see Note 14). Remove plate and dry with hairdryer (see Note 6). Separated lipids are now ready for visualization and quantification.

3.5.2 Separation of diacylglycerols

For separation of diacylglycerols a one-step solvent system is applied *(19)*. Prepare lipid extracts (Section 3.1.1) and dissolve lipids in an appropriate volume of $CHCl_3$/methanol (2:1; v/v). Load lipid extracts on the TLC plate and develop the TLC with chloroform/acetone/acetate (90:8:1, per vol.) for ~20 min. Dry the TLC plate with a hairdryer.

Separated lipids can be visualized and quantified (see Notes 6-7 and 12-14).

3.5.3 Visualizing separated lipids and quantification

To quantify sterols and steryl esters, TLC plate can be directly scanned at a wavelength of 275 nm. Peaks of standards with known amounts loaded are used for calibration. The peak areas of individual samples are set in relation to standards.

To quantify other lipids visualization is needed as follows (Fig. 2):

1. Put the TLC plate into a charring solution and keep it there for 15-20 sec (see Note 15).
2. Put TLC plate into an oven and heat for 30 min at 100°C.
3. After heating separated lipids and standards become visible as bands and can be scanned at 400 nm wavelengths using a TLC scanner. Amounts of individual lipids are calculated relative to standards as described above (see Note 16).

3.6 Sterol analysis by Gas Liquid Chromatography- Mass Spectrometry

The analysis of sterols from yeast was described previously *(9, 20)*. Here we summarize the method for the analysis of *P. pastoris* sterols by GLC-MS.

3.6.1 Sample preparation

The size of biological samples required for sterol analysis depends on the content of sterols. For analyzing the sterol composition from total cell extracts the amount of 0.3 mg protein is sufficient. For subcellular fractions the sample size can differ strongly and has to be estimated empirically. As examples, mitochondrial fractions containing 0.5 mg protein, plasma membrane fractions containing 1 mg protein, peroxisomal fractions containing 0.25 mg protein, and lipid droplet fractions containing 0.02-0.03 mg protein are sufficient.

1. Alkaline hydrolysis. Put the following reagents into a 15 ml glass tube: 0.6 ml methanol; 0.4 ml 0.5% pyrogallol in methanol; 0.4 ml 60% KOH; 5 µl of cholesterol solution (2 mg/ml) as an internal standard; and an appropriate amount of the specimen to be analyzed.
2. Close tubes tightly, wrap in aluminum foil to protect the sample from light, and put the tube into a water bath for 2 h at 90°C (see Note 17).
3. Extract lipids by adding 1 ml of *n*-heptane and mix the sample vigorously for 30 sec. Centrifuge tubes for 3 min at 250 x g. Transfer the upper phase into a new tube. Repeat the extraction twice with 1 ml of *n*-heptane and combine upper phases.
4. Dry extracts under a stream of nitrogen and store at -20°C.
5. For analysis, dissolve extracts in 10 µl pyridine, add 10 µl of N'O'-bis(trimethylsilyl)-trifluoracetamide, incubate for 10 min and dilute with 50 µl ethyl acetate (see Note 18). Transfer samples to glass acquisition vials.

3.6.2 GLC-MS analysis

GLC-MS analysis can be performed on a gas chromatograph equipped with a mass selective detector and a MS capillary column (crosslinked 5% Phenyl Methyl Siloxane) with 30 m×0.25 mm×0.25 µm film thickness.

1. Aliquots of 1 µl are injected at 270°C injection temperature in the splitless mode with helium as a carrier gas at a constant flow rate of 0.9 ml/min. The temperature program is as follows: 1 min at 100°C and 10°C/min to 250°C and 3°C/min to 310°C.
2. Mass spectra are obtained in scan mode with 3.27 scans/sec using a scan range of 200-500 amu. Individual sterols are identified according to their retention times (Fig. 3A) and mass fragmentation pattern (Fig. 3B, see Note 19) using appropriate chromatography software. For quantification of individual sterols, integrated peak areas are related to the internal standard cholesterol peak area.

3.7 Analysis of non-polar lipid and phospholipid species by HPLC coupled mass spectrometry

The procedure for lipid analysis by HPLC/MS has been described previously in much detail *(21, 22)*. Here we provide a protocol for the analysis of molecular species of triacylglycerols and phospholipids.

1. Prepare lipid extracts as described in section 3.1.1. The amount of extracted lipids and downstream dilution factors depend on the sample and lipid class being analyzed and should be adjusted empirically (see Note 20).
2. Dissolve lipids in 500 µl $CHCl_3$/methanol (1:1; v/v) and add 5 µM TG (species 51:0) and 5 µM PC (species 24:0) as internal standards. Transfer 30 µl to the acquisition vial and use 3 µl injection volume for HPLC-MS.
3. Use a reversed-phase C18 column (reversed-phase C18; 100 × 1 mm i.d., 1.9 µm particle size) employing solvent A and solvent B for chromatographic separation of lipid species. The gradient changes from 35 % to 70 % solvent B within 4 min and further to 100 % solvent B within 16 min. These conditions are held constant for 10 min at a flow rate of 250 µl/min. Mass spectrometry is performed by HPLC directly coupled to a FT-ICR-MS hybrid mass spectrometer equipped with an ionMax ESI source. The mass spectrometer is operated at a mass accuracy of <2 ppm with external calibration and resolution of 200,000 full width at half height at 400 *m/z*. The spray voltage is set at 5,000 V, the capillary voltage at 35 V, the tube lens at 120 V and the capillary temperature at 250°C. Peak areas are calculated by QuanBrowser for all lipid species identified according to their exact mass and retention time.

4 Notes

1. Glass tubes need to be closed tightly with organic solvent resistant seals. Make sure that no evaporation of solvent occurs by using intact glass tubes and caps with gaskets.
2. Removal of the protein containing interphase without losing substantial amounts of the organic phase is critical, especially when absolute quantifications are required. Therefore, it is recommended to leave some residual proteins in the interphase, which still can be removed during further steps of phase separation. Alternatively, protein interphases can be left intact during the entire extraction process, and the organic phase can be collected by penetrating the protein layer with a small glass pipette.
3. Dried lipid extracts can be stored in -20° till needed.
4. Extracted phospholipids should be applied as a spot of about 3-5 mm in diameter ~2 cm from the left and the lower margins of a Silica gel 60 TLC plate.
5. TLC chambers have to be saturated with solvents for about 30 min before usage.
6. Do not overheat the Silica gel 60 TLC plate.
7. At this stage, the plates can be stored overnight in the dark. Iodine should be completely removed by spraying the plate with distilled water and heating at ~50°C in the oven, or by evaporating on air in a hood.
8. Moistening the TLC with phosphate-free distilled water facilitates scrapping off the respective spots.
9. The tube should be put into the heating block only to half of the height thus allowing circulation and condensation of acid fumes. It is important that this step is performed in a hood because the hot acids may give rise to hazardous fumes. After 30 min the liquid in the tubes should be colorless or slightly yellow. If it is dark yellow or brownish, it can be bleached by addition of 5-10 µl 30 % H_2O_2.
10. Use an appropriate UPLC column, e.g. with dimensions 100 mm × 1 mm, 1 µm.
11. Optimize MS parameters to maximize detector response.
12. For loading TLC plates manually, glass syringes with 25-100 µl volume are suitable. Try to load bands as thin as possible.
13. The amounts of standards to load should be estimated empirically and depend on the samples to be analyzed.
14. TLC plates should not get in contact with front or side walls of the chamber during development.
15. Avoid keeping TLC plates in charring solution for more than 1 min.

16. Alternatively to densitometric scanning procedures, bands visualized on TLC plates can be digitalized at high resolution, and any graphic analyzing software (e.g., ImageJ, CorelDRAW) can be used for calculating amounts of standards and individual lipids.
17. After heating samples in the water bath, the color of the mixture should turn yellow.
18. This step should be performed directly before GLC-MS analysis.
19. Retention times of sterols can differ slightly depending on the samples, but the overall pattern is similar.
20. As an example, 0.3 mg protein from a cell homogenate is sufficient for non-polar lipid and phospholipid species analysis.

Acknowledgements

This work was supported by the Austrian Science Fund FWF (project TRP009 and DK Molecular Enzymology to GD), the Federal Ministry of Economy, Family and Youth (BMWFJ), the Federal Ministry of Traffic, Innovation and Technology (bmvit), the Styrian Business Promotion Agency SFG, the Standortagentur Tirol and ZIT – Technology Agency of the City of Vienna through the COMET-Funding Program managed by the Austria Research Promotion Agency FFG, and by the Austrian Centre of Industrial Biotechnology (ACIB GmbH).

References

1. G. Daum, N.D. Lees, M. Bard, et al. (1998) Biochemistry, cell biology and molecular biology of lipids of *Saccharomyces cerevisiae*, Yeast 14, 1471–1510.

2. J.R. Van Brocklyn and J.B. Williams (2012) The control of the balance between ceramide and sphingosine-1-phosphate by sphingosine kinase: oxidative stress and the seesaw of cell survival and death, Comp. Biochem. Phys. Part B, Biochem. Mol. Biol. 163, 26–36.

3. A.X.S. Santos and H. Riezman (2012) Yeast as a model system for studying lipid homeostasis and function, FEBS Lett. 586, 2858–2867.

4. M. Sud, E. Fahy, D. Cotter, et al. (2007) LMSD: LIPID MAPS structure database, Nucl. Acids Res. 35, D527–532.

5. E. Fahy, S. Subramaniam, R.C. Murphy, et al. (2009) Update of the LIPID MAPS comprehensive classification system for lipids, J. Lipid Res. 50 Suppl, S9–14.

6. D. Peretti, N. Dahan, E. Shimoni, et al. (2008) Coordinated lipid transfer between the endoplasmic reticulum and the Golgi complex requires the VAP proteins and is essential for Golgi-mediated transport, Mol. Biol. Cell. 19, 3871–3884.

7. M. Schnabl, G. Daum, and H. Pichler (2005) Multiple lipid transport pathways to the plasma membrane in yeast, Biochim. Biophys. Acta. 1687, 130–140.

8. E. Zinser, C.D. Sperka-Gottlieb, E.V. Fasch, et al. (1991) Phospholipid synthesis and lipid composition of subcellular membranes in the unicellular eukaryote *Saccharomyces cerevisiae*, J. Bacteriol. 173, 2026–2034.

9. G. Tuller, T. Nemec, C. Hrastnik, et al. (1999) Lipid composition of subcellular membranes of an FY1679-derived haploid yeast wild-type strain grown on different carbon sources, Yeast 15, 1555–1564.

10. M. Ståhlman, C.S. Ejsing, K. Tarasov, et al. (2009) High-throughput shotgun lipidomics by quadrupole time-of-flight mass spectrometry, J. Chromatography 877, 2664–2672.

11. C. Klose, M.A. Surma, and K. Simons (2013) Organellar lipidomics--background and perspectives, Curr. Op. Cell Biol. 25, 406–413.

12. J. Folch, M. Lees, and G.H. Sloane Stanley (1957) A simple method for the isolation and purification of total lipids from animal tissues, J. Biol. Chem. 226, 497–509.

13. J.E. Markham, J. Li, E.B. Cahoon, et al. (2006) Separation and identification of major plant sphingolipid classes from leaves, J. Biol. Chem. 281, 22684–22694.

14. C. Buré, J.-L. Cacas, F. Wang, et al. (2011) Fast screening of highly glycosylated plant sphingolipids by tandem mass spectrometry, Rapid Comm. Mass Spectr. 25, 3131–3145.

15. R.M. Broekhuyse (1968) Phospholipids in tissues of the eye. I. Isolation, characterization and quantitative analysis by two-dimensional thin-layer chromatography of diacyl and vinyl-ether phospholipids, Biochim. Biophys. Acta. 152, 307–315.

16. J.E. Markham and J.G. Jaworski (2007) Rapid measurement of sphingolipids from Arabidopsis thaliana by reversed-phase high-performance liquid chromatography coupled to electrospray ionization tandem mass spectrometry, Rapid Comm. Mass Spectr. 21, 1304–1314.

17. C.S. Ejsing, T. Moehring, U. Bahr, et al. (2006) Collision-induced dissociation pathways of yeast sphingolipids and their molecular profiling in total lipid extracts: a study by quadrupole TOF and linear ion trap-orbitrap mass spectrometry, J. Mass Spectr. 41, 372–389.

18. V.A. Ivashov, K. Grillitsch, H. Koefeler, et al. (2013) Lipidome and proteome of lipid droplets from the methylotrophic yeast *Pichia pastoris*, Biochim. Biophys. Acta. 1831, 282–290.

19. C. Heier, U. Taschler, S. Rengachari, et al. (2010) Identification of Yju3p as functional orthologue of mammalian monoglyceride lipase in the yeast *Saccharomyces cerevisiae*, Biochim. Biophys. Acta. 1801, 1063–1071.

20. M.A. Quail and S.L. Kelly (1996) The extraction and analysis of sterols from yeast, Meth. Mol. Biol. 53, 123–131.

21. J. Hartler, M. Trötzmüller, C. Chitraju, et al. (2011) Lipid Data Analyzer: unattended identification and quantitation of lipids in LC-MS data, Bioinformatics 27, 572–577.

22. A. Fauland, H. Köfeler, M. Trötzmüller, et al. (2011) A comprehensive method for lipid profiling by liquid chromatography-ion cyclotron resonance mass spectrometry, J. Lipid Res. 52, 2314–2322.

Figures and legends

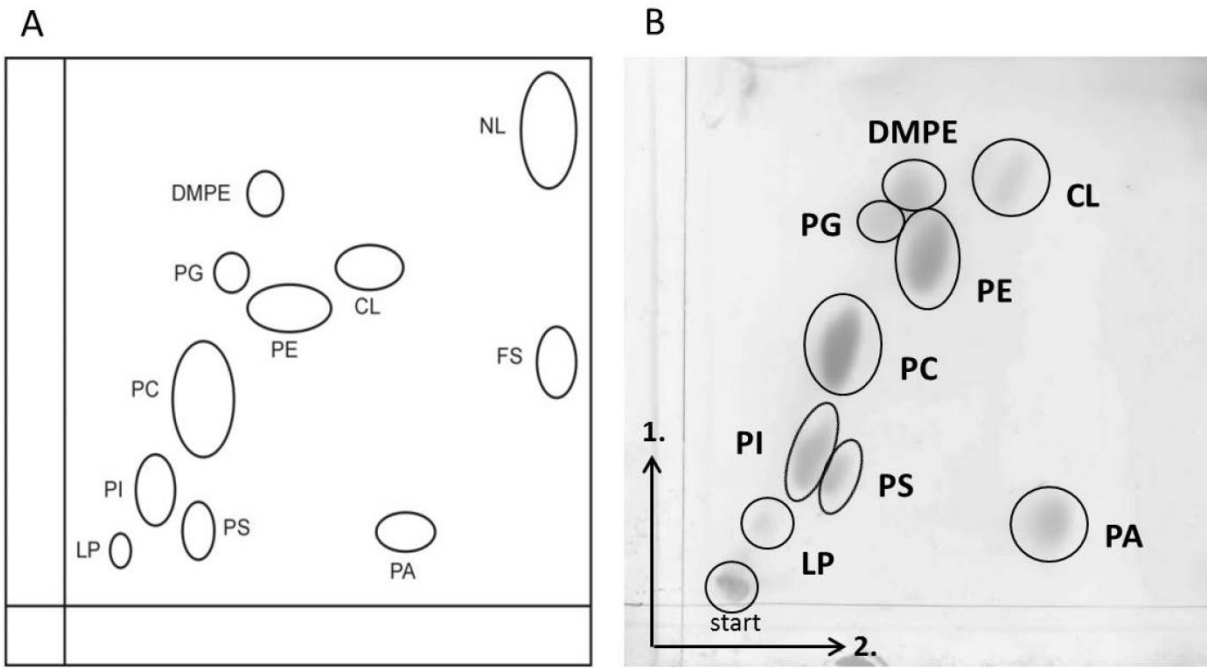

Figure 1: Phospholipid separation by two-dimensional thin layer chromatography

Phospholipids are extracted from samples containing 1-2 mg protein and applied to two-dimensional thin layer chromatography (2D-TLC) as described in section 3.3.1. Figure 1A indicates how phospholipids should typically separate in a 2D-TLC. Figure 1B shows the phospholipid profile of a *P. pastoris* microsomal fraction after 2D-TLC separation and iodine vapor staining. Numbers indicate running directions and the solvent system. CL: cardiolipin; DMPE: dimethylphosphatidylethanolamine; FS: fatty acids; LP: lysophospholipids; NL: neutral lipids; PA: phosphatidic acid; PC: phosphatidylcholine; PE: phosphatidylethanolamine; PG: phosphatidylglycerol; PI: phosphatidylinositol; PS: phosphatidylserine; start: lipids are applied to the TLC plate at this point.

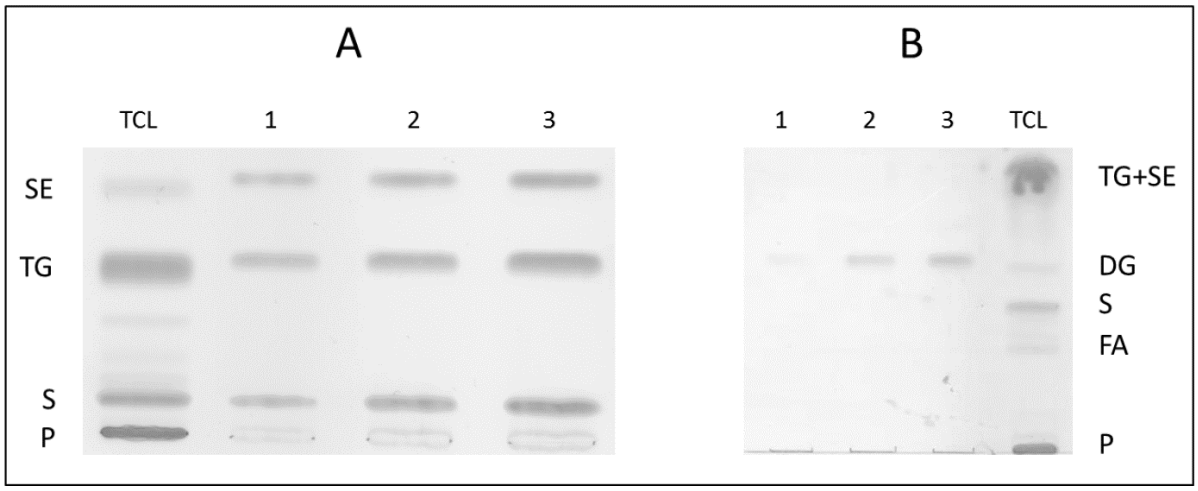

Figure 2: Non-polar lipids separated by TLC and visualized

Pichia pastoris cells were grown on YPD to the stationary phase (26 h). Total cellular lipids (TCL) were extracted from cell homogenates containing 0.3 mg protein and applied onto TLC plates. Lipids were separated by a two-step (A) or one-step procedure (B) and visualized by charring and heating. P- phospholipids, S- sterols, TG- triacylglycerols, SE- steryl esters, FA- fatty acids, DG- diacylglycerols. Increasing amounts of the following standards were loaded in lanes 1-3 of plate A: 3, 6, and 10 µg ergosterol; 10, 20, 40 µg triolein; 2, 4, 6 µg cholesterol oleate. TLC plate B was loaded with 0.7, 3.3, and 5 µg of 1,2-diolein standard in lanes 1-3.

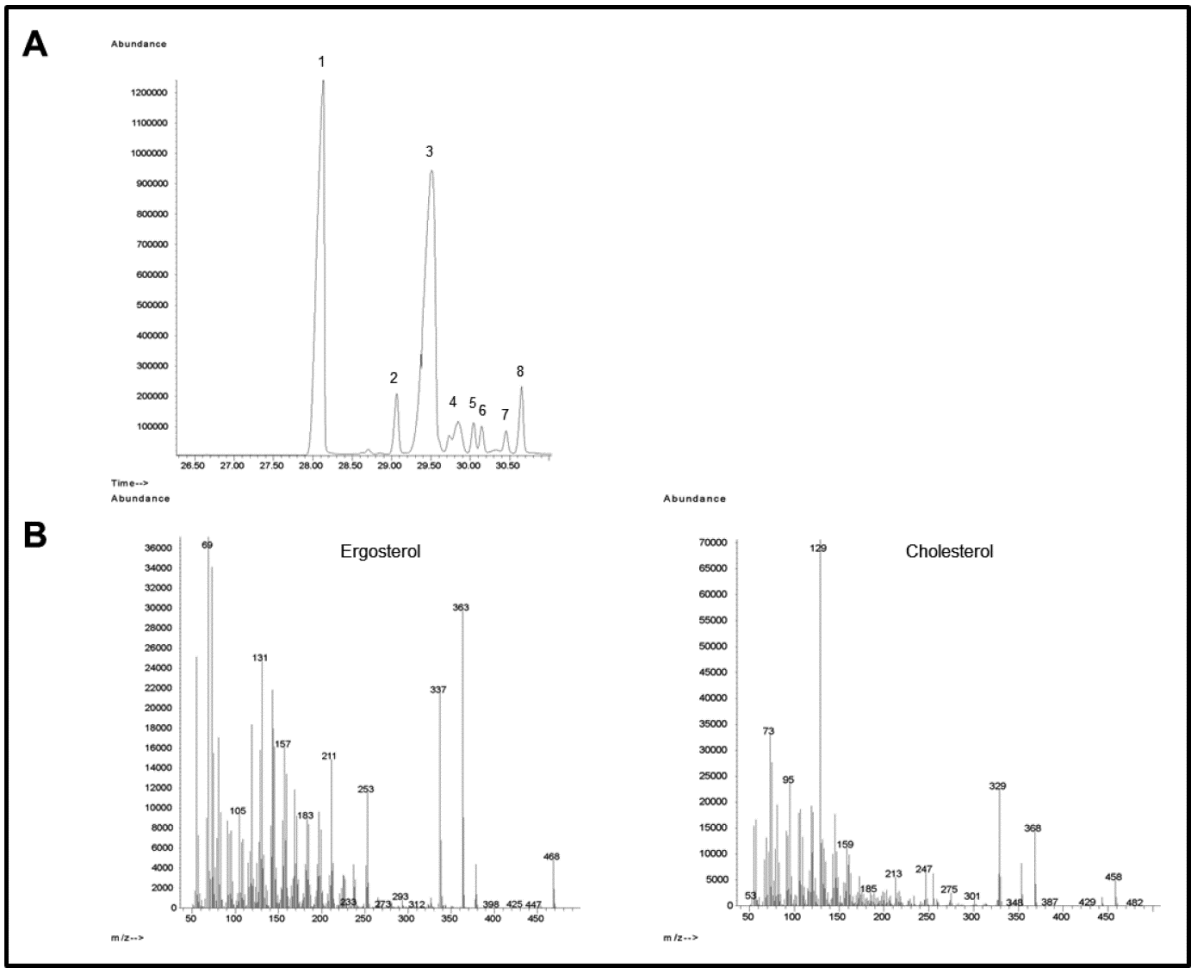

Figure 3: Example of GLC chromatogram and mass fragmentation patterns of *Pichia pastoris* total cell sterols

Cells were grown on YPD to the stationary phase (26 h). Sterols were extracted from homogenates containing 0.3 mg protein and analyzed by gas liquid chromatography/mass spectrometry. A- GLC pattern. Numbered peaks represent individual sterols as follows: 1- cholesterol as internal standard, 2- zymosterol, 3- ergosterol, 4- 4-methylzymosterol, 5- fecosterol, 6- episterol, 7- lanosterol, 8- 4,14-dimethylcholesta-8,24-dienol. B- mass fragmentation pattern of ergosterol and cholesterol.

Chapter V

The lipidome and proteome of microsomes from the methylotrophic yeast *Pichia pastoris*

Lisa Klug[a‡], Pablo Tarazona[b‡], Clemens Gruber[c,d‡], Karlheinz Grillitsch[e], Brigitte Gasser[c,f], Martin Trötzmüller[g], Harald Köfeler[g], Erich Leitner[h], Ivo Feussner[b], Diethard Mattanovich[c,f], Friedrich Altmann[c,d], Günther Daum[a*]

[a]Institute of Biochemistry, Graz University of Technology, Austria; [b]Department for Plant Biochemistry, Albrecht-von-Haller Institute for Plant Sciences, Georg-August-University, Goettingen, Germany; [c]Austrian Centre of Industrial Biotechnology, Vienna, Austria; [d]Department of Chemistry, BOKU University of Natural Resources and Life Sciences Vienna, Austria; [e]Austrian Centre of Industrial Biotechnology, Graz, Austria; [f]Department of Biotechnology, BOKU University of Natural Resources and Life Sciences Vienna, Austria; [g]Core Facility for Mass Spectrometry, Center for Medical Research, Medical University of Graz, Austria; [h]Institute of Analytical Chemistry and Food Chemistry, Graz University of Technology, Austria;

[‡] Contributed equally and should be considered as co-first authors.

[*]Corresponding author: Günther Daum, Institute of Biochemistry, Graz University of Technology; Petersgasse 12/2, A-8010 Graz, Austria; Tel.: +43 316 873 6462; Fax: +43 316 873 6952; E-mail: guenther.daum@tugraz.at

Keywords:

Pichia pastoris, microsomes, endoplasmic reticulum, lipidome, proteome, sphingolipids, phospholipids, sterols, fatty acids

Abbreviations:

ER, endoplasmic reticulum; M30, 30,000 g microsomes; M40, 40,000 g microsomes; BM, bulk membranes; PMSF, phenylmethylsulfonyl fluoride; SDS, Sodium dodecyl sulfate; DTT, dithiothreitol; Cer, ceramide; HexCer, hexosyl ceramide; LCB, long chain base; MS, mass spectrometry; cww, cell wet weight; T_d, doubling time.

Abstract

The methylotrophic yeast *Pichia pastoris* is a popular yeast expression system for the production of heterologous proteins in biotechnology. Interestingly, cell organelles which play an important role in this process have so far been insufficiently investigated. For this reason, we started a systematic approach to isolate and characterize organelles from *P. pastoris*. In this study, we present a procedure to isolate microsomal membranes at high purity. These samples represent endoplasmic reticulum (ER) fractions which were subjected to molecular analysis of lipids and proteins. Organelle lipidomics included a detailed analysis of glycerophospholipids, fatty acids, sterols and sphingolipids. The microsomal proteome analyzed by mass spectrometry identified typical proteins of the ER known from other cell types, especially *Saccharomyces cerevisiae*, but also a number of unassigned gene products. The lipidome and proteome analysis of *P. pastoris* microsomes are prerequisite for a better understanding of functions of this organelle and for modifying this compartment for biotechnological applications.

1 Introduction

Pichia pastoris is a popular host for the production of heterologous proteins, but is also used as model organism for peroxisome and secretory organelle proliferation [1–4]. While methanol induced promoters are employed to produce proteins in small and medium scale with great success, there are significant technical and safety issues favoring the use of glucose based expression systems in large industrial scale production [4], which calls for investigations of *P. pastoris* biochemistry and cell biology under these conditions. As *P. pastoris* proved to be very efficient for the production of secretory proteins [5], a detailed analysis of components of the secretory pathway is of great interest. Recently, we performed a computational genome wide analysis for gene products involved in protein folding and secretion in eight different yeast species, including *P. pastoris* and the model yeast *Saccharomyces cerevisiae*. Essential functions of the secretory pathway are apparently conserved among yeasts, while high diversity was identified for the chaperone family of J proteins, for peptidyl-prolyl isomerases, and for Golgi localized mannosyl transferases [6].

Organelle analysis of *P. pastoris* [7–9] is meant to complement biotechnological studies and to provide insight into components and functions of subcellular compartments which are involved in protein expression. In the present study, we focus on the characterization of *P. pastoris* microsomes (M30, M40) representing the endoplasmic reticulum (ER) of the cell. The ER forms a membrane network of tubules, vesicles and cisternae [10] which is connected to the nuclear envelope in the form of a continuum and linked to other organelles such as mitochondria or the plasma membrane through membrane contact sites [11,12]. Two types of ER subfractions are known. The rough ER with ribosomes attached is involved in protein synthesis and represents the starting point of the protein secretory pathway [11], whereas the smooth ER contributes to carbohydrate metabolism, lipid synthesis and calcium storage [12,13]. The secretory pathway includes the ER, the Golgi and the plasma membrane. Secretory proteins synthesized at the rough ER are shuttled via membrane vesicles to the Golgi and further to the plasma membrane where the cargo is released into the extracellular environment [6,14]. Due to the fact that the ER is also the major site of phospholipid, sphingolipid and sterol synthesis, lipids have also to be transported from the ER to other organelles. Non-vesicular and vesicular pathways were suggested as possible lipid transport pathways [15,16]. Non-vesicular transport most likely takes place at membrane contact sites which are found between ER and Golgi, plasma membrane, mitochondria and endosomes

respectively [17–20]. Thus, besides its importance for cell metabolic processes the ER acts as the major gateway for proteins and lipids to final destinations.

In the present study, we describe the biochemical characterization of *P. pastoris* microsomal subfractions. This analysis is based on the isolation of highly purified microsomes, quality control by Western Blot analysis, conventional biochemical lipid and protein analysis, and -omics studies by mass spectrometry of lipids and proteins. The detailed information about lipidome and proteome of microsomes provides insight into the molecular composition of this important organelle and access to functional aspects of this subcellular fraction.

2 Experimental procedures

2.1 Strains and culture conditions

The wild type strain *P. pastoris* CBS7435 was used throughout this study. YPD medium containing 1 % yeast extract, 2 % peptone and 2 % glucose was used to cultivate this strain. Pre-cultures were grown at 25°C or 30°C for 48 h in baffled Erlenmeyer flasks with shaking at 130 rpm. Main cultures were grown in 300 ml YPD medium in 2 l Erlenmeyer flask with baffles which were inoculated with an aliquot of the pre-culture to an OD_{600} of 0.1. Cells were grown at 30°C for 22 hours (T_d ~ 2.9 h) or at 25°C for 26 hours (T_d ~ 3.2 h) with shaking to the late exponential phase.

2.2 Isolation of Microsomes

Microsomes were isolated from the *P. pastoris* CBS7435 wild type strain grown to the late exponential growth phase as described above. Cell fractionation was performed by the following procedure. Cells were harvested and converted to spheroplasts by using Zymolyase 20T [8]. After 1 h of enzymatic treatment, spheroplasts were homogenized in Tris-mannitol buffer (0.6 M mannitol, 10 mM Tris/HCl, pH 7.4) containing PMSF (1 M, 2 µl/g cww) with 15 strokes in a Dounce Homogenizer. Homogenates were centrifuged at 5,500 rpm at 4°C for 5 min in a Sorvall RC 6 Plus centrifuge using a SS-34 rotor. This procedure was repeated twice with the obtained pellet after resuspension in Tris-mannitol buffer. Combined supernatants (crude homogenate) were centrifuged at 10,000 rpm at 4°C for 10 min. The resulting supernatant was further centrifuged at 13,000 rpm at 4°C for 30 min. The obtained supernatant was centrifuged at 16,000 rpm (30,000 g) at 4°C for 30 min. The pellet (M30) was re-suspended in Tris/HCl, pH 7.4, and the supernatant was centrifuged at 18,500 rpm (40,000 g) at 4°C for 30 min. The resulting pellet (M40) was re-suspended in Tris/HCl, pH 7.4. The microsomal fractions M30 and M40 were stored at -70°C. For mass spectrometric analysis, M30 and M40 were washed once with water and fractions were directly sedimented in an Eppendorf tube using a Beckman Coulter Optima TLX table top ultracentrifuge with a TLA100.4 rotor. M30 was sedimented at 30,000 g and M40 at 40,000 g for 30 min at 4°C. Organelles were stored at -70°C.

2.3 Preparation of bulk membranes

Bulk membranes (BM) were isolated from *P. pastoris* CBS7435 wild type strain grown to the late exponential growth phase as described above. Preparation of BM was performed by two different procedures. For the first method, Zymolyase 20T [8] was used for cell spheroplasting, and homogenate was prepared as described for the isolation of microsomes (see section 2.2). For the second method, a mechanical cell disruption was employed. Cells were harvested at the late exponential growth phase and re-suspended in water (2.8 ml/g cww). After addition of Tris/HCl buffer (0.5 M, pH 8.5, 170 µl/g cww), EDTA (0.5 M, pH 8.0, 34 µl/g cww) and PMSF (1 M, 2 µl/g cww) cells were mechanically disrupted with glass beads in the Merckenschlager disintegrator for 3 min under cooling with CO_2. Glass beads were sedimented and the supernatant was centrifuged for 10 min at 2,500 rpm at 4°C in a Sorvall RC 5B Plus centrifuge using a Sorvall GSA rotor. The supernatant from this step was used as homogenate.

Homogenates obtained from both methods were centrifuged at 45,000 rpm (100,000 g) for 45 min at 4°C in a Thermo Scientific Sorvall WX Ultra Series centrifuge using a T865 rotor. The resulting pellet was used as bulk membranes (BM-Zym: obtained from cells disrupted with Zymolyase; BM-MS: obtained from cells disrupted with glass beads in the Merckenschlager). For mass spectrometric analysis bulk membranes were washed once with water and sedimented in a Beckman Coulter Optima TLX table top ultracentrifuge with a TLA100.4 rotor. Pellets were stored at -70°C.

2.4 Protein analysis

Homogenate and microsomes were diluted 1:10 with water. Proteins were precipitated with trichloroacetic acid on ice at least for 1 h. After washing, precipitated proteins were solubilized in 0.1 % SDS, 0.1 M NaOH at 37°C for 30 min. Protein quantification was performed as described by Lowry et al. [21]. SDS-polyacrylamide gel electrophoresis was carried out by the method of Laemmli [22] using gradient SDS gels (18 % to 12.5 %). Ten µg protein of each sample was loaded per lane. Gels were either stained with Coomassie Brilliant Blue or used for Western Blot analysis according to Haid and Suissa [23]. Primary polyclonal antibodies raised in rabbits and monoclonal antibodies raised in mouse were directed against *S. cerevisiae* proteins. For detection, peroxidase conjugated secondary antibodies and a chemiluminescent signal detection solution (SuperSignal® West Pico Chemiluminescent

Substrate, Thermo Scientific, Rockford, IL, USA) were used to visualize immune-reactive proteins.

2.5 Proteome analysis by mass spectrometry

Proteome analysis of homogenate and microsomal fractions were performed in three steps including (i) sample preparation; (ii) sample analysis by mass spectrometry, and (iii) data processing. Two different strategies were employed for sample preparation. For in-solution analysis of proteins, organelle pellets were solubilized in 0.1 M ammonium bicarbonate buffer (ABC buffer) containing 0.1 % RapiGest SF [24]. Samples were reduced using 15 mM DTT and carbamidomethylated (55 mM iodoacetamide), and proteins were precipitated for purification (acetone to aqueous phase = 4:1; v/v). Homogenates were directly used for reduction and protein precipitation. The pellet was dissolved in 0.1 M ABC buffer and digested over night with trypsin (Promega Sequencing Grade Trypsin; Enzyme:Substrate 1:50) at 37°C. Alternatively, samples were digested in gel. The pellets were solubilized in SDS sample buffer (250 mM Tris/HCl pH 6.8, 2 % SDS, 25 % glycerol, 20 mM DTT, 10 µl bromophenol blue) and separated on a 12 % SDS gel [22]. Three zones of equal size in Coomassie blue stained gel were cut out and digested in gel as described previously [25–27].

For analysis, about 3 µg of each digest were loaded onto a BioBasic C18 column (BioBasic-18, 150 x 0.18 mm, 5 µm, Thermo Scientific) using 0.1 % formic acid as aqueous solvent. A gradient from 5 to 70 % acetonitrile was developed over 105 min at a flow rate of 1.5 µl/min. Detection was performed with an ion trap mass spectrometer equipped with the standard ESI source (Bruker amaZon speed ETD) in the positive ion, DDA mode (= switching to MSMS mode for eluting peaks). Instrument calibration was performed using the ESI calibration mixture (Agilent, Low Concentration Tuning Mix).

Alternatively, the samples from the in-solution digestion were analyzed using a Q-TOF MS (Bruker maxis 4G ETD) equipped with the ESI nano online source. Peptides were separated on a C-18 column (Acclaim® PepMap100 C18 column, Thermo, 250 * 0.1 mm, 3 µm packing, flow: 0.4 µl/ min) employing a gradient from 90 % solvent A / 10 % solvent B to 32 % solvent B in 70 min. After this phase a 30 min gradient elution from 32 % to 75 % B was employed to facilitate elution of large peptides. Solvent A is 0.1 % formic acid in water, and Solvent B is 0.1 % formic acid in acetonitrile. Finally, the column was equilibrated for 15 min at starting conditions (95 % A, 5 % B). MS scans were recorded in the range of 150-2200 Da, and the 10 highest peaks, each, were selected for fragmentation.

For data processing, the analysis files were converted to mgf files (mascot generic format) using Data Analysis 4.0, Bruker. MASCOT searches (ion trap: parent and fragment mass error 0.4 Da; QTOF: parent mass error 7 ppm fragment mass error 0.05 Da) were performed employing the ProteinScape software (Bruker). Proteins identified by only one peptide or having sequence coverage of less than 4 % were excluded from further analysis. Signal peptides were predicted using SignalP, whereas TM HMM was employed to predict transmembrane domains.

2.6 Lipid analysis

Lipids with the exception of sphingolipids (see below, section 2.6.5), were extracted from homogenate (H) and microsomal fractions (M30, M40) following the procedure of Folch et al. [28]. For fatty acid and phospholipid analysis, lipids were extracted from samples containing 1-2 mg protein. Diacylglycerols were extracted from samples corresponding to 0.4 mg protein, and triacylglycerols from samples containing 0.2 mg protein. For the analysis of sterols as well as for species analysis of phospholipids, diacylglycerols, triacylglycerols and sphingolipids samples with 0.3 mg protein were used. Extracted lipids were dried under a stream of nitrogen and stored at -20°C.

2.6.1 Fatty acid analysis

Lipids were extracted as described above, and fatty acids were converted to fatty acid methyl esters by methanolysis using 2.5 % sulphuric acid in methanol and heating at 80°C for 90 min. Fatty acid methyl esters were extracted in a mixture of light petroleum and water (3/1; per vol.) and analyzed by gas liquid chromatography (Hewlett-Packard 6890 Gas-chromatograph) using a HP-INNOWax capillary column (15 m x 0.25 mm i.d. x 0.50 µm film thickness) with helium as carrier gas. Fatty acids were identified by comparison to the fatty acid methyl ester standard mix GLC-68B (NuCheck, Inc., Elysian, MN, USA) and hexacosanoic acid methyl ester standard (Sigma Aldrich, Vienna).

2.6.2 Phospholipid analysis

Individual phospholipids were separated by two-dimensional thin-layer chromatography on Silica gel 60 plates using chloroform/methanol/25 % NH_3 (65/35/5 per vol.) as the first, and chloroform/acetone/methanol/acetic acid/water (50/20/10/10/5, per vol.) as the second solvent system. Phospholipids were detected by staining with iodine vapor. Stained spots were scraped off and phospholipids were quantified by the procedure of Broekhuyse [29]. For total phospholipid analysis, aliquots of dried lipid extracts were directly subjected to phosphate determination using phosphate as standard.

For phospholipid species analysis by LC-MS lipids extracted as described above were dissolved in chloroform/methanol (1/1; v/v) and spiked with a set of 28 internal standards. Internal standardization and data acquisition by HPLC coupled to a FT-ICR-MS hybrid mass spectrometer (LTQ-FT, Thermo Scientific) was described previously by Fauland et al. [30]. Data processing takes into account exact mass and retention time and was performed by Lipid Data Analyzer according to Hartler et al. [31].

2.6.3 Diacylglycerol and triacylglycerol analysis

Diacylglycerols (DG) and triacylglycerols (TG) were extracted and separated by thin layer chromatography (TLC) using Silica Gel 60 plates (Merck). DG chromatograms were developed in an ascending manner using chloroform/acetone/acetic acid (45/4/0.5; per vol.) as a solvent system. TG chromatograms were developed in an ascending manner by a two-step developing system. First, light petroleum/diethyl ether/acetic acid (35/15/1; per vol.) was used as mobile phase, and chromatograms were developed to half-distance of the plate. Then, plates were dried briefly and chromatograms were further developed to the top of the plate using light petroleum/diethyl ether (49/1; v/v) as the second mobile phase.

Bands were visualized by dipping the plate for 15 s into a solution consisting of 0.63 g $MnCl_2.4H_2O$, 60 ml water, 60 ml methanol, and 4 ml concentrated sulphuric acid, and incubated in a heating chamber at 105°C for at least 30 min. Then, DG and TG bands were identified and quantified by comparison to appropriate standards (diolein, triolein) and densitometric scanning at 400 nm with a TLC Scanner (CAMAG TLC Scanner 3).

2.6.4 Sterol analysis

Sterol analysis was performed as described by Quail and Kelly [32]. After alkaline hydrolysis of lipid extracts using cholesterol as internal standard, gas liquid chromatography/ mass spectrometry (GLC/MS) was carried out with a Hewlett-Packard 5890 Gas-Chromatograph equipped with a mass selective detector (HP 5972), using an HP 5-MS capillary column (30 m x 0.25 mm i.d. x 0.25 µm film thickness). Sample aliquots of 1 µl were injected in the splitless mode at 270°C injection temperature with helium as carrier gas and with a flow rate set at 0.9 ml/ min in constant flow mode. The temperature program was 100°C for 1 min, 10°C/ min to 250°C, and 3°C/ min to 310°C. Sterols were identified by their mass fragmentation pattern.

2.6.5 Sphingolipid analysis

Bulk membranes and microsomal preparations containing 300 µg protein were spiked with 30 µl of the internal standard mix as an extraction control (0.15 nmol *N*-(dodecanoyl)-sphing-4-enine, 0.15 nmol *N*-(dodecanoyl)-1-β-glucosyl-sphing-4-enine, 4.5 nmol C17 sphinganine, Avanti Polar Lipids, Inc., Alabaster, AL, USA), suspended in 6 ml propan-2-ol/hexane/water (60:26:14; per vol) and incubated at 60°C for 30 min slightly modifying a protocol described previously [33]. During the incubation, samples were shortly vortexed and sonicated after 0, 10, 20 and 30 min. Then, the extracts were cleared from cell debris by centrifugation, dried under a stream of nitrogen, redissolved in 800 µl tetrahydrofuran/methanol/water (4:4:1; per vol.) [34] and stored under argon at -20°C. For analysis, samples were resolubilized by gentle heating and sonication.

UPLC-nanoESI-MS/MS was initiated by Ultra Performance Liquid Chromatography (UPLC) performed on an ACQUITY UPLC® system (Waters Corp., Milford, MA, USA) equipped with an ACQUITY UPLC® HSS T3 Column (100 mm × 1 mm, 1 µm; Waters Corp., Milford, MA, USA). Aliquots of 2 µl were injected in the partial loop with needle overfill mode. The flow rate was 0.12 ml/min, and the separation temperature was 35°C. Inositol containing sphingolipids were separated by linear gradient elution as follows: 65 % solvent B held for 2 min, linear increase to 100 % solvent B for 8 min, 100 % solvent B held for 2 min and equilibration to 65 % solvent B in 2 min. Ceramides (Cer) and hexosylceramides (HexCer) were separated as follows: 80 % solvent B held for 2 min, linear increase to 100 % solvent B for 8 min, 100 % solvent B held for 2 min and equilibration to 80

% solvent B in 2 min. Solvent B was tetrahydrofuran/methanol/20 mM ammonium acetate containing 0.1 % (v/v) acetic acid; and solvent A was methanol/20 mM ammonium acetate containing 0.1 % (v/v) acetic acid. Chip-based nanoelectrospray ionization was achieved with a TriVersa Nanomate® (Advion, Ithaca, NY, USA) in the positive ion mode with 5 μm internal diameter nozzles, a flow rate of 209 nl/ min and a voltage of 1.5 kV. Detection of sphingolipid molecular species was carried out with a 4000 QTRAP® tandem mass spectrometer (AB Sciex, Framingham, MA, USA) by monitoring (i) the transition from $[M+H]^+$ molecular ions to dehydrated long chain base (LCB) fragments for Cer, HexCer and LCB; and (ii) the loss of phosphoinositol containing head groups for inositol containing sphingolipids [35,36]. Dwell time was 30 ms and MS parameters were optimized to maximize detector response.

3 Results

3.1 Isolation of microsomes from *P. pastoris* and quality control

P. pastoris cells were harvested at the late exponential growth phase and microsomal fractions were isolated as described under Experimental Procedures. Figure 1A shows the protein profiles of homogenate and the two microsomal fractions M30 and M40 as analyzed by SDS-PAGE. The protein patterns of both microsomal fractions look similar to each other and also to the pattern of the homogenate indicating that M30 and M40 are major subcellular fractions. Western blot analysis (Figure 1B) and the calculation of the relative enrichment/depletion of the signal intensities from marker proteins (Figure 1C) revealed marked enrichment of M30 and M40 over the homogenate as judged by the appearance of the HDEL microsomal marker. This antibody is directed against a C-terminal tetrapeptide found in ER resident soluble proteins from the yeast. In contrast, other organelle markers such as the outer mitochondrial membrane protein porin (Por1p), the Golgi marker Emp47p or the cytosolic glyceraldehyde-3-phosphate-dehydrogenase (GAPDH) were markedly depleted or even missing in M30 and M40 indicating only marginal contamination with other cellular fractions. This result led us to conclude that high quality microsomal fractions were obtained employing the described protocol. Since the ER is in close contact to the plasma membrane we also used the plasma membrane marker beta-1,3-glucanosyltransferase Gas1p for quality control. Gas1p was hardly detectable in the homogenate and in the M40 fraction, and present only at low amount in M30 compared to highly purified plasma membrane. Thus, cross-contamination of microsomes with plasma membrane was also very low. A possible peroxisomal contamination was tested by using an antibody directed against the peroxisomal membrane protein Pex3p. It has to be noted, however, that under growth conditions chosen for this study peroxisomes do not proliferate. Not unexpectedly, a slight signal of Pex3p was found in the M30 fraction. It is well known that in un-induced yeast cells Pex3p is retained in the ER [37,38]. The delta(24)-sterol C-methyltransferase Erg6p was used as another marker protein. Erg6p was detected in the homogenate and also at a lower amount in M30. This result is in line with previous findings [17] describing the dual localization of Erg6p in lipid droplets and in the ER.

3.2 Lipid analysis of *P. pastoris* microsomes

3.2.1 Fatty acids

Fatty acids are components of glycerophospholipids, sphingolipids and storage lipids such as triacylglycerols and steryl esters [39,40]. Since fatty acids are building blocks of membrane lipids, they contribute to the physical properties of these cell structures [41]. Table 1 shows the fatty acid composition of microsomal membranes M30 and M40 compared to the homogenate. Oleic acid (18:1) and linoleic acid (18:2) are the predominant fatty acids in the homogenate and in M30. In these samples, palmitic acid (16:0), linolenic acid (18:3) and the very long chain cerotic acid (26:0) were also found at substantial amounts, whereas the amounts of other fatty acids were below 5 % each. Consequently, homogenate (H) and M30 exhibit a high degree of unsaturation. In contrast, the major fatty acids of M40 are palmitic acid (16:0) followed by oleic acid (18:1) and linoleic acid (18:2). The amount of linolenic acid was decreased whereas the level of cerotic acid was increased in M40 compared to homogenate. This pattern resulted in a marked shift of the ratio of unsaturated to saturated fatty acids to a lower value in M40.

3.2.2 Diacylglycerols and triacylglycerols

Although diacylglycerols (DG) and triacylglycerols (TG) are not typical membrane lipids and rather stored in lipid droplets [42,43], substantial amounts of these non-polar lipids were found in microsomes (Figure 2A). The level of DG appears to be similar in homogenate (H) and in M30 and M40, whereas TG accumulated in M30 by a factor of 5 in comparison to homogenate and M40. Interestingly, DG and TG species of M30 and M40 were different from the homogenate (Figure 2B). Major DG species were C34 followed by C36. All of these species contained at least one mono-unsaturated fatty acid. Noteworthy, C38 species were only found in the homogenate but not in the microsomes. A detailed list of possible fatty acid combinations is shown in Supplemental Table S1. Molecular species of TG showed a higher diversity (Figure 2C). In TG, saturated molecular species were completely missing. The majority of TG species contained 54 C-atoms followed by 52 C-atoms. Microsomes harbor more C54 species, whereas the homogenate is enriched in C52 and C56 TG species.

3.2.3 Glycerophospholipids

Glycerophospholipids are important components of the ER because they determine membrane features which play an important role in diverse functions such as protein and lipid synthesis and transport [44]. Figure 3 summarizes the results of the phospholipid analysis of *P. pastoris* microsomal membranes and homogenate. M30 showed the highest phospholipid to protein ratio compared to homogenate and M40 (Figure 3A). The total phospholipid content of M40 microsomes was similar to the homogenate. Analysis of individual phospholipids (Figure 3B) demonstrated that phosphatidylcholine (PC) is the major phospholipid in all samples followed by phosphatidylethanolamine (PE). PC values of microsomes are not markedly different from homogenate. A slight decrease of PE in M40 microsomes was observed. Levels of phosphatidic acid (PA), phosphatidylinositol (PI) and lysophospholipids (LP) were slightly increased in microsomes whereas only traces of cardiolipin (CL) were found.

The species patterns of the major phospholipids PC, PE, PI and PS in homogenate, M30 and M40 were analyzed by mass spectrometry (Figure 4). The analysis of the fatty acids of *P. pastoris* homogenate and microsomes as shown in Table 1 served as a basis for possible combinations of these fatty acids in phospholipids (Supplemental Table S2). In PC and PE, C34 and C36 species with different degrees of unsaturation were predominant. In contrast, PS contained a limited set of C34:1, C34:2 and C34:3 species. The different species patterns of PS, PE and PC are interesting because these three phospholipids are biosynthetically linked through the pathway of aminoglycerophospholipid formation [45]. The species pattern of PI is also limited to C34:1 and C34:2 as major components. Noteworthy, saturated phospholipid species were not found in PC, PS and PI, and only at a small amount in PE.

Comparing phospholipid species from the homogenate to M30 and M40 fractions some minor changes were observed. As examples, C36:5 and C36:6 species of PC were slightly increased in microsomes at the expense of C34:1 and C36:2. C32 and C34 species of PE were increased in microsomes at the expense of C36 species; and a decrease of C34:1 in PI from microsomes was compensated by an increase of C34:3.

3.2.4 Sterols

Sterols of the yeast as of other cell types exist as membrane components or as storage components in the form of steryl esters [46–49]. Sterols from *P. pastoris* homogenate and

microsomes were analyzed by gas-liquid chromatography/mass spectrometry. The content of ergosterol in the homogenate and the M40 fraction showed comparable levels (5-7 µg/mg protein), whereas in M30 a 3-fold increase of the ergosterol to protein ratio was detected (~16 µg/mg protein). Ergosterol precursors (ergosta-7,22-dien, episterol, lanosterol, 4-methyl-zymosterol, 4,4-dimethylcholeta-8,24-dien) were also found in all three fractions although only at trace amounts (<0.5 µg/mg protein).

3.2.5 Sphingolipids

The simplest membrane sphingolipids in yeast are ceramides (Cer) which contain a long chain base (sphingoid base) with an acyl chain attached via an amide bond. Different polar head groups containing hexosyl and inositolphosphoryl units can be bound to ceramides giving rise to hexosylceramides (HexCer), inositolphosphorylceramides (IPC), mannosylinositolphosphorylceramides (MIPC), and mannosyldiinositolphosphorylceramides ($M(IP)_2C$) [50,51].

All these sphingolipid classes from bulk membranes and microsomal preparations of *P. pastoris* were analyzed at the molecular level by UPLC-nanoESI-MS/MS. Bulk membranes were prepared as a control by two different cell disruption methods (Zymolyase or Merckenschlager) which did not, however, affect the outcome of the analysis (Figure 5). Microsomes M30 and M40 were isolated as described above. The application of a reversed phase chromatographic separation was crucial for the identification, exclusion of false positives and discernment between isobaric species and allowed the profiling of 87 sphingolipid molecular species (Figure 5).

The analysis of ceramides and hexosylceramides showed high similarity of species distributions in bulk membranes and microsomal fractions (Figure 5, Cer and HexCer). Ceramides containing five different long chain bases (18:0;2, 18:1;2, 18:2;2, 19:2:2 and 18:0;3) and eight different saturated fatty acyl chains (16:0;0, 16:0;1, 18:0;0, 18:0;1, 24:0;0, 24:0;1, 26:0;0 and 26:0;1) were detected in both bulk membranes and microsomal fractions (Figure 5, Cer). Ceramides harboring a dihydroxy long chain base contained in all cases a C16 or C18 fatty acyl chain. In contrast, ceramides harboring a trihydroxy long chain base mainly contained α-hydroxylignoceryl (24:0;1) and α-hydroxycerotyl (26:0;1) chains.

Hesoxylceramides contained exclusively dihydroxy long chain bases and α-hydroxy C16 and C18 fatty acyl chains (Figure 5, HexCer). The accumulation of hexosylceramides increased with unsaturation and methylation of the long chain base. The major species

consists of a diunsaturated and methylated long chain base (19:2;2). This methylated long chain base was only detected in hexosylceramides and at very low levels in ceramides.

The major inositol containing sphingolipids contained a trihydroxy long chain base (18:0;3) acylated with α-hydroxylignoceryl (24:0;1) or α-hydroxycerotyl (26:0;1) chains, giving rise to 42:0;4 and 44:0;4 species (Figure 5, IPC; MIPC and $M(IP)_2C$). Minor species may also contain saturated dihydroxy long chain bases and non hydroxylated fatty acyl chains. In contrast to ceramides and hexosylceramides, some inositol containing sphingolipids harbored dihydroxy acyl chains, such as dihydroxylignoceryl (24:0;2) and dihydroxycerotyl (26:0;2) giving rise to the pentahydroxy species 42:0;5 and 44:0;5, respectively. Comparison of profiles of inositol containing sphingolipids in bulk membranes and microsomal fractions showed accumulation of several pentahydroxy species, e.g. 42:0;5 in the microsomal fractions, whereas several tetrahydroxy species, e.g. IPC(42:0;4) and IPC(44:0;5) were preferentially found in bulk membranes.

3.3 Proteome analysis of *P. pastoris* microsomes

For proteome analysis of *P. pastoris* microsomes, M30 and M40 fractions were prepared in three biological replicates. The proteomes of these fractions were analyzed by (i) ion trap mass spectrometry and (ii) Q-TOF mass spectrometry. Additionally, homogenates of *P. pastoris* prepared as described in section 2.2 were analyzed.

Microsomal proteins, which were detected in at least two of the three biological replicates, were identified through annotation in the Universal Protein Resource Knowledgebase (http://www.uniprot.org/help/uniprotkb). If necessary, functional annotation was manually curated in addition by individual BLAST search and by protein domain search. As summarized in a Venn diagram (Figure 6), in microsomes, 294 proteins were detected compared to more than 620 polypeptides in the homogenate. Among the 294 microsomal proteins, 126 (~43 %) were exclusively found in the ER fractions but not in the homogenate, whereas 168 proteins were detected in the homogenate as well. Details are shown in the Supplemental Table S3. The former group of proteins was considered as highly enriched in microsomal fractions. Proteins found in all three fractions (H, M30, M40) were mostly present at lower amounts in the homogenate than in microsomes (see Supplemental Table S3).

Among the proteins enriched in the microsomal fractions, several components of core ER functions were present including subunits of the translocon pore, the signal peptidase complex, and the OST complex involved in protein N-glycosylation (see Table 2 and

Supplemental Table S3). Furthermore, several enzymes involved in N- and O-glycosylation, GPI anchor biosynthesis, and lipid biosynthesis, as well as ER resident chaperones and foldases were found. It has to be noted that several proteins of the latter group such as the Hsp70 chaperone, Kar2p and protein disulfide isomerase Pdi1p were also detected in the homogenate, confirming their high abundance in the total cell extract (up to 30 % of total ER protein). Another large group of proteins detected were proteins which are travelling through the ER on the way to their final cellular destination such as the Golgi, the vacuole or the cell surface (plasma membrane and cell wall). Approximately 70 of 294 gene products are involved in cytoplasmic translation. Most members of this group are components of the ribosome (63 ribosomal proteins) which are attached to the cytosolic side of the ER membrane during co-translational translocation, and cytosolic chaperones involved in co- and post-translational translocation of the nascent polypeptides across the ER membrane through the Sec61p and Ssh1p translocon pore complexes (for recent review see [6]). Some mitochondrial membrane proteins were also detected, especially in M30. Our proteome analysis also identified microsomal enzymes involved in lipid metabolism. A group of fatty acid synthesizing and elongating proteins such as Fas1p, Sur4p or Ole1p was detected as well as proteins involved in phospholipid metabolism such as Cho2p, Sac1p and Gpt2p. Moreover, some enzymes of sterol and sphingolipid metabolism, like Lcb1p, Lcb2p and several Erg-proteins were identified in the microsomal fractions. Enzymes of lipid metabolism predicted to be localized in the ER were more abundant in M30, as are also ER resident chaperones, proteins involved in ER glycosylation and mitochondrial proteins. In contrast, ER proteins with unknown function were enriched in M40, where also the majority of ER-to-Golgi transport proteins and Golgi glycosylation enzymes were found. No preference for either M30 or M40 was observed for the other functional categories (Table 2 and Supplemental Table S3).

From the microsomal proteome identified here, 99 proteins were already annotated as ER-localized or ER-associated and 63 polypeptides as ribosomal proteins, whereas 20 proteins have not yet been assigned to a biological function. Ten of these proteins were predicted to be localized to the ER. One third of all detected proteins are involved in carbohydrate and lipid metabolic processes or transmembrane transport. It is well known that the ER contributes to all of these processes. Furthermore, ER proteins also participate in the other processes shown in Table 3 such as protein targeting, glycosylation and folding [52–54]. Interestingly, only one component of the peroxisomal import machinery was found, which has

been reported to be assembled in the ER membrane, confirming that peroxisome biosynthesis is not highly active in glucose grown *P. pastoris*.

In Table 3 the top 25 hits of proteins detected in M30 and M40 are listed. The ranking is based on mean values of protein scores from mass spectrometry. The highest scores were attributed to Sec63p, a component of the protein targeting and ER import machinery; Ost1p, a protein involved in protein glycosylation in the ER lumen; and Emp47p which is an integral membrane component of ER-derived COPII coated vesicles. The top 25 list also includes proteins involved in the protein secretory process (Sec-proteins), lipid metabolism and protein glycosylation. A complete list of all 294 proteins found in microsomes with detailed information about occurrences in M30, M40 and the homogenate as well as their biological function is shown in the Supplemental Table S3.

4 Discussion

In the present study we report an isolation protocol for ER fractions (microsomes) from the methylotrophic yeast *P. pastoris* which is a valuable microorganism in biotechnology. The protocol used for isolation of M30 and M40 microsomes was adapted from methods originally designed for *Saccharomyces cerevisiae* and is based on various steps of differential centrifugation.

Although the high purity of microsomal fractions was confirmed by Western Blot analysis, contamination with other subcellular fractions could not be excluded. Such contaminations can be derived either from unwanted co-fractionation of other cellular compartments/components or from ER associated components which represent biologically relevant structural and functional links of the ER to other organelles. The long list of proteins detected in microsomal fractions allows interpretations in both directions, although a vast proportion of polypeptides detected in our proteomic approach appear to be "true" ER proteins. Within the cell, ER proteins comprise a predominant portion of total proteins as can also be seen from the protein patterns on SDS Gels (see Fig. 1) and from our proteome analysis which provides for the first time a deeper insight into the protein molecular equipment of microsomes from *P. pastoris* (see Table 2 and 3 and Supplemental Table 3).

The finding that the proteomes of M30 and M40 microsomal fractions were rather similar was not surprising. The question remained why two different populations of microsomal vesicles were obtained. A possible explanation for this finding may be differences in the lipid patterns. As shown in Table 1 and Figure 2, the degree of fatty acid desaturation and the phospholipid to protein ratio as well as the ergosterol content were markedly different in M30 and M40. These properties may contribute to differences in the sedimentation behavior of the two microsomal vesicles populations.

An interesting observation in our lipidome study was the finding that almost all phospholipid species detected contained at least one unsaturated fatty acid. Since *P. pastoris* does not only produce monounsaturated fatty acids like *S. cerevisiae* [53], but also polyunsaturated acyl chains, a high degree of unsaturation in the membranes may be reached and may influences membrane properties. Moreover, enzymes embedded in membranes might rely on certain conditions in their environment.

Another important observation derived from the lipidome analysis is the phospholipid class specific pattern of species. These differences can be explained by the biosynthetic origin of the respective phospholipids. PS and PI are derived from the same precursor, CDP-

diacylglycerol [54,55]. Although PS and PI synthases are distinct enzymes, their specificity appears to be similar resulting in PS and PI species patterns with a large portion on C34:1 and C34:2. The pattern of species in the aminoglycerophospholipid biosynthetic route (PS – PE – PC) becomes less specific. This is also due to a second biosynthetic route, the CDP-ethanolamine/choline pathway contributes to PE and PC formation. These facts result in the broad and almost randomized pattern of PC species (see Figure 3).

Sterols and sphingolipids are synthesized in the ER and delivered to other organelles, mostly to the plasma membrane where they contribute to stability/rigidity of the membrane [56,57]. Interestingly, a number of sterol biosynthetic enzymes (Erg-proteins) were found as prominent components of the ER in our proteome study (see Table 2, Table 3 and Supplemental Table S3). Nevertheless, *P. pastoris* has to be regarded as a low sterol yeast since sterol levels in all organelle membranes (our own observations and [7,8]) as well as in lipid droplets in the form of steryl esters [9] are low. Similar to sterols, the concentration of inositol containing sphingolipids in ER membranes appears to be low compared to the plasma membrane (our own unpublished observations).

Detection of substantial amounts of DG and TG in microsomes was surprising because these components are mainly found as storage lipids in lipid droplets. However, it has to be noted that enzymes of TG synthesis in *P. pastoris* identified recently [58] are also ER components.

In conclusion, our study presented here describes an in depth analysis of microsomal compartments at lipid and protein levels. We regard these analytical data as important for a deeper knowledge of *P. pastoris* organelles and to understanding organelle bound processes of this yeast in more detail.

Acknowledgements

This work has been supported by Austrian Science Fund FWF (project TRP 9 to G. D.), the Federal Ministry of Economy, Family and Youth (BMWFJ), the Federal Ministry of Traffic, Innovation and Technology (bmvit), the Styrian Business Promotion Agency SFG, the Standortagentur Tirol and ZIT – Technology Agency of the City of Vienna through the COMET-Funding Program managed by the Austrian Research Promotion Agency FFG, and by the Austrian Centre of Industrial Biotechnology (ACIB GmbH). EQ BOKU VIBT GmbH is acknowledged for providing LC-MS/MS instrumentation. P. T. is supported by the Microbiology and Biochemistry program of the Goettingen Graduate School of Neurosciences and Molecular Biology (GGNB).

References

[1] M. Bollok, D. Resina, F. Valero, P. Ferrer, Recent patents on the *Pichia pastoris* expression system: expanding the toolbox for recombinant protein production, Recent Pat. Biotechnol., 3 (2009) 192–201.

[2] E. Papanikou, B.S. Glick, The yeast Golgi apparatus: Insights and mysteries, FEBS Lett., 583 (2009) 3746–3751.

[3] C. Ma, G. Agrawal, S. Subramani, Peroxisome assembly: matrix and membrane protein biogenesis, J. Cell Biol., 193 (2011) 7–16.

[4] B. Gasser, R. Prielhofer, H. Marx, M. Maurer, J. Nocon, M. Steiger, V. Puxbaum, M. Sauer, D. Mattanovich, *Pichia pastoris*: protein production host and model organism for biomedical research, Future Microbiol., 8 (2013) 191–208.

[5] L.M. Damasceno, C.-J. Huang, C.A. Batt, Protein secretion in *Pichia pastoris* and advances in protein production, Appl. Microbiol. Biotechnol., 93 (2012) 31–39.

[6] M. Delic, M. Valli, A.B. Graf, M. Pfeffer, D. Mattanovich, B. Gasser, The secretory pathway: Exploring yeast diversity, FEMS Microbiol. Rev., (2013) 1-43.

[7] T. Wriessnegger, G. Gübitz, E. Leitner, E. Ingolic, J. Cregg, B.J. de la Cruz, G. Daum, Lipid composition of peroxisomes from the yeast *Pichia pastoris* grown on different carbon sources, Biochim. Biophys. Acta, 1771 (2007) 455–461.

[8] T. Wriessnegger, E. Leitner, M.R. Belegratis, E. Ingolic, G. Daum, Lipid analysis of mitochondrial membranes from the yeast *Pichia pastoris*, Biochim. Biophys. Acta, 1791 (2009) 166–172.

[9] V.A. Ivashov, K. Grillitsch, H. Koefeler, E. Leitner, D. Baeumlisberger, M. Karas, G. Daum, Lipidome and proteome of lipid droplets from the methylotrophic yeast *Pichia pastoris*, Biochim. Biophys. Acta, 1831 (2012) 282-290.

[10] W.A. Prinz, L. Grzyb, M. Veenhuis, J.A. Kahana, P.A. Silver, T.A. Rapoport, Mutants affecting the structure of the cortical endoplasmic reticulum in *Saccharomyces cerevisiae*, J. Cell Biol., 150 (2000) 461–474.

[11] P. Shindiapina, C. Barlowe, Requirements for transitional endoplasmic reticulum site structure and runction in *Saccharomyces cerevisiae*, Mol. Biol. Cell, 21 (2010) 1530–1545.

[12] G.K. Voeltz, M.M. Rolls, T.A. Rapoport, Structural organization of the endoplasmic reticulum, EMBO Rep., 3 (2002) 944–950.

[13] E.M. Lynes, T. Simmen, Urban planning of the endoplasmic reticulum (ER): How diverse mechanisms segregate the many functions of the ER, Biochim. Biophys. Acta, 1813 (2011) 1893–1905.

[14] J. Hou, K.E.J. Tyo, Z. Liu, D. Petranovic, J. Nielsen, Metabolic engineering of recombinant protein secretion by *Saccharomyces cerevisiae*, FEMS Yeast Res., 12 (2012) 491–510.

[15] N.A. Baumann, D.P. Sullivan, H. Ohvo-Rekilä, C. Simonot, A. Pottekat, Z. Klaassen, C.T. Beh, A.K. Menon, Transport of newly synthesized sterol to the sterol-enriched plasma membrane occurs via nonvesicular equilibration, Biochem., 44 (2005) 5816–5826.

[16] M. Schnabl, G. Daum, H. Pichler, Multiple lipid transport pathways to the plasma membrane in yeast, Biochim. Biophys. Acta, 1687 (2005) 130–140.

[17] H. Pichler, B. Gaigg, C. Hrastnik, G. Achleitner, S.D. Kohlwein, G. Zellnig, A. Perktold, G. Daum, A subfraction of the yeast endoplasmic reticulum associates with the plasma membrane and has a high capacity to synthesize lipids, Eur. J. Biochem., 268 (2001) 2351–2361.

[18] R.J. Perry, N.D. Ridgway, Molecular mechanisms and regulation of ceramide transport, Biochim. Biophys. Acta, 1734 (2005) 220–234.

[19] D. Peretti, N. Dahan, E. Shimoni, K. Hirschberg, S. Lev, Coordinated lipid transfer between the endoplasmic reticulum and the Golgi complex requires the VAP proteins and is essential for Golgi-mediated transport, Mol. Biol. Cell, 19 (2008) 3871–3884.

[20] G. Achleitner, B. Gaigg, A. Krasser, E. Kainersdorfer, S.D. Kohlwein, A. Perktold, G. Zellnig, G. Daum, Association between the endoplasmic reticulum and mitochondria of yeast facilitates interorganelle transport of phospholipids through membrane contact, Eur. J. Biochem., 264 (1999) 545–553.

[21] O.H. Lowry, N.J. Rosebrough, A.L. Farr, R.J. Randall, Protein measurement with the Folin phenol reagent, J. Biol. Chem., 193 (1951) 265–275.

[22] U.K. Laemmli, Cleavage of structural proteins during the assembly of the head of bacteriophage T4, Nature, 227 (1970) 680–685.

[23] A. Haid, M. Suissa, Immunochemical identification of membrane proteins after sodium dodecyl sulfate-polyacrylamide gel electrophoresis, Meth. Enzymol., 96 (1983) 192–205.

[24] F. Wu, D. Sun, N. Wang, Y. Gong, L. Li, Comparison of surfactant-assisted shotgun methods using acid-labile surfactants and sodium dodecyl sulfate for membrane proteome analysis, Anal. Chim. Acta, 698 (2011) 36–43.

[25] M. Dragosits, J. Stadlmann, J. Albiol, K. Baumann, M. Maurer, B. Gasser, M. Sauer, F. Altmann, P. Ferrer, D. Mattanovich, The effect of temperature on the proteome of recombinant *Pichia pastoris*, J. Proteome Res., 8 (2009) 1380–1392.

[26] D. Kolarich, F. Altmann, N-Glycan analysis by matrix-assisted laser desorption/ionization mass spectrometry of electrophoretically separated nonmammalian proteins: Application to peanut allergen Ara h 1 and olive pollen allergen Ole e 1, Anal. Biochem., 285 (2000) 64–75.

[27] D. Kolarich, F. Altmann, E. Sunderasan, Structural analysis of the glycoprotein allergen Hev b 4 from natural rubber latex by mass spectrometry, Biochim. Biophys. Acta, 1760 (2006) 715–720.

[28] J. Folch, M. Lees, G.H. Sloane Stanley, A simple method for the isolation and purification of total lipides from animal tissues, J. Biol. Chem., 226 (1957) 497–509.

[29] R.M. Broekhuyse, Phospholipids in tissues of the eye I Isolation, characterization and quantitative analysis by two-dimensional thin-layer chromatography of diacyl and vinyl-ether phospholipids, Biochim. Biophys. Acta, 152 (1968) 307–315.

[30] A. Fauland, H. Köfeler, M. Trötzmüller, A. Knopf, J. Hartler, A. Eberl, C. Chitraju, E. Lankmayr, F. Spener, A comprehensive method for lipid profiling by liquid chromatography-ion cyclotron resonance mass spectrometry, J. Lipid Res., 52 (2011) 2314–2322.

[31] J. Hartler, M. Trötzmüller, C. Chitraju, F. Spener, H.C. Köfeler, G.G. Thallinger, Lipid Data Analyzer: unattended identification and quantitation of lipids in LC-MS data, Bioinformatics, 27 (2011) 572–577.

[32] M.A. Quail, S.L. Kelly, The extraction and analysis of sterols from yeast, Methods Mol. Biol., 53 (1996) 123–131.

[33] J.E. Markham, J. Li, E.B. Cahoon, J.G. Jaworski, Separation and identification of major plant sphingolipid classes from leaves, J. Biol. Chem., 281 (2006) 22684–22694.

[34] C. Buré, J.-L. Cacas, F. Wang, K. Gaudin, F. Domergue, S. Mongrand, J.-M. Schmitter, Fast screening of highly glycosylated plant sphingolipids by tandem mass spectrometry, Rapid Comm. Mass Spectrom., 25 (2011) 3131–3145.

[35] J.E. Markham, J.G. Jaworski, Rapid measurement of sphingolipids from *Arabidopsis thaliana* by reversed-phase high-performance liquid chromatography coupled to

electrospray ionization tandem mass spectrometry, Rapid Comm. Mass Spectrom., 21 (2007) 1304–1314.

[36] C.S. Ejsing, T. Moehring, U. Bahr, E. Duchoslav, M. Karas, K. Simons, A. Shevchenko, Collision-induced dissociation pathways of yeast sphingolipids and their molecular profiling in total lipid extracts: a study by quadrupole TOF and linear ion trap–orbitrap mass spectrometry, J. of Mass Spectrom., 41 (2006) 372–389.

[37] D. Hoepfner, D. Schildknegt, I. Braakman, P. Philippsen, H.F. Tabak, Contribution of the endoplasmic reticulum to peroxisome formation, Cell, 122 (2005) 85–95.

[38] Y.Y.C. Tam, A. Fagarasanu, M. Fagarasanu, R.A. Rachubinski, Pex3p initiates the formation of a preperoxisomal compartment from a subdomain of the endoplasmic reticulum in *Saccharomyces cerevisiae*, J. Biol. Chem., 280 (2005) 34933–34939.

[39] G. Daum, N.D. Lees, M. Bard, R. Dickson, Biochemistry, cell biology and molecular biology of lipids of *Saccharomyces cerevisiae*, Yeast, 14 (1998) 1471–1510.

[40] T. Czabany, K. Athenstaedt, G. Daum, Synthesis, storage and degradation of neutral lipids in yeast, Biochim. Biophys. Acta, 1771 (2007) 299–309.

[41] J. Petschnigg, H. Wolinski, D. Kolb, G. Zellnig, C.F. Kurat, K. Natter, S.D. Kohlwein, Good fat, essential cellular requirements for triacylglycerol synthesis to maintain membrane homeostasis in Yeast, J. Biol. Chem., 284 (2009) 30981–30993.

[42] S. Rajakumari, R. Rajasekharan, G. Daum, Triacylglycerol lipolysis is linked to sphingolipid and phospholipid metabolism of the yeast *Saccharomyces cerevisiae*, Biochim. Biophys. Acta, 1801 (2010) 1314–1322.

[43] K. Athenstaedt, G. Daum, *YMR313c/TGL3* encodes a novel triacylglycerol lipase located in lipid particles of *Saccharomyces cerevisiae*, J. Biol. Chem., 278 (2003) 23317–23323.

[44] T.A. Lagace, N.D. Ridgway, The role of phospholipids in the biological activity and structure of the endoplasmic reticulum, Biochim. Biophys. Acta, 1833 (2013) 2499–2510.

[45] S.A. Henry, S.D. Kohlwein, G.M. Carman, Metabolism and regulation of glycerolipids in the Yeast *Saccharomyces cerevisiae*, Genetics, 190 (2012) 317–349.

[46] E. Zinser, C.D. Sperka-Gottlieb, E.V. Fasch, S.D. Kohlwein, F. Paltauf, G. Daum, Phospholipid synthesis and lipid composition of subcellular membranes in the unicellular eukaryote *Saccharomyces cerevisiae*, J. Bacteriol., 173 (1991) 2026–2034.

[47] E. Zinser, F. Paltauf, G. Daum, Sterol composition of yeast organelle membranes and subcellular distribution of enzymes involved in sterol metabolism, J. Bacteriol., 175 (1993) 2853–2858.

[48] M. Bard, D.A. Bruner, C.A. Pierson, N.D. Lees, B. Biermann, L. Frye, C. Koegel, R. Barbuch, Cloning and characterization of *ERG25*, the *Saccharomyces cerevisiae* gene encoding C-4 sterol methyl oxidase, Proc. Nat. Acad. Sci. U.S.A., 93 (1996) 186–190.

[49] R. Leber, K. Landl, E. Zinser, H. Ahorn, A. Spök, S.D. Kohlwein, F. Turnowsky, G. Daum, Dual localization of squalene epoxidase, Erg1p, in yeast reflects a relationship between the endoplasmic reticulum and lipid particles, Mol. Biol. Cell, 9 (1998) 375–386.

[50] R.C. Dickson, Thematic review series: Sphingolipids: New insights into sphingolipid metabolism and function in budding yeast, J. Lipid Res., 49 (2008) 909–921.

[51] P. Ternes, T. Wobbe, M. Schwarz, S. Albrecht, K. Feussner, I. Riezman, J.M. Cregg, E. Heinz, H. Riezman, I. Feussner, D. Warnecke, Two pathways of sphingolipid biosynthesis are separated in the yeast *Pichia pastoris*, J. Biol. Chem., 286 (2011) 11401–11414.

[52] M. Aebi, R. Bernasconi, S. Clerc, M. Molinari, N-glycan structures: recognition and processing in the ER, Trends in Biochem. Sci., 35 (2010) 74–82.

[53] G. Tuller, T. Nemec, C. Hrastnik, G. Daum, Lipid composition of subcellular membranes of an FY1679-derived haploid yeast wild-type strain grown on different carbon sources, Yeast, 15 (1999) 1555–1564.

[54] N.M. Jani, J.M. Lopes, Regulated transcription of the *Saccharomyces cerevisiae* phosphatidylinositol biosynthetic gene, *PIS1*, yields pleiotropic effects on phospholipid synthesis, FEMS Yeast Res., 9 (2009) 552–564.

[55] H.-S. Choi, A. Sreenivas, G.-S. Han, G.M. Carman, Regulation of phospholipid synthesis in the Yyeast *cki1Δ eki1Δ* mutant defective in the Kennedy pathway: The *Cho1*-encoded phosphatidylserine synthase is regulated by mRNA stability, J. Biol. Chem., 279 (2004) 12081–12087.

[56] G. van Meer, D.R. Voelker, G.W. Feigenson, Membrane lipids: where they are and how they behave, Nat. Rev. Mol. Cell Biol., 9 (2008) 112–124.

[57] S. Gulati, Y. Liu, A.B. Munkacsi, L. Wilcox, S.L. Sturley, Sterols and sphingolipids: Dynamic duo or partners in crime?, Prog. Lipid Res., 49 (2010) 353–365.

[58] V.A. Ivashov, G. Zellnig, K. Grillitsch, G. Daum, Identification of triacylglycerol and steryl ester synthases of the methylotrophic yeast *Pichia pastoris*, Biochim. Biophys. Acta, 1831 (2013) 1158–1166.

Table 1: Fatty acid composition of *P. pastoris* microsomes

Fatty acids from homogenate (H) and microsomes (M30, M40) were analyzed by GLC. Results are shown as relative amounts of total fatty acids (%). Data are mean values of two independent experiments analyzed in replicates (n=4). Maximum standard deviation was ±5%.

	Relative amount of total fatty acids (weight %)										
	C14:0	**C16:0**	**C16:1**	**C18:0**	**C18:1**	**C18:2**	**C18:3**	**C20:1**	**C20:2**	**C26:0**	**unsat.:sat.**
H	0.5	16.0	3.0	3.7	24.4	24.4	14.8	0.0	4.5	8.1	2.5
M30	0.4	18.4	3.5	3.5	26.1	26.0	13.5	1.0	3.4	5.7	2.6
M40	0.7	32.7	3.0	5.2	15.8	13.3	6.4	2.0	6.4	11.2	0.9

Table 2: Categories of proteins detected in the microsomes

Proteome analysis was performed by mass spectrometry from *P. pastoris* 30,000 g microsomes (M30) and 40,000 g microsomes (M40). Proteins were analyzed from 3 independent experiments by i) ion trap MS and by ii) Q-TOF MS as described the methods section. Proteins detected more often in M30 are underlined, while proteins detected more often in M40 are in italics. Proteins that were only found in the microsomal fractions M30 and M40, but not in the homogenate are highlighted in bold. Details can be found in Supplemental Table S3.

Function	**Detected proteins**
Translocation across ER membrane	**Sec61**, **Sec63**, **Sec66**, **Sec72**, Ssh1, ***Sss1***
Signal peptidase complex	***Sec11***, **Spc2**, **Spc3**
ER protein glycosylation	N-glycosylation: **Alg2**, Dpm1, **Gtb1**, *Psa1*, **Rot2** OST-complex: **Ost1**, **Ost2**, ***Ost3***, Swp1, Wbp1 O-glycosylation: **Pmt1**, Pmt2
ER Golgi vesicle transport	ER to Golgi: Arf1, **Emp24**, **Emp47**, **Erp5**, ***Erv14***, ***Erv25***, Sec18, *Ykt6* Golgi to ER: ***Get1***, **Get2**, ***Sec22*** Golgi - endosome/vacuole: Vps1,Vti1, ***Ykt6***, ***Ypt32***, *Ypt52* Golgi to PM: Bmh2, Sec4, ***Snc2***, *Sso2*
GPI anchor biosynthesis	**Gpi8**, **Gpi16**, **Gpi17**
ER resident chaperones & foldases	chaperones: Cne1, **Erj5**, Kar2, **Lhs1** PPIases: Cpr5, ***Fpr2*** oxidative folding: **Ero1**, Pdi1, **Mpd1**, **ERp38**
Other ER resident proteins	Rtn1, Sbf1, **Gsf2**, Gtt1, *Cbr1*, *Yop1*
Lipid metabolism	sterol biosynthesis: ***Erg1***, *Erg2*, ***Erg3***, Erg5, Erg6, **Erg9**, *Erg10*, **Erg11**, **Erg25**, **Erg26**, **Hmg1**, Ncp1, **Nsg2** fatty acid metabolism: Faa1, ***Fad2***, Fas1, **Fen1**, Ifa38, ***Ole1***, **Sur4** phospholipid metabolism: Ayr1, **Cho2**, *Pct1*, Sac1, **Slc1** sphingolipid metabolism: **Dpl1**, Hfd1, Lcb1, **Lcb2**, **Slm1**, PAS_chr4_0465 lipid metabolism: **Tcb1**, **Tcb3**, ***PAS_chr2-1_0835*** others: Het1, **Stt4**

Golgi	glycosylation: **Gda1**, ***Kre2***, Ktr1, ***Ktr4***, ***Mnn2-2***, **Mnn9**, Vrg4 other: **Pmr1**
Ribosome/translation	64 ribosomal proteins of the small and the large subunit associated to ribosomes: Tma19, ***Bfr1*** translation control: *Asc1*, *Dbp2*, Ded1, Efb1, Eft2, Tef2, Tef4-1, *Tif1*, Yef3 chaperones: **Caj1**, Cpr1, Hsp31, Hsp82, **Sis1**, Ssa1, Ssb2, Sse1, Ydj1
Mitochondria	respiratory chain (inner membrane): **Cox4**, **Cox5B**, Nde1, Qcr2 other membrane proteins: ***Fmp52***, Ggc1, Mir1, Odc1, Pet9, Por1 F1F0 ATP synthase: Atp1, Atp2, Atp4, Atp5, Atp7, Atp20 translocase: Ssc1, **Tom22**, Tom40
Vacuole	Cps1, **Pep4**, **Vac8**, ***Vma6***, **Vph1**, Vps70, **Ycf1**
Cell surface	plasma membrane transporters and proteins: Ady2-1, Ady2-2, Aqy1, **Ctr1**, **Dip5**, **Ena**2, **Fre1**, Hxt7, **Ist2**, ***Nce102***, **Ste6**, **Pdr5-1**, **Pdr5-2**, **Pga3**, Pma1, ***Pun1***, Ras1, **Rsr1**, **Sit1**, **Sng1**, **Snq2**, Sur7, **Yck2**, **Yps1-2** cell wall proteins: ***Bgl2***, **Flo5-1**, Fks1, Gas1-1, **Gas1-2**, **Gas3**, Scw10, **YJL171C** proteins involved in cell polarity: Act1, **Rgd1**, Rho1, **Rho3**, **Cdc42** eisosomes: Eis1, Lsp1, ***Seg1***, Pil1
Other	ERAD: Cdc48 ER-nuclear membrane: Pom33, Gsp1 peroxisome: ***Pex14*** histone: Hta2, *Htb2*, Hhf1 core metabolism: Adh2, Cdc19, Eno1, Gnd2, Pgk1, *Sah1*, Sam1, Ser3, Tal1-1, Tdh3 unknown: **PAS_chr1-4_0091**, ***PAS_chr2-1_0218***, **PAS_chr2-1_0254**, **PAS_chr2-2_0082**, PAS_chr2-2_0394, PAS_chr3_0261, **PAS_chr3_0692**, **PAS_chr3_1023**, *PAS_chr4_0320*, Phm7 other: ***Fra1-1***, Phb2, **Rsp5**, **Uro1**, Ynk1
Unknown function, predicted to be ER localized	***Emc7***, ***Irc22***, **Msc7**, ***PAS_chr1-3_0136***, *PAS_chr2-1_0046*, ***PAS_chr2-2_0124***, ***PAS_chr3_0249***, ***PAS_chr3_1178***, **Yet3**, YNR021W

Table 3: The Top 25 proteins of *P. pastoris* microsomes

Proteome analysis was performed by mass spectrometry from *P. pastoris* 30,000 g microsomes (M30) and 40,000 g microsomes (M40). Proteins were analyzed from 3 independent experiments by i) ion trap MS and by ii) Q-TOF MS. The Top 25 proteins (i) ranked by protein score (1, highest score) derived from the ion scores during MS (proteins with a protein score higher than 70 and a minimum of two peptides identified were accepted); (ii) found in both microsomal fractions, but not in the homogenate; and (iii) at least in two out of three preparations were included. R: Rank, MM: molecular mass; kDa: Kilo Dalton; SP: predicted signal peptide (SignalP 40 Server); SA: predicted signal anchor (SignalP 40 Server); TMH: predicted transmembrane helices (TMHMM2,0). Numbers indicate the amount of TMHs. n: no; y: yes;

R	Probe ID	Short Name *P. pastoris*	Short Name *S. cerevisiae*	Systematic Name *S. cerevisiae*	Protein description of *S. cerevisiae* homolog in Saccharomyces Genome Database	MM [kDa]	SP	SA	TMH
1	Pipas_chr4_0395	SEC63	SEC63	YOR254C	Essential subunit of Sec63 complex (Sec63p, Sec62p, Sec66p and Sec72p); with Sec61 complex, Kar2p/BiP and Lhs1p forms a channel competent for SRP-dependent and post-translational SRP-independent protein targeting and import into the ER	73.6	n	y	3
2	Pipas_chr3_0741	OST1	OST1	YJL002C	Alpha subunit of the oligosaccharyl transferase complex of the ER lumen, which catalyzes asparagine-linked glycosylation of newly synthesized proteins	52.2	y	n	1
3	Pipas_chr4_0432	EMP47	EMP47	YFL048C	Integral membrane component of endoplasmic reticulum-derived COPII-coated vesicles, which function in ER to Golgi transport	53.6	y	n	1
4	Pipas_chr2-1_0212	PMT1	PMT1	YDL095W	Protein O-mannosyltransferase of the ER membrane; transfers mannose from dolichyl phosphate-D-mannose to protein serine and threonine residues; involved in ER quality control; amino terminus faces cytoplasm, carboxyl terminus faces ER lumen	89.5	n	n	9
5	Pipas_chr1-4_0604	ERG26	ERG26	YGL001C	C-3 sterol dehydrogenase, catalyzes the second of three steps required to remove two C-4 methyl groups from an intermediate in ergosterol biosynthesis	38.0	n	n	0

6	Pipas_chr3_0957	ERG11	ERG11	YHR007C	Lanosterol 14-alpha-demethylase; catalyzes the C-14 demethylation of lanosterol to form 4,4"-dimethyl cholesta-8,14,24-triene-3-beta-ol in the ergosterol biosynthesis pathway; member of the cytochrome P450 family; associated and coordinately regulated with the P450 reductase Ncp1p	58.8	n	y	0
7	Pipas_chr3_0488	TCB1	TCB1	YOR086C	Lipid-binding ER protein involved in ER-plasma membrane tethering; one of 6 proteins (Ist2p, Scs2p, Scs22p, Tcb1p, Tcb2p, Tcb3p) that connect ER to the plasma membrane (PM) and regulate PM phosphatidylinositol-4-phosphate (PI4P) levels by controlling access of Sac1p phosphatase to its substrate PI4P in the PM; contains three calcium and lipid binding domains; non-tagged protein also localizes to mitochondria; C-termini of Tcb1p, Tcb2p and Tcb3p interact	129.2	n	n	3
8	Pipas_chr2-1_0448	SEC72	SEC72	YLR292C	Non-essential subunit of Sec63 complex (Sec63p, Sec62p, Sec66p and Sec72p); with Sec61 complex, Kar2p/BiP and Lhs1p forms a channel competent for SRP-dependent and post-translational SRP-independent protein targeting and import into the ER	22.0	n	n	0
9	Pipas_chr2-1_0564	ERP5	ERP5	YHR110W	Protein with similarity to Emp24p and Erv25p, member of the p24 family involved in ER to Golgi transport	27.3	y	y	1
10	Pipas_chr2-1_0433	SEC66	SEC66	YBR171W	Non-essential subunit of Sec63 complex (Sec63p, Sec62p, Sec66p and Sec72p); with Sec61 complex, Kar2p/BiP and Lhs1p forms a channel competent for SRP-dependent and post-translational SRP-independent protein targeting and import into the ER	22.6	n	y	1
11	Pipas_chr1-3_0134	ERJ5	ERJ5	YFR041C	Type I membrane protein with a J domain is required to preserve the folding capacity of the endoplasmic reticulum; loss of the non-essential ERJ5 gene leads to a constitutively induced unfolded protein response	35.0	y	n	1
12	Pipas_chr1-3_0202	SEC61	SEC61	YLR378C	Essential subunit of Sec61 complex (Sec61p, Sbh1p, and Sss1p); forms a channel for SRP-dependent protein import and retrograde transport of misfolded proteins out of the ER; with Sec63 complex allows SRP-independent protein import into ER	52.5	n	y	8

13	Pipas_chr1-1_0120	TCB3	TCB3	YML072C	Cortical ER protein involved in ER-plasma membrane tethering; one of 6 proteins (Ist2p, Scs2p, Scs22p, Tcb1p, Tcb2p, Tcb3p) that connect ER to the plasma membrane (PM) and regulate PM phosphatidylinositol-4-phosphate (PI4P) levels by controlling access of Sac1p phosphatase to its substrate PI4P in the PM; localized to the bud via specific mRNA transport; non-tagged protein detected in a phosphorylated state in mitochondria; C-termini of Tcb1p, Tcb2p and Tcb3p interact	155.2	n	n	1
14	Pipas_chr3_1259	ERV25	ERV25	YML012W	Protein that forms a heterotrimeric complex with Erp1, Erp2p, and Emp24, member of the p24 family involved in endoplasmic reticulum to Golgi transport	30.6	y	y	0
15	Pipas_chr2-1_0342	GSF2	GSF2	YML048W	ER localized integral membrane protein that may promote secretion of certain hexose transporters, including Gal2p; involved in glucose-dependent repression	44.9	n	n	0
16	Pipas_chr1-4_0187	SEC11	SEC11	YIR022W	18kDa catalytic subunit of the Signal Peptidase Complex (SPC; Spc1p, Spc2p, Spc3p, and Sec11p) which cleaves the signal sequence of proteins targeted to the endoplasmic reticulum (2, 3 and see Summary Paragraph) Name Description SECretory 4	19.3	n	y	1
17	Pipas_chr4_0504	NCE102	NCE102	YPR149W	Protein of unknown function; contains transmembrane domains; involved in secretion of proteins that lack classical secretory signal sequences; component of the detergent-insoluble glycolipid-enriched complexes (DIGs)	18.3	y	y	4
18	Pipas_chr2-1_0589	SPC2	SPC2	YML055W	Subunit of signal peptidase complex (Spc1p, Spc2p, Spc3p, Sec11p), which catalyzes cleavage of N-terminal signal sequences of proteins targeted to the secretory pathway; homologous to mammalian SPC25	20.0	n	y	2
19	Pipas_chr3_1157	YPS1-2	YPS1	YLR120C	Aspartic protease, member of the yapsin family of proteases involved in cell wall growth and maintenance; attached to the plasma membrane via a glycosylphosphatidylinositol (GPI) anchor	60.5	y	n	0
20	Pipas_chr1-3_0125	MPD1	MPD1	YOR288C	Member of the protein disulfide isomerase (PDI) family; interacts with and inhibits the chaperone activity of Cne1p; MPD1 overexpression in a pdi1 null mutant suppresses defects in Pdi1p functions such as carboxypeptidase Y maturation	33.5	y	n	0

21	Pipas_chr2-1_0633	EMP24	EMP24	YGL200C	Component of the p24 complex; binds to GPI anchor proteins and mediates their efficient transport from the ER to the Golgi; integral membrane protein that associates with endoplasmic reticulum-derived COPII-coated vesicles	22.6	y	n	0
22	Pipas_chr3_0733	LCB2	LCB2	YDR062W	Component of serine palmitoyltransferase, responsible along with Lcb1p for the first committed step in sphingolipid synthesis, which is the condensation of serine with palmitoyl-CoA to form 3-ketosphinganine	62.6	n	y	1
23	Pipas_chr4_0254	MSC7	MSC7	YHR039C	Protein of unknown function, green fluorescent protein (GFP)-fusion protein localizes to the endoplasmic reticulum; msc7 mutants are defective in directing meiotic recombination events to homologous chromatids	71.0	n	y	1
24	Pipas_chr3_0053	ERG25	ERG25	YGR060W	C-4 methyl sterol oxidase, catalyzes the first of three steps required to remove two C-4 methyl groups from an intermediate in ergosterol biosynthesis; mutants accumulate the sterol intermediate 4,4-dimethylzymosterol	37.2	n	y	0
25	Pipas_chr2-1_0038	YET3	YET3	YDL072C	Protein of unknown function; YET3 null mutant decreases the level of secreted invertase; homolog of human BAP31 protein;protein abundance increases in response to DNA replication stress	21.9	n	y	3

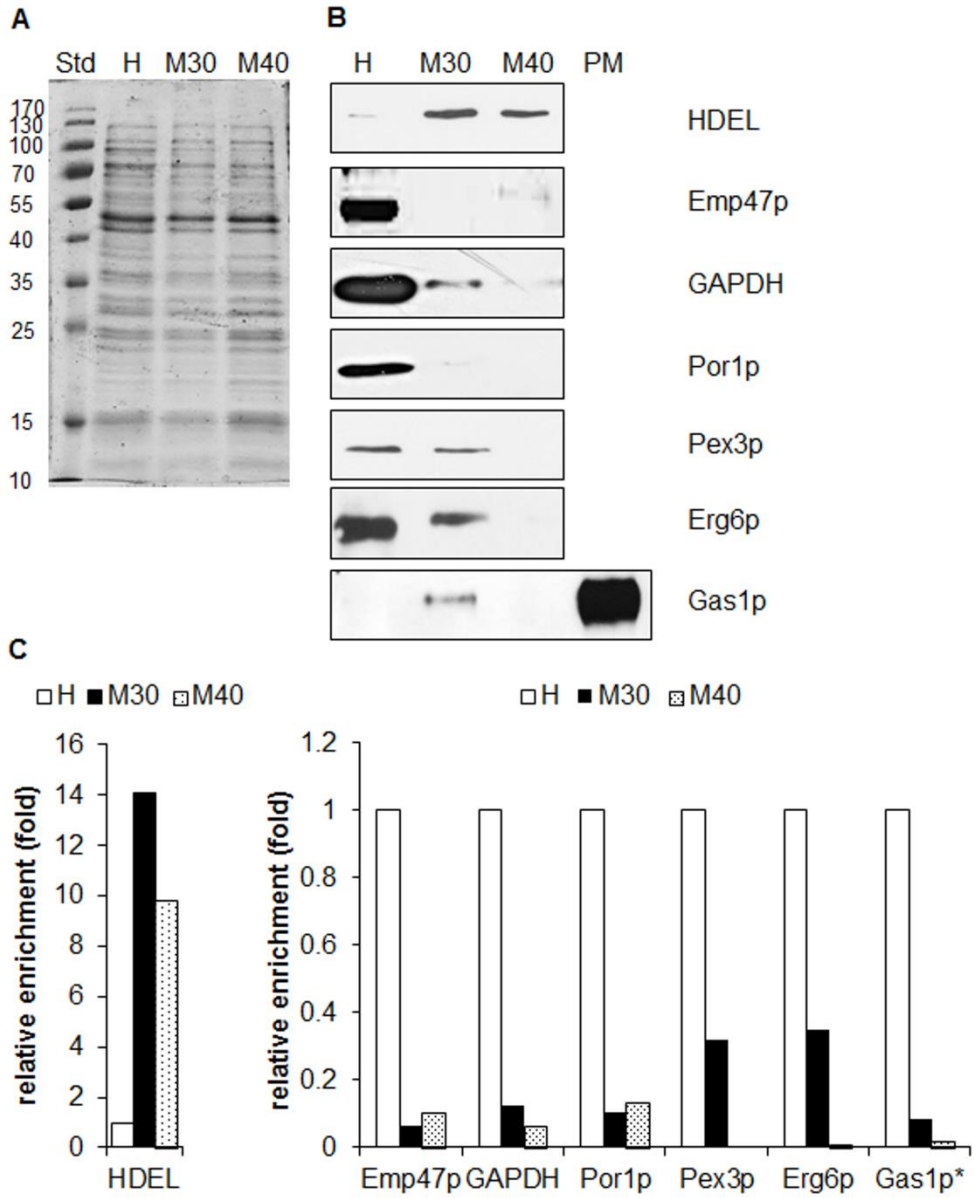

Figure 1: Protein profile and quality control of *P. pastoris* microsomes

A) Coomassie Blue stained SDS-Gel and B) Western Blot analysis of homogenate (H) and microsomes (M30, M40). 10 µg protein of each sample was loaded per lane. Antibodies against a microsomal HDEL-sorting signal, Golgi protein Emp47p, cytosolic glyceraldehyde-3-phosphate-dehydrogenase (GAPDH), mitochondrial protein Por1p, peroxisomal membrane protein Pex3p, lipid droplet/ER protein Erg6p and plasma membrane (PM) protein Gas1p were used. C) Relative enrichment/depletion of marker proteins detected by Western Blot. Homogenate and plasma membrane signal intensities were set at 1. The enrichment/depletion of protein signals detected in microsomes was calculated over the homogenate or the plasma membrane. *Plasma membrane was used to monitor Gas1p, which could not be detected in the homogenate. Data are mean values of at least two independent Western Blot analyses.

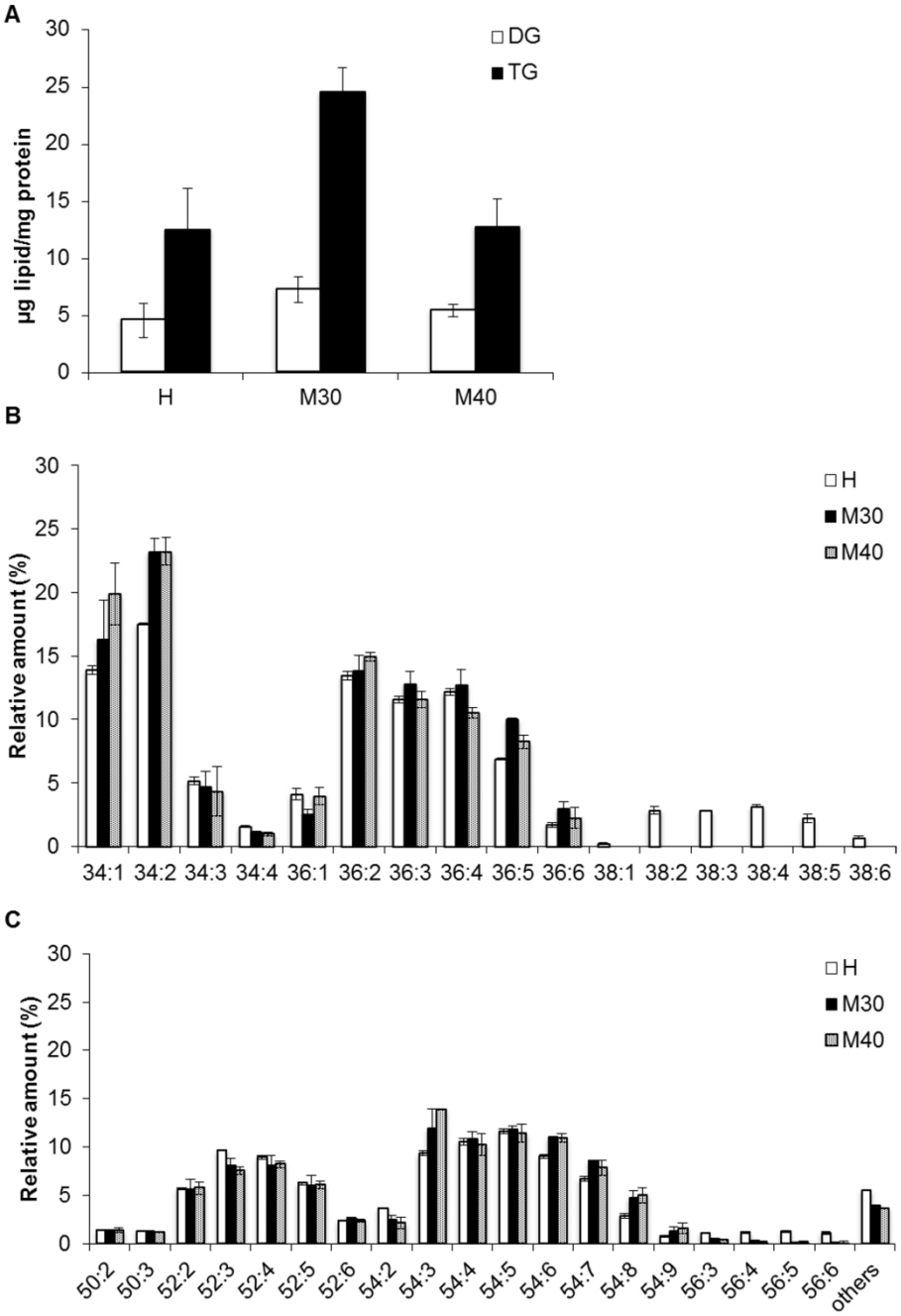

Figure 2: Analysis of diacylglycerols and triacylglycerols from *P. pastoris* microsomes

A) Diacylglycerols (DG) and triacylglycerols (TG) were analyzed from *P. pastoris* homogenate (H), 30,000 g microsomes (M30) and 40,000 g microsomes (M40) as described in the methods section. Data are mean values from two independent experiments analyzed in replicates (n=4). Error bars indicate standard deviation.

B) Molecular species of diacylglycerols and C) triacylglycerols from homogenate (H) and microsomes (M30, M40) were analyzed by LC-MS. Results are shown as relative amounts (%). Data are mean values from two independent experiments analyzed in replicates (n=4). Error bars indicate standard deviation.

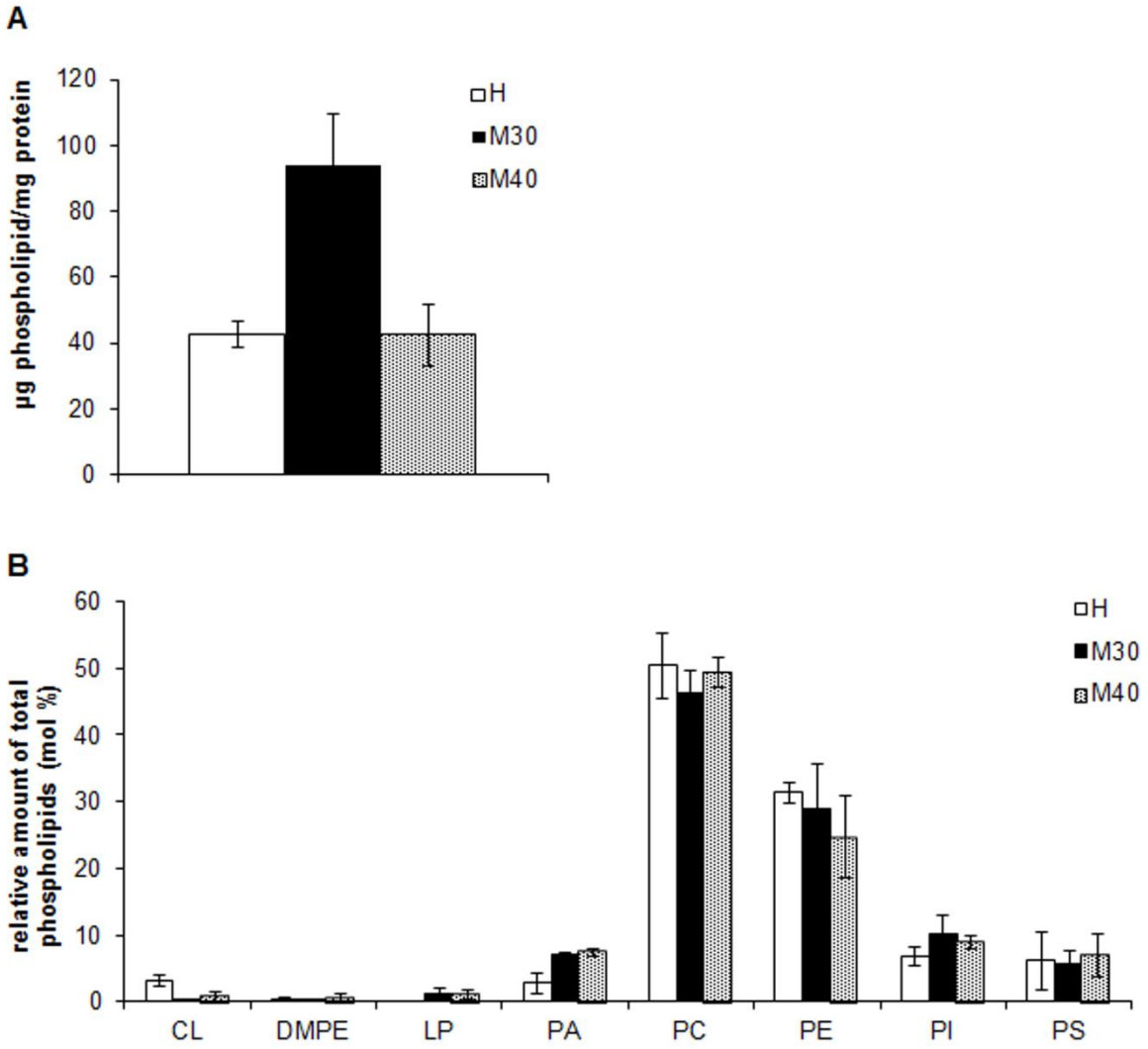

Figure 3: Total and individual phospholipids of *P. pastoris* microsomes

A) Total phospholipids were extracted and analyzed as described in the methods section from homogenate (H) and microsomes (M30, M40). Data are mean values of three independent experiments analyzed in replicates (n=6). Error bars indicate standard deviation.

B) Individual phospholipids from homogenate (H) and microsomes (M30, M40) were separated by two-dimensional TLC and quantified as described in the methods section. After iodine staining phospholipid spots were scratched off and the phosphate content was analyzed. The relative distribution of cardiolipin (CL), dimethylphosphatidylethanolamine (DMPE), lysophospholipids (LP), phosphatidic acid (PA), phosphatidylcholine (PC), phosphatidylethanolamine (PE), phosphatidylinositol (PI) and phosphatidylserine (PS) is shown as mol % of total phospholipids. Data are mean values of three independent experiments analyzed in replicates (n=6). Error bars indicate standard deviation.

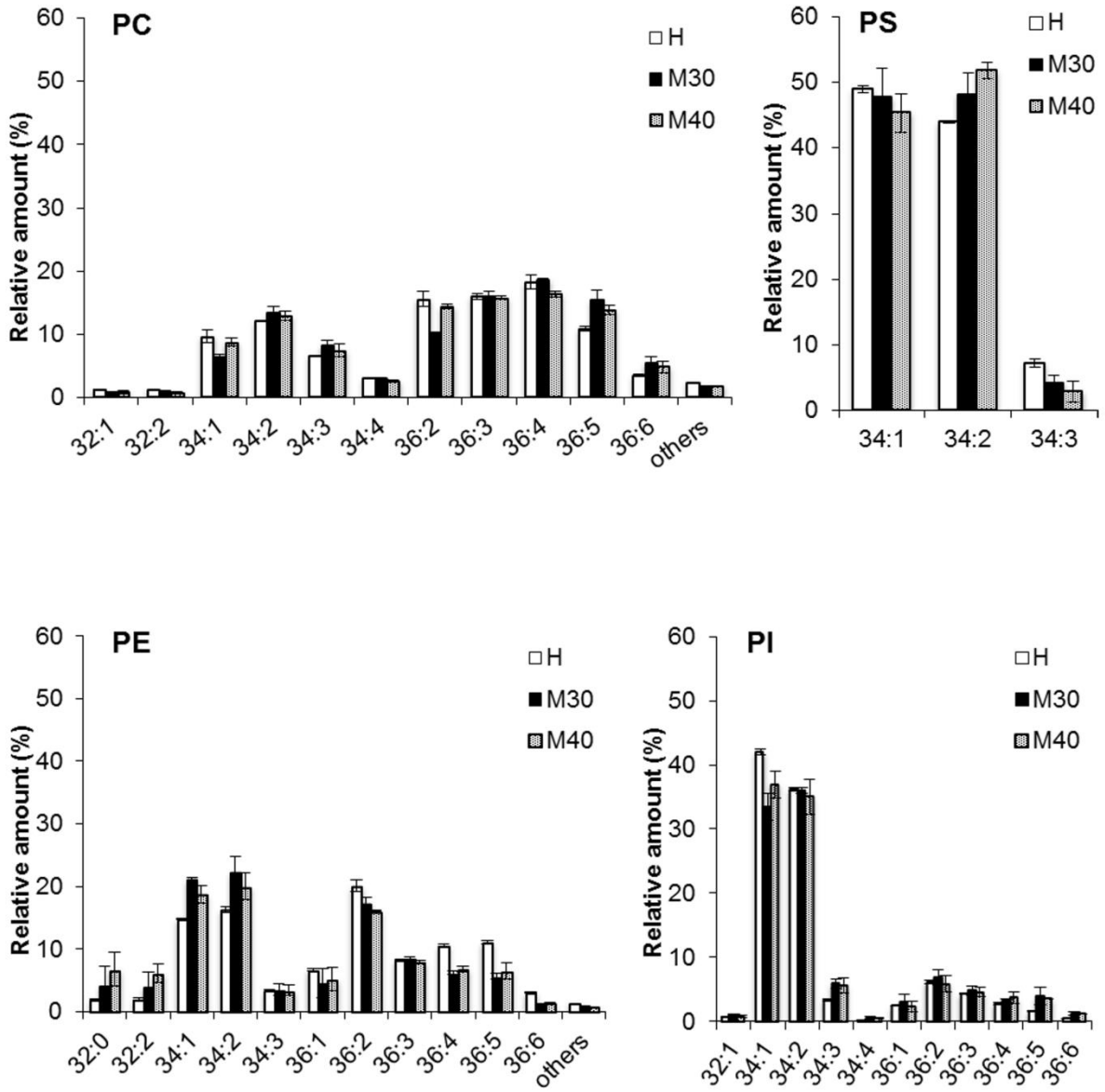

Figure 4: Molecular species of individual phospholipids from *P. pastoris* microsomes

Molecular species of phosphatidylcholine (PC), phosphatidylethanolamine (PE), phosphatidylinositol (PI) and phosphatidylserine (PS) from homogenate (H) and microsomes (M30, M40) were analyzed by LC-MS. Results are shown as relative amounts (%). Data are mean values of two independent experiments. Measured values deviate less than ±4.5% from the mean value.

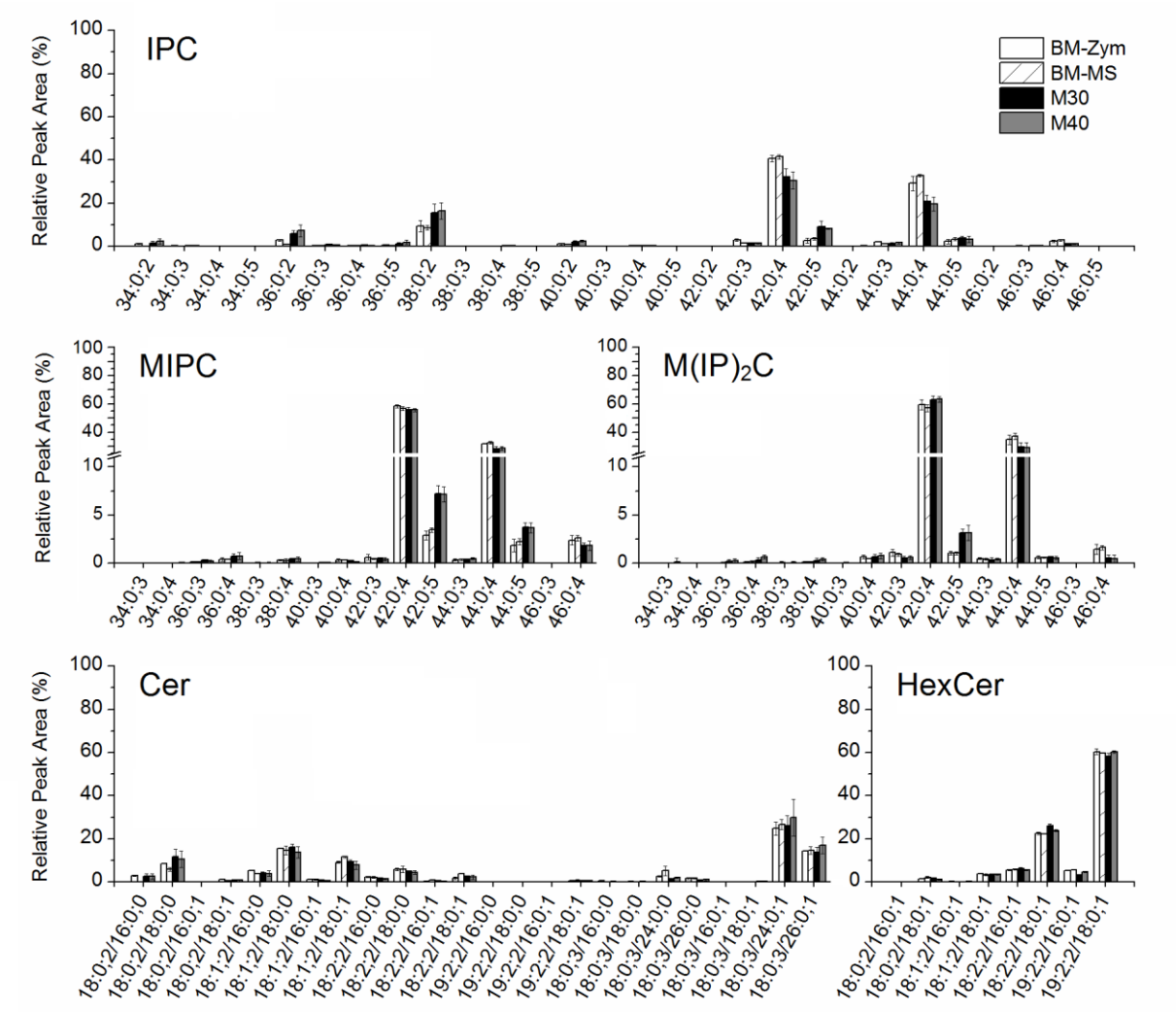

Figure 5: Sphingolipids of *P. pastoris* microsomes

Sphingolipids were extracted from *P. pastoris* bulk membranes (BM-Zym or BM-MS) and M30 and M40 microsomal fractions as described in the methods section and analyzed by UPLC-nanoESI-MS/MS. Molecular species of inositolphosphorylceramides (IPC), mannosylinositolphosphorylceramides (MIPC), mannosyldiinositolphosphorylceramides ($M(IP)_2C$), ceramides (Cer) and hexosylceramides (HexCer) were identified. Results are shown as relative peak areas (%). Data were obtained from two independent BM, M30 and M40 preparations, two replicates each (n=4). Error bars indicate standard deviation.

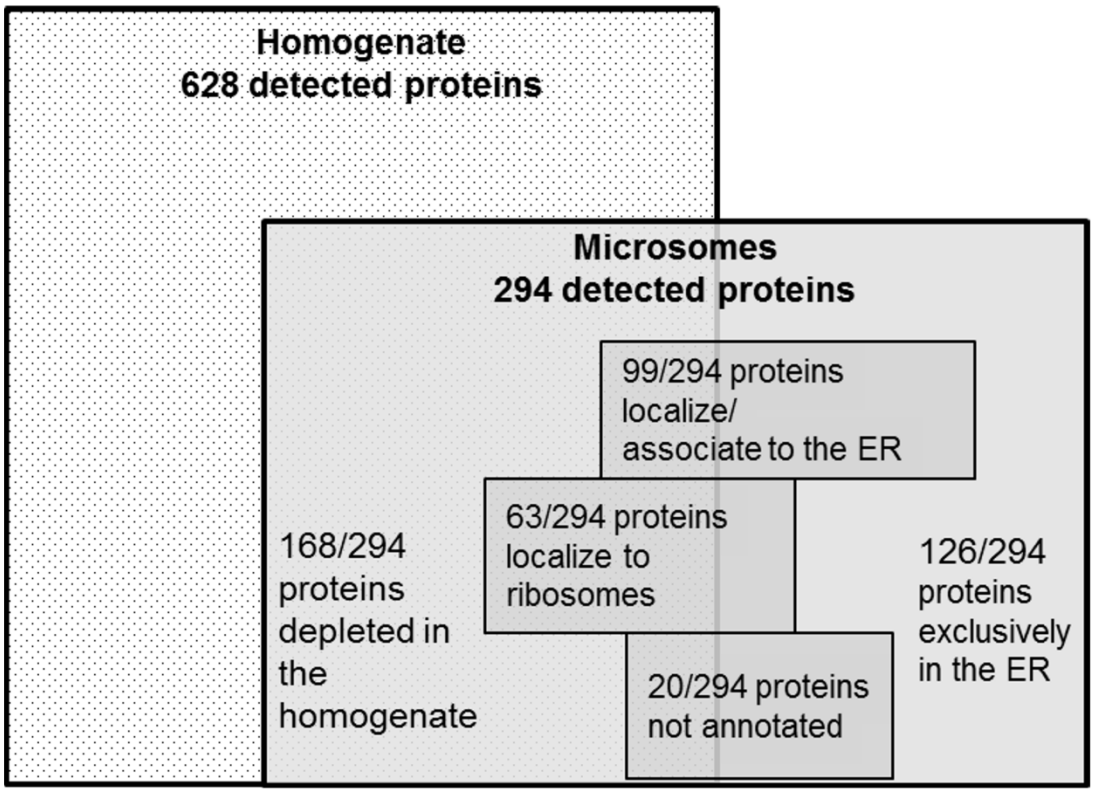

Figure 6: Venn diagram of *P. pastoris* microsomal proteome

Proteome analysis was performed by mass spectrometry from *P. pastoris* homogenate, 30,000 g microsomes (M30) and 40,000 g microsomes (M40). Proteins were analyzed from 3 independent experiments by (i) ion trap MS and (ii) Q-TOF MS as described in the Methods section. Distribution and localization of detected proteins are indicated.

Supplemental Table S1: Possible fatty acid combinations of diacylglycerols and triacylglycerols from *P. pastoris* microsomes

Possible combinations of acyl chains in diacylglycerols (DG) and triacylglycerols (TG) from homogenate (H) and microsomes (M30, M40) are listed, based on the detected fatty acids, in Table 1.

Diacylglycerol species	*Possible fatty acid combination (based on detected fatty acids shown in Table 1)*
C34:1	C16:0-C18:1; C16:1-C18:0
C34:2	C16:0-C18:2; C16:1-C18:1; C14:0-C20:2; C14:1-C20:1
C34:3	C16:0-C18:3; C16:1-C18:2;
C34:4	C16:1-C18:3;
C36:1	C16:0-C20:1; C16:1-C20:0; C18:0-C18:1
C36:2	C16:0-C20:2; C16:1-C20:1; C18:0-C18:2; C18:1-C18:1
C36:3	C16:1-C20:2; C18:0-C18:3; C18:1-C18:2
C36:4	C18:1-C18:3; C18:2-C18-2
C36:5	C18:2-C18:3
C36:6	C18:3-C18:3
C38:1	C18:0-C20:1
C38:2	C18:0-C20:1; C18:1-C20:1
C38:3	C18:1-C20:2; C18:2-C20:1
C38:4	C18:2-C20:2; C18:3-C20:1
C38:5	C18:3-C20:2
Triacylglycerol species	*Possible fatty acid combination (based on detected fatty acids shown in Table 1)*
C50:2	C14:0-C18:1-C18:1; C14:0-C18:0-C18:2; C14:0-C16:0-C20:2; C14:0-C16:1-C20:1; C16:0-C16:0-C18:2; C16:0-C16:1-C18:1; C16:1-C16:1-C18:0
C50:3	C14:0-C18:1-C18:2; C14:0-C18:0-C18:3; C14:0-C16:1-C20:2; C16:0-C16:0-C18:3; C16:0-C16:1-C18:2; C16:1-C16:1-C18:1
C52:2	C14:0-C18:0-C20:2; C14:0-C18:1-C20:1; C16:0-C18:0-C18:2; C16:1-C18:0-C18:1
C52:3	C14:0-C18:1-C20:2; C14:0-C18:2-C20:1; C16:0-C18:0-C18:3; C16:0-C18:1-C18:2; C16:1-C18:0-C18:2; C16:1-C18:1-C18:1
C52:4	C14:0-C18:2-C20:2; C14:0-C18:3-C20:1; C16:0-C18:1-C18:3; C16:0-C18:2-C18:2; C16:1-C18:0-C18:3; C16:1-C18:1-C18:2
C52:5	C14:0-C18:3-C20:2; C16:0-C18:2-C18:3; C16:1-C18:1-C18:3; C16:1-C18:2-C18:2
C52:6	C16:0-C18:3-C18:3; C16:1-C18:2-C18:3
C54:2	C14:0-C20:1-C20:1; C16:0-C18:0-C20:2; C16:0-C18:1-C20:1; C16:1-C18:0-C20:1; C18:0-C18:0-C18:0; C18:0-C18:1-C18:1

C54:3	C14:0-C20:1-C20:2; C16:0-C18:1-C20:2; C16:0-C18:2-C20:1; C16:1-C18:0-C20:2; C16:1-C18:1-C20:1; C18:0-C18:0-C18:3; C18:0-C18:1-C18:2; C18:1-C18:1-C18:1
C54:4	C14:0-C20:2-C20:2; C16:0-C18:2-C20:2; C16:0-C18:3-C20:1; C16:1-C18:2-C20:1; C18:0-C18:1-C18:3; C18:0-C18:2-C18:2; C18:1-C18:1-C18:2
C54:5	C16:0-C18:3-C20:2; C16:1-C18:2-C20:2; C16:1-C18:3-C20:1; C18:0-C18:2-C18-3; C18:1-C18:1-C18:3
C54:6	C16:1-C18:3-C20:2; C18:0-C18:3-C18:3; C18:1-C18:2-C18:3; C18:2-C18:2-C18:2
C54:7	C18:1-C18:3-C18:3; C18:2-C18:2-C18:3
C54:8	C18:2-C18:3-C18:3
C54:9	C18:3-C18:3-C18:3
C56:3	C18:0-C18:1-C20:2; C18:0-C18:2-C20:1; C18:1-C18:1-C20:1
C56:4	C18:0-C18:2-C20:2; C18:0-C18:3-C20:1; C18:1-C18:1-C20:2; C18:1-C18:2-C20:1
C56:5	C18:0-C18:3-C20:2; C18:1-C18:2-C20:2; C18:1-C18:3-C20:1; C18:2-C18:2-C20:1
C56:6	C18:1-C18:3-C20:2; C18:2-C18:2-C20:2; C18:2-C18:3-C20:1

Supplemental Table S2: Possible fatty acid combinations of individual phospholipid species from *P. pastoris* microsomes

Possible combinations of acyl chains of molecular species of phosphatidylcholine (PC), phosphatidylethanolamine (PE), phosphatidylinositol (PI) and phosphatidylserine (PS) from homogenate (H) and microsomes (M30, M40) are listed, based on the detected fatty acids, in Table 1.

Phospholipid species	*Possible fatty acid combination (based on detected fatty acids from table 1)*
C32:0	C14:0-C18:0; C16:0-C16:0
C32:1	C14:0-C18:1; C16:0-C16:1
C32:2	C14:0-C18:2; C16:1-C16:1
C34:0	C16:0-C18:0
C34:1	C16:0-C18:1; C16:1-C18:0
C34:2	C16:0-C18:2; C16:1-C18:1; C14:0-C20:2; C14:1-C20:1
C34:3	C16:0-C18:3; C16:1-C18:2; C14:1-C20:2
C34:4	C16:1-C18:3;
C36:1	C16:0-C20:1; C16:1-C20:0; C18:0-C18:1
C36:2	C16:0-C20:2; C16:1-C20:1; C18:0-C18:2; C18:1-C18:1
C36:3	C16:1-C20:2; C18:0-C18:3; C18:1-C18:2
C36:4	C18:1-C18:3; C18:2-C18-2
C36:5	C18:2-C18:3
C36:6	C18:3-C18:3

Supplemental Table S3: Microsomal proteome of *P. pastoris.*

Detected proteins from proteome analysis by mass spectrometry, which was performed from *P. pastoris* 30,000 g microsomes (M30) and 40,000 g microsomes (M40), are listed. Proteins were analyzed from 3 independent experiments by i) ion trap MS and by ii) Q-TOF MS. Uniport_ID: Name of protein entry in Uniprot Database, in most cases for *P. pastoris* strain GS115. Short_Name: Short protein name; names are assigned based on homology to *Saccharomyces cerevisiae.* Short_Name_Sc: Short protein name of *S. cerevisiae* homolog. Description: Information about gene/protein function as given in *Saccharomyces* Genome Database or NCBI. Functional category: manual curation of protein function and localization of *S. cerevisiae* homolog. Signal peptide: prediction of cleavable signal peptides by SignalP 4.0 (1: presence, 0: absence). Signal anchor: prediction of transmembrane signal anchors by SignalP 4.0 (1: presence, 0: absence); GPI anchors are also indicated. TMD: prediction of transmembrane helices by TMHMM 2.0 (TMH, number of transmembrane helices; 0: absence). MM: molecular mass in kDa. pI: isoelectric point. rank in total extract: ranking of proteins in total cell extract out of 685 detected proteins (1: highest score; 685: lowest score; 0: not detected). M30, M40: number out of 3 microsome preparations in which a certain protein was detected in fraction M30 or M40. #Peptides: maximum number of peptides identified in microsomal fractions M30/M40. SC [%]: maximal sequence coverage of identified protein in microsomal fractions M30/M40. Abbreviations: ER: endoplasmic reticulum; cyto: cytosol; LP: lipid particle; MOM: mitochondrial outer membrane; PM: plasma membrane; localization data for *S. cerevisiae* homolog.

Uniprot_ID	Short_Name	Short_Name_Sc	Description	Functional category	Signal peptide	Signal anchor	TMD	MW [kDa]	pI	rank in total extract	M30	M40	# Peptides	SC [%]
C4QYF3	BGL2	BGL2	Endo-beta-1,3-glucanase, major protein of the cell wall, involved in cell wall maintenance	cell wall	1	0	0	33.9	3.9	0	2	3	4	17.0
C4R1D2	FKS1	FKS1	Catalytic subunit of 1,3-beta-D-glucan synthase, functionally redundant with alternate catalytic subunit Gsc2p; binds to regulatory subunit Rho1p; involved in cell wall synthesis and maintenance; localizes to sites of cell wall remodeling	cell wall	0	0	TMH, 14	215.1	8.1	38	3	3	28	21.9
C4QYW7	FLO5-1	FLO5	Lectin-like cell wall protein (flocculin) involved in flocculation, binds to mannose chains on the surface of other cells	cell wall	1	0	TMH, 1	51.2	4.2	0	2	2	3	9.6

C4QVL4	GAS1-1	GAS1	Beta-1,3-glucanosyltransferase, required for cell wall assembly; localizes to the cell surface via a glycosylphosphatidylinositol (GPI) anchor; also found at the nuclear periphery	cell wall	1	0	GPI anchor	57.3	3.9	172	3	3	8	17.7
C4QVL5	GAS1-2	GAS1	Beta-1,3-glucanosyltransferase, required for cell wall assembly; localizes to the cell surface via a glycosylphosphatidylinositol (GPI) anchor; also found at the nuclear periphery	cell wall	1	0	GPI anchor	58.3	3.8	0	3	3	8	21.9
C4R9F4	GAS3	GAS3	Low abundance member of the GAS family of GPI-containing proteins; putative 1,3-beta-glucanosyltransferase; localizes to the cell wall;	cell wall	1	0	GPI anchor	53.8	4.0	0	3	1	4	13.1
C4QVL7	SCW10	SCW10	Cell wall protein with similarity to glucanases	cell wall	1	0	0	35.9	4.8	141	2	2	2	13.2
C4R2B9	YJL171C	YJL171C	GPI-anchored cell wall protein of unknown function; induced in response to cell wall damaging agents and by mutations in genes involved in cell wall biogenesis; sequence similarity to YBR162C/TOS1, a covalently bound cell wall protein	cell wall	1	0	GPI anchor	44.5	4.0	0	2	0	2	9.4
C4R796	CAJ1	CAJ1	Nuclear type II J heat shock protein of the E. coli dnaJ family, contains a leucine zipper-like motif, binds to non-native substrates for presentation to Ssa3p, may function during protein translocation, assembly and disassembly	chaperone	0	0	0	47.7	5.8	0	3	3	7	28.8
C4QVQ4	CPR1	CPR1	Cytoplasmic peptidyl-prolyl cis-trans isomerase (cyclophilin), catalyzes the cis-trans isomerization of peptide bonds N-terminal to proline residues	chaperone	0	0	0	18.0	6.1	80	3	3	5	32.1
C4R5A4	HSP31	HSP31	Possible chaperone and cysteine protease with similarity to E. coli Hsp31; member of the DJ-1/ThiJ/PfpI superfamily	chaperone	0	0	0	25.4	6.0	295	3	1	2	25.3
C4QXI5	HSP82	HSP82	Hsp90 chaperone required for pheromone signaling and negative regulation of Hsf1p; docks with Tom70p for mitochondrial preprotein delivery; promotes telomerase DNA binding and nucleotide addition; interacts with Cns1p, Cpr6p, Cpr7p, Sti1p	chaperone	0	0	0	80.9	4.7	24	3	3	15	32.2
C4R2Q1	SIS1	SIS1	Type II HSP40 co-chaperone that interacts with the HSP70 protein Ssa1p; not functionally redundant with Ydj1p due to due to substrate specificity	chaperone	0	0	0	37.0	9.2	0	3	3	11	46.2
C4R887	SSA1	SSA1	ATPase involved in protein folding and nuclear localization signal (NLS)-directed nuclear transport; member of heat shock protein 70 (HSP70) family; forms a chaperone complex with Ydj1p; localized to the nucleus, cytoplasm, and cell wall	chaperone	0	0	0	69.6	4.7	8	3	3	21	50.2

C4R5E4	SSB2	SSB2	Cytoplasmic ATPase that is a ribosome-associated molecular chaperone, functions with J-protein partner Zuo1p; may be involved in the folding of newly-synthesized polypeptide chains; member of the HSP70 family	chaperone	0	0	0	66.5	4.9	6	3	2	20	50.4
C4R9F1	SSE1	SSE1	ATPase that is a component of the heat shock protein Hsp90 chaperone complex; binds unfolded proteins; member of the heat shock protein 70 (HSP70) family; localized to the cytoplasm	chaperone	0	0	0	78.7	5.0	65	2	0	5	8.5
C4R2Z2	YDJ1	YDJ1	Type I HSP40 co-chaperone involved in regulation of the HSP90 and HSP70 functions; involved in protein translocation across membranes; member of the DnaJ family	chaperone	0	0	0	43.4	5.8	245	3	2	8	29.1
C4R0S8	ADH2	ADH2	Glucose-repressible alcohol dehydrogenase II, catalyzes the conversion of ethanol to acetaldehyde; involved in the production of certain carboxylate esters	core metabolism	0	0	0	37.0	5.8	9	2	0	4	22.9
C4R1P9	CDC19	CDC19	Pyruvate kinase, functions as a homotetramer in glycolysis to convert phosphoenolpyruvate to pyruvate, the input for aerobic (TCA cycle) or anaerobic (glucose fermentation) respiration	core metabolism	0	0	0	55.5	6.1	50	3	3	11	46.1
C4R3H8	ENO1	ENO1	Enolase I, a phosphopyruvate hydratase that catalyzes the conversion of 2-phosphoglycerate to phosphoenolpyruvate during glycolysis and the reverse reaction during gluconeogenesis	core metabolism	0	0	0	46.5	5.3	22	3	3	8	33.9
C4R430	GND2	GND2	6-phosphogluconate dehydrogenase (decarboxylating), catalyzes an NADPH regenerating reaction in the pentose phosphate pathway; required for growth on D-glucono-delta-lactone	core metabolism	0	0	0	53.9	5.9	16	3	1	8	22.2
C4QY07	PGK1	PGK1	3-phosphoglycerate kinase, catalyzes transfer of high-energy phosphoryl groups from the acyl phosphate of 1,3-bisphosphoglycerate to ADP to produce ATP; key enzyme in glycolysis and gluconeogenesis	core metabolism	0	0	0	44.1	8.7	17	3	1	6	29.1
C4R5W1	SAH1	SAH1	S-adenosyl-L-homocysteine hydrolase, catabolizes S-adenosyl-L-homocysteine which is formed after donation of the activated methyl group of S-adenosyl-L-methionine (AdoMet) to an acceptor	core metabolism	0	0	0	48.6	5.3	21	2	3	7	24.5
C4R5U7	SAM2	SAM2	S-adenosylmethionine synthetase, catalyzes transfer of the adenosyl group of ATP to the sulfur atom of methionine	core metabolism	0	0	0	42.3	6.1	64	2	1	3	9.9
C4R1C8	SER3	SER3	3-phosphoglycerate dehydrogenase, catalyzes the first step in serine and glycine biosynthesis	core metabolism	0	0	0	51.0	5.8	143	2	0	1	5.8

C4R245	TAL1-1	TAL1	Transaldolase, enzyme in the non-oxidative pentose phosphate pathway; converts sedoheptulose 7-phosphate and glyceraldehyde 3-phosphate to erythrose 4-phosphate and fructose 6-phosphate	core metabolism	0	0	0	35.5	4.9	31	2	0	6	22.2
C4R0P1	TDH3	TDH3	Glyceraldehyde-3-phosphate dehydrogenase, isozyme 3, involved in glycolysis and gluconeogenesis; tetramer that catalyzes the reaction of glyceraldehyde-3-phosphate to 1,3 bis-phosphoglycerate; detected in the cytoplasm and cell wall	core metabolism	0	0	0	35.6	6.3	4	3	3	15	58.0
C4R1J7	EIS1	EIS1	Component of the eisosome that is required for proper eisosome assembly; similarity to Ykl050cp and Uso1p	eisosome	0	0	0	91.3	5.8	258	2	2	8	15.8
C4R3X5	LSP1	LSP1	Primary component of eisosomes, which are large immobile patch structures at the cell cortex associated with endocytosis, along with Pil1p and Sur7p; member of the BAR domain family	eisosome	0	0	0	33.9	4.7	69	3	3	17	76.8
C4R5L9	PAS_chr3_0802	SEG1	Component of eisosome required for proper eisosome assembly; precedes Pil1p/Lsp1p during eisosome formation and controls eisosome length and shape; Seg1p-GFP diffusely distributed and forms heterogeneous patches at the plasma membranebuds, also found in medium and large buds; may interact with ribosomes	eisosome	0	0	0	86.9	9.7	0	0	2	2	3.9
C4QYV1	PIL1	PIL1	Primary component of eisosomes, which are large immobile cell cortex structures associated with endocytosis; member of the BAR domain	eisosome	0	0	0	35.2	4.9	49	3	3	19	78.6
C4R0B4	CNE1	CNE1	Calnexin; integral membrane ER chaperone involved in folding and quality control of glycoproteins; chaperone activity is inhibited by Mpd1p, with which Cne1p interacts; 24% identical to mammalian calnexin; Ca+ binding not yet shown in yeast	ER chaperone	0	0	TMH, 1	63.0	4.4	320	3	2	14	28.0
C4QWL5	CPR5	CPR5	Peptidyl-prolyl cis-trans isomerase (cyclophilin) of the endoplasmic reticulum, catalyzes the cis-trans isomerization of peptide bonds N-terminal to proline residues	ER chaperone	1	0	0	24.7	4.6	498	3	2	13	66.2
C4QVC1	ERJ5	ERJ5	Type I membrane protein with a J domain is required to preserve the folding capacity of the endoplasmic reticulum	ER chaperone	1	0	TMH, 1	35.0	10.2	0	2	2	5	25.8
C4QVU1	ERO1	ERO1	Thiol oxidase required for oxidative protein folding in the endoplasmic reticulum	ER chaperone	1	0	0	60.2	4.8	0	3	1	4	12.3
C4QWA2	ERp38	NA	Protein disulfide isomerase; multifunctional protein of ER lumen	ER chaperone	1	0	0	42.0	5.9	0	3	2	8	35.2

C4R379	FPR2	FPR2	Membrane-bound peptidyl-prolyl cis-trans isomerase (PPIase); expression pattern suggests possible involvement in ER protein trafficking	ER chaperone	1	0	0	16.6	5.8	0	1	2	1	9.9
C4R0D7	GSF2	GSF2	ER localized integral membrane protein that may promote secretion of certain hexose transporters	ER chaperone	0	0	0	44.9	4.7	0	2	2	5	19.5
C4R2T6	GTT1	GTT1	ER associated glutathione S-transferase capable of homodimerization	ER chaperone	0	0	0	27.4	9.0	280	3	2	3	14.4
C4QZS3	KAR2	KAR2	ATPase involved in protein import into the ER, also acts as a chaperone to mediate protein folding in the ER and may play a role in ER export of soluble proteins; regulates the unfolded protein response via interaction with Ire1p	ER chaperone	1	0	TMH, 1	74.2	4.6	89	3	3	35	49.0
C4QV45	LHS1	LHS1	Molecular chaperone of the endoplasmic reticulum lumen, involved in polypeptide translocation and folding; nucleotide exchange factor for the ER lumenal Hsp70 chaperone Kar2p; regulated by the unfolded protein response pathway	ER chaperone	1	0	TMH, 1	99.5	4.9	0	2	1	10	19.0
C4QVB2	MPD1	MPD1	Member of the protein disulfide isomerase (PDI) family; interacts with and inhibits the chaperone activity of Cne1p; MPD1 overexpression in a pdi1 null mutant suppresses defects in Pdi1p functions such as carboxypeptidase Y maturation	ER chaperone	1	0	0	33.5	10.0	0	3	2	4	23.2
C4R938	PDI1	PDI1	Protein disulfide isomerase; multifunctional protein resident in the endoplasmic reticulum lumen, essential for the formation of disulfide bonds in secretory and cell-surface proteins, unscrambles non-native disulfide bonds	ER chaperone	1	0	0	52.6	4.4	98	3	2	27	65.6
C4R6Z9	CBR1	CBR1	Microsomal cytochrome b reductase, not essential for viability	ER cytochrome	0	1	TMH, 1	30.7	9.1	508	1	2	13	56.3
C4R2W7	ARF1	ARF1	ADP-ribosylation factor, GTPase of the Ras superfamily involved in regulation of coated vesicle formation in intracellular trafficking within the Golgi	ER Golgi vesicle transport	0	0	0	20.6	5.8	234	3	2	4	43.6
C4QZN3	BMH2	BMH2	14-3-3 protein; controls proteome at post-transcriptional level, binds proteins and DNA, involved in regulation of many processes including exocytosis, vesicle transport, Ras/MAPK signaling, and rapamycin-sensitive signaling	ER Golgi vesicle transport	0	0	0	29.0	4.6	91	3	2	8	54.1
C4R1A2	EMP24	EMP24	Component of the p24 complex; binds to GPI anchor proteins and mediates their efficient transport from the ER to the Golgi; integral membrane protein that associates with endoplasmic reticulum-derived COPII-coated vesicles	ER Golgi vesicle transport	1	0	0	22.6	7.8	0	2	2	4	33.0

C4R7V8	EMP47	EMP47	Integral membrane component of endoplasmic reticulum-derived COPII-coated vesicles, which function in ER to Golgi transport	ER Golgi vesicle transport	1	0	TMH, 1	53.6	6.0	0	2	2	8	27.3
C4R125	ERP5	ERP5	Protein with similarity to Emp24p and Erv25p, member of the p24 family involved in ER to Golgi transport	ER Golgi vesicle transport	1	1	TMH, 1	27.3	9.4	0	3	2	7	30.0
C4QXT6	ERV14	ERV14	Protein localized to COPII-coated vesicles, involved in vesicle formation and incorporation of specific secretory cargo	ER Golgi vesicle transport	0	1	TMH, 3	19.2	9.4	0	1	2	1	6.7
C4R371	ERV25	ERV25	Protein that forms a heterotrimeric complex with Erp1, Erp2p, and Emp24, member of the p24 family involved in endoplasmic reticulum to Golgi transport	ER Golgi vesicle transport	1	0	0	30.6	9.2	0	2	3	7	31.0
C4R7S7	GET1	GET1	SSubunit of the GET complex; involved in insertion of proteins into the ER membrane; required for the retrieval of HDEL proteins from the Golgi to the ER in an ERD2 dependent fashion and for normal mitochondrial morphology and inheritance	ER Golgi vesicle transport	1	0	TMH, 3	23.2	9.6	0	1	2	3	23.7
C4R3U0	GET2	GET2	Subunit of the GET complex; involved in insertion of proteins into the ER membrane; required for the retrieval of HDEL proteins from the Golgi to the ER in an ERD2 dependent fashion and for meiotic nuclear division	ER Golgi vesicle transport	0	0	TMH, 3	34.4	5.3	0	2	2	1	4.5
C4R495	SEC18	SEC18	ATPase required for vesicular transport between ER and Golgi, the 'priming' step in homotypic vacuole fusion, autophagy, and protein secretion	ER Golgi vesicle transport	0	0	0	84.0	6.5	308	2	2	11	18.9
C4R427	SEC22	SEC22	R-SNARE protein; assembles into SNARE complex with Bet1p, Bos1p and Sed5p; cycles between the ER and Golgi complex; involved in anterograde and retrograde transport between the ER and Golgi; synaptobrevin homolog	ER Golgi vesicle transport	0	0	TMH, 1	24.7	9.5	0	1	2	3	21.5
C4R3N7	SEC4	SEC4	Rab family GTPase essential for vesicle-mediated exocytic secretion and autophagy; associates with the exocyst component Sec15p and may regulate polarized delivery of transport vesicles to the exocyst at the plasma membrane	ER Golgi vesicle transport	0	0	0	22.8	5.4	424	2	1	2	15.2
C4QZ68	SNC2	SNC2	Vesicle membrane receptor protein (v-SNARE) involved in the fusion between Golgi-derived secretory vesicles with the plasma membrane; member of the synaptobrevin/VAMP family of R-type v-SNARE proteins	ER Golgi vesicle transport	0	0	TMH, 1	12.3	10.1	0	2	3	2	31.8
C4QY09	SSO2	SSO2	Plasma membrane t-SNARE involved in fusion of secretory vesicles at the plasma membrane; syntaxin homolog	ER Golgi vesicle transport	0	0	TMH, 1	32.7	5.1	441	2	3	6	35.3
C4QZ31	VPS1	VPS1	Dynamin-like GTPase required for vacuolar sorting; also involved in actin cytoskeleton organization, endocytosis, late Golgi-retention of some proteins, regulation of peroxisome	ER Golgi vesicle transport	0	0	0	76.6	7.8	176	3	3	6	17.1

			biogenesis											
C4R6G6	VTI1	VTI1	Protein involved in cis-Golgi membrane traffic; v-SNARE that interacts with two t-SNARES, Sed5p and Pep12p; required for multiple vacuolar sorting pathways	ER Golgi vesicle transport	0	0	TMH, 1	25.2	5.5	617	2	2	5	30.6
C4QZ63	YKT6	YKT6	Vesicle membrane protein (v-SNARE) with acyltransferase activity; involved in trafficking to and within the Golgi, endocytic trafficking to the vacuole, and vacuolar fusion; membrane localization due to prenylation at the carboxy-terminus	ER Golgi vesicle transport	0	0	0	22.7	6.5	0	1	2	2	11.5
C4QYQ7	YPT32	YPT32	Rab family GTPase involved in the exocytic pathway; mediates intra-Golgi traffic or the budding of post-Golgi vesicles from the trans-Golgi	ER Golgi vesicle transport	0	0	0	24.5	4.9	0	1	2	2	15.9
C4QXL9	YPT52	YPT52	Rab family GTPase, similar to Ypt51p and Ypt53p and to mammalian rab5; required for vacuolar protein sorting and endocytosis	ER Golgi vesicle transport	0	0	0	23.1	5.5	597	1	3	5	27.7
C4R716	YPT6	YPT6	Rab family GTPase, Ras-like GTP binding protein involved in the secretory pathway, required for fusion of endosome-derived vesicles with the late Golgi, maturation of the vacuolar carboxypeptidase Y	ER Golgi vesicle transport	0	0	0	22.8	4.8	0	1	2	5	28.6
C4QVL8	RTN1	RTN1	ER membrane protein that interacts with Sey1p to maintain ER morphology; interacts with exocyst subunit Sec6p, with Yip3p, and with Sbh1p;	ER membrane	0	1	TMH, 2	32.5	8.7	165	2	2	10	35.2
C4R4C6	SPF1	SPF1	P-type ATPase, ion transporter of the ER membrane involved in ER function and Ca2+ homeostasis; required for regulating Hmg2p degradation	ER membrane	0	1	TMH, 6	136.0	5.8	288	3	2	18	20.6
C4R0Z7	YOP1	YOP1	Membrane protein that interacts with Yip1p to mediate membrane traffic; interacts with Sey1p to maintain ER morphology; overexpression leads to cell death and accumulation of internal cell membranes	ER membrane	0	1	TMH, 2	19.4	9.2	430	2	3	5	31.0
C4R0L5	GPI16	GPI16	Transmembrane protein subunit of the glycosylphosphatidylinositol transamidase complex that adds GPIs to newly synthesized proteins; human PIG-Tp homolog	ER, GPI synthesis	1	0	TMH, 1	69.3	5.4	0	2	1	2	9.2
C4R4N8	GPI17	GPI17	Transmembrane protein subunit of the glycosylphosphatidylinositol transamidase complex that adds GPIs to newly synthesized proteins; human PIG-Sp homolog	ER, GPI synthesis	0	1	TMH, 2	56.4	4.5	0	2	1	4	11.8
C4R7C0	GPI8	GPI8	ER membrane glycoprotein subunit of the glycosylphosphatidylinositol transamidase complex that adds glycosylphosphatidylinositol (GPI) anchors to newly synthesized proteins; human PIG-K protein is a functional	ER, GPI synthesis	1	0	0	43.8	5.0	0	2	1	3	14.7

			homolog											
C4QZ40	ALG2	ALG2	Mannosyltransferase that catalyzes two consecutive steps in the N-linked glycosylation pathway; alg2 mutants exhibit temperature-sensitive growth and abnormal accumulation of the lipid-linked oligosaccharide Man2GlcNAc2-PP-Dol	ER, protein glycosylation	0	0	TMH, 1	53.4	5.8	0	2	1	3	14.1
C4QVT1	DPM1	DPM1	Dolichol phosphate mannose (Dol-P-Man) synthase of the ER membrane, catalyzes the formation of Dol-P-Man from Dol-P and GDP-Man; required for glycosyl phosphatidylinositol membrane anchoring, O mannosylation, and protein glycosylation	ER, protein glycosylation	0	0	TMH, 1	28.9	5.8	199	3	3	15	51.2
C4R3S3	GTB1	GTB1	Glucosidase II beta subunit, forms a complex with alpha subunit Rot2p, involved in removal of two glucose residues from N-linked glycans during glycoprotein biogenesis in the ER	ER, protein glycosylation	1	0	0	57.6	4.6	0	2	1	5	11.8
C4R5F4	OST1	OST1	Alpha subunit of the oligosaccharyltransferase complex of the ER lumen, which catalyzes asparagine-linked glycosylation of newly synthesized proteins	ER, protein glycosylation	1	0	TMH, 1	52.2	5.4	0	3	2	8	19.4
C4R236	OST2	OST2	Epsilon subunit of the oligosaccharyltransferase complex of the ER lumen, which catalyzes asparagine-linked glycosylation of newly synthesized proteins	ER, protein glycosylation	0	1	TMH, 3	15.2	10.2	0	2	1	2	21.5
C4R8E5	OST3	OST3	Gamma subunit of the oligosaccharyltransferase complex of the ER lumen, which catalyzes asparagine-linked glycosylation of newly synthesized proteins; Ost3p is important for N-glycosylation of a subset of proteins	ER, protein glycosylation	1	0	TMH, 5	37.0	8.6	0	1	2	2	15.0
C4QZZ6	PMT1	PMT1	Protein O-mannosyltransferase, transfers mannose from dolichyl phosphate-D-mannose to protein Ser/Thr residues; involved in O-glycosylation which is essential for cell wall rigidity; involved in ER quality control	ER, protein glycosylation	0	0	TMH, 9	89.5	6.8	0	3	2	8	16.0
C4R044	PMT2	PMT2	Protein O-mannosyltransferase, transfers mannose residues from dolichyl phosphate-D-mannose to protein Ser/Thr residues; involved in ER quality control; acts in a complex with Pmt1p	ER, protein glycosylation	0	1	TMH, 7	85.1	7.9	509	3	2	8	17.9
C4R5U0	PSA1	PSA1	GDP-mannose pyrophosphorylase (mannose-1-phosphate guanyltransferase), synthesizes GDP-mannose from GTP and mannose-1-phosphate in cell wall biosynthesis; required for normal cell wall structure	ER, protein glycosylation	0	0	0	39.8	5.9	191	1	2	2	9.1
C4R1R0	ROT2	ROT2	Glucosidase II catalytic subunit required for normal cell wall synthesis	ER, protein glycosylation	1	0	0	103.7	5.4	0	3	1	5	8.3

C4QVN9	SWP1	SWP1	Delta subunit of the oligosaccharyl transferase glycoprotein complex, which is required for N-linked glycosylation of proteins in the endoplasmic reticulum	ER, protein glycosylation	1	0	TMH, 2	27.2	9.4	639	2	2	5	26.4
C4R0M2	WBP1	WBP1	Beta subunit of the oligosaccharyl transferase (OST) glycoprotein complex; required for N-linked glycosylation of proteins in the endoplasmic reticulum	ER, protein glycosylation	1	0	TMH, 2	48.9	4.4	682	3	2	14	44.1
C4QXP7	SEC11	SEC11	18kDa catalytic subunit of the Signal Peptidase Complex (SPC; Spc1p, Spc2p, Spc3p, and Sec11p) which cleaves the signal sequence of proteins targeted to the endoplasmic reticulum	ER, signal peptidase	0	1	TMH, 1	19.3	9.8	0	2	2	6	39.2
C4R152	SPC2	SPC2	Subunit of signal peptidase complex (Spc1p, Spc2p, Spc3p, Sec11p), which catalyzes cleavage of N-terminal signal sequences of proteins targeted to the secretory pathway; homologous to mammalian SPC25	ER, signal peptidase	0	1	TMH, 2	20.0	7.5	0	2	2	3	31.4
C4R969	SPC3	SPC3	Subunit of signal peptidase complex (Spc1p, Spc2p, Spc3p, Sec11p), which catalyzes cleavage of N-terminal signal sequences of proteins targeted to the secretory pathway; homologous to mammalian SPC22/23	ER, signal peptidase	0	1	TMH, 1	20.5	9.4	0	1	2	2	23.2
C4QVJ2	SEC61	SEC61	Essential subunit of Sec61 complex (Sec61p, Sbh1p, and Sss1p); forms a channel for SRP-dependent protein import and retrograde transport of misfolded proteins out of the ER	ER, translocon	0	1	TMH, 8	52.5	9.4	0	3	3	8	17.2
C4R7S0	SEC63	SEC63	Essential subunit of Sec63 complex (Sec63p, Sec62p, Sec66p and Sec72p); with Sec61 complex, Kar2p/BiP and Lhs1p forms a channel competent for SRP-dependent and post-translational SRP-independent protein targeting and import into the ER	ER, translocon	0	1	TMH, 3	73.6	4.8	0	3	2	13	29.7
C4R0N2	SEC66	SEC66	Non-essential subunit of Sec63 complex (Sec63p, Sec62p, Sec66p and Sec72p); with Sec61 complex, Kar2p/BiP and Lhs1p forms a channel competent for SRP-dependent and post-translational SRP-independent protein targeting and import into the ER	ER, translocon	0	1	TMH, 1	22.6	5.7	0	3	2	5	44.8
C4R0Q1	SEC72	SEC72	Non-essential subunit of Sec63 complex (Sec63p, Sec62p, Sec66p and Sec72p); with Sec61 complex, Kar2p/BiP and Lhs1p forms a channel competent for SRP-dependent and post-translational SRP-independent protein targeting and import into the ER	ER, translocon	0	0	0	22.0	5.2	0	3	2	7	41.5
C4QZ15	SSH1	SSH1	Subunit of the Ssh1 translocon complex; Sec61p homolog involved in co-translational pathway of protein translocation; not essential	ER, translocon	0	1	TMH, 10	52.6	8.6	589	2	2	2	7.1
C4QVV4	SSS1	SSS1	Subunit of the Sec61p translocation complex (Sec61p-Sss1p-Sbh1p) that forms a channel for passage of secretory proteins through the endoplasmic reticulum membrane, and of the	ER, translocon	0	1	TMH, 1	7.2	10.3	0	2	3	1	15.6

			Ssh1p complex (Ssh1p-Sbh2p-Sss1p); interacts with Ost4p and Wbp1p											
C4R518	EMC7	NA	Protein of unknown function (DUF2012);Starch-binding domain-like, homolog of mammalian ER membrane protein complex subunit 7	ER, unknown	1	0	0	24.0	6.5	0	1	2	3	18.2
C4R0M5	IRC22	IRC22	Putative protein of unknown function; green fluorescent protein (GFP)-fusion localizes to the ER	ER, unknown	1	0	TMH, 1	24.7	5.0	0	2	3	7	41.3
C4R7B0	MSC7	MSC7	Protein of unknown function, green fluorescent protein (GFP)-fusion protein localizes to the endoplasmic reticulum	ER, unknown	0	1	TMH, 1	71.0	6.7	0	2	2	3	8.3
C4QVC3	PAS_chr1-3_0136	SHE10	putative secreted protein, does not contain GPI anchor modification site	ER, unknown	1	0	0	90.8	4.1	0	0	2	4	7.4
C4QZH2	PAS_chr2-1_0046	YPR063C	ER-localized protein of unknown function; Uncharacterised protein family (UPF0139)	ER, unknown	0	1	0	11.7	10.1	676	1	2	2	25.9
C4R2S8	PAS_chr2-2_0124	YOL107W	Eukaryotic integral membrane protein (DUF1751)	ER, unknown	0	1	TMH, 5	40.2	7.8	0	1	2	4	19.3
C4R400	PAS_chr3_0249	NA	CUE domain;UBA-like	ER, unknown	0	1	TMH, 1	17.8	9.9	0	0	2	2	13.4
C4R496	PAS_chr3_1178	YDR056C	Putative protein of unknown function; green fluorescent protein (GFP)-fusion protein localizes to the endoplasmic reticulum	ER, unknown	1	0	0	20.4	7.6	0	0	2	3	28.8
C4QZG4	YET3	YET3	Protein of unknown function; YET3 null mutant decreases the level of secreted invertase; homolog of human BAP31 protein	ER, unknown	0	1	TMH, 3	21.9	9.4	0	2	2	2	21.2
C4R4M7	YNR021W	YNR021W	Protein of unknown function (DUF1682); green fluorescent protein (GFP)-fusion protein localizes to the endoplasmic reticulum	ER, unknown	1	1	0	42.6	8.6	300	3	3	9	35.7
C4R9A6	CDC48	CDC48	ATPase involved in ubiquitin-mediated protein degradation; Cdc48p-Npl4p-Ufd1p complex participates in ER-associated degradation (ERAD)	ERAD	0	0	0	91.1	4.7	18	2	2	8	18.0
C4R886	PAS_chr4_0551	POM33	Transmembrane nucleoporin involved in nuclear pore complex (NPC) distribution, assembly or stabilization; highly conserved across species, orthologous to human TMEM33 and paralogous to Per33p	ER-nuclear membrane	0	1	TMH, 5	31.1	10.4	343	3	2	2	11.7
C4QY43	PMR1	PMR1	High affinity Ca2+/Mn2+ P-type ATPase required for Ca2+ and Mn2+ transport into Golgi; involved in Ca2+ dependent protein sorting and processing	Golgi	0	0	TMH, 6	101.0	5.1	0	2	2	9	18.5

C4R6M2	GDA1	GDA1	Guanosine diphosphatase located in the Golgi, involved in the transport of GDP-mannose into the Golgi lumen by converting GDP to GMP after mannose is transferred its substrate	Golgi, protein glycosylation	1	1	TMH, 1	59.9	5.1	0	2	2	7	19.3
C4R3V8	KRE2	KRE2	Alpha1,2-mannosyltransferase of the Golgi involved in protein mannosylation	Golgi, protein glycosylation	0	1	TMH, 1	45.5	6.1	0	1	2	4	17.4
C4R3V9	KTR1	KTR1	Alpha-1,2-mannosyltransferase involved in O- and N-linked protein glycosylation; type II membrane protein; member of the KRE2/MNT1 mannosyltransferase family	Golgi, protein glycosylation	0	1	TMH, 1	46.7	5.9	553	3	3	20	60.0
C4QXA8	KTR4	KTR4	Putative mannosyltransferase involved in protein glycosylation; member of the KRE2/MNT1 mannosyltransferase family	Golgi, protein glycosylation	0	1	TMH, 1	49.9	6.0	0	0	2	2	5.5
C4QX95	MNN2-2	MNN2	Alpha-1,2-mannosyltransferase, responsible for addition of the first alpha-1,2-linked mannose to form the branches on the mannan backbone of oligosaccharides, localizes to an early Golgi compartment	Golgi, protein glycosylation	0	1	TMH, 1	77.4	5.3	0	1	2	5	10.5
C4R6V4	MNN9	MNN9	Subunit of Golgi mannosyltransferase complex also containing Anp1p, Mnn10p, Mnn11p, and Hoc1p that mediates elongation of the polysaccharide mannan backbone; forms a separate complex with Van1p that is also involved in backbone elongation	Golgi, protein glycosylation	0	1	TMH, 1	42.4	8.6	0	2	2	5	25.6
C4R5Y9	VRG4	VRG4	Golgi GDP-mannose transporter; regulates Golgi function and glycosylation in Golgi	Golgi, protein glycosylation	0	1	TMH, 10	36.3	0.0	411	2	1	3	14.6
C4R2J6	HHF1	HHF1	Histone H4, core histone protein required for chromatin assembly and chromosome function; contributes to telomeric silencing; N-terminal domain involved in maintaining genomic integrity	histone	0	0	0	11.4	11.8	120	2	2	5	49.5
C4R0M8	HTA2	HTA2	Histone H2A, core histone protein required for chromatin assembly and chromosome function; DNA damage-dependent phosphorylation by Mec1p facilitates DNA repair; acetylated by Nat4p	histone	0	0	0	13.9	10.8	299	2	2	3	45.4
C4R0M7	HTB2	HTB2	Histone H2B, core histone protein required for chromatin assembly and chromosome function; Rad6p-Bre1p-Lge1p mediated ubiquitination regulates transcriptional activation, meiotic DSB formation and H3 methylation	histone	0	0	0	14.4	10.5	167	1	3	2	15.9
C4R6Q5	FAD2	NA	delta 12-fatty acid desaturase	lipid metabolism	0	0	TMH, 5	48.5	8.9	0	1	2	4	11.7
C4R2Q5	HET1	NA	Glycolipid transfer protein (GLTP);Sphingolipid transfer protein Het1, no S. cerevisiae homolog	lipid metabolism	0	0	0	22.1	7.6	128	2	2	3	22.6

C4QZ99	LCB1	LCB1	Component of serine palmitoyltransferase, responsible along with Lcb2p for the first committed step in sphingolipid synthesis, which is the condensation of serine with palmitoyl-CoA to form 3-ketosphinganine	lipid metabolism	0	0	0	61.7	5.4	598	3	2	10	25.5
C4R5E6	LCB2	LCB2	Component of serine palmitoyltransferase, responsible along with Lcb1p for the first committed step in sphingolipid synthesis, which is the condensation of serine with palmitoyl-CoA to form 3-ketosphinganine	lipid metabolism	0	1	TMH, 1	62.6	9.0	0	2	2	4	9.6
C4R7Z3	PAS_chr4_0465	NA	sphingolipid C9-methyltransferase, S-adenosyl-L-methionine-dependent; introduces the methyl group at the C9-position of fungal glucosylceramides (experimentally verified)	lipid metabolism	0	1	TMH, 1	56.2	6.6	344	3	3	10	36.4
C4QVT8	FAS1	FAS1	Beta subunit of fatty acid synthetase, which catalyzes the synthesis of long-chain saturated fatty acids; contains acetyltransacylase, dehydratase, enoyl reductase, malonyl transacylase, and palmitoyl transacylase activities	lipid metabolism, cyt, LP	0	0	0	229.6	6.2	2	2	2	6	5.3
C4QY22	ERG10	ERG10	Acetyl-CoA C-acetyltransferase (acetoacetyl-CoA thiolase), cytosolic enzyme that transfers an acetyl group from one acetyl-CoA molecule to another, forming acetoacetyl-CoA; involved in the first step in mevalonate biosynthesis	lipid metabolism, cyto	0	0	0	41.7	6.1	55	1	2	5	17.9
C4QYE4	SLM1	SLM1	Phosphoinositide PI4,5P(2) binding protein, forms a complex with Slm2p; acts downstream of Mss4p in a pathway regulating actin cytoskeleton organization in response to stress; phosphorylated by the TORC2 complex	lipid metabolism, eisosome, PM	0	0	0	77.4	9.1	0	3	2	14	24.3
C4QXE9	CHO2	CHO2	Phosphatidylethanolamine methyltransferase (PEMT), catalyzes the first step in the conversion of phosphatidylethanolamine to phosphatidylcholine during the methylation pathway of phosphatidylcholine biosynthesis	lipid metabolism, ER	0	1	TMH, 8	103.1	8.6	0	2	0	2	3.6
C4R8D3	DPL1	DPL1	Dihydrosphingosine phosphate lyase, regulates intracellular levels of sphingolipid long-chain base phosphates (LCBPs), degrades phosphorylated long chain bases, prefers C16 dihydrosphingosine-l-phosphate as a substrate	lipid metabolism, ER	0	1	0	63.8	6.2	0	3	0	4	9.3
C4R632	ERG11	ERG11	Lanosterol 14-alpha-demethylase; catalyzes the C-14 demethylation of lanosterol to form 4,4"-dimethyl cholesta-8,14,24-triene-3-beta-ol in the ergosterol biosynthesis pathway; member of the cytochrome P450 family	lipid metabolism, ER	0	1	0	58.8	8.5	0	3	2	8	24.1
C4R749	ERG2	ERG2	C-8 sterol isomerase, catalyzes the isomerization of the delta-8 double bond to the delta-7 position at an intermediate step in ergosterol biosynthesis	lipid metabolism, ER	0	1	0	23.3	5.2	576	1	2	1	11.2
C4QYY9	ERG26	ERG26	C-3 sterol dehydrogenase, catalyzes the second of three steps required to remove two C-4 methyl groups from an intermediate in ergosterol biosynthesis	lipid metabolism, ER	0	0	0	38.0	7.8	0	3	2	7	44.1

C4QY87	ERG3	ERG3	C-5 sterol desaturase, catalyzes the introduction of a C-5(6) double bond into episterol, a precursor in ergosterol biosynthesis; mutants are viable, but cannot grow on non-fermentable carbon sources	lipid metabolism, ER	0	0	TMH, 4	44.7	8.9	0	1	2	3	14.1
C4R4R9	ERG5	ERG5	C-22 sterol desaturase, a cytochrome P450 enzyme that catalyzes the formation of the C-22(23) double bond in the sterol side chain in ergosterol biosynthesis; may be a target of azole antifungal drugs	lipid metabolism, ER	0	1	0	60.1	6.1	146	2	2	11	27.3
C4R513	FEN1	FEN1	Fatty acid elongase, involved in sphingolipid biosynthesis; acts on fatty acids of up to 24 carbons in length; mutations have regulatory effects on 1,3-beta-glucan synthase, vacuolar ATPase, and the secretory pathway	lipid metabolism, ER	0	1	TMH, 7	38.3	9.8	0	3	0	2	12.0
C4R2G2	HMG1	HMG1	One of two isozymes of HMG-CoA reductase that catalyzes the conversion of HMG-CoA to mevalonate, which is a rate-limiting step in sterol biosynthesis; localizes to the nuclear envelope; overproduction induces the formation of karmellae	lipid metabolism, ER	0	1	TMH, 6	107.1	9.2	0	3	2	11	17.1
C4R7N6	IFA38	IFA38	Microsomal beta-keto-reductase; contains oleate response element (ORE) sequence in the promoter region; mutants exhibit reduced VLCFA synthesis, accumulate high levels of dihydrosphingosine, phytosphingosine and medium-chain ceramides	lipid metabolism, ER	0	1	TMH, 3	36.4	10.0	449	3	2	4	18.2
C4QV83	NSG2	NSG2	Protein involved in regulation of sterol biosynthesis; specifically stabilizes Hmg2p, one of two HMG-CoA isoenzymes that catalyze the rate-limiting step in sterol biosynthesis	lipid metabolism, ER	0	0	TMH, 3	33.0	5.9	0	2	0	2	7.8
C4QZJ9	OLE1	OLE1	Delta(9) fatty acid desaturase, required for monounsaturated fatty acid synthesis and for normal distribution of mitochondria	lipid metabolism, ER	0	0	TMH, 4	55.9	9.7	0	1	2	5	19.0
C4QZ02	SAC1	SAC1	Phosphatidylinositol phosphate (PtdInsP) phosphatase involved in hydrolysis of PtdIns[4]P; transmembrane protein localizes to ER and Golgi; involved in protein trafficking and processing, secretion, and cell wall maintenance	lipid metabolism, ER	0	0	TMH, 2	68.6	8.9	239	3	2	8	16.6
C4R3Y7	SUR4	SUR4	Elongase, involved in fatty acid and sphingolipid biosynthesis; synthesizes very long chain 20-26-carbon fatty acids from C18-CoA primers; involved in regulation of sphingolipid biosynthesis	lipid metabolism, ER	0	0	TMH, 6	38.0	9.7	0	3	2	2	12.1
C4QW59	TCB3	TCB3	Lipid-binding protein, localized to the bud via specific mRNA transport; non-tagged protein detected in a phosphorylated state in mitochondria; GFP-fusion protein localizes to the cell periphery; C-termini of Tcb1p, Tcb2p and Tcb3p interact	lipid metabolism, ER	0	0	TMH, 1	155.2	6.5	0	3	2	9	10.3

C4R2Z6	AYR1	AYR1	NADPH-dependent 1-acyl dihydroxyacetone phosphate reductase found in lipid particles, ER, and mitochondrial outer membrane; involved in phosphatidic acid biosynthesis; required for spore germination; capable of metabolizing steroid hormones	lipid metabolism, ER, LP	0	0	TMH, 1	32.2	9.5	339	2	2	3	20.9
C4R3L8	ERG1	ERG1	Squalene epoxidase, catalyzes the epoxidation of squalene to 2,3-oxidosqualene; plays an essential role in the ergosterol-biosynthesis pathway and is the specific target of the antifungal drug terbinafine	lipid metabolism, ER, LP	0	0	TMH, 3	55.1	5.9	0	0	2	5	15.7
C4R4C9	ERG6	ERG6	Delta(24)-sterol C-methyltransferase, converts zymosterol to fecosterol in the ergosterol biosynthetic pathway by methylating position C-24; localized to both lipid particles and mitochondrial outer membrane	lipid metabolism, ER, LP	0	0	0	43.3	5.4	108	3	2	14	48.3
C4R0N3	PAS_chr2-1_0835	LOA1	Acyltransferase;Glycerol-3-phosphate (1)-acyltransferase	lipid metabolism, ER, LP	0	1	TMH, 1	32.2	10.1	0	0	2	4	27.6
C4R470	ERG9	ERG9	Farnesyl-diphosphate farnesyl transferase (squalene synthase), joins two farnesyl pyrophosphate moieties to form squalene in the sterol biosynthesis pathway	lipid metabolism, ER, MOM	0	0	0	50.6	5.4	0	3	1	3	14.7
C4R3E6	ERG25	ERG25	C-4 methyl sterol oxidase, catalyzes the first of three steps required to remove two C-4 methyl groups from an intermediate in ergosterol biosynthesis; mutants accumulate the sterol intermediate 4,4-dimethylzymosterol	lipid metabolism, ER, PM	0	1	0	37.2	9.3	0	2	2	2	10.5
C4R1Y4	PCT1	PCT1	Cholinephosphate cytidylyltransferase, also known as CTP:phosphocholine cytidylyltransferase, rate-determining enzyme of the CDP-choline pathway for phosphatidylcholine synthesis, inhibited by Sec14p, activated upon lipid-binding	lipid metabolism, ER-Golgi	0	0	0	42.2	9.8	0	1	2	11	31.1
C4R4Q0	TCB1	TCB1	Lipid-binding protein containing three calcium and lipid binding domains; non-tagged protein localizes to mitochondria and GFP-fusion protein localizes to the cell periphery; C-termini of Tcb1p, Tcb2p and Tcb3p interact	lipid metabolism, ER-PM	0	0	TMH, 3	129.2	6.1	0	3	2	12	16.6
C4QVE4	SLC1	SLC1	1-acyl-sn-glycerol-3-phosphate acyltransferase, catalyzes the acylation of lysophosphatidic acid to form phosphatidic acid, a key intermediate in lipid metabolism; enzymatic activity detected in lipid particles and microsomes	lipid metabolism, LP	0	1	TMH, 1	31.8	5.8	0	2	1	2	10.8
C4R1R9	FAA1	FAA1	Long chain fatty acyl-CoA synthetase, activates imported fatty acids with a preference for C12:0-C16:0 chain lengths; functions in long chain fatty acid import; accounts for most acyl-CoA synthetase activity; localized to lipid particles	lipid metabolism, LP, ER	0	0	0	78.3	9.0	41	3	3	27	41.7
C4R901	NCP1	NCP1	NADP-cytochrome P450 reductase; involved in ergosterol biosynthesis; associated and coordinately regulated with Erg11p	lipid metabolism, MOM	0	1	0	77.5	5.0	263	2	2	15	38.1

C4QV87	STT4	STT4	Phosphatidylinositol-4-kinase that functions in the Pkc1p protein kinase pathway; required for normal vacuole morphology, cell wall integrity, and actin cytoskeleton organization	lipid metabolism, PM	0	0	0	208.8	6.4	0	2	0	9	9.3
C4R0F7	COX4	COX4	Subunit IV of cytochrome c oxidase, the terminal member of the mitochondrial inner membrane electron transport chain; precursor N-terminal 25 residues are cleaved during mitochondrial import; phosphorylated; spermidine enhances translation	mitochondria	0	0	0	18.1	9.0	0	3	1	3	35.4
C4R526	COX5B	COX5B	Subunit Vb of cytochrome c oxidase, which is the terminal member of the mitochondrial inner membrane electron transport chain	mitochondria	0	0	TMH, 1	17.6	10.1	0	2	1	3	22.4
C4QXS0	FMP52	FMP52	Protein of unknown function, localized to the mitochondrial outer membrane; induced by treatment with 8-methoxypsoralen and UVA irradiation	mitochondria	0	0	0	23.8	9.5	0	2	3	3	23.6
C4QZ00	MIR1	MIR1	Mitochondrial phosphate carrier, imports inorganic phosphate into mitochondria	mitochondria	0	0	0	32.9	9.7	105	3	2	11	71.5
C4QY16	NDE2	NDE2	Mitochondrial external NADH dehydrogenase, catalyzes the oxidation of cytosolic NADH; Nde1p and Nde2p are involved in providing the cytosolic NADH to the mitochondrial respiratory chain	mitochondria	0	0	0	62.7	9.4	192	2	0	4	9.7
C4R3D1	ODC1	ODC1	Mitochondrial inner membrane transporter, exports 2-oxoadipate and 2-oxoglutarate from the mitochondrial matrix to the cytosol for lysine and glutamate biosynthesis and lysine catabolism; suppresses, in multicopy, an fmc1 null mutation	mitochondria	0	1	0	32.1	10.0	451	2	1	2	16.0
C4R760	PET9	PET9	Major ADP/ATP carrier of the mitochondrial inner membrane, exchanges cytosolic ADP for mitochondrially synthesized ATP; also imports heme and ATP; phosphorylated	mitochondria	0	0	TMH, 3	33.2	10.2	25	3	3	16	48.4
C4R1Z2	POR1	POR1	Mitochondrial porin (voltage-dependent anion channel), outer membrane protein required for the maintenance of mitochondrial osmotic stability and mitochondrial membrane permeability; phosphorylated	mitochondria	0	0	0	29.6	9.4	11	3	2	14	62.9
C4R1V5	QCR2	QCR2	Subunit 2 of the ubiquinol cytochrome-c reductase complex, which is a component of the mitochondrial inner membrane electron transport chain; phosphorylated; transcription is regulated by Hap1p, Hap2p/Hap3p, and heme	mitochondria	0	0	0	37.4	9.0	103	2	0	4	15.1
C4R4C3	SSC1	SSC1	Hsp70 family ATPase, constituent of the import motor component of the Translocase of the Inner Mitochondrial membrane (TIM23 complex); involved in protein translocation and folding; subunit of SceI endonuclease	mitochondria	0	0	0	69.7	5.3	45	2	1	3	14.1

C4R225	TOM22	TOM22	Component of the TOM (translocase of outer mitochondrial membrane) complex responsible for initial import of mitochondrially directed proteins; acts as a receptor for precursor proteins and mediates interaction between TOM and TIM complexes	mitochondria	0	0	TMH, 1	16.3	3.7	0	2	1	2	23.5
C4R7R5	TOM40	TOM40	Component of the TOM (translocase of outer membrane) complex responsible for recognition and initial import steps for all mitochondrially directed proteins; constitutes the core element of the protein conducting pore	mitochondria	0	0	0	42.7	5.5	379	3	0	3	14.4
C4R4Y8	ATP1	ATP1	Alpha subunit of the F1 sector of mitochondrial F1F0 ATP synthase, which is a large, evolutionarily conserved enzyme complex required for ATP synthesis; phosphorylated	mitochondrial F1F0 ATP synthase	0	0	0	58.7	9.6	14	3	2	14	34.6
C4R2N5	ATP2	ATP2	Beta subunit of the F1 sector of mitochondrial F1F0 ATP synthase, which is a large, evolutionarily conserved enzyme complex required for ATP synthesis; phosphorylated	mitochondrial F1F0 ATP synthase	0	0	0	54.0	5.0	3	3	2	20	54.5
C4R5N6	ATP20	ATP20	Subunit g of the mitochondrial F1F0 ATP synthase; reversibly phosphorylated on two residues; unphosphorylated form is required for dimerization of the ATP synthase complex	mitochondrial F1F0 ATP synthase	0	0	0	15.8	10.3	293	2	0	1	14.6
C4R4M3	ATP4	ATP4	Subunit b of the stator stalk of mitochondrial F1F0 ATP synthase, which is a large, evolutionarily conserved enzyme complex required for ATP synthesis; contributes to the oligomerization of the complex; phosphorylated	mitochondrial F1F0 ATP synthase	0	0	0	25.3	9.5	255	3	2	6	39.2
C4QWD4	ATP5	ATP5	Subunit 5 of the stator stalk of mitochondrial F1F0 ATP synthase, which is an evolutionarily conserved enzyme complex required for ATP synthesis; homologous to bovine subunit OSCP (oligomycin sensitivity-conferring protein); phosphorylated	mitochondrial F1F0 ATP synthase	0	0	0	21.7	9.6	100	2	1	6	54.6
C4QWF3	ATP7	ATP7	Subunit d of tmitochondrial F1F0 ATP synthase, which is a large, evolutionarily conserved enzyme complex required for ATP synthesis	mitochondrial F1F0 ATP synthase	0	0	0	19.7	7.6	158	2	2	5	39.4
C4R0Q2	GSP1	GSP1	Ran GTPase, GTP binding protein (mammalian Ranp homolog) involved in the maintenance of nuclear organization, RNA processing and transport; regulated by Srm1p, Rna1p, Yrb1p, Yrb2p, Yrp4p, Yrb30p, Cse1p and Kap95p	nuclear membrane	0	0	0	24.1	6.6	214	3	3	4	36.2
C4QW50	FRA1-1	FRA1	Protein involved in negative regulation of transcription of iron regulon; forms an iron independent complex with Fra2p, Grx3p, and Grx4p; cytosolic; mutant fails to repress transcription of iron regulon and is defective in spore formation	other	0	0	0	79.2	6.3	0	1	2	2	13.6

C4QYK6	PHB2	PHB2	Subunit of the prohibitin complex (Phb1p-Phb2p), a 1.2 MDa ring-shaped inner mitochondrial membrane chaperone that stabilizes newly synthesized proteins; determinant of replicative life span; involved in mitochondrial segregation	other	0	1	TMH, 1	33.4	10.3	614	2	0	1	5.6
C4R0F0	RSP5	RSP5	E3 ubiquitin ligase of the NEDD4 family; involved in regulating many cellular processes including MVB sorting, heat shock response, transcription, endocytosis, and ribosome stability	other	0	0	0	87.7	5.8	0	2	2	9	14.9
C4R2A9	URO1	NA	Uricase; Urate oxidase, degardes uric acid to allantoin; no S. cerevisiae homolog	other	0	0	0	34.7	7.8	0	2	2	6	30.5
C4R300	YNK1	YNK1	Nucleoside diphosphate kinase, catalyzes the transfer of gamma phosphates from nucleoside triphosphates, usually ATP, to nucleoside diphosphates by a mechanism that involves formation of an autophosphorylated enzyme intermediate	other	0	0	0	17.0	6.2	99	2	2	4	34.9
C4R8Y8	PEX14	PEX14	Peroxisomal membrane peroxin that is a central component of the peroxisomal protein import machinery; interacts with both PTS1 (Pex5p) and PTS2 (Pex7p), peroxisomal matrix protein signal recognition factors and membrane receptor Pex13p	peroxisomal membrane	0	0	0	46.6	4.8	0	1	2	2	10.8
C4QW99	ADY2-1	ADY2	Acetate transporter required for normal sporulation; phosphorylated in mitochondria	plasma membrane	0	0	TMH, 6	28.4	6.2	235	3	3	3	16.0
C4R1C0	ADY2-2	ADY2	Acetate transporter required for normal sporulation; phosphorylated in mitochondria	plasma membrane	0	0	TMH, 6	29.0	5.8	405	3	2	3	13.8
C4R5H7	AQY1	AQY1	Spore-specific water channel that mediates the transport of water across cell membranes, developmentally controlled; may play a role in spore maturation, probably by allowing water outflow, may be involved in freeze tolerance	plasma membrane	0	1	TMH, 6	29.9	6.5	303	3	2	3	21.1
C4R733	CTR1	CTR1	High-affinity copper transporter of the plasma membrane, mediates nearly all copper uptake under low copper conditions; transcriptionally induced at low copper levels and degraded at high copper levels	plasma membrane	0	0	TMH, 3	25.1	5.5	0	2	1	6	37.9
C4R7E9	DIP5	DIP5	Dicarboxylic amino acid permease, mediates high-affinity and high-capacity transport of L-glutamate and L-aspartate; also a transporter for Gln, Asn, Ser, Ala, and Gly	plasma membrane	0	0	TMH, 12	65.3	9.6	0	3	3	7	13.5
C4QX33	ENA2	ENA2	P-type ATPase sodium pump, involved in Na+ efflux to allow salt tolerance; likely not involved in Li+ efflux	plasma membrane	0	0	TMH, 10	120.4	5.3	0	3	3	29	34.6
C4R659	FRE1	FRE1	Ferric reductase and cupric reductase, reduces siderophore-bound iron and oxidized copper prior to uptake by	plasma membrane	1	0	TMH, 7	76.8	8.4	0	3	3	12	21.3

			transporters; expression induced by low copper and iron levels											
C4QYV2	HXT7	HXT7	High-affinity glucose transporter of the major facilitator superfamily, nearly identical to Hxt6p, expressed at high basal levels relative to other HXTs, expression repressed by high glucose levels	plasma membrane	0	1	TMH, 11	59.5	7.5	338	3	3	11	24.8
C4R0V8	IST2	IST2	Plasma membrane protein that may be involved in osmotolerance, localizes to the mother cell in small-budded cells and to the bud in medium- and large-budded cells	plasma membrane	0	0	TMH, 6	99.0	6.8	0	3	1	4	8.1
C4R835	NCE102	NCE102	Protein of unknown function; contains transmembrane domains; involved in secretion of proteins that lack classical secretory signal sequences; component of the detergent-insoluble glycolipid-enriched complexes (DIGs)	plasma membrane	1	1	TMH, 4	18.3	10.0	0	2	3	5	29.8
C4QZH7	PAS_chr2-1_0050	STE6	Plasma membrane ATP-binding cassette (ABC) transporter required for the export of a-factor	plasma membrane	0	0	TMH, 11	142.4	5.9	0	3	3	16	15.7
C4QX02	PDR5-1	PDR5	Plasma membrane ATP-binding cassette (ABC) transporter, multidrug transporter actively regulated by Pdr1p; also involved in steroid transport, cation resistance, and cellular detoxification during exponential growth	plasma membrane	0	0	TMH, 12	170.3	6.0	0	3	3	43	35.9
C4R284	PDR5-2	PDR5	Plasma membrane ATP-binding cassette (ABC) transporter, multidrug transporter actively regulated by Pdr1p; also involved in steroid transport, cation resistance, and cellular detoxification during exponential growth	plasma membrane	0	0	TMH, 13	167.7	8.7	0	3	1	9	7.8
C4QZY3	PGA3	PGA3	Putative cytochrome b5 reductase, localized to the plasma membrane; may be involved in regulation of lifespan; required for maturation of Gas1p and Pho8p, proposed to be involved in protein trafficking	plasma membrane	0	1	TMH, 2	34.6	5.3	0	2	2	7	40.0
C4QVS9	PMA1	PMA1	Plasma membrane H+-ATPase, pumps protons out of the cell; major regulator of cytoplasmic pH and plasma membrane potential; P2-type ATPase; Hsp30p plays a role in Pma1p regulation	plasma membrane	0	0	TMH, 9	97.8	4.8	20	3	3	46	48.0
C4QXM7	PUN1	PUN1	Plasma membrane protein with a role in cell wall integrity; co-localizes with Sur7p in punctate membrane patches; null mutant displays decreased thermotolerance; transcription induced upon cell wall damage and metal ion stress	plasma membrane	0	1	TMH, 4	33.6	4.3	0	2	3	1	5.2
C4R8L5	RAS1	RAS1	GTPase involved in G-protein signaling in the adenylate cyclase activating pathway, plays a role in cell proliferation; localized to the plasma membrane; homolog of mammalian RAS proto-oncogenes	plasma membrane	0	0	0	23.7	4.8	237	3	3	8	48.8

C4R235	RSR1	RSR1	GTP-binding protein of the ras superfamily required for bud site selection, morphological changes in response to mating pheromone, and efficient cell fusion; localized to the plasma membrane; significantly similar to mammalian Rap GTPases	plasma membrane	0	0	0	25.7	9.6	0	2	1	2	15.2
C4R573	SIT1	SIT1	Ferrioxamine B transporter, member of the ARN family of transporters that specifically recognize siderophore-iron chelates; transcription is induced during iron deprivation and diauxic shift; potentially phosphorylated by Cdc28p	plasma membrane	0	0	TMH, 14	70.6	8.8	0	2	1	4	7.4
C4R175	SNG1	SNG1	Protein involved in resistance to nitrosoguanidine (MNNG) and 6-azauracil (6-AU); expression is regulated by transcription factors involved in multidrug resistance	plasma membrane	0	0	TMH, 7	54.3	5.7	0	3	1	3	7.9
C4R070	SNQ2	SNQ2	Plasma membrane ATP-binding cassette (ABC) transporter, multidrug transporter involved in multidrug resistance and resistance to singlet oxygen species	plasma membrane	0	0	TMH, 12	164.7	5.2	0	3	3	33	32.9
C4R6D4	SUR7	SUR7	Plasma membrane protein that localizes to furrow-like invaginations (MCC patches); component of eisosomes; associated with endocytosis, along with Pil1p and Lsp1p; sporulation and plasma membrane sphingolipid content are altered in mutants	plasma membrane	0	1	TMH, 4	31.7	4.7	473	3	3	6	27.0
C4R8A4	YCK2	YCK2	Palmitoylated plasma membrane-bound casein kinase I isoform; shares redundant functions with Yck1p in morphogenesis, proper septin assembly, endocytic trafficking; provides an essential function overlapping with that of Yck1p	plasma membrane	0	0	0	57.6	10.1	0	3	1	4	12.0
C4R3Q7	YPS1-2	YPS1	Aspartic protease, member of the yapsin family of proteases involved in cell wall growth and maintenance; attached to the plasma membrane via a glycosylphosphatidylinositol (GPI) anchor	plasma membrane	1	0	0	60.5	4.0	0	3	2	5	11.2
Q9P4D1	ACT1	ACT1	Actin, structural protein involved in cell polarization, endocytosis, and other cytoskeletal functions	polarity	0	0	0	41.7	5.2	29	3	3	3	20.5
C4R8L6	RGD1	RGD1	GTPase-activating protein (RhoGAP) for Rho3p and Rho4p, possibly involved in control of actin cytoskeleton organization	polarity	0	0	0	70.6	6.3	0	2	1	6	13.5
C4R3P3	RHO1	RHO1	GTP-binding protein of the rho subfamily of Ras-like proteins, involved in establishment of cell polarity; regulates protein kinase C (Pkc1p) and the cell wall synthesizing enzyme 1,3-beta-glucan synthase (Fks1p and Gsc2p)	polarity	0	0	0	22.0	5.2	388	3	3	6	48.7
C4R0N5	RHO3	RHO3	Non-essential small GTPase of the Rho/Rac subfamily of Ras-like proteins involved in the establishment of cell polarity; GTPase activity positively regulated by the GTPase activating protein (GAP) Rgd1p	polarity	0	0	0	26.4	4.9	0	2	1	3	20.9

C4QZP2	CDC42	CDC42	Small rho-like GTPase, essential for establishment and maintenance of cell polarity; mutants have defects in the organization of actin and septins	polyrity	0	0	0	21.3	6.2	0	2	2	2	14.1
C4QXC0	ASC1	ASC1	G-protein beta subunit and guanine nucleotide dissociation inhibitor for Gpa2p; ortholog of RACK1 that inhibits translation; core component of the small (40S) ribosomal subunit; represses Gcn4p in the absence of amino acid starvation	ribosome/translation	0	0	0	34.7	6.3	73	1	2	3	13.3
C4QYF5	BFR1	BFR1	Component of mRNP complexes associated with polyribosomes; implicated in secretion and nuclear segregation; multicopy suppressor of BFA (Brefeldin A) sensitivity	ribosome/translation	0	0	0	58.3	9.5	0	0	2	7	16.2
C4R751	DBP2	DBP2	Essential ATP-dependent RNA helicase of the DEAD-box protein family, involved in nonsense-mediated mRNA decay and rRNA processing	ribosome/translation	0	0	0	58.6	9.5	202	1	2	6	15.3
C4R6Z1	DED1	DED1	ATP-dependent DEAD (Asp-Glu-Ala-Asp)-box RNA helicase, required for translation initiation of all yeast mRNAs	ribosome/translation	0	0	0	66.4	7.9	63	2	2	5	13.5
C4R0H3	EFB1	EFB1	Translation elongation factor 1 beta; stimulates nucleotide exchange to regenerate EF-1 alpha-GTP for the next elongation cycle; part of the EF-1 complex, which facilitates binding of aminoacyl-tRNA to the ribosomal A site	ribosome/translation	0	0	0	23.3	4.1	133	2	1	4	38.9
C4QZQ5	EFT2	EFT2	Elongation factor 2 (EF-2), also encoded by EFT1; catalyzes ribosomal translocation during protein synthesis; contains diphthamide, the unique posttranslationally modified histidine residue specifically ADP-ribosylated by diphtheria toxin	ribosome/translation	0	0	0	93.4	6.3	10	3	3	24	39.9
C4R305	RPL10	RPL10	Protein component of the large (60S) ribosomal subunit, responsible for joining the 40S and 60S subunits; regulates translation initiation; has similarity to rat L10 ribosomal protein and to members of the QM gene family	ribosome/translation	0	0	0	25.5	10.6	227	3	2	11	50.9
C4R8K3	RPL11B	RPL11B	Protein component of the large (60S) ribosomal subunit; involved in ribosomal assembly; depletion causes degradation of proteins and RNA of the 60S subunit	ribosome/translation	0	0	0	19.9	10.5	296	2	3	5	31.6
C4QWD2	RPL12B	RPL12B	Protein component of the large (60S) ribosomal subunit; rpl12a rpl12b double mutant exhibits slow growth and slow translation	ribosome/translation	0	0	0	17.8	10.0	123	2	3	8	62.4
C4R7T7	RPL13B	RPL13B	Protein component of the large (60S) ribosomal subunit; not essential for viability	ribosome/translation	0	0	0	22.2	11.3	144	2	3	4	34.0
C4R389	RPL14B	RPL14B	Protein component of the large (60S) ribosomal subunit	ribosome/translation	0	0	0	14.9	4.6	266	2	3	5	42.9

C4R1C9	RPL15B	RPL15B	Protein component of the large (60S) ribosomal subunit; binds to 5.8 S rRNA	ribosome/translation	0	0	0	24.2	11.9	221	2	2	5	34.3
C4R759	RPL16A	RPL16A	N-terminally acetylated protein component of the large (60S) ribosomal subunit, binds to 5.8 S rRNA	ribosome/translation	0	0	0	22.7	10.7	250	2	3	9	37.2
C4R2U4	RPL17B	RPL17B	Protein component of the large (60S) ribosomal subunit	ribosome/translation	0	0	0	19.1	10.4	345	3	3	7	52.4
C4QY71	RPL18B	RPL18B	Protein component of the large (60S) ribosomal subunit	ribosome/translation	0	0	0	20.6	11.4	138	3	3	4	29.6
C4R3I6	RPL19B	RPL19B	Protein component of the large (60S) ribosomal subunit; rpl19a and rpl19b single null mutations result in slow growth, while the double null mutation is lethal	ribosome/translation	0	0	0	23.5	11.8	139	2	2	7	39.2
C4QWC5	RPL1B	RPL1B	N-terminally acetylated protein component of the large (60S) ribosomal subunit; rpl1a rpl1b double null mutation is lethal	ribosome/translation	0	0	0	24.5	10.3	126	2	2	8	44.7
C4R3E7	RPL20A	RPL20A	Protein component of the large (60S) ribosomal subunit	ribosome/translation	0	0	0	21.5	10.3	110	2	2	8	42.0
C4QVD0	RPL23A	RPL23A	Protein component of the large (60S) ribosomal subunit	ribosome/translation	0	0	0	14.4	11.0	81	3	2	5	39.4
C4QZL3	RPL24B	RPL24B	Ribosomal protein L30 of the large (60S) ribosomal subunit; not essential for translation but may be required for normal translation rate	ribosome/translation	0	0	0	17.9	11.5	488	3	2	5	26.6
C4R910	RPL25	RPL25	Primary rRNA-binding ribosomal protein component of the large (60S) ribosomal subunit; binds to 25S rRNA via a conserved C-terminal motif	ribosome/translation	0	0	0	15.7	10.1	380	2	2	5	49.3
C4R1K3	RPL28	RPL28	Ribosomal protein of the large (60S) ribosomal subunit; may have peptidyl transferase activity	ribosome/translation	0	0	0	16.5	11.5	615	2	2	5	43.6
C4QWG6	RPL2A-1	RPL2A	Protein component of the large (60S) ribosomal subunit	ribosome/translation	0	0	0	27.2	11.6	183	2	2	3	21.7
C4QWG6	RPL2A-2	RPL2A	Protein component of the large (60S) ribosomal subunit	ribosome/translation	0	0	0	27.2	11.6	183	2	2	3	21.7
C4R6Z0	RPL3	RPL3	Protein component of the large (60S) ribosomal subuni; involved in the replication and maintenance of killer double stranded RNA virus	ribosome/translation	0	0	0	43.6	10.7	79	2	2	7	21.6

C4QZL4	RPL30	RPL30	Protein component of the large (60S) ribosomal subunit; involved in pre-rRNA processing in the nucleolus; autoregulates splicing of its transcript	ribosome/translation	0	0	0	11.6	10.2	261	2	2	2	29.9
C4R731	RPL31B	RPL31B	Protein component of the large (60S) ribosomal subunit; associates with the karyopherin Sxm1p; loss of both Rpl31p and Rpl39p confers lethality	ribosome/translation	0	0	0	13.6	10.1	218	2	3	6	53.8
C4R6D3	RPL32	RPL32	Protein component of the large (60S) ribosomal subunit, has similarity to rat L32 ribosomal protein; overexpression disrupts telomeric silencing	ribosome/translation	0	0	0	15.2	11.3	0	2	2	3	36.4
C4QXY6	RPL33A	RPL33A	N-terminally acetylated ribosomal protein L37 of the large (60S) ribosomal subunitrpl33a null mutant exhibits slow growth while rpl33a rpl33b double null mutant is inviable	ribosome/translation	0	0	0	12.1	10.7	462	1	2	5	39.3
C4QWQ6	RPL35B	RPL35B	Protein component of the large (60S) ribosomal subunit	ribosome/translation	0	0	0	13.9	11.1	364	2	2	3	20.0
C4QZ92	RPL36A	RPL36A	N-terminally acetylated protein component of the large (60S) ribosomal subunit; binds to 5.8 S rRNA	ribosome/translation	0	0	0	11.5	12.0	0	2	3	4	29.7
C4QYD7	RPL38	RPL38	Protein component of the large (60S) ribosomal subunit	ribosome/translation	0	0	0	9.0	10.7	275	2	3	2	37.2
C4R0U2	RPL40A	RPL40A	Fusion protein, that is cleaved to yield ubiquitin and a ribosomal protein of the large (60S) ribosomal subunit with similarity to rat L40; ubiquitin may facilitate assembly of the ribosomal protein into ribosomes	ribosome/translation	0	0	0	14.6	10.7	0	2	2	5	46.1
C4R487	RPL43B	RPL43B	Protein component of the large (60S) ribosomal subunit	ribosome/translation	0	0	0	10.1	11.4	663	0	2	3	35.9
C4QV16	RPL4A	RPL4A	N-terminally acetylated protein component of the large (60S) ribosomal subunit	ribosome/translation	0	0	0	36.9	11.2	77	3	3	14	48.4
C4QWU8	RPL5	RPL5	Protein component of the large (60S) ribosomal subunit; binds 5S rRNA and is required for 60S subunit assembly	ribosome/translation	0	0	0	34.1	8.9	78	3	3	9	44.1
C4R6Y3	RPL6B	RPL6B	Protein component of the large (60S) ribosomal subunit; binds to 5.8S rRNA	ribosome/translation	0	0	0	18.6	9.0	71	2	2	9	78.4
C4QZE7	RPL7A	RPL7A	Protein component of the large (60S) ribosomal subunit; contains a conserved C-terminal Nucleic acid Binding Domain (NDB2)	ribosome/translation	0	0	0	27.9	10.0	66	3	3	11	55.3
C4QWG3	RPL8B	RPL8B	Ribosomal 60S subunit protein L8B; mutation results in decreased amounts of free 60S subunits	ribosome/translation	0	0	0	26.8	10.1	101	2	2	12	60.1

C4QWY6	RPL9B	RPL9B	Protein component of the large (60S) ribosomal subunit	ribosome/translation	0	0	0	21.7	9.8	129	3	3	11	55.5
C4QV50	RPP0	RPP0	Conserved ribosomal protein P0 of the ribosomal stalk, which is involved in interaction between translational elongation factors and the ribosome	ribosome/translation	0	0	0	33.7	4.5	95	3	3	10	36.2
C4QYK0	RPS0B	RPS0B	Protein component of the small (40S) ribosomal subunit; required for maturation of 18S rRNA along with Rps0Ap; deletion of either RPS0 gene reduces growth rate, deletion of both genes is lethal	ribosome/translation	0	0	0	29.2	4.4	181	3	3	5	25.5
C4R9C0	RPS10A	RPS10A	Protein component of the small (40S) ribosomal subunit	ribosome/translation	0	0	0	13.2	9.5	212	1	3	6	56.8
C4R146	RPS11B	RPS11B	Protein component of the small (40S) ribosomal subunit	ribosome/translation	0	0	0	17.6	11.1	281	1	2	6	56.8
C4R4Z8	RPS12	RPS12	Protein component of the small (40S) ribosomal subunit	ribosome/translation	0	0	0	15.6	4.4	466	1	3	5	41.7
C4R7Y4	RPS13	RPS13	Protein component of the small (40S) ribosomal subunit	ribosome/translation	0	0	0	17.1	10.9	163	3	3	8	57.6
C4R0T7	RPS14A	RPS14A	Ribosomal protein 59 of the small subunit, required for ribosome assembly and 20S pre-rRNA processing	ribosome/translation	0	0	0	15.2	11.6	106	3	3	7	61.8
C4QYM1	RPS15	RPS15	Protein component of the small (40S) ribosomal subunit	ribosome/translation	0	0	0	16.4	10.8	286	2	1	3	27.6
C4R7T8	RPS16B	RPS16B	Protein component of the small (40S) ribosomal subunit	ribosome/translation	0	0	0	16.4	10.8	224	3	2	5	48.3
C4R1R2	RPS17B	RPS17B	Ribosomal protein 51 (rp51) of the small (40s) subunit	ribosome/translation	0	0	0	15.7	10.7	97	3	3	6	61.0
C4R1R7	RPS18A	RPS18A	Protein component of the small (40S) ribosomal subunit	ribosome/translation	0	0	0	17.7	10.9	114	3	3	10	61.4
C4QY72	RPS19B	RPS19B	Protein component of the small (40S) ribosomal subunit, required for assembly and maturation of pre-40 S particles	ribosome/translation	0	0	0	16.7	9.8	271	2	2	5	45.3
C4R853	RPS1B	RPS1B	Ribosomal protein 10 (rp10) of the small (40S) subunit	ribosome/translation	0	0	0	28.9	10.4	56	3	3	11	53.9

C4QYX3	RPS2	RPS2	Protein component of the small (40S) subunit, essential for control of translational accuracy; phosphorylation by C-terminal domain kinase I (CTDK-I) enhances translational accuracy; methylated on one or more arginine residues by Hmt1p	ribosome/translation	0	0	0	28.2	10.4	121	3	3	9	47.1
C4R2D3	RPS20	RPS20	Protein component of the small (40S) ribosomal subunit; overproduction suppresses mutations affecting RNA polymerase III-dependent transcription	ribosome/translation	0	0	0	13.5	10.5	319	2	3	5	41.5
C4R0T8	RPS22A-2	RPS22A	Protein component of the small (40S) ribosomal subunit	ribosome/translation	0	0	0	14.6	10.4	290	3	3	3	43.8
C4R7L7	RPS23A	RPS23A	Ribosomal protein 28 (rp28) of the small (40S) ribosomal subunit, required for translational accuracy	ribosome/translation	0	0	0	15.9	11.6	0	2	2	3	46.2
C4R7F4	RPS24A	RPS24A	Protein component of the small (40S) ribosomal subunit	ribosome/translation	0	0	0	15.4	10.9	329	3	2	7	48.1
C4R256	RPS25A	RPS25A	Protein component of the small (40S) ribosomal subunit	ribosome/translation	0	0	0	12.0	10.6	348	2	1	4	45.4
C4R1A3	RPS27B	RPS27B	Protein component of the small (40S) ribosomal subunit	ribosome/translation	0	0	0	8.9	10.2	634	1	2	2	29.3
C4QWN4	RPS27B-2	RPS27B	Protein component of the small (40S) ribosomal subunit	ribosome/translation	0	0	0	9.0	10.5	524	2	2	1	19.5
C4QXU7	RPS28B	RPS28B	Protein component of the small (40S) ribosomal subunit	ribosome/translation	0	0	0	7.6	11.3	0	1	2	3	41.8
C4QVA2	RPS3	RPS3	Protein component of the small (40S) ribosomal subunit, has apurinic/apyrimidinic (AP) endonuclease activity; essential for viability	ribosome/translation	0	0	0	26.9	9.8	61	2	3	12	47.7
C4R7A1	RPS4B	RPS4B	Protein component of the small (40S) ribosomal subunit	ribosome/translation	0	0	0	31.7	9.6	82	3	3	9	37.2
C4R5H6	RPS5	RPS5	Protein component of the small (40S) ribosomal subunit, the least basic of the non-acidic ribosomal proteins; phosphorylated in vivo; essential for viabilityns	ribosome/translation	0	0	0	24.6	9.9	62	3	3	5	44.3
C4R6U6	RPS6B-2	RPS6B	Protein component of the small (40S) ribosomal subunit	ribosome/translation	0	0	0	27.0	10.7	179	2		7	28.0
C4R762	RPS7B	RPS7B	Protein component of the small (40S) ribosomal subunit; interacts with Kti11p; deletion causes hypersensitivity to	ribosome/translation	0	0	0	21.3	9.7	161	3	3	9	56.9

			zymocin											
C4QX43	RPS8A	RPS8A	Protein component of the small (40S) ribosomal subunit	ribosome/translation	0	0	0	22.5	10.9	122	2	2	6	41.0
C4QYE8	RPS9B	RPS9B	Protein component of the small (40S) ribosomal subunit	ribosome/translation	0	0	0	22.2	10.3	189	2	3	7	40.9
C4QZB0	TEF2	TEF2	Translational elongation factor EF-1 alpha; also encoded by TEF1; functions in the binding reaction of aminoacyl-tRNA (AA-tRNA) to ribosomes; may also have a role in tRNA re-export from the nucleus	ribosome/translation	0	0	0	50.1	9.8	15	3	3	21	61.2
C4R6V3	TEF4-1	TEF4	Gamma subunit of translational elongation factor eEF1B, stimulates the binding of aminoacyl-tRNA (AA-tRNA) to ribosomes by releasing eEF1A (Tef1p/Tef2p) from the ribosomal complex	ribosome/translation	0	0	0	47.1	6.1	37	3	2	6	23.7
C4R506	TIF2	TIF2	Translation initiation factor eIF4A, identical to Tif1p; DEA(D/H)-box RNA helicase that couples ATPase activity to RNA binding and unwinding; forms a dumbbell structure of two compact domains connected by a linker; interacts with eIF4G	ribosome/translation	0	0	0	45.0	4.8	27	2	3	6	25.6
C4R0Y3	TMA19	TMA19	Protein that associates with ribosomes	ribosome/translation	0	0	0	18.5	4.2	236	3	1	2	19.2
C4R6N9	YEF3	YEF3	Gamma subunit of translational elongation factor eEF1B, stimulates the binding of aminoacyl-tRNA (AA-tRNA) to ribosomes by releasing eEF1A (Tef1p/Tef2p) from the ribosomal complex; contains two ABC cassettes; binds and hydrolyzes ATP	ribosome/translation	0	0	0	116.6	5.5	5	3	3	16	22.8
C4QXE7	PAS_chr1-4_0091	SNL1	BAG domain;BAG domain	unknown	0	1	0	25.1	9.8	0	2	2	4	23.0
C4R004	PAS_chr2-1_0218	NA	hypothetical protein	unknown	0	0	0	14.7	4.8	0	2	3	4	33.6
C4R042	PAS_chr2-1_0254	NA	PH domain;PH domain-like	unknown	0	0	0	50.2	5.8	0	2	1	7	20.2
C4R2X3	PAS_chr2-2_0082	NA	Polyketide cyclase / dehydrase and lipid tra;Bet v1-like	unknown	0	0	0	16.1	7.6	0	2	2	2	31.7
C4R1Z0	PAS_chr2-2_0394	NA	Stomatin-like protein / Band 7 family;Band 7/SPFH domain	unknown	0	0	0	35.9	5.7	162	3	2	4	16.2

C4R412	PAS_chr3_0261	GTT3	Rho termination factor, N-terminal domain;Rho N-terminal domain-like	unknown	0	0	TMH, 3	39.0	4.5	203	2	2	3	14.1
C4R5A5	PAS_chr3_0692	NA	NAD dependent epimerase/dehydratase family;NAD(P)-binding Rossmann-fold domains	unknown	0	0	0	35.8	5.9	0	3	2	6	22.0
C4R699	PAS_chr3_1023	PAR32	Protein of unknown function (DUF3602)	unknown	0	0	0	16.1	9.1	0	2	2	3	29.1
C4R7I8	PAS_chr4_0320	NA	Protein of unknown function (DUF3812)	unknown	0	0	0	92.7	4.7	194	1	2	7	10.1
C4QV09	PHM7	PHM7	Protein of unknown function, expression is regulated by phosphate levels	unknown	0	1	TMH, 10	100.6	8.3	157	3	3	13	18.0
C4R8M0	CPS1	CPS1	Vacuolar carboxypeptidase yscS; expression is induced under low-nitrogen conditions	vacuole	0	1	TMH, 1	65.8	5.0	174	3	3	14	43.5
C4R6G8	PEP4	PEP4	Vacuolar aspartyl protease (proteinase A), required for the posttranslational precursor maturation of vacuolar proteinases; important for protein turnover after oxidative damage	vacuole	1	0	0	44.3	4.5	0	2	2	3	15.9
C4QXF8	VAC8	VAC8	Phosphorylated and palmitoylated vacuolar membrane protein that interacts with Atg13p, required for the cytoplasm-to-vacuole targeting (Cvt) pathway; interacts with Nvj1p to form nucleus-vacuole junctions	vacuole	0	0	0	60.7	4.7	0	2	2	8	22.1
C4R2G6	VMA6	VMA6	Subunit d of the five-subunit V0 integral membrane domain of vacuolar H+-ATPase (V-ATPase), an electrogenic proton pump found in the endomembrane system; stabilizes VO subunits; required for V1 domain assembly on the vacuolar membrane	vacuole	0	0	0	39.6	4.4	0	1	2	5	20.4
C4R6H4	VPH1	VPH1	Subunit a of vacuolar-ATPase V0 domain, one of two isoforms (Vph1p and Stv1p); Vph1p is located in V-ATPase complexes of the vacuole while Stv1p is located in V-ATPase complexes of the Golgi and endosomes	vacuole	0	0	TMH, 7	92.0	4.9	0	2	1	4	6.2
C4R5N2	VPS70-1	VPS70	Protein of unknown function involved in vacuolar protein sorting	vacuole	0	1	TMH, 1	94.6	6.5	256	2	2	4	13.6
C4QZ04	YCF1	YCF1	Vacuolar glutathione S-conjugate transporter of the ATP-binding cassette family, has a role in detoxifying metals such as cadmium, mercury, and arsenite	vacuole	0	0	TMH, 14	169.2	9.3	0	2	2	6	5.3
					39	**57**	**118**							

Chapter VI

Identification of the *CRD1* gene encoding cardiolipin synthase from *Pichia pastoris*

Lisa Klug and Günther Daum*

Institute of Biochemistry, Graz University of Technology, Graz, Austria

Keywords:

Cardiolipin, synthase, *Pichia pastoris*, mitochondria, phospholipids

*Corresponding author: Günther Daum, Institute of Biochemistry, Graz University of Technology, Petersgasse 12/II, A-8010 Graz, Austria, Tel.: +43 316 873 6462; Fax: +43 316 873 6952; E-mail address: guenther.daum@tugraz.at

Abbreviations:

ATP, adenosine triphosphate; CL, cardiolipin; DNA, deoxyribonucleic acid; EDTA, ethylenediamine tetraacetic acid; PMSF, phenylmethylsulfonylfluoride; RNA, ribonucleic acid; rpm, rounds per minute; RT-PCR, real time PCR; SDS, sodium dodecyl sulfate; TLC, thin layer chromatography

Abstract

The anionic phospholipid cardiolipin (CL) has a unique dimeric structure and plays an important role in bioenergetics, respiration and mitochondrial function. Here we describe identification of CL synthase from the methylotrophic yeast *Pichia pastoris*. The gene locus was identified by homology blast search, and the function of the *Pichia pastoris CRD1* gene product as CL synthase was proven by complementation of defects in a *S. cerevisiae crd1*Δ deletion strain. Expression of the *Pichia* gene in *S. cerevisiae* led to compensation of the temperature sensitive phenotype and restored CL formation in *S. cerevisiae crd1*Δ. Overexpression of *CRD1* in *Pichia pastoris* caused changes in the phospholipid pattern and improved growth under aerobic conditions. Thus, CL seems to play also an important role in *Pichia pastoris.*

1 Introduction

Biological membranes are composed of phospholipids, sterols and sphingolipids. Besides the structural function of lipids, they also serve as a matrix for various cellular processes [1]. One phospholipid with special properties is cardiolipin (CL). Its structure is unique among all phospholipids and its localization is mainly restricted to one organelle, the mitochondria. The name cardiolipin has been chosen due to its first isolation from beef heart in the early 1940s [2]. Structural differences to other phospholipids are given by the fact that CL is a lipid dimer consisting of two glycerophosphate backbones with four fatty acyl chains [3]. CL is synthesized by condensation of the phospholipid phosphatidylglycerol with cytidine-diphosphate diacylglycerol which is derived from phosphatidic acid. This reaction is catalyzed by cardiolipin synthase [4]. After its biosynthesis, CL undergoes acyl chain remodeling, where it is de-acetylated and re-acetylated to yield a functional CL molecule [5–7]. In contrast to other phospholipids, which are synthesized mainly in the endoplasmic reticulum and then transported to their final destination, CL synthesis takes place in mitochondria where the largest portion of the functional molecule remains [8]. CL is primarily localized to the inner mitochondrial membrane [9] where it acts as a supporter of several cellular processes and is important for the maintenance of mitochondria integrity [10,11]. It is required for a mitochondrial respiration [12] and thus for cellular ATP production [13] by stabilizing and activating proteins and complexes of the respiratory chain. Furthermore, an involvement of CL in programmed cell death, the so called apoptosis, has been demonstrated [14–16]. CL electrostatically anchors the pro-apoptotic factor cytochrome c to the inner mitochondrial membrane and regulates its release which induces apoptosis. The contribution of CL in mitochondrial functions suggests that its loss, depletion or alteration in the acyl chain composition will lead to mitochondria dysfunction and trigger pathological processes associated to compromised mitochondrial function. Indeed, alterations in CL biology were demonstrated in Ischemia and Reperfusion, heart failure or the Barth syndrome [17,18].

In higher eukaryotes, CL is essential for life, while the yeast *Saccharomyces cerevisiae* is still viable in the absence of CL [19]. Thus, *S. cerevisiae* has become a useful model organism to study CL biosynthesis and acyl chain remodeling. In contrast, lipid biochemistry in general and cardiolipin synthesis in especial has not been studied intensively with the methylotrophic yeast *Pichia pastoris,* although this microorganism has become a popular expression system

for heterologous protein production in industry and applied research [20]. In our laboratory an initiative has been launched several years ago to study organelles from *Pichia pastoris* in some detail [21–24]. As part of these studies, we wished to get a deeper insight into the phospholipid metabolism of *Pichia pastoris.* During these investigations, we also studied CL as a major phospholipid of mitochondrial membranes and focused on its synthesis and the enzyme involved. For this purpose, we first identified the *CRD1* gene encoding the CL synthase in *Pichia pastoris* CBS7435 wild type strain. Here we show that the gene product expressed in a *S. cerevisiae crd1*Δ strain was able to complement for the temperature sensitive growth phenotype and to restore CL synthesis. Furthermore, we demonstrate that expression of the *CRD1* gene in *Pichia pastoris* under an inducible promoter influenced growth of the microorganism. Deletion of the *CRD1* gene failed so far. The reason for this failure may be the fact that *Pichia pastoris* is a strictly aerobic organism, and CL as a cofactor for mitochondrial function and respiration may be essential for cell viability.

2 Experimental procedures

2.1 Strains and culture conditions

Strains used in these studies are described in Table 1. *E. coli* strains were grown at 37°C, *S. cerevisiae* strains at 30°C or 37°C, and *P. pastoris* strains at 30°C. Liquid cultures were incubated with shaking at 130 rpm. For *P. pastoris* baffled Erlenmeyer flasks were used. The Oxoid anaerobic system was used for anaerobic growth tests.

Full media (YP) containing 1 % yeast extract, 2 % peptone and the respective carbon source or synthetic minimal media (MM) containing 0.67% yeast nitrogen base with ammonium sulfate but without amino acids, the respective carbon source and amino acid supplements were used for yeast cultivation. For details see Table 2. LB(A) media containing 1% tryptone, 0.5% yeast extract, 0.5% sodium chloride with or without ampicillin (100 µg/ml) were used for bacteria cultivation. For preparation of agar plates, 2% agar was added to the respective media. For anaerobic growth, agar plates were supplemented with 20 µg/ml ergosterol and 0.06% Tween 80 as a source of oleic acid.

2.2 Growth phenotype analysis

For complementation studies, the *S. cerevisiae* strains BY4741, BY4741 *crd1*Δ, BY4741 *crd1*Δ [pYes2] and BY4741 *crd1*Δ [pYes2_Pp_*CRD1*] were grown over night in the respective medium (MMD, MMD –ura) at 30°C. For growth phenotype analysis of *P. pastoris*, the wild type CBS7435 and the CBS7435 GalP-*CRD1* construct were grown over night in the respective medium (YPD, YPD^{G418}). One OD unit was harvested and cells were suspended in 1 ml sterile ddH_2O. Serial dilutions were prepared in sterile water, and 5 µl of each serial dilution were spotted onto agar plates containing different carbon sources. Plates were incubated either at 30°C or at 37°C for 2 – 4 days.

For growth in liquid media, *P. pastoris* wild type CBS7435 and the CBS7435 GalP-*CRD1* were precultured in full medium in baffled Erlenmeyer flasks shaking at 130 rpm at 30°C for 2 days. Main cultures on YPD, YPGal and YPLac were inoculated with the precultures to an OD_{600} of 0.1 and incubated with shaking at 130 rpm at 30°C. Over a time

period of 48 hours, samples were taken from the main cultures at defined time points, and the OD_{600} was optically determined.

2.3 Bioinformatical studies

DNA sequences were obtained from http://www.ncbi.nlm.nih.gov/pubmed/. Blast search was performed using a Lalign alignment software provided by http://www.expasy.org/. Clustal Omega multiple protein sequence alignment software provided by http://www.ebi.ac.uk/services/proteins was used for protein homology studies. A conserved domain search software provided by http://www.ncbi.nlm.nih.gov/Structure/cdd/cdd.shtml was used to identify protein domains.

2.4 Genetic techniques

All enzymes, buffers, kits and plasmids used for genetic manipulations are commercially available. Primers used in this study are shown in Table 3.

2.4.1 Cloning of the *P. pastoris CRD1* gene into *S. cerevisiae* BY4741 *crd1Δ*

Plasmid pYes2 was isolated from *E. coli* Top10 [pYes2] cells using a commercial available plasmid isolation kit. After disruption of *P. pastoris* CBS7435 cells with glass beads in 500µl lysis buffer (100 mM Tris/HCl pH 8.0, 50 mM EDTA pH 8.0, 1% SDS), genomic DNA was isolated by adding 275 µl 7M ammonium acetate and 500 µl chloroform. Genomic DNA was precipitated with isopropanol, washed with 70% ethanol and dissolved in sterile ddH_2O. The putative *P. pastoris CRD1* gene was amplified by a standard PCR from the genomic DNA using primers 1 and 2. Plasmid pYes2 and amplified gene were cut with XbaI and BamHI. The cut plasmid and the insert were ligated using T4 DNA ligase, and the vector construct was transformed into competent *E. coli* Top10 cells by chemical transformation [25]. Cells were plated onto LBA plates and incubated at 37°C. Clones were streaked out onto new LBA plates and checked by colony PCR using primers 3 and 4. As a control, plasmid pYes2_*CRD1* was isolated from several positive clones, cut with StuI or BamHI and XbaI and sequenced. After verification, pYes2_*CRD1* was isolated from one positive clone and

transformed into *S. cerevisiae* BY4741 *crd1*Δ cells by a standard lithium acetate transformation method [26]. As a control, cells were also transformed with the empty vector. Transformed cells were plated onto MMD –ura plates and incubated at 30°C. Clones were streaked out onto new MMD –ura plates and checked by colony PCR using primers 5 and 6. Plasmids were isolated from positive clones and sequenced.

2.4.2 Replacement of the native promoter of the *P. pastoris CRD1* gene by an inducible promoter

Plasmids pYes2 and pFA6a-KanMX6 isolated from *E. coli* Top10 [pYes2] and Top10 [pFA6a-KanMX6] cells using a commercially available plasmid isolation kit served as templates for the amplification of the galactose promoter (GalP) and the Geneticin (G418) resistance cassette by a standard PCR. Primers 7 and 8 were used for amplifying the G418 resistance cassette; and primers 9 and 10 for amplification of the GalP. The *P. pastoris CRD1* gene was amplified by standard PCR from genomic DNA isolated as described above using primers 11 and 12. Amplified single fragments were used as templates for an overlap PCR performed by a standard protocol. The overlap PCR revealed a fragment which contains a 5´ flanking region homologous to a sequence ~ 1000 bp upstream of the *CRD1* ORF, the G418 resistance cassette, the inducible Gal promoter and the whole *CRD1* gene. This fragment was transformed into *P. pastoris* CBS7435 by electroporation using a condensed protocol [27]. Cells were plated onto $YPGal^{G418}$ plates and incubated at 30°C. Obtained clones were checked by colony PCR using the primer combination 13/14 and 12/15; and genomic DNA was isolated from the positives and sequenced.

2.4.3 Real time PCR

For RT-PCR, the *P. pastoris* CBS7435 and the CBS7435 GalP-*CRD1* strains and the *S. cerevisiae* BY4741 strain were precultured in baffled Erlenmeyer flasks in YPD with shaking at 130 rpm for 2 days at 30°C. Cells were shifted to either fresh YPD medium or to YPGal medium for main cultures, and cells were grown at 30°C to the mid logarithmic growth phase. Cells were harvested and total RNA was isolated using an RNeasy kit from Quiagen as described by the manufacturer. After DNase I digestion, RT-PCR was performed using the

SuperScript III Platinum SYBR Green one-step quantitative RT-PCR kit (Invitrogen) by following the manufacturer's instructions. Primers 16 and 17 were used for amplification of the *Pichia CRD1* gene; and primers 18 and 19 for the *Pichia ARG4* gene as a reference gene. Primers 20 and 21 were used for amplification of the *Saccharomyces CRD1* gene; and primers 22 and 23 for the *Saccharomyces ARG4* gene as a reference gene. Reactions were performed in sealed MicroAmp Optical 96-Well Reaction Plates, and amplification was measured using an ABI 7500 instrument (Applied Biosystems). Samples were quantified using the comparative Ct method (ΔΔCt) described by Livak and Schmittgen [28]. With this method, the differences in *CRD1* mRNA expression after *ARG4* normalization relative to the control were calculated.

2.5 Isolation of mitochondria

The *P. pastoris* CBS7435 and the GalP-*CRD1* strain were precultured in baffled Erlenmeyer flasks in YPD with shaking at 130 rpm for 2 days at 30°C. Cells were shifted to either fresh YPD medium or to YPGal medium for main culture. The *S. cerevisiae* strains BY4741, BY4741 *crd1*Δ, BY4741 *crd1*Δ [pYes2] and BY4741 *crd1*Δ [pYes2_*CRD1*] were precultured in Erlenmeyer flasks in MMGal with shaking at 130 rpm for 2 days at 30°C and shifted to fresh MMGal medium for main cultures.

Mitochondria were isolated from cells grown to the late exponential growth phase at 30°C. Cell fractionation was performed by the following procedure. Cells were harvested and converted to spheroplasts by using Zymolyase 20T [22]. After 1 h of enzymatic treatment, spheroplasts were homogenized in Tris-mannitol buffer (0.6 M mannitol, 10 mM Tris/HCl, pH 7.4) containing PMSF (1 M, 2 µl/g cww) with 15 strokes in a Dounce Homogenizer. Homogenates were centrifuged at 5,500 rpm at 4°C for 5 min in a Sorvall RC 6 Plus centrifuge using an SS-34 rotor. This procedure was repeated twice with the obtained pellet after resuspension in Tris-mannitol buffer. Combined supernatants (crude homogenate) were centrifuged at 10,000 rpm at 4°C for 10 min. The resulting pellet was suspended in Tris-mannitol buffer and centrifuged at 5,500 rpm at 4°C for 5 min to remove residual cell debris. The obtained supernatant was centrifuged at 10,000 rpm at 4°C for 10 min. The pellet (mitochondria) was suspended in Tris/HCl, pH 7.4 and stored at -70°C.

2.6 Protein analysis

Homogenate and mitochondria were diluted 1:10 with water. Proteins were precipitated with trichloroacetic acid (final concentration 10%) on ice at least for 1 h. After washing, precipitated proteins were solubilized in 0.1 % SDS, 0.1 M NaOH at 37°C for 30 min. Protein quantification was performed as described by Lowry et al. [29]. For the quality control of the isolated mitochondria, SDS-polyacrylamide gel electrophoresis was carried out by the method of Laemmli [30] using 12.5 % SDS gels. Ten µg protein of each sample were loaded per lane. Gels were used for Western Blot analysis according to Haid and Suissa [31]. Primary polyclonal antibodies raised in rabbits were directed against *S. cerevisiae* proteins. For detection, peroxidase conjugated secondary antibodies and a chemiluminescent signal detection solution (SuperSignal® West Pico Chemiluminescent Substrate, Thermo Scientific, Rockford, IL, USA) were used to visualize immune-reactive proteins.

2.7 Phospholipid analysis

Lipids were extracted following the procedure of Folch et al. [32]. For phospholipid analysis, lipids were extracted from samples containing 1-2 mg protein. Extracted lipids were dried under a stream of nitrogen and stored at -20°C.

Individual phospholipids were separated by two-dimensional thin-layer chromatography on Silica gel 60 plates using chloroform/methanol/25 % NH_3 (65/35/5 per vol.) as the first; and chloroform/acetone/methanol/acetic acid/water (50/20/10/10/5, per vol.) as the second solvent system. Phospholipids were detected by staining spots on plates with iodine vapor. Stained spots were scraped off, and phospholipids were quantified by the procedure of Broekhuyse [33]. For total phospholipid analysis, aliquots of dried lipid extracts were directly subjected to phosphate determination using phosphate as standard.

3 Results

3.1 Bioinformatical identification of the *CRD1* gene in *P. pastoris* CBS7435

Since the gene encoding the cardiolipin synthase in the *P. pasto*ris wild type strain CBS7435 has not yet been annotated, we first performed a bioinformatical screening. In a blast search, the *CRD1* gene from *S. cerevisiae*, the *CRD1* gene from the *P. pastoris* strain GS115 and the whole genome of the *P. pastoris* strain CBS7435 were compared (Lalign alignment; http://www.expasy.org/). This blast search identified the gene locus 0636 on chromosome 3 of the CBS7435 strain as potential *CRD1* gene, which shared 56% sequence homology to the *CRD1* gene from *S. cerevisiae*, and 87% sequence homology to the GS115 CL synthase encoding gene. The identified open reading frame was annotated to encode for a putative membrane protein. Clustal Omega multiple protein sequence alignment software (http://www.ebi.ac.uk/services/proteins) was used to evaluate the homologies of the translated products. Both *Pichia* proteins shared about 38% sequence homology to the *S. cerevisiae* Crd1p and about 90% to each other as shown in Figure 1A. The CBS7435 protein encoded by Chr. 3_0636 consists of 340 amino acids and differs in the first 32 amino acids from the CL synthase from the GS115 strain which consists of 308 amino acids. The remaining amino acids showed a hundred percent homology. A conserved domain search from the CBS7435 putative Crd1p using a conserved domain search software (http://www.ncbi.nlm.nih.gov/Structure/cdd/cdd.shtml) revealed several domains involved in lipid metabolism belonging to the CDP-alcohol phosphatidyltransferase superfamily (Figure 1B). These domains harbor the ability to catalyze the displacement of CMP from a CDP-alcohol by a second alcohol forming a phosphodiester bond. The most important finding was the presence of a cardiolipin synthase domain. Taken together, our bioinformatical investigations confirmed that the gene locus 0636 on chromosome 3 codes for the CL synthase in *P. pastoris* wild type strain CBS7435.

3.2 Expression of the putative *CRD1* gene from *P. pastoris* CBS7435 in a *S. cerevisiae crd1Δ* deletion strain

Although putative *CRD1* genes from *P. pastoris* CBS7435 and GS115 were identified by computational studies, the function of the respective gene products has not yet been proven by biochemical methods. To address this question, the *CRD1* gene from *P. pastoris* CBS7435 was cloned into a *S. cerevisiae crd1Δ* strain. The growth phenotype (Figure 2) and the phospholipid composition (Figure 3) were analyzed from the *S. cerevisiae* wild type strain BY4741, the BY4741 *crd1Δ* deletion strain and the deletion strain harboring a vector containing the putative *CRD1* gene from *P. pastoris* CBS7435 expressed under the control of a galactose promoter. For phenotype analysis, drop tests were performed on different carbon sources, and plates were incubated at 30°C or 37°C. As can be seen from Figure 2, the BY4741 *crd1Δ* strain showed a growth defect at the elevated temperature. This defect was also observed in a control strain which harbored the empty vector. When the *CRD1* gene from *P. pastoris* was expressed in the *crd1Δ* background, the growth defect at 37°C was compensated independent of the carbon source. The compensating effect was also observed at 30°C when lactate was used as carbon source. At this temperature the deletion strain showed reduced viability which was rescued by expression of the *P. pastoris CRD1* gene.

To further verify the identity of the CL synthase from *P. pastoris* CBS7435, mitochondria were isolated from the *S. cerevisiae* wild type, the *crd1Δ* deletion strain and the deletion strain expressing the *CRD1* gene from *P. pastoris*. Strains were grown on MM containing galactose as carbon source. Galactose induces the Gal promoter and thus the expression of the *P. pastoris CRD1* gene in the deletion strain. Phospholipids were extracted from the mitochondria and analyzed by two-dimensional TLC. This analysis showed that CL was synthesized in wild type, whereas in the *S. cerevisiae crd1Δ* deletion strain no CL was formed (Figure 3A). Expression of the *P. pastoris CRD1* gene in the deletion strain rescued CL synthesis as shown by the presence of the CL spot on the TLC plate. The relative amounts of individual phospholipids from mitochondria were examined by phosphate determination. Levels of PC, PI and some minor phospholipids were similar in all three strains. In contrast, PE was markedly increased in the deletion strain over the wild type, whereas CL was completely absent (Figure 3B). In the strain expressing the *P. pastoris CRD1* gene PE was still slightly increased over the wild type, and CL was formed to approximately 70% of the wild type control.

Conclusively, complementation of the growth defect of a *S. cerevisiae crd1Δ* strain by expression of the *P. pastoris* CBS7435 *CRD1* gene and phospholipid analysis identified the gene coding for CL synthase in *P. pastoris*.

3.3 Anaerobic growth of the *P. pastoris* CBS7435 wild type strain

Due to the fact that CL is involved in mitochondria integrity, cell respiration and energy production, we investigated the ability of the *P. pastoris* CBS7435 wild type strain to grow under anaerobic conditions. As a control, the *S. cerevisiae* BY4741 and the BY4741 *crd1Δ* strain were also tested. The three strains were streaked out on agar plates containing different carbon sources. Media were supplemented with ergosterol and Tween 80. The plates were incubated in an anaerobic jar at 30°C at least for four days. Figure 4 demonstrates that *P. pastoris* CBS7435 was not viable under anaerobic conditions. In contrast, both *Saccharomyces* strains were able to grow in the absence of oxygen. These results indicate that *P. pastoris* CBS7435 wild type strain is a strict aerobic organism. This fact may be the reason why deletion of the *P. pastoris CRD1* gene failed so far. It may be possible that CL is essential for maintaining mitochondrial respiration in *P. pastoris*, and lack of CL synthesis may thus lead to loss of viability.

3.4 Replacement of the native *CRD1* promoter by an inducible galactose promoter

By overlap PCR, a DNA fragment consisting of homologous sequences to the up- and downstream flanking region of the *P. pastoris* chromosomal *CRD1* open reading frame, a geneticin resistance gene and the complete *CRD1* gene under the control of a galactose promoter (GalP) was constructed. This fragment was transformed into the *P. pastoris* CBS7435 wild type strain. Through homologous recombination, the chromosomal native promoter of the *CRD1* gene was replaced by the inducible galactose promoter. The strategy for the promoter replacement is shown in Figure 5. Positive clones were selected by geneticin resistance and confirmed by colony PCR and sequencing. Finally, a strain named *P. pastoris* CBS7435-GalP-*CRD1* was obtained where the *CRD1* gene expression is under control of the galactose promoter.

The galactose promoter described above is induced by galactose or lactate and repressed by glucose. However, this promoter cannot be completely switched off under repressive conditions. Even when the galactose promoter was repressed a basal expression level of the *CRD1* gene remained. To test the growth phenotype of the constructed strain, we performed drop tests on inducing and repressing carbon sources and determined growth in liquid cultures (Figure 6). The GalP-*CRD1* construct was compared to the wild type. Repression of the galactose promoter did not change the growth behavior of the GalP-*CRD1* strain, neither on plates nor in liquid cultures (Figures 6A and D). A positive effect on growth was observed when the galactose promoter was induced on galactose as well as lactate containing media (Figures 6B-D). The most significant difference was discovered when plates with a low concentration of galactose were used for the drop tests. This result led us to hypothesize that overexpression of *CRD1* in *P. pastoris* may improve cell mass production.

3.5 *CRD1* gene expression of the *P. pastoris* CBS7435-GalP-*CRD1* strain

To confirm that the increased growth under inducing conditions was the result of enhanced *CRD1* gene expression we performed RT-PCR analysis with wild type and the strain bearing the GalP-*CRD1* construct. Precultures were grown on glucose and main cultures were grown on glucose medium or galactose medium. At the mid logarithmic growth phase RNA was isolated and RT-PCR was performed. Results are shown in Figure 7. Shifting the GalP-*CRD1* strain from glucose to a fresh glucose medium which represses the galactose inducible promoter, did not change the *CRD1* gene expression at all. This result was in line with the above described growth phenotype. When the galactose promoter was induced by shifting the cells from glucose to a galactose medium, a marked increase of the *CRD1* gene expression over the wild type level was detected. Thus, the growth phenotype correlated with the gene expression of *CRD1*. We also compared the *CRD1* gene expression levels of *P. pastoris* to the *S. cerevisiae* BY4741 strain which was set at 1. Independent of the carbon source the level of *CRD1* gene expression was higher in *P. pastoris* than in *S. cerevisiae*. When cells were shifted from glucose to galactose, the difference between the two wild type strains was only moderate, but induction of the galactose promoter led again to a strong increase of mRNA synthesis.

3.6 Phospholipid analysis of the *P. pastoris* CBS7435-GalP-*CRD1* strain

Since CL is a mitochondrial phospholipid, we isolated mitochondria from the WT and the GalP-*CRD1* construct and determined the distribution of individual phospholipids and the amount of total phospholipids. Precultures of the strains were grown on glucose and shifted for the main cultures to fresh glucose or galactose media, respectively, and mitochondria were isolated at the late logarithmic growth phase. Lipids were extracted from mitochondria and subjected to phospholipid analysis. Interestingly, the relative distribution of individual phospholipids from wild type and the GalP-*CRD1* strain was similar independent of the carbon source (Figure 8A). In contrast, the amount of total phospholipids was changed (Figure 8B). Repressing the galactose promoter led to a reduction of the total phospholipid amount in comparison to wild type. Under inducible conditions, the amount of total phospholipids in mitochondria from the GalP-*CRD1* strain was increased over wild type as well as over the GalP-*CRD1* strain which was grown on glucose. Also the amount of CL was increased in the GalP-*CRD1* strain after promoter induction in comparison to the wild type and the GalP-*CRD1* strain grown on glucose (Figure 8C). Taken together, the results of the phospholipid analysis suggested that an improved *CRD1* gene expression led to an overall increase of phospholipid synthesis in *P. pastoris*, while the distribution of the individual phospholipids is not influenced.

4 Discussion

Due to the fact that *Pichia pastoris* has become a very important biotechnological tool used in the industry for the production of heterologous proteins, it is obvious to study cell biological and biochemical properties of this organism more in detail. Several investigations concerning *Pichia* organelles and their lipidome and proteome have already been performed in our laboratory [21–24]. These studies also led us to investigate phospholipid metabolism of *P. pastoris* in more detail as phospholipids are the basis of all organelle membranes.

In the present work, we focused on the synthesis of CL, a unique phospholipid which is primarily found in mitochondria. In *S. cerevisiae*, the enzyme catalyzing CL synthesis is encoded by the *CRD1* gene. To identify the respective gene in *P. pastoris* and to characterize the gene product we have chosen a stepwise approach. First, we performed bioinformatical studies to identify the *CRD1* gene in *P. pastoris* CBS7435. Secondly, we expressed the *CRD1* gene from *Pichia pastoris* in a *S. cerevisiae crd1*Δ deletion strain and showed (i) complementation of the growth defect in *S. cerevisiae crd1*Δ by the *P. pastoris* gene; as well as (ii) reconstitution of the ability to synthesize CL. Thus we clearly identified the *CRD1* gene encoding for the CL synthase in *P. pastoris* by function. Finally, we investigated effects of *CRD1* overexpression in *P. pastoris.*

To address the question as to the physiological role of CL in *P. pastoris* and especially in mitochondria we tried to delete the *CRD1* gene, but without success. As *P. pastoris* is a strictly aerobic microorganism (see Figure 4) one might speculate that CL which is important for respiration is essential for growth. The influence of the CL level on the growth behavior of *P. pastoris* was also demonstrated with a strain overexpressing *CRD1* under an inducible promoter. At present it is difficult to interpret why the amount of total mitochondrial phospholipids was increased in the overexpressing strain, while the distribution of the individual phospholipids was not altered. Thus, the link between CL metabolism and the rest of the lipid biosynthetic network in *P. pastoris* remains to be investigated.

References

1 Van Meer G, Voelker DR & Feigenson GW (2008) Membrane lipids: where they are and how they behave. *Nat. Rev. Mol. Cell Biol.* **9**, 112–124.

2 Pangborn MC (1942) Isolation and purification of a serologically active phospholipid from beef heart. *J. Biol. Chem.* **143**, 247–256.

3 Lewis RNAH & McElhaney RN (2009) The physicochemical properties of cardiolipin bilayers and cardiolipin-containing lipid membranes. *Biochim. Biophys. Acta* **1788**, 2069–2079.

4 Schlame M, Rua D & Greenberg ML (2000) The biosynthesis and functional role of cardiolipin. *Progr. Lipid Res.* **39**, 257–288.

5 Gu Z, Valianpour F, Chen S, Vaz FM, Hakkaart GA, Wanders RJA & Greenberg ML (2004) Aberrant cardiolipin metabolism in the yeast *taz1* mutant: a model for Barth syndrome. *Mol. Microbiol.* **51**, 149–158.

6 Beranek A, Rechberger G, Knauer H, Wolinski H, Kohlwein SD & Leber R (2009) Identification of a cardiolipin-specific phospholipase encoded by the gene *CLD1* (*YGR110W*) in yeast. *J. Biol. Chem.* **284**, 11572–11578.

7 Schlame M (2013) Cardiolipin remodeling and the function of tafazzin. *Biochim. Biophys. Acta* **1831**, 582–588.

8 Joshi AS, Zhou J, Gohil VM, Chen S & Greenberg ML (2009) Cellular functions of cardiolipin in yeast. *Biochim. Biophys. Acta* **1793**, 212–218.

9 Daum G (1985) Lipids of mitochondria. *Biochim. Biophys. Acta* **822**, 1–42.

10 Jiang F, Ryan MT, Schlame M, Zhao M, Gu Z, Klingenberg M, Pfanner N & Greenberg ML (2000) Absence of cardiolipin in the *crd1* null mutant results in decreased mitochondrial membrane potential and reduced mitochondrialfunction. *J. Biol. Chem.* **275**, 22387–22394.

11 Chen S, Tarsio M, Kane PM & Greenberg ML (2008) Cardiolipin mediates cross-talk between mitochondria and the vacuole. *Mol. Biol. Cell* **19**, 5047–5058.

12 Zhang M, Mileykovskaya E & Dowhan W (2002) Gluing the respiratory chain together. Cardiolipin is required for supercomplex formation in the inner mitochondrial membrane. *J. Biol. Chem.* **277**, 43553–43556.

13 Acehan D, Malhotra A, Xu Y, Ren M, Stokes DL & Schlame M (2011) Cardiolipin affects the supramolecular organization of ATP synthase in mitochondria. *Biophys. J.* **100**, 2184–2192.

14 Rytömaa M, Mustonen P & Kinnunen PK (1992) Reversible, nonionic, and pH-dependent association of cytochrome c with cardiolipin-phosphatidylcholine liposomes. *J. Biol. Chem.* **267**, 22243–22248.

15 Ott M, Zhivotovsky B & Orrenius S (2007) Role of cardiolipin in cytochrome c release from mitochondria. *Cell Death Differ.* **14**, 1243–1247.

16 Sinibaldi F, Fiorucci L, Patriarca A, Lauceri R, Ferri T, Coletta M & Santucci R (2008) Insights into cytochrome c−cardiolipin interaction. Role played by ionic strength. *Biochem.* **47**, 6928–6935.

17 Chicco AJ & Sparagna GC (2007) Role of cardiolipin alterations in mitochondrial dysfunction and disease. *Am. J. Physiol.* **292**, C33–C44.

18 Claypool SM & Koehler CM (2012) The complexity of cardiolipin in health and disease. *Trends Biochem. Sci.* **37**, 32–41.

19 Jiang F, Rizavi HS & Greenberg ML (1997) Cardiolipin is not essential for the growth of *Saccharomyces cerevisiae* on fermentable or non-fermentable carbon sources. *Mol. Microbiol.* **26**, 481–491.

20 Gasser B, Prielhofer R, Marx H, Maurer M, Nocon J, Steiger M, Puxbaum V, Sauer M & Mattanovich D (2013) *Pichia pastoris*: protein production host and model organism for biomedical research. *Future Microbiol.* **8**, 191–208.

21 Wriessnegger T, Gübitz G, Leitner E, Ingolic E, Cregg J, De la Cruz BJ & Daum G (2007) Lipid composition of peroxisomes from the yeast *Pichia pastoris* grown on different carbon sources. *Biochim. Biophys. Acta* **1771**, 455–461.

22 Wriessnegger T, Leitner E, Belegratis MR, Ingolic E & Daum G (2009) Lipid analysis of mitochondrial membranes from the yeast *Pichia pastoris*. *Biochim. Biophys. Acta* **1791**, 166–172.

23 Ivashov VA, Grillitsch K, Koefeler H, Leitner E, Baeumlisberger D, Karas M & Daum G (2013) Lipidome and proteome of lipid droplets from the methylotrophic yeast *Pichia pastoris*. *Biochim. Biophys. Acta* **1831**, 282-290.

24 Klug L, Tarazona P, Gruber C, Grillitsch K, Gasser B, Trötzmüller M, Köfeler H, Leitner E, Feussner I, Mattanovich D, Altmann F & Daum G (2014) The lipidome and proteome of microsomes from the methylotrophic yeast *Pichia pastoris*. *Biochim. Biophys. Acta* **1841**, 215–226.

25 Froger A & Hall JE (2007) Transformation of plasmid DNA into *E. coli* using the heat shock method. *J. Vis. Exp*. **6**, http://www.jove.com/index/Details.stp?ID=253, doi: 10.3791/253

26 Gietz RD, Schiestl RH, Willems AR & Woods RA (1995) Studies on the transformation of intact yeast cells by the LiAc/SS-DNA/PEG procedure. *Yeast* **11**, 355–360.

27 Lin-Cereghino J, Wong WW, Xiong S, Giang W, Luong LT, Vu J, Johnson SD & Lin-Cereghino GP (2005) Condensed protocol for competent cell preparation and transformation of the methylotrophic yeast *Pichia pastoris*. *Biotechniques* **38**, 44–48.

28 Livak KJ & Schmittgen TD (2001) Analysis of relative gene expression data using real-time quantitative PCR and the 2−ΔΔCT method. *Methods* **25**, 402–408.

29 Lowry OH, Rosebrough NJ, Farr AL & Randall RJ (1951) Protein measurement with the Folin phenol reagent. *J. Biol. Chem.* **193**, 265–275.

30 Laemmli UK (1970) Cleavage of structural proteins during the assembly of the head of bacteriophage T4. *Nature* **227**, 680–685.

31 Haid A & Suissa M (1983) Immunochemical identification of membrane proteins after sodium dodecyl sulfate-polyacrylamide gel electrophoresis. *Meth. Enzymol.* **96**, 192–205.

32 Folch J, Lees M & Sloane Stanley GH (1957) A simple method for the isolation and purification of total lipids from animal tissues. *J. Biol. Chem.* **226**, 497–509.

33 Broekhuyse RM (1968) Phospholipids in tissues of the eye. Isolation, characterization and quantitative analysis by two-dimensional thin-layer chromatography of diacyl and vinyl-ether phospholipids. *Biochim. Biophys. Acta* **152**, 307–315.

Table 1: Strains used in this study.

Strain	**Genotype**	**Origin**
S. cerevisiae BY4741	MATa; *his3*Δ 1; *leu2*Δ 0; *met15*Δ 0; *ura3*Δ 0	Euroscarf
S. cerevisiae BY4741 *crd1*Δ	MATa; *his3*Δ 1; *leu2*Δ 0; *met15*Δ 0; *ura3*Δ 0; *YDL142c*::kanMX4	Euroscarf
S. cerevisiae BY4741 *crd1*Δ [pYes2]	MATa; *his3*Δ 1; *leu2*Δ 0; *met15*Δ 0; *ura3*Δ 0; *YDL142c*::kanMX4; [pYes2]	This study
S. cerevisiae BY4741 *crd1*Δ [pYes2_Pp_*CRD1*]	MATa; *his3*Δ 1; *leu2*Δ 0; *met15*Δ 0; *ura3*Δ 0; *YDL142c*::kanMX4; [pYes2_P.p.*CRD1*]	This study
E. coli Top10	F- mcrA Δ(mrr-hsdRMS-mcrBC) φ80lacZΔM15 ΔlacX74 nupG recA1 araD139 Δ(ara-leu)7697 galE15 galK16 rpsL(StrR) endA1 λ-	Invitrogen
E. coli Top10 [pYes2]	As above transformed with [pYes2]	Our laboratory
E. coli Top10 [pFA6a_KanMX6]	As above transformed with [pFA6a-KanMX6]	Our laboratory
E. coli Top10 [pYes2_Pp_*CRD1*]	As above transformed with [pYes2_P.p.*CRD1*]	This study
P. pastoris CBS7435	MATa; Mut^+; His^+;	ACIB
P. pastoris CBS7435 GalP-*CRD1*	MATa; Mut^+; His^+; $G418^R$-GalP-CRD1	This study

Table 2: Growth media used in this study.

YP, yeast peptone full medium; MM, synthetic minimal medium.

Growth medium	**Carbon source, amino acid supplement**
YPD	2% glucose
YPGal	2% galactose
YPLac	2.66% lactate, 0.1% glucose
$YPGal^{G418}$	2% galactose, 0.5 mg/ml geneticin
MMD	2% glucose, all amino acids
MMGal	2% galactose, all amino acids
MMLac	2.66% lactate, 0.1% glucose, all amino acids
MMGly	3% glycerol, all amino acids
MMEtOH	3% ethanol, all amino acids
MMGly/EtOH	2% glycerol, 2% ethanol, all amino acids
MMD -ura	2% glucose, amino acid mix without uracil
MMGal -ura	2% galactose, amino acid mix without uracil

Table 3: Primers used in this study.

Bold: restriction enzyme cutting sites; bold and underlined: homologous sequences to the used templates; fwd, forward; rev, reverse.

Number	Name	5' => 3' sequence	direction
1	XbaI-CRD1	**ggatcc**ttatttggcattttctttatttaatattctgac	fwd
2	CRD1-BamHI	**tctaga**atgactctccaggaagggcg	rev
3	pYes2 control fwd	ttaacagatatataaatgcaaaaactgca	fwd
4	pYes2 control rev	gtataatgttacatgcgtacacgc	rev
5	CRD1 control fwd	cgaccccaaacgggtatatt	fwd
6	CRD1 control rev	ctgcatccttgctgaaaaca	rev
7	5'CRD1-lfhr-KanMX6 fwd	**tctgccgaaagagacaatctaaat**gggttaattaaggcgcgc	fwd
8	KanMX6 rev	gaattcgagctcgtttaaactgg	rev
9	3'KanMX-GAL1-P fwd	**ccagtttaaacgagctcgaattc**agtacggattagaagccgcc	fwd
10	GAL1-P-5'crd1 rev	**gattcaacctctgaaaggattcga**gttttttctccttgacgttaaagt	rev
11	3'FR GAL1-P - CRD1 fwd	**aggagaaaaaac**tcgaatcctttcagaggttgaatc atgactctccag	fwd
12	CRD1 rev	ttatttggcattttctttatttaatattctgactgc	rev
13	kan-gal-crd1 control fwd	ttcagtcgtcactcatggtga	fwd
14	kan-gal-crd1 control rev	gaaaacataggacagcccactt	rev
15	KanMX control fwd	gattcctgtttgtaattgtcctttt	fwd
16	RT-PP crd1 fwd	tgggattatcggccatctactacaga	fwd
17	RT-PP crd1 rev	cttgcttatcgtagttggcctcacc	rev
18	RT-PP arg4 fwd	tcctccggtggcagttctt	fwd
19	RT-PP arg4 rev	tccattgactcccgttttgag	rev
20	RT-SC crd1 fwd	gaccttcccaactatcaaaatggaaca	fwd
21	RT-SC crd1 rev	ttctatcttcgaaatcctcctcggttt	rev
22	RT-SC arg4 fwd	gacatgcaagaagacaaagagccacta	fwd
23	RT-SC arg4 rev	gtgagagcagcttccatcttttcctta	rev

A

```
Crd1p S. cerevisiae S288c                1    ------------------------------------MIQMVPIYSCSALLRRTIPKR---PFYHVLSGLTVRFKVN--P  38
Crd1p P. pastoris GS115                  1    ---------------------------------MYFGGAVRRVAFVSGGPFHHLTMPTLRALPPLAVVNLLSVRHLTNKSP  48
Put. membrane prot. P. pastoris CBS7435  1    MTLQEGRPQTGVLARSPISFLANLIFFPIQLFMYFGGAVRRVAFVSGGPFHHLTMPTLRALPPLAVVNLLSVRHLTNKSP  80

Crd1p S. cerevisiae S288c                39   QLNYNLFR--------------DLTRREYATNPSKTPHIKSK------------LLNIPNILTLSRIGCTPFIGLFIITN  92
Crd1p P. pastoris GS115                  49   QRKQTMITKTKEIGKKMSIETVETTKKIKENTLAKSKELKESFSSMIPSEYHENIYTIPNILTFTRLLSAPIIGYLIVHN  128
Put. membrane prot. P. pastoris CBS7435  81   QRKQTMITKTKEIGKKMSIETVETTKKIKENTLAKSKELKESFSSMIPSEYHENIYTIPNILTFTRLLSAPIIGYLIVHN  160

Crd1p S. cerevisiae S288c                93   NLTPALGLFAFSSITDFMDGYIARKYGLKTIAGTILDPLADKLLMITTTLALSVPSGPQIIPVSIAAIILGRDVLLAISA  172
Crd1p P. pastoris GS115                  129  HVTSALSLFTYSCITDFIDGYIARKYNMKSVVGTVIDPMADKSLMIICTACMAQS---HQIPMYVAVIILGRDVLLGLSA  205
Put. membrane prot. P. pastoris CBS7435  161  HVTSALSLFTYSCITDFIDGYIARKYNMKSVVGTVIDPMADKSLMIICTACMAQS---HQIPMYVAVIILGRDVLLGLSA  237

Crd1p S. cerevisiae S288c                173  LFIRYSTLKLKYPGRVAWNSYWDIVRYPSAEVRPSQLSKWNTFFQMVYLGSGVL---LLLYEKEEGCEKTEEDFEDRKQD  249
Crd1p P. pastoris GS115                  206  IYYRYVSLPRPKTFKRFWD-----FSIPSAEVRPTTISKINTGLQMVYIGSSMIKPVLIPYLTSDSSAMV----------  270
Put. membrane prot. P. pastoris CBS7435  238  IYYRYVSLPRPKTFKRFWD-----FSIPSAEVRPTTISKINTGLQMVYIGSSMIKPVLIPYLTSDSSAMV----------  302

Crd1p S. cerevisiae S288c                250  FQKAFSYLGYVTATTTIMSGVSYALKRNAFKLLK-----  283
Crd1p P. pastoris GS115                  271  LQGLFA-LEITVAISTILSGLSYVFSKDAVRILNKENAK  308
Put. membrane prot. P. pastoris CBS7435  303  LQGLFA-LEITVAISTILSGLSYVFSKDAVRILNKENAK  340
```

B

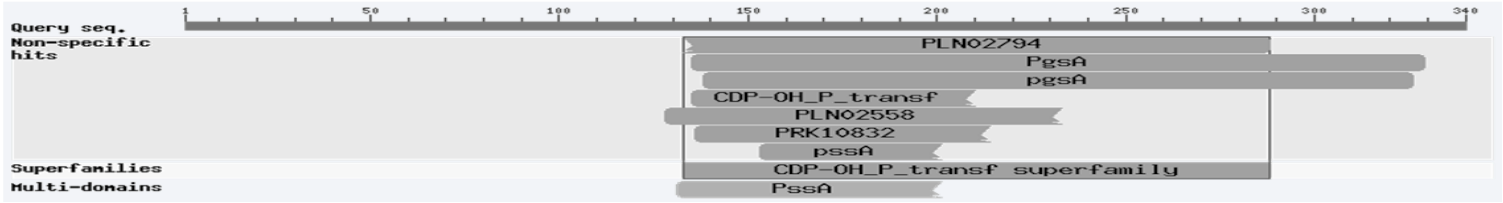

Figure 1: Bioinformatical identification of the *CRD1* gene in *P. pastoris* CBS7435.A) Protein alignment of the cardiolipin synthases (Crd1p) from *S. cerevisiae* BY4741 and *P. pastoris* GS115 and the putative membrane protein from *P. pastoris* CBS7435. B) Conserved domains found in the putative membrane protein from *P. pastoris* CBS7435. PLN02794, cardiolipin synthase; PgsA/pgsA, phosphatidylglycerophosphate synthase; CDP-OH_P_transf, CDP-alcohol phosphatidyltransferase; PLN02558, CDP-diacylglycerol-glycerol-3-phosphate/ 3-phosphatidyltransferase; PRK10832, phosphatidylglycerophosphate synthetase; PssA/pssA, phosphatidylserine synthase. Software used for this bioinformatical studies is mentioned under experimental procedures.

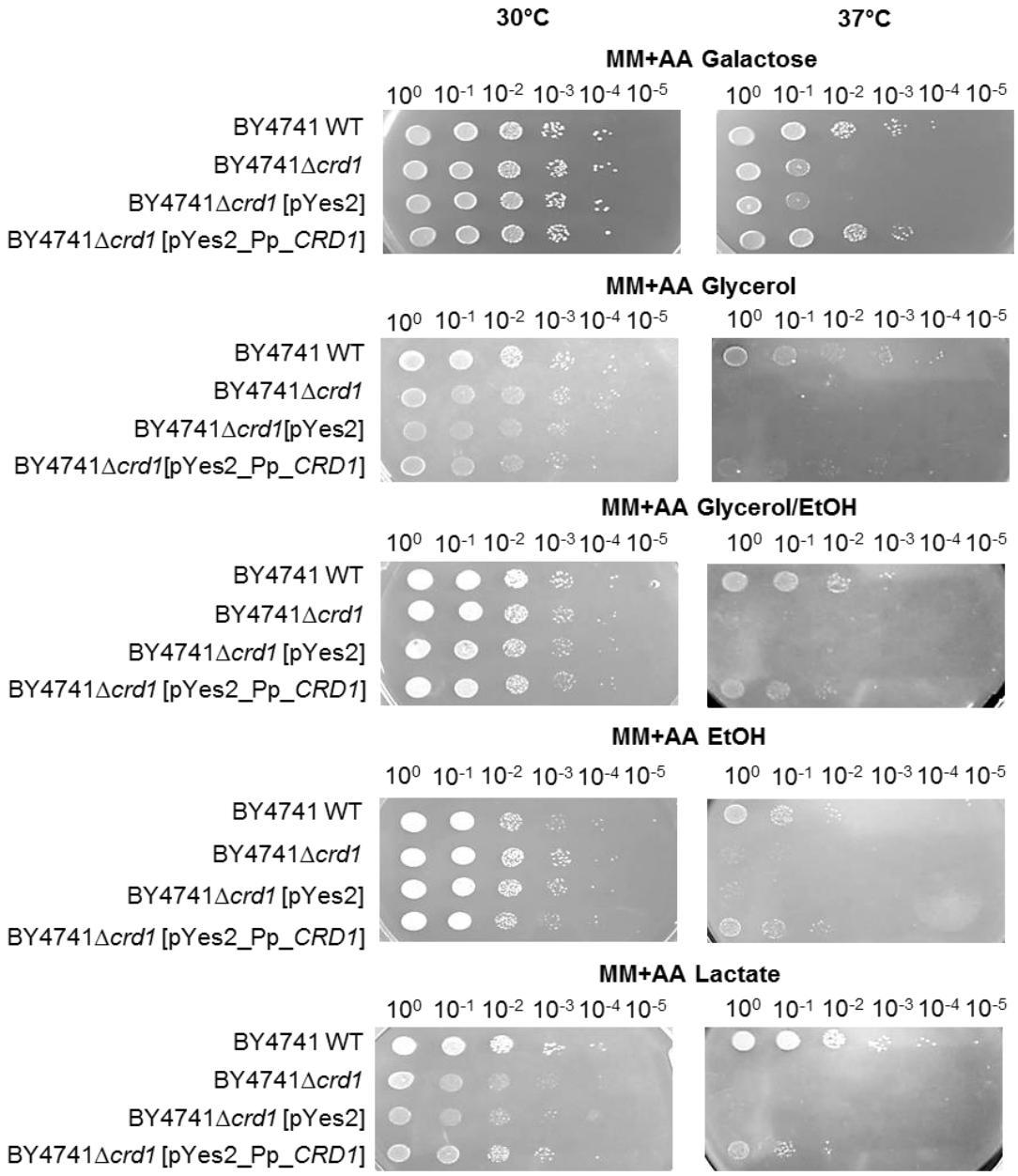

Figure 2: Growth phenotypic analysis of the *S. cerevisiae* strain BY4741 *crd1*Δ expressing the *CRD1* gene from *P. pastoris*.

The *S. cerevisiae* strains BY4741, BY4741 *crd1*Δ, BY4741 *crd1*Δ [pYes2] and BY4741 *crd1*Δ [pYes2_Pp_*CRD1*] were grown over night in the respective medium (MMD, MMD – ura) at 30°C. One OD unit of cells was harvested and resuspended in 1 ml sterile ddH_2O. Serial dilutions were prepared in sterile water, and 5 µl of each serial dilution was spotted onto agar plates containing different carbon sources. Plates were incubated either at 30°C or at 37°C for 2 – 4 days. WT, wild type; Pp, *Pichia pastoris*; MM, minimal medium; EtOH, ethanol; AA, all amino acid mix.

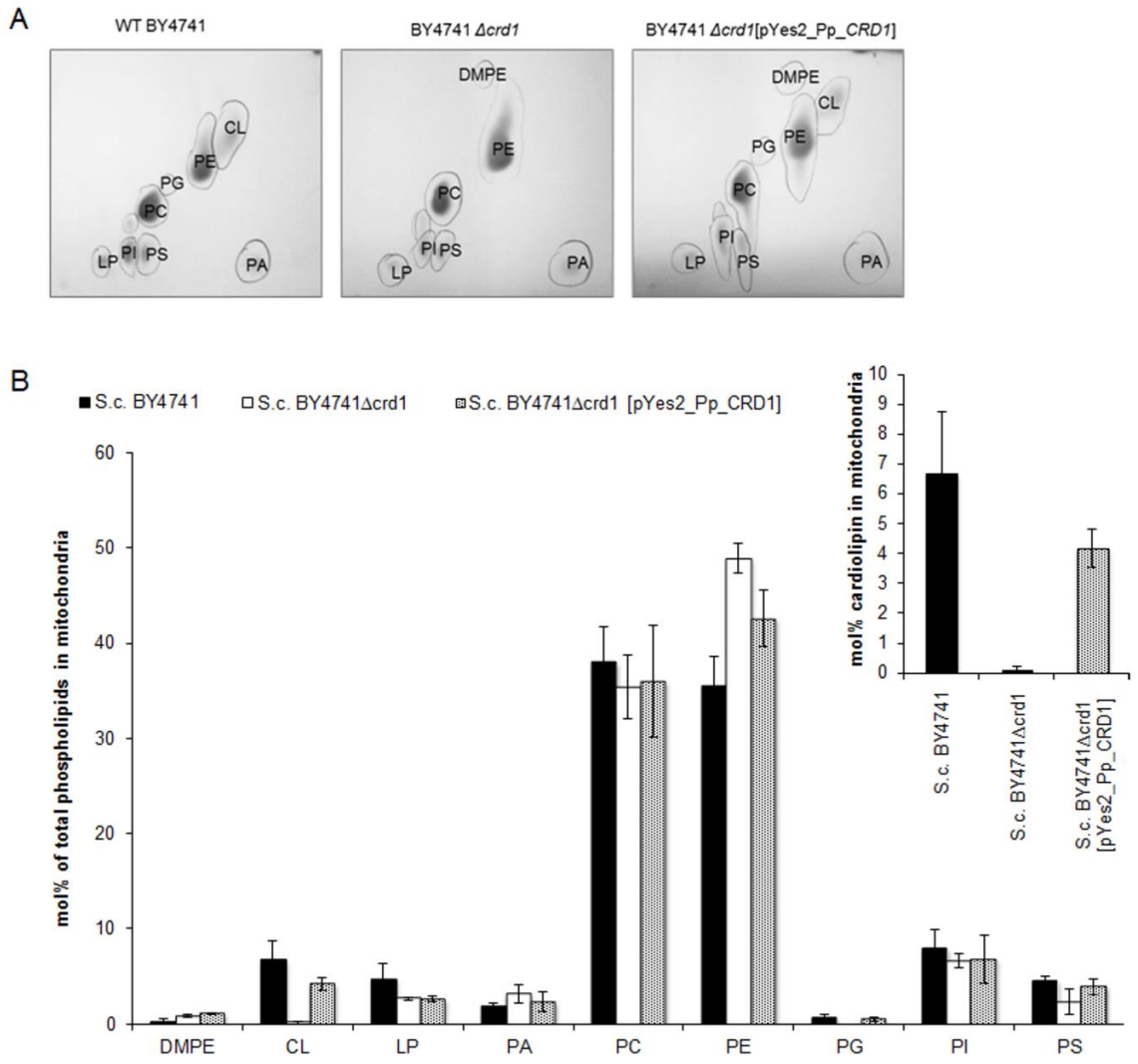

Figure 3: Individual phospholipids of the *S. cerevisiae* strain BY4741 *crd1*Δ expressing the *CRD1* gene from *P. pastoris*.

Mitochondria were isolated from the *S. cerevisiae* strains BY4741, BY4741 *crd1*Δ and BY4741 *crd1*Δ [pYes2_Pp_*CRD1*], and lipids were extracted. Individual phospholipids were separated by two-dimensional thin-layer chromatography (TLC), stained with iodine vapor and quantified as described in the experimental procedures. A) Individual phospholipids in mitochondria from *S. cerevisiae* strains BY4741, BY4741 *crd1*Δ and BY4741 *crd1*Δ [pYes2_Pp_*CRD1*] separated on TLC-plates and stained with iodine vapor. B) The amounts of cardiolipin (CL), dimethylphosphatidylethanolamine (DMPE), lysophospholipids (LP), phosphatidic acid (PA), phosphatidylcholine (PC), phosphatidylethanolamine (PE), phosphatidylinositol (PI) and phosphatidylserine (PS) in mitochondria from *S. cerevisiae* strains BY4741, BY4741 *crd1*Δ and BY4741 *crd1*Δ [pYes2_Pp_*CRD1*] are shown as mol% of total phospholipids. Data are mean values of two independent experiments analyzed in replicates (n=4). Error bars indicate standard deviation. Pp, *Pichia pastoris*.

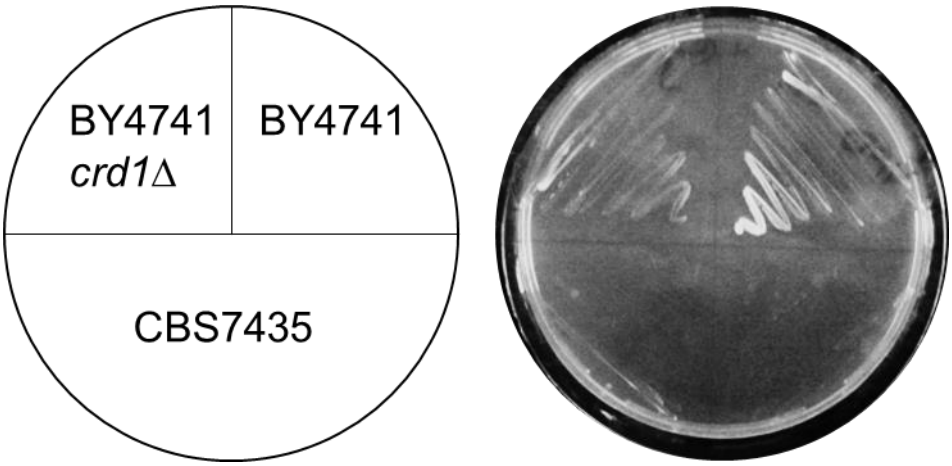

Figure 4: Anaerobic growth of the *P. pastoris* CBS7435.

Anaerobic growth of *P. pastoris* CBS7435 and the *S. cerevisiae* strains BY4741 and BY4741 *crd1*Δ as references was tested on plates. Strains were streaked out onto agar plates supplemented with ergosterol and Tween 80 and containing different carbon sources. Plates were incubated anaerobically at 30°C. Growth on YPD is shown as an example.

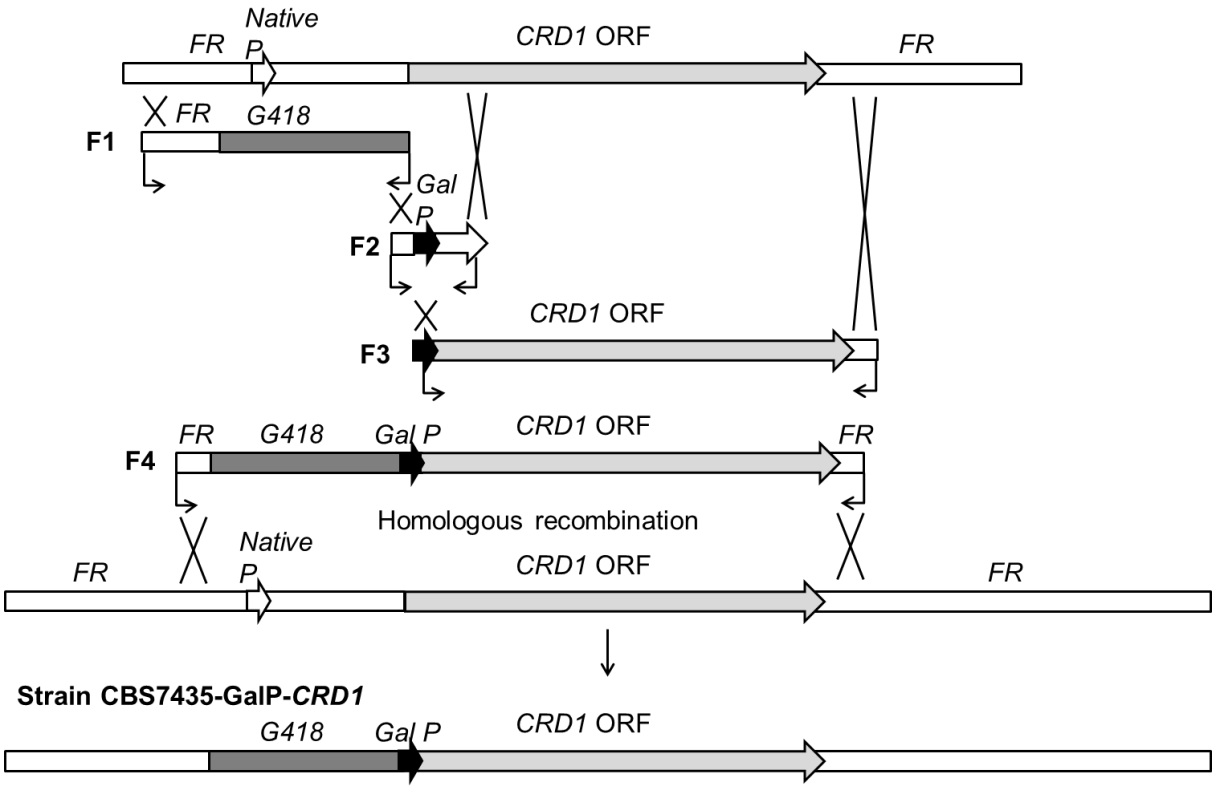

Figure 5: Strategy for the exchange of the native *CRD1* promoter by an inducible promoter in *P. pastoris* CBS7435.

The native promoter of the *CRD1* gene from *P. pastoris* CBS7435 was replaced by the inducible galactose promoter as described under experimental procedures. F, fragment; FR, flanking region; ORF, open reading frame; P, promoter; Gal, galactose; G418, geneticin.

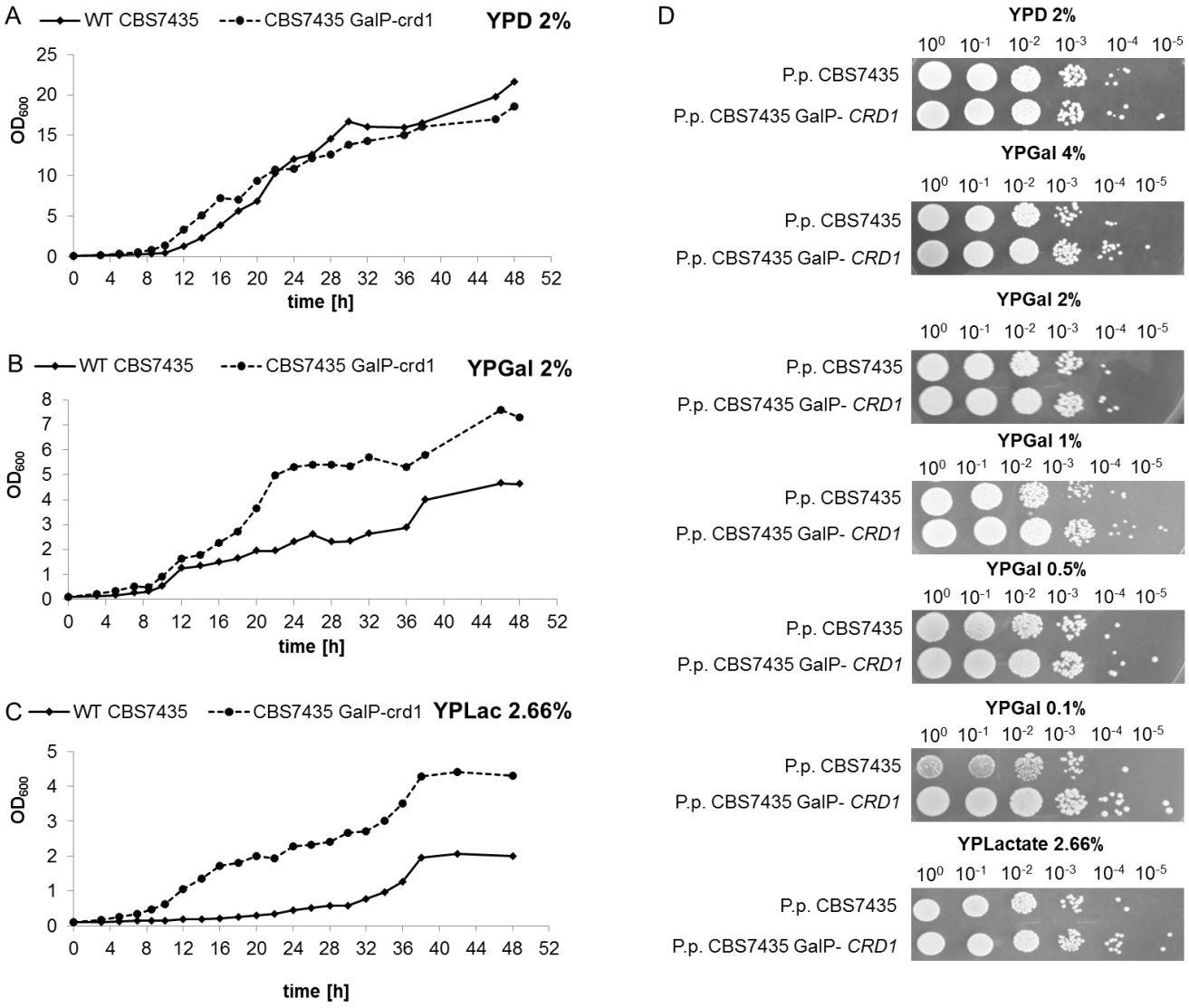

Figure 6: Growth phenotype analysis of the *P. pastoris* CBS7435-GalP-*CRD1* strain.

P. pastoris wild type CBS7435 and CBS7435 GalP-*CRD1* were cultivated as described under experimental procedures. Over a time period of 48 hours, samples were taken from cultures grown on A) YPD, B) YPGal and C) YPLac, and the OD_{600} was determined. D) Growth behavior of *P. pastoris* CBS7435 and CBS7435-GalP-*CRD1* was examined by drop tests as described under experimental procedures. Serial dilutions were prepared and 5 µl of each dilution was spotted onto agar plates containing different carbon sources. Plates were incubated at 30°C for 2 – 4 days. WT, wild type; GalP, galactose promoter; YP, yeast peptone full medium; D, glucose; Gal, galactose; Lac, lactate; P.p., *Pichia pastoris.* OD_{600}, optical density was measured at 600 nm.

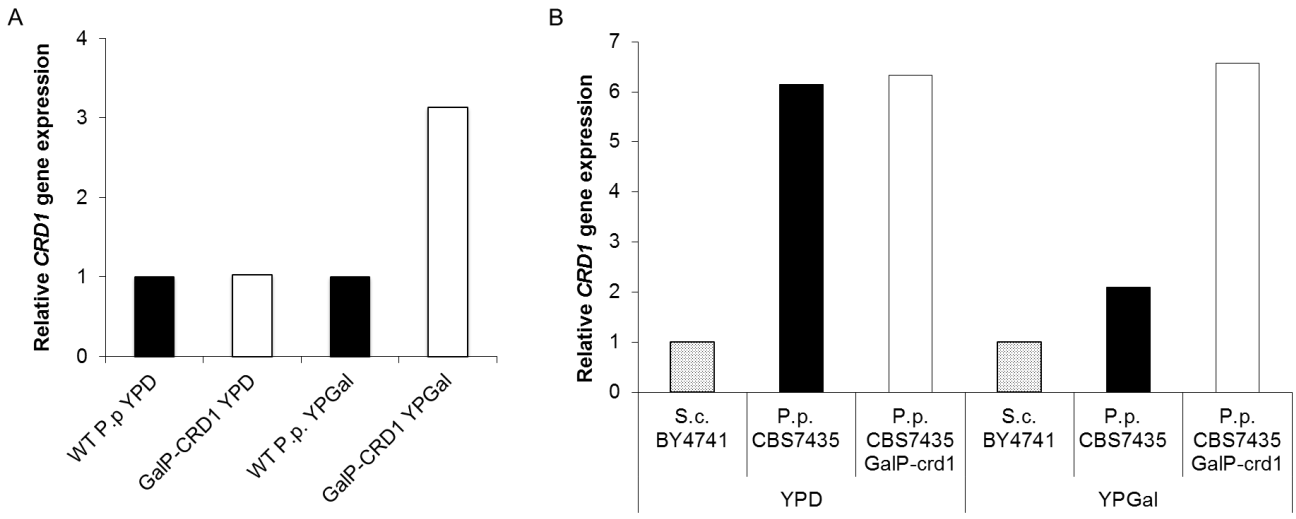

Figure 7: Expression of *CRD1* in *P. pastoris* CBS7435-GalP-*CRD1*.

Relative expression of the *CRD1* gene from *P. pastoris* CBS7435 and CBS7435 GalP-*CRD1* strains and *S. cerevisiae* BY4741 was determined and quantified by real time PCR as described under experimental procedures. For RNA isolation, strains were precultured on glucose (YPD) and shifted to fresh glucose (YPD) or galactose media (YPGal) for the main culture. A) *CRD1* gene expression of *P. pastoris* CBS7435-GalP-*CRD1* relative to the *P. pastoris* wild type CBS7435; and B) *CRD1* gene expression of the *P. pastoris* wild type strain CBS7435 and CBS7435-GalP-*CRD1* relative to the *S. cerevisiae* wild type strain BY4741 after shifting the cells from YPD to a promoter repressing (YPD) or a promoter inducing (YPGal) medium. WT, wild type; GalP, galactose promoter; YP, yeast peptone full medium; D, glucose; Gal, galactose; Lac, lactate; OD_{600}, optical density measured at 600 nm; P.p., *Pichia pastoris*; S.c. *Saccharomyces cerevisiae*.

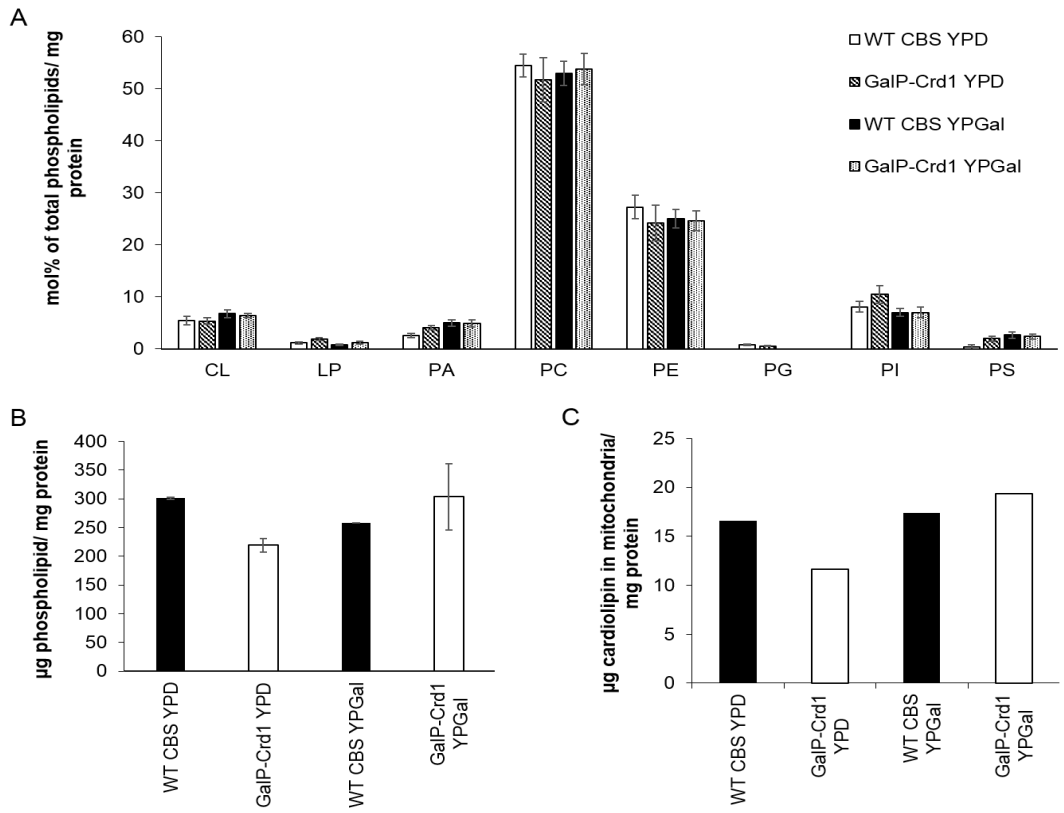

Figure 8: Phospholipid analysis of the *P. pastoris* CBS7435-GalP-*CRD1* strain.

Mitochondria were isolated from *P. pastoris* strains CBS7435 and CBS7435 GalP-*CRD1* after shifting the cells from YPD to a promoter repressing (YPD) or a promoter inducing (YPGal) medium. Individual phospholipids were separated by two-dimensional thin-layer chromatography (TLC), stained with iodine vapor and quantified as described under experimental procedures. Total phospholipids were directly quantified by phosphate determination. A) The amounts of cardiolipin (CL), dimethylphosphatidylethanolamine (DMPE), lysophospholipids (LP), phosphatidic acid (PA), phosphatidylcholine (PC), phosphatidylethanolamine (PE), phosphatidylinositol (PI) and phosphatidylserine (PS) in mitochondria from *P. pastoris* CBS7435 and CBS7435 GalP-*CRD1* are shown as mol% of total phospholipids. Data are mean values of two independent experiments analyzed in replicates (n=4). Error bars indicate standard deviation. B) Total phospholipids of mitochondria from the *P. pastoris* strains CBS7435 and the CBS7435 GalP-*CRD1* are shown in µg/mg protein. Data are mean values of two independent experiments analyzed in replicates (n=4). Error bars indicate standard deviation. C) Amounts of CL were calculated from analysis A and B and expressed as µg CL in mitochondria per mg protein. WT, wild type; GalP, galactose promoter; YP, yeast peptone full medium; D, glucose; Gal, galactose; P.p., *Pichia pastoris*.

Chapter VII

General discussion

Since fundamental information about *Pichia pastoris* cell biological and biochemical characteristics is rather rare, a project to characterize organelle membranes of *P. pastoris* was initiated in our laboratory some years ago. This Thesis was part of the "Pichia lipidomics" project and was primarily dedicated to the investigation of microsomes and phospholipid metabolism in this yeast. During this study two main objectives were addressed. First, we isolated microsomes which represent the endoplasmic reticulum from *P. pastoris* and studied lipidome and proteome of this subcellular compartment in detail. Secondly, we identified the gene responsible for the formation of the mitochondrial phospholipid cardiolipin. Moreover, we provided an overview about lipid metabolism in yeast and summarized the entire methodology employed in our laboratory for isolation of organelles and biomembranes from *P. pastoris* and the lipid analytical techniques required for their characterization.

The lipidome and proteome of *P. pastoris* microsomes

In the present study we established an isolation protocol for ER fractions (microsomes) from the methylotrophic yeast *P. pastoris*. The protocol used for isolation of M30 and M40 microsomes was adapted from methods originally designed for *S. cerevisiae* and is based on various steps of differential centrifugation. Microsomal fractions were obtained at high quality and their lipidome and proteome was analyzed.

The lipidome studies revealed that almost all phospholipid species detected contained at least one unsaturated fatty acid. Since *P. pastoris* does not only produce monounsaturated fatty acids like *S. cerevisiae* [1] but also polyunsaturated acyl chains, a high degree of unsaturation in the membranes is reached thus influencing membrane properties and membrane protein functions.

Another interesting finding derived from the lipidome analysis was the glycerophospholipid class specific pattern of species. Although PS and PI synthases are

distinct enzymes, their specificity appears to be similar resulting in PS and PI species patterns with a large portion on C34:1 and C34:2. These observations may be explained by the biosynthetic origin of the respective phospholipids. PS and PI are derived from the same precursor, CDP-diacylglycerol [2,3]. The pattern of aminoglycerophospholipid species (PS – PE – PC) is less specific as shown by the high diversity of species containing unsaturated C34 and C36. The fact that PE and PC are synthesized by two different biosynthetic routes, the CDP-ethanolamine/choline pathway and the methylation pathway, may contribute to the broad and almost randomized pattern of PC and PE species.

Although DG and TG are primarily found in lipid droplets, substantial amounts of these lipids were also detected in microsomes. This finding may be explained by the fact that enzymes of TG synthesis in *P. pastoris* identified recently [4] are also ER components.

P. pastoris is a "low sterol yeast" since sterol levels in all organelle membranes (our own observations and [5,6]) as well as in lipid droplets in the form of steryl esters [7] are low. Similar to sterols, the concentration of inositol containing sphingolipids in ER membranes appears to be low compared to the plasma membrane (our own unpublished observations). The complex hexosylceramides and inositol containing ceramides seem to evolve from different ceramide species.

The large number of proteins detected in microsomal fractions as well as the protein profile indicated that ER proteins comprise a predominant portion of total proteins in the cell. Beside proteins involved in glycosylation, secretion and translation, a number of lipid biosynthetic enzymes were found as prominent components of the ER in our proteome study. These investigations provide for the first time a deeper insight into the protein molecular equipment of microsomes from *P. pastoris.*

Identification of the cardiolipin synthase in *P. pastoris*

In this thesis, phospholipid metabolism in *P. pastoris* was also studied by investigating cardiolipin (CL) synthesis. The enzyme catalyzing CL formation is the mitochondrial CL synthase. To identify the respective gene from *P. pastoris* and to characterize the gene product we have chosen a stepwise approach. First, we identified the *CRD1* gene in *P. pastoris* CBS7435 by bioinformatical studies. Secondly, we expressed the *CRD1* gene from *P. pastoris* in a *S. cerevisiae crd1*Δ deletion strain and showed (i) complementation of the growth defect in *S. cerevisiae crd1*Δ by the *P. pastoris* gene; as well as (ii) reconstitution of the ability to synthesize CL. Thus, we identified the *CRD1* gene encoding for the CL synthase

in *P. pastoris* by function. Finally, we investigated effects of *CRD1* overexpression in *P. pastoris.*

To address the question as to the physiological role of CL in *P. pastoris* and especially in mitochondria we tried to delete the *CRD1* gene, but without success. As *P. pastoris* is a strictly aerobic microorganism one might speculate that CL which is important for respiration is essential for growth. The influence of the CL level on the growth behavior of *P. pastoris* was also demonstrated with a strain overexpressing *CRD1* under an inducible promoter. At present it is difficult to interpret why the amount of total mitochondrial phospholipids was increased in the overexpressing strain, while the distribution of the individual phospholipids was not altered. Thus, the link between CL metabolism and the rest of the lipid biosynthetic network in *P. pastoris* remains to be investigated.

Conclusion

In conclusion, this Thesis contributes to our understanding of lipid metabolism in yeast. The design of methods for organelle isolation, lipidome and proteome analysis was a major step forward in our knowledge of *P. pastoris* cellular and molecular biology. Methods developed during this study were specifically applied to characterize microsomal compartments at the lipid and protein levels. Moreover, this work extended our knowledge of *P. pastoris* lipid biosynthesis by investigation CL synthase.

Pichia pastoris has become a very important biotechnological tool used in the industry for the production of heterologous proteins. Thus, it is obvious that a good knowledge of cell biological and biochemical properties of this organism is required to understand and manipulate biotechnological processes at the molecular level. Several investigations with *Pichia* organelles, their lipidome and their proteome have already been performed in our laboratory [5–8]. These studies have demonstrated the value of these investigations, but also the further need to study lipid metabolism and membrane biology of *P. pastoris* in more detail.

References:

[1] G. Tuller, T. Nemec, C. Hrastnik, G. Daum, Lipid composition of subcellular membranes of an FY1679-derived haploid yeast wild-type strain grown on different carbon sources, Yeast, 15 (1999) 1555–1564.

[2] N.M. Jani, J.M. Lopes, Regulated transcription of the *Saccharomyces cerevisiae* phosphatidylinositol biosynthetic gene, *PIS1*, yields pleiotropic effects on phospholipid synthesis, FEMS Yeast Res., 9 (2009) 552–564.

[3] H.-S. Choi, A. Sreenivas, G.-S. Han, G.M. Carman, Regulation of phospholipid synthesis in the yeast *cki1Δ eki1Δ* mutant defective in the Kennedy pathway; The Cho1-encoded phosphatidylserine synthase is regulated by mRNA stability, J. Biol. Chem., 279 (2004) 12081–12087.

[4] V.A. Ivashov, G. Zellnig, K. Grillitsch, G. Daum, Identification of triacylglycerol and steryl ester synthases of the methylotrophic yeast *Pichia pastoris*, Biochim. Biophys. Acta, 1831 (2013) 1158–1166.

[5] T. Wriessnegger, G. Gübitz, E. Leitner, E. Ingolic, J. Cregg, B.J. de la Cruz, G. Daum, Lipid composition of peroxisomes from the yeast *Pichia pastoris* grown on different carbon sources, Biochim. Biophys. Acta, 1771 (2007) 455–461.

[6] T. Wriessnegger, E. Leitner, M.R. Belegratis, E. Ingolic, G. Daum, Lipid analysis of mitochondrial membranes from the yeast P*ichia pastoris*, Biochim. Biophys. Acta, 1791 (2009) 166–172.

[7] V.A. Ivashov, K. Grillitsch, H. Koefeler, E. Leitner, D. Baeumlisberger, M. Karas, G. Daum, Lipidome and proteome of lipid droplets from the methylotrophic yeast *Pichia pastoris*, Biochim. Biophys. Acta, 1831 (2013) 282-290.

[8] L. Klug, P. Tarazona, C. Gruber, K. Grillitsch, B. Gasser, M. Trötzmüller, H. Köfeler, E. Leitner, I. Feussner, D. Mattanovich, F. Altmann, G. Daum, The lipidome and proteome of microsomes from the methylotrophic yeast *Pichia pastoris*, Biochim. Biophys. Acta, 1841 (2014) 215–226.

List of Publications

1. M. Spanova, D. Zweytick, K. Lohner, L. Klug, E. Leitner, A. Hermetter, G. Daum, Influence of squalene on lipid particle/droplet and membrane organization in the yeast *Saccharomyces cerevisiae*, Biochim. Biophys. Acta, 1821 (2012) 647–653.

2. L. Klug, P. Tarazona, C. Gruber, K. Grillitsch, B. Gasser, M. Trötzmüller, H. Köfeler, E. Leitner, I. Feussner, D. Mattanovich, F. Altmann, G. Daum, The lipidome and proteome of microsomes from the methylotrophic yeast *Pichia pastoris*, Biochim. Biophys. Acta, 1841 (2014) 215–226.

3. L. Klug, V. Ivashov, K. Grillitsch and G. Daum, *Pichia pastoris* lipidomics, in Pichia protocols (Methods in Molecular Biology), Springer protocols, Third edition (2013), manuscript submitted.
4. V. Ivashov, L. Klug, K. Grillitsch and G. Daum, Isolation of *Pichia* organelles, in Pichia protocols (Methods in Molecular Biology), Springer protocols, Third edition (2013) manuscript submitted
5. L. Klug, G. Daum, Yeast lipid metabolism at a glance, FEMS Yeast Res., Minireview, manuscript under revision
6. K. Grillitsch, P. Tarazona, L. Klug, T. Wriessnegger, G. Zellnig, E. Leitner, I. Feussner and G. Daum, Isolation and characteristics of the plasma membrane from the yeast *Pichia pastoris*, Biochim. Biophys. Acta, manuscript submitted

Contributions to Conferences

Dates (M-Y)	Title of Conference	Type of presentation
02-2011	7th Doc Day, Graz, Austria	Poster
08/09-2011	52nd International Conference on the Bioscience of Lipids (ICBL), Warsaw, Poland	Poster
02/03-2012	Pichia 2012, Alpbach, Austria	Poster
03-2012	4th International Graz Symposium on Lipid and Membrane Biology, Graz, Austria	Attended
09-2012	4th Annual Meeting 2012 of the Austrian Association of Molecular Life Sciences and Biotechnology, Graz, Austria,	Attended
06-2013	5th Conference on Physiology of Yeast and Filamentous Fungi, Montpellier, France	Poster
02-2014	11th Doc Day, Graz, Austria	Poster

Curriculum Vitae

Personal data:

Full name:	Lisa Theresa Romana Klug
Grade:	Bakk. rer. nat., MSc.
Nationality:	Austria
Date of birth:	21.01.1982
Place of birth:	Leutschach, Austria
Address:	Kleegasse 4/19, 8020 Graz, Austria
E-mail:	klug.lisa@gmail.com
Cell phone number:	0043 650 2101000

Education:

September 2010 –

March 2014 PhD student at the Institute of Biochemistry, Graz University of Technology, Graz, Austria within the framework of the Doctoral School Molecular Biomedical Sciences and Biotechnology of the Karl-Franzens-University and Graz University of Technology (NAWI Graz)

Subject: ***Pichia pastoris*** **Lipidomics**
Supervisor: Ao.Univ.-Prof. Dipl.-Ing. Dr.techn. tit.Univ.-Prof. Daum Günther

February 2009 –

August 2010 Master thesis at the Institute of Molecular Biosciences, Karl-Franzens University, Graz, Austria

Subject: **Cell death of *Saccharomyces cerevisiae* during chronological aging triggered by methionine restriction**
Supervisors: Dr. Kai-Uwe Fröhlich and Dr. Christoph Ruckenstuhl

October 2008 –

January 2009 — Project lab at the Institute of Molecular Biosciences, Karl-Franzens University, Graz, Austria

Subject: **Cell survival of *Saccharomyces cerevisiae* under various methionine concentrations during chronological aging**

2007-2010 — Undergraduate Education, Master Molecular Microbiology, Karl-Franzens University, Graz, Austria.

2003-2007 — Undergraduate Education, Bachelor Molecular Biology, Karl-Franzens University, Graz, Austria

2000-2003 — Undergraduate Education, Master Biology, Karl-Franzens University, Graz, Austria

June 2000 — School Leaving examination

1992-2000 — Secondary School BG/BRG Leibnitz, Austria

1988-1992 — Primary School Gleinstätten, Austria

Teaching activities:

SS 2012/ SS2013 — Supervisor Lab Course Immunological Methods ("LU Immunologische Methoden")

SS 2009/ SS2010 — Tutor Lab Course Molecular Biology I ("LU Molekularbiologische Übungen I")

SS 2009/ WS 2009/ SS2010 — Tutor Lab Course Microbiology for Biologists ("LU Mikrobiologische Übungen für Biologen")

SS 2009 – SS 2010 — Performance of "open lab" courses for non-scientific public consisting of a seminar and an experimental part

SS2009 — Collaboration in molecular cooking (Podiumsdiskussion der siebten Fakultät "Leben am Limit")

Soft skills: Seminar in scientific communications (co-organisation of the "long night of research 2009")

Seminar in project management (co-organisation of a meeting "science with flavour, kitchen meets research laboratory" in June 2010)

Practical Experience:

2003	Summer job at Fresenius Kabi Graz, Department for microbiological quality control of infusion solutions for the pharmaceutical use, Graz, Austria
2004	Temporary work at Hennes & Mauritz Gmbh, Sales, Graz, Austria
2003-2008	Part-time employment at Fresenius Kabi Graz, Department for microbiological quality control of infusion solutions for the pharmaceutical use, Graz, Austria

Languages:

German (native)
English (fluent)
French (A1/2)